

Direct synthesis of hydrogen peroxide in a wall-coated capillary microreactor

Citation for published version (APA):

Paunovic, V. (2015). *Direct synthesis of hydrogen peroxide in a wall-coated capillary microreactor*. [Phd Thesis 1 (Research TU/e / Graduation TU/e), Chemical Engineering and Chemistry]. Technische Universiteit Eindhoven.

Document status and date:

Published: 01/01/2015

Document Version:

Publisher's PDF, also known as Version of Record (includes final page, issue and volume numbers)

Please check the document version of this publication:

- A submitted manuscript is the version of the article upon submission and before peer-review. There can be important differences between the submitted version and the official published version of record. People interested in the research are advised to contact the author for the final version of the publication, or visit the DOI to the publisher's website.
- The final author version and the galley proof are versions of the publication after peer review.
- The final published version features the final layout of the paper including the volume, issue and page numbers.

[Link to publication](#)

General rights

Copyright and moral rights for the publications made accessible in the public portal are retained by the authors and/or other copyright owners and it is a condition of accessing publications that users recognise and abide by the legal requirements associated with these rights.

- Users may download and print one copy of any publication from the public portal for the purpose of private study or research.
- You may not further distribute the material or use it for any profit-making activity or commercial gain
- You may freely distribute the URL identifying the publication in the public portal.

If the publication is distributed under the terms of Article 25fa of the Dutch Copyright Act, indicated by the "Taverne" license above, please follow below link for the End User Agreement:

www.tue.nl/taverne

Take down policy

If you believe that this document breaches copyright please contact us at:

openaccess@tue.nl

providing details and we will investigate your claim.

Direct synthesis of hydrogen peroxide in a wall-coated capillary microreactor

PROEFSCHRIFT

ter verkrijging van de graad van doctor aan de
Technische Universiteit Eindhoven, op gezag van de
rector magnificus prof.dr.ir.F.P.T.Baaijens,
voor een commissie aangewezen door het College
voor Promoties, in het openbaar te verdedigen op
donderdag 15 oktober 2015 om 16:00 uur

door

Violeta Paunovic

geboren te Prijepolje, Servië

Dit proefschrift is goedgekeurd door de promotoren en de samenstelling van de promotiecommissie is als volgt:

voorzitter:	prof.dr.ir. R.A.J. Janssen
1 ^e promotor:	prof.dr.ir. J.C. Schouten
Copromotor(en):	dr.ir. T.A. Nijhuis
leden:	prof.dr. Y. Cheng (Tsinghua University) prof.dr. F. Kapteijn (TUD) prof.dr.ir. E.J.M. Hensen
adviseur(s):	dr. V. Ordonsky (Université Lille)

"Experience is what you get when you didn't get what you wanted."

Randy Pausch, The Last Lecture (2007)

To my Serbian and my German family...

This work was financially supported by the National Research School Combination Catalysis Controlled by Chemical Design (NRSC-Catalysis) program of The Netherlands Organisation for Scientific Research (NWO) in the Netherlands.

Direct synthesis of hydrogen peroxide in a wall-coated capillary microreactor/
by Violeta Paunovic.

Eindhoven: Technische Universiteit Eindhoven, 2015.

A catalogue record is available from the Eindhoven University of Technology
Library

ISBN: 978-90-386-3907-9

Cover design by Violeta Paunović and Bogdan Kalušević.

Printed by GVO printers & designers B.V.

Table of contents

1. Introduction.....	1
1.1. Direct synthesis vs. Anthraquinone autooxidation process.....	1
1.2. Catalyst.....	6
1.3. Role of promoters.....	8
1.4. Solvent.....	11
1.5. Reactor concepts.....	12
1.5.1. Microreactors and the Direct Synthesis.....	14
1.6. Objectives and Outline.....	18
2. Catalyst coating on prefabricated capillary microchannels for the direct synthesis of hydrogen peroxide.....	23
2.1. Introduction.....	24
2.2. Experimental.....	26
2.2.1. Deposition of the catalytic layer on capillary wall- Coating procedure.....	26
2.2.2. Preparation of the silica wash-coat solution and capillary pretreatment...	28
2.2.3. Coating analysis.....	29
2.2.4. Deposition of Au-Pd catalyst.....	30
2.2.5. Microchannel catalyst testing.....	31
2.2.5.1. Flow pattern.....	31
2.3. Results.....	32
2.3.1. Colloidal silica coatings.....	33
2.3.1.1. Dynamic coating of capillary microchannels - coating uniformity....	33
2.3.2. Slurry coatings.....	37
2.3.3. Sol-gel coatings.....	39
2.3.4. Activity of Au-Pd catalyst supported on SiO ₂ wash-coats in a microchannel in the direct synthesis of hydrogen peroxide.....	42
2.4. Conclusions.....	45
3. Direct synthesis of H₂O₂ over Au-Pd catalyst in a wall-coated microchannel.....	49
3.1. Introduction.....	49
3.2. Materials and Methods.....	51
3.2.1. Preparation of microchannel wash-coats.....	51
3.2.2. Catalyst preparation.....	52

3.2.3. Catalyst characterization.....	53
3.2.4. Catalyst testing.....	54
3.2.4.1. Slurry catalyst testing.....	54
3.2.4.2. Microchannel catalyst testing.....	55
3.3. Results and Discussion.....	56
3.3.1. Catalyst characterization.....	56
3.3.2. Catalyst testing.....	59
3.4. Conclusions.....	65
4. Direct synthesis of H₂O₂ in a wall-coated microchannel over Au-Pd catalyst- microchannel performance study.....	69
4.1. Introduction.....	69
4.2. Materials and Methods.....	72
4.2.1. Preparation of microchannel wash-coats.....	72
4.2.2. Catalyst preparation.....	72
4.2.3. Direct synthesis of hydrogen peroxide in a wall-coated microchannel.....	73
4.3. Results and Discussion.....	74
4.3.1. Effect of operating conditions on the catalyst performance in a microchannel.....	75
4.3.2. Effect of external and internal mass transfer effects.....	84
4.3.3. Towards the application of direct synthesis.....	85
4.3.4. Hydrogen peroxide direct synthesis - Potential and challenges.....	88
4.4. Conclusion.....	90
5. Direct synthesis of H₂O₂ over Au-Pd catalyst- Kinetic study.....	95
5.1. Introduction.....	96
5.2. Materials and Methods.....	98
5.2.1. Deposition of silica layer.....	99
5.2.2. Deposition of Au-Pd catalyst.....	99
5.2.3. Direct synthesis of hydrogen peroxide in a microchannel-kinetic experiments.....	100
5.2.4. Hydrogenation of hydrogen peroxide in semi-batch reactor-kinetic experiments.....	100
5.2.5. Parameter determination.....	102
5.3. Results and Discussion.....	102
5.3.1. Characterization of Au-Pd catalysts.....	102
5.3.2. Reaction.....	104
5.3.3. Catalyst oxidation state alternation and activity.....	106

Chapter 1: Introduction

5.3.4. External and internal mass transfer in microchannel.....	107
5.3.5. Hydrogenation kinetics.....	108
5.3.6. Kinetics of direct formation reaction.....	111
5.3.7. Hydrogen peroxide concentration –the validation of kinetic expressions.....	116
5.4. Conclusions.....	116
Appendix 5A: Derivation of L-H kinetic expressions for hydrogenation of hydrogen peroxide.....	118
Appendix5B: Derivation of main L-H kinetic rate expressions for direct formation reaction.....	119
6. Direct synthesis of H₂O₂ over Au-Pd catalyst- Effect of co-solvent addition.....	127
6.1. Introduction.....	127
6.2. Materials and Methods.....	130
6.2.1. Catalyst preparation.....	130
6.2.2. Catalyst characterization.....	131
6.2.3. Direct synthesis of hydrogen peroxide and peroxide decomposition experiments.....	131
6.3. Results and Discussion.....	133
6.3.1. Catalyst characterization.....	133
6.3.2. Direct synthesis of hydrogen peroxide in presence of a co-solvent.....	133
6.3.2.1. Reactant-co-solvent interaction.....	139
6.3.2.2. Solvent/co-solvent-catalyst interactions.....	140
6.3.2.3. Type of metal affected and the amount of solvent.....	145
6.3.2.4. Direct synthesis of hydrogen peroxide in a wall-coated microchannel.....	146
6.3.3. FTIR adsorption of CO, acetonitrile and methanol over Au, Pd and Au-Pd catalysts supported on silica.....	153
6.3.3.1. FTIR of adsorbed CD ₃ CN.....	155
6.3.3.2. FTIR of adsorbed CH ₃ OH.....	156
6.3.4. Hydrogen peroxide decomposition in water/co-solvent mixture.....	157
6.4. Conclusions.....	160
Appendix 6A: Decomposition of H ₂ O ₂ in the presence of co-solvent.....	162
7. Conclusions & Outlook.....	169
7.1. Conclusions.....	169
7.2. Outlook.....	172
7.2.1. Application of solid acid as a catalyst support.....	173

7.2.2. Polyelectrolyte multilayers (PEM) AuPd catalyst as an upgrade in the catalyst preparation procedure.....	174
List of publications.....	177
Acknowledgments	181
Curriculum Vitae	185

Summary

Direct synthesis of hydrogen peroxide in a wall-coated capillary microreactor

Hydrogen peroxide is one of the most environmentally friendly and versatile commercial chemicals today with application in the paper and pulp industry, disinfectant, in semi-conductors and in the production of chemicals. Nevertheless, the Anthraquinone auto-oxidation (AO) process that is currently used for large-scale production of hydrogen peroxide cannot be considered an environmentally friendly process. The direct synthesis of hydrogen peroxide has been recognized as the best green alternative to the current AO process. In this process, hydrogen and oxygen are reacting directly over a heterogeneous catalyst to give hydrogen peroxide and water as the only by-product of the reaction. The safety hazards associated with the application of potentially explosive gas mixtures complicating the application of this process in a conventional reactor are eliminated by performing the reaction in a wall-coated microchannel reactor.

The first part of this thesis deals with the development of the catalyst for the direct synthesis reaction, a methodology to deposit the catalytic layer on prefabricated capillary microchannels and testing performance of the wall-coated microchannel reactor. Deposition of the catalytic layer on microchannel walls ensures a lower pressure drop in comparison to a micro-packed bed and proper catalyst wetting and contacting with the liquid phase used to collect the peroxide from the catalyst surface. The catalytic layers inside the microchannel consist of silica coatings with embedded AuPd nanoparticles as an active catalytic phase. Those catalytic coatings were prepared in a step-wise fashion, first a layer of silica support material is coated on the microchannel wall followed by deposition of the active catalytic phase. This ensures that active nanoparticles remain accessible for reactants on the catalyst surface (not entrapped in catalyst pores by binder material used in the coating procedure) and retain their activity. Catalytic tests performed indicated that there is a superior activity for colloidal AuPd bimetallic nanoparticles prepared using a two-phase synthesis procedure in comparison to impregnated AuPd catalysts. An important advantage of using a capillary channel microreactor is the possibility to use H_2/O_2 concentrations that would be considered explosive in traditional reactors. Operating the microreactor within what would have been the explosive regime in a conventional reactor results in a higher selectivity and productivity.

Summary

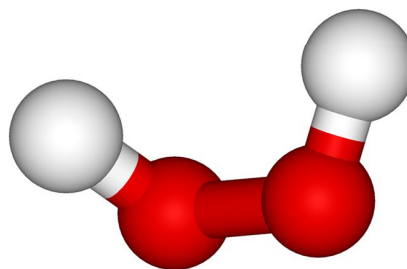
A microchannel performance study was carried out evaluating the maximum peroxide concentration achievable in the aqueous phase. It was assessed that the generation of higher hydrogen peroxide concentrations in the aqueous phase suffers from selectivity impairment. In order to improve H₂ efficiency of the process, the recommendation was given to couple the direct synthesis with a competitive in-situ oxidation reaction consuming peroxide which would prevent its non-selective transformation to water.

The second part of the thesis is devoted to a kinetic study of direct synthesis over AuPd colloidal nanoparticles and the application of alternative liquid phases in order to improve the selectivity. A study of the kinetics of the reactions involved in the hydrogen peroxide direct synthesis was performed in order to obtain the overall rate expression to be used to predict peroxide concentration at the reactor outlet. For this purpose, the reactions of direct formation of peroxide and peroxide reduction in the presence of hydrogen were studied separately. The decomposition reaction is eliminated by the addition of sulfuric acid, typically applied in direct synthesis, but in the conventional AO process for peroxide stabilization against decomposition. The kinetic model is in line with the mechanism that suggests that the direct formation of hydrogen peroxide from hydrogen and oxygen proceeds through hydrogen adsorption, pairwise dissociation, but not spill-over of H-species over the bimetallic AuPd surface as commonly observed with Pd catalysts. Peroxide concentration values predicted by an overall kinetic model and values experimentally measured at the outlet of the microchannel with a catalytic layer deposited on the wall are in good agreement. The final part of the thesis discusses the effect of organic solvents on the direct synthesis reaction and the corresponding yield improvements that can be obtained by carefully choosing a solvent/co-solvent mixture as the alternative liquid phase.

The concept developed in this thesis shows that it is possible to use safely high hydrogen and oxygen concentrations in a wall-coated microchannel reactor, resulting in both productivity and selectivity improvements and eliminates the need for high operating pressures required in conventional reactors. In addition, the peroxide concentrations achievable at the reactor outlet are in the range required for small-scale on-site on-demand applications.

Introduction

The direct synthesis of hydrogen peroxide



1

1.1. Direct synthesis vs. Anthraquinone autooxidation process

Hydrogen peroxide is one of the most widely used chemicals today with an annual market of around 370 kt (2013). From a chemical point of view, it is a green oxidant which donates oxygen giving water as the only by-product, while being more reactive and selective in comparison to molecular oxygen. Hydrogen peroxide is applied in textile, paper and pulp industry as a bleaching agent, as a disinfectant in pharmaceutical, food and cosmetic industry, oxidant in water treatment or selective oxidant in chemical synthesis ^[1,2]. Many of those applications are motivated by more stringent standards and legislations.

The state of the art process to produce hydrogen peroxide is two-stage cyclical anthraquinone auto-oxidation process (AO), which involves hydrogenation of anthraquinone working solution over a hydrogenation catalyst followed by the oxidation of the anthraquinone working solution giving the hydrogen peroxide in the organic phase (Fig. 1.1). The major disadvantages of the AO process are its complexity and the waste

generation caused by accumulation of permanently hydrogenated alkyanthraquinone products hydroanthrahydroquinones, oxantrones and anthrones [3]. The hydrogen peroxide generated in working solution is further extracted using a water phase and distilled in order to generate the desired peroxide content. In order to be economically viable, the process needs to run on a large scale of at least 40kt/year for each production unit. The world's largest plants situated in Antwerp and Thailand are designed to produce 230 and 330 kt/year of hydrogen peroxide respectively. The productivity of the AO process is expressed per amount of the working solution applied and ranges between 7-15 g_{H₂O₂}/kg of working solution (Fig. 1.2). Besides the complexity of such a large scale process, the transportation of concentrated peroxide solutions to the customer sites requires special precautions related to the safety. Eventually, the various applications of hydrogen peroxide on a customer site require a concentration in a range of 1-10 wt%. Standard grades of hydrogen peroxide, typically used for bleaching and other industrial processes, contain sufficient stabilizers to keep decomposition under control in a wide variety of applications. In some applications, special grades are required which contain significantly lower concentrations of stabilizers. Grades required for chemical synthesis often need to contain less stabilizing compounds, which could interfere with synthetic reactions. High(er) purity grades are also applied in aseptic packaging, food industry, water treatment and electronics. Stabilizers added typically involve metal chelating agents and colloids including stannates, pyrophosphates and organophosphonates.

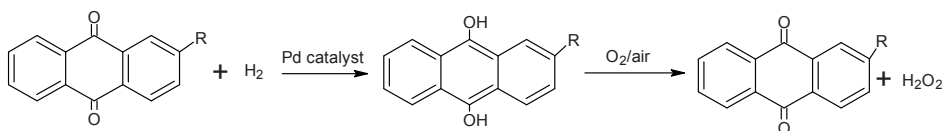


Figure 1.1. Hydrogen peroxide synthesis through hydrogenation of alkyanthraquinone and oxidation of corresponding hydroquinone.

Special safety measures are required during hydrogen peroxide storage at the customer site. Storage tanks and associated piping need to be equipped with relief devices to ensure safety in case of pressure build-up as a consequence of peroxide decomposition. Storage of solutions at temperatures higher than 20 °C can accelerate decomposition. In general, elevated temperatures of storage vessels along with the persistent bubbling is an indication of rapid peroxide decomposition. If the cooling of the tank is insufficient and temperature exceeds 40°C, the peroxide solution stored needs to be diluted and/or disposed. Due to safety risks associated with both storage and transportation of hydrogen peroxide, the necessity for operating the process on a small-to-medium scale (2-10 kt/year) has been recognized [4]. Such a process needs to be performed in a compact

Chapter 1: Introduction

closed modular plant with catalyst and/or working solution regeneration/replacement frequency not shorter than 3 months. A mini-plant based on the current AO process is typically configured not to be equipped with the regeneration unit for the working solution ^[4], to reduce its complexity. The working solution is intended to be replaced periodically by a fresh working solution and/or by a refreshed working solution which was withdrawn from the reactor. In addition, a mini-plant might be equipped with alumina beds to control the acidity of the working solution. A requirement that this modular unit needs to fulfill is fast start-up and fast shut-down. For the hydrogenation step of the AO process a palladium or palladium/silver catalyst is used, in the form of a fixed-bed or suspended catalyst. Hydrogen fed to the system is often diluted allowing easier control over the hydrodynamic/flow regime in the reactor. 30-80% of total hydrogen fed is intended to be converted. Hydrogen peroxide extraction is performed using deionized water, which contains additives for stabilizing hydrogen peroxide, for adjusting the pH and/or for corrosion protection.

The direct synthesis of hydrogen peroxide is a green alternative to the current Anthraquinone autoxidation (AO) process (Fig. 1.3). Besides the green label, the direct synthesis route has been of interest for many years because of potential capital savings, mainly when integrated with the production of chemical intermediates. The economic justification to commercialize the direct synthesis reaction is based on small-scale on-site production ^[5]. Still, despite a vast amount of literature available on the direct synthesis reaction and announcements of pilot plants successfully running, the latest of which reported by Degussa in 2009, no commercial process is available yet. The major challenges associated with the direct synthesis of hydrogen peroxide (DS) are the explosiveness of the hydrogen-oxygen mixtures over a very wide range of concentrations (4-96%) and the poor selectivity towards hydrogen peroxide as the desired product. To achieve a high selectivity towards peroxide, it is necessary to design the catalyst that favors direct synthesis reaction over the thermodynamically preferred direct formation of water from H₂ and O₂. In addition, the catalyst should catalyze as little as possible further transformation of peroxide to water through hydrogenation and the decomposition reaction.

The direct synthesis is a three-phase process which involves a H₂-O₂ mixture as gas-phase, a solvent and the solid catalyst phase. The role of the liquid phase used is to collect and solubilize the hydrogen peroxide formed, since pure hydrogen peroxide is highly unstable

The direct synthesis of hydrogen peroxide

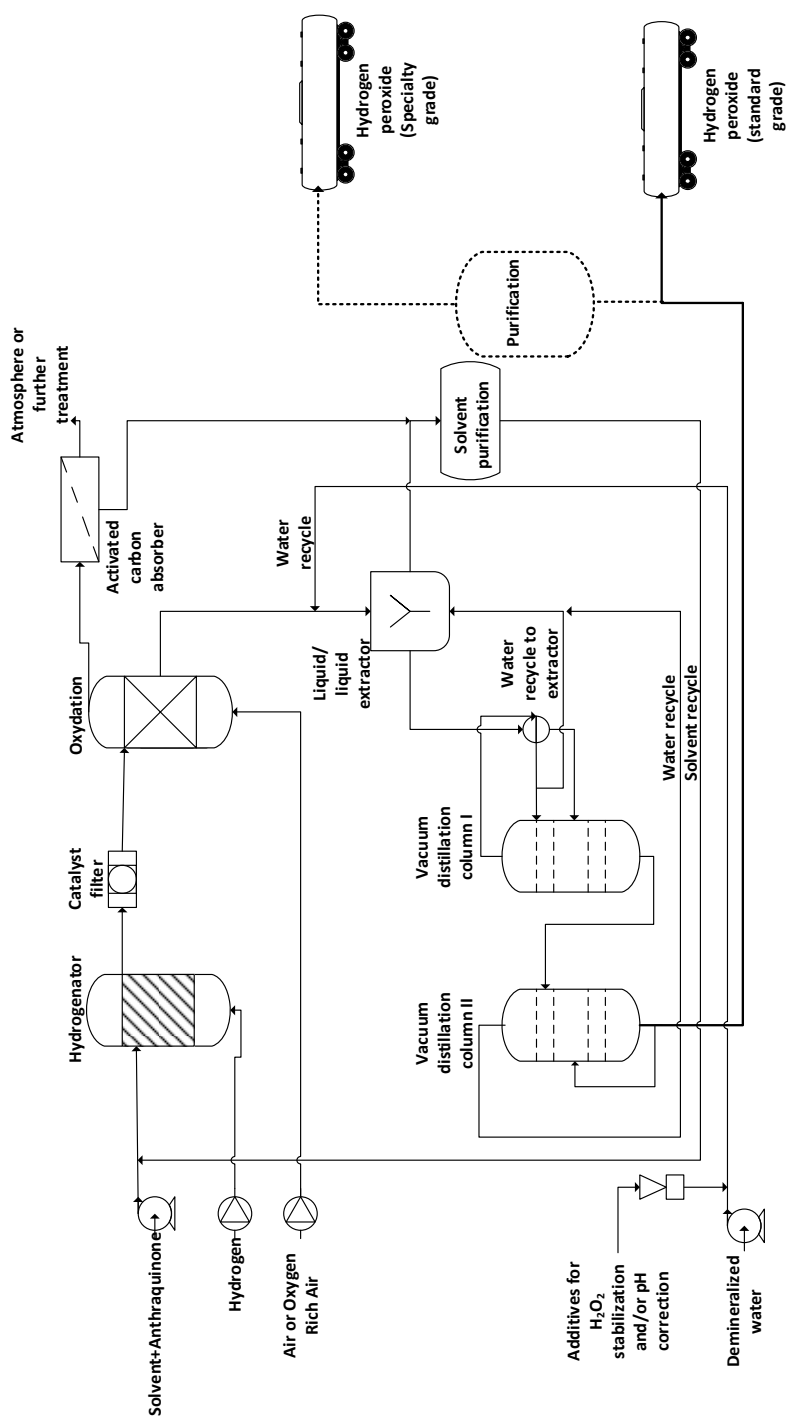


Figure 1.2. Scheme of the Anthraquinone auto-oxidation process (AO) [3,4].

Chapter 1: Introduction

peroxide, the necessity for operating the process on a small-to-medium scale (2-10 kt/year) has been recognized ^[4]. Such a process needs to be performed in a compact closed modular plant with catalyst and/or working solution regeneration/replacement frequency not shorter than 3 months. A mini-plant based on the current AO process is typically configured not to be equipped with the regeneration unit for the working solution ^[4], to reduce its complexity. The working solution is intended to be replaced periodically by a fresh working solution and/or by a refreshed working solution which was withdrawn from the reactor. In addition, a mini-plant might be equipped with alumina beds to control the acidity of the working solution. A requirement that this modular unit needs to fulfill is fast start-up and fast shut-down. For the hydrogenation step of the AO process a palladium or palladium/silver catalyst is used, in the form of a fixed-bed or suspended catalyst. Hydrogen fed to the system is often diluted allowing easier control over the hydrodynamic/flow regime in the reactor. 30-80% of total hydrogen fed is intended to be converted. Hydrogen peroxide extraction is performed using deionized water, which contains additives for stabilizing hydrogen peroxide, for adjusting the pH and/or for corrosion protection.

The direct synthesis of hydrogen peroxide is a green alternative to the current Anthraquinone autoxidation (AO) process (Fig. 1.3). Besides the green label, the direct synthesis route has been of interest for many years because of potential capital savings, mainly when integrated with the production of chemical intermediates. The economic justification to commercialize the direct synthesis reaction is based on small-scale on-site production ^[5]. Still, despite a vast amount of literature available on the direct synthesis reaction and announcements of pilot plants successfully running, the latest of which reported by Degussa in 2009, no commercial process is available yet. The major challenges associated with the direct synthesis of hydrogen peroxide (DS) are the explosiveness of the hydrogen-oxygen mixtures over a very wide range of concentrations (4-96%) and the poor selectivity towards hydrogen peroxide as the desired product. To achieve a high selectivity towards peroxide, it is necessary to design the catalyst that favors direct synthesis reaction over the thermodynamically preferred direct formation of water from H₂ and O₂. In addition, the catalyst should catalyze as little as possible further transformation of peroxide to water through hydrogenation and the decomposition reaction.

The direct synthesis is a three-phase process which involves a H₂-O₂ mixture as gas-phase, a solvent and the solid catalyst phase. The role of the liquid phase used is to collect and solubilize the hydrogen peroxide formed, since pure hydrogen peroxide is highly unstable

and decomposes to water and oxygen. Water is most often applied as a solvent in the direct synthesis considering that it is non-flammable and non-toxic, allowing for the safest operation.

Besides water, short chain alcohols or mixtures of alcohols and water are typically used in direct synthesis as a liquid phase. In a recent review on direct synthesis, García-Serna et al.^[5] discuss the economics of AO and DS process, concluding that the DS process can compete with the AO process only if it is able to reduce CAPEX by avoiding typically applied concentration steps in AO process (extraction, distillation) and produce hydrogen peroxide solutions directly in a concentrations required for further application. It was estimated that a H₂O₂ concentration required would be 15 wt% of H₂O₂ in case of aqueous solutions and 9 wt% for methanol/alcohol solutions. They further emphasize that the reactor technology needs to provide high conversions (>99%) with a selectivity over 20 %.

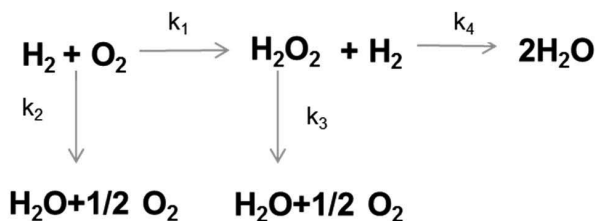


Figure 1.3. Scheme of the direct synthesis from hydrogen and oxygen.

1.2. Catalyst

Catalysts applied in direct synthesis typically involve noble-metals Au, Pd, Pt, Ag^[6-13]. The activity of Ru, Rh or Cu was also tested in the direct synthesis reaction^[14] however the productivities achieved were well below the values observed with Pd, Pt or Au. Generally speaking, the direct comparison of the catalytic performance between different papers and patents is very difficult, considering that the reaction conditions applied, including temperatures, pressures, presence or absence of promoters, solvents, gas-phase composition, flow rates, reactor types vary from case to case. Still, some general trends can be identified. Since the first patent on the direct synthesis reaction in 1914^[15] until 2002^[7], Palladium has been recognized as the best catalyst for direct conversion of H₂ and O₂ to H₂O₂. Addition or alloying of Pd with Au or Pt seems to significantly improve the Pd performance in the direct synthesis. Early theoretical studies on the energetics of the direct synthesis reaction indicated that Au might be even more active in the direct synthesis than Pt or Pd owing to the high stability of the hydroperoxide species formed on

Chapter 1: Introduction

the Au surface ^[16]. Nevertheless, the extensive research done by Hutchings et al. shows that gold catalysts alone are significantly less active than palladium, while Au-Pd alloys exhibit much higher activities and selectivity in comparison to their monometallic analogues ^[17]. The most simplistic explanation of the role of Au added to Pd in this kind of bimetallic catalyst is to “dilute” the Pd surface and to isolate Pd sites. It is believed that significant isolation of Pd sites in bimetallic alloy catalyst prevents O₂ dissociation and increases the selectivity towards the peroxide ^[18]. On the other hand, the majority of the recently reported industrial research on direct synthesis catalysts with emphasis on Degussa, mainly relies on Pd or Pd/Pt alloys. In fact, the series of patents issued between 2005-2012 ^{[10-13][19]} and assumingly related to announcement of an integrated pilot plant for the PO production from propylene and directly synthesized hydrogen peroxide deals with a nano Pt/Pd catalyst with a crystal face exposure of FCC 110 or 111 ^[11]. The experimental investigation of the effect of Pd alloying with Pt or Au is accompanied with theoretical DFT calculations ^[20,21]. According to Todorovic et al. non-selective formation of water is caused by O₂ dissociation on Pt, OOH dissociation on Pt and H₂O₂ decomposition on Au surfaces ^[20]. Still, the experimentally observed selectivity for a certain Au-Pd catalyst could have not been explained on the bases of the calculated barriers for the involved reaction steps. Li et al. suggested that less active gold atoms on the Au-Pd surface weaken the interaction of H₂O₂ with the metal surface suppressing the decomposition and facilitating the desorption of peroxide from the catalyst surface ^[21].

For the direct synthesis reaction, supported catalysts tend to be preferred due to the ease of separation especially when considering larger scale processes. The tremendous effect that the support has on the selectivity towards the peroxide has been supported by at least two direct studies on the influence of the nature of the support on the direct synthesis and side reactions when catalyzed by Au-Pd, Au or Pd ^[22,23]. Although reported productivity values for some supports tend to deviate a bit among the two references, the general trend observed is that supports with a lower isoelectric point show a better performance in direct synthesis, which is especially obvious in case of Au-Pd catalyst. This is in relation with the fact that some supports are very active in hydrogenating or decomposing hydrogen peroxide. MgO as a support with a high isoelectric point exhibits very high hydrogenation and decomposition rates (817 and 535 mol/kg^h respectively), while carbon is the least active in catalyzing side reactions that consume peroxide formed (117 and 41 mol/kg^h respectively). In addition, it has been reported that a treatment of the support with acids can further improve the overall Au-Pd catalyst performance in direct synthesis ^[9,24]. While nitric or acetic acid support treatment results in higher activity and selectivity towards peroxide, treatment with HCl seems to be detrimental, at least in

case of Au-Pd supported on carbon. Contrary to the expectations, the same effect is not evident for Au and Pd monometallic catalysts supported on carbon.

The most important parameter that might influence the catalytic activity of Pd or Au-Pd bimetallic catalysts is the oxidation state of the palladium under reaction conditions, considering the presence of both reductive and oxidative species in the direct synthesis. It is well known that the oxidation state of Pd catalysts switches between metallic and oxide depending on the temperature and oxygen concentration. The oxidation state of palladium and its influence on the direct synthesis reaction is still under discussion. Some studies suggest that the catalytic activity achieved with PdO is much higher in comparison to Pd⁰ [25], which might be associated with lower hydrogenation/decomposition rates when compared to their metallic analogues [26], while some authors made a contradictory conclusion that metallic palladium is responsible for the high activity and selectivity [27,28]. Choudhary et al. associated the drop of the H₂ conversion and H₂O₂ selectivity with reaction time to surface/subsurface oxide formation as a consequence of the Pd⁰ oxidation with the H₂O₂ formed [29], despite the fact that they earlier reported lower hydrogenation and decomposition H₂O₂ rates on PdO [26]. In addition, some authors associated elution of Pd from the support material and reactor to PdO formation under reaction conditions and its dissolution in acidic liquid medium [30]. Knowing that long-term stability of the catalyst can be affected by the catalyst oxidation state, the questions regarding the presence of oxide phase, conditions under which PdO is formed and its influence on the catalyst activity or potentially deactivation or leaching are becoming even more significant.

1.3. Role of promoters

The side reactions involved in the consumption of hydrogen peroxide and water formation can be inhibited to certain extent by adding acid and/ or halogen as promoters. Typically, acids such as HNO₃, H₂SO₄, HCl, HBr, H₃PO₄ are added directly in the liquid phase. Nevertheless, solid acids also proved to be equally efficient. Blanco-Brieva et al. performed the direct synthesis reaction in methanol using a palladium catalyst supported on sulfonic acid-functionalized silica [31]. With the liquid phase containing additionally maximum of 24 ppm HBr, the selectivity achieved was over 80 % (for 0.5 % peroxide solution), meaning that the solid-acid is also able to prevent peroxide transformation to water. Moreover, treatment of a carbon or silica support with HNO₃ before the deposition of the metal component of the catalyst leads to reduction in side reaction rates resulting in a higher selectivity^[9].

The effect of acid addition on the direct peroxide synthesis yield was initially observed by Prospelova [32,33]. After addition of a mineral acid such as HCl, the hydrogen peroxide

Chapter 1: Introduction

decomposition over Pd catalyst was suppressed. The explanation of the acid role was also given by the same author, who suggested that protons from the acid prevent dissociation of H_2O_2 which is structurally an acid. It is assumed that decomposition of hydrogen peroxide proceeds through the formation of HO_2^- species. Accumulation of H^+ ions on the Pd surface in the form of a unique layer hinders both the penetration of HO_2^- and decomposition of hydrogen peroxide. Even the specification of commercially available standard grades of hydrogen peroxide, emphasizes that standard grades are acidic solutions with the pH range of 0.7-2.2 depending on the peroxide content ^[34]. This is necessary in order to ensure a long stability of hydrogen peroxide solutions. Metal chelating agents are not sufficient stabilizers to ensure stability of peroxide solutions.

The role of acid was confirmed in many subsequent publications. In fact, studies were performed in order to compare the effects of different mineral acids. It has been confirmed that besides the proton, the associated anion of the mineral acids also has an influence on observed reaction rate and selectivity. Typically non-coordinating anions, such as sulfate, phosphate, nitrate, etc., are assumed not to block catalytically active sites in the direct synthesis ^{[35][36]}, while coordinating anions, such as chloride, bromide and iodide are responsible for catalyst poisoning ^[37].

Next to the enhancement of selectivity, the addition of acid might also play a role in the long-term catalyst stability ^[5]. There are reports in the literature that suggest that addition of acid might cause a leaching of active metal from catalyst support. Namely, Choudhry et al. ^[33] emphasized that phosphoric acid is the most convenient for direct synthesis reaction due to low corrosiveness, lowest palladium leaching rate and additionally, stabilizing effect of phosphate anion. One of the ways to acidify the aqueous medium without introduction of mineral acid is the application of CO_2 (instead of N_2) as a diluent gas at high pressure. Upon the dissolution in water, carbonic acid is formed. This process is pressure dependent, meaning that after depressurization acid is removed from the solution. The promotional effect of CO_2 gas as a diluent in the direct synthesis has been proven for the Au-Pd catalyst ^[39], while the addition of phosphoric acid seemed to be deteriorating due to inhibiting effect of phosphate anion at given concentration. In a later publication it was shown that the optimum pH in case of Au-Pd/C is around 2, while in case of Au-Pd/MgO the optimum pH in terms of hydrogen peroxide productivity lies well below 1 ^[40]. The general rule introduced is that the reaction should be operated at a pH equal or lower than the isoelectric point of the support applied.

Besides the acid, the liquid medium used in direct synthesis of hydrogen peroxide contains halogen ions in relatively small concentrations. It has been demonstrated through a

number of publications that its additions hinders the metal catalyzed decomposition of hydrogen peroxide ^[6]. The promoting effect of bromide reflected through the selectivity improvement is consistent with selective catalyst poisoning via blockage of highly active sites on the catalyst surface responsible for dissociative adsorption of O₂ and re-adsorption/dissociation of H₂O₂^[41]. Liu et al. ^[28] showed that Br ions are much more effective than Cl, presumably due to a stronger bromide interaction with palladium. The advantage of bromide is reflected in an inhibition of palladium leaching from the support ^[28]. Interestingly, among the halides fluoride ions proved not to be effective in direct synthesis for selectivity improvement, while iodide seems to strongly poison the catalyst, resulting in complete catalyst deactivation. It needs to be emphasized that chloride and bromide anions exhibit the promoting effect only in the presence of protons ^[37]. Besides the suppression of hydrogen peroxide decomposition, it has been documented that Br ions, depending on the concentration, can reduce the rate of the peroxide reduction with H₂ ^[42]. However, the curiosity is that a fluoride anion is acting as a promoter of hydrogen peroxide decomposition when a reduced palladium catalyst is used ^[37]. Combinations of two different halogen ions might have a synergistic effect on the promoting direct synthesis over side reactions ^[43]. It is interesting to notice that a combination of F and I ions is not deactivating the catalyst, but moreover increases the selectivity. Still, the highest selectivity is observed when combining Cl with Br or I ^[43].

Many authors tend to believe that Pd alloying with a second metal such as platinum or gold has a similar effect as halogen ions in liquid medium, increasing the selectivity towards hydrogen peroxide. The promotional effect of bromide was proven in case of Au-Pd catalyst as well. Carbon and MgO supported Au-Pd catalysts pretreated with solutions of NaBr in small concentrations (0.00034–0.044 wt%) showed an enhancement in the peroxide yield during the direct synthesis ascribed to the poisoning effect of hydrogenation and decomposition catalytic sites ^[44]. This effect was more pronounced in case of a MgO supported catalyst. Higher NaBr loadings (0.5-8.3 wt%) proved to be detrimental. Still, the findings made are sometimes unclear and contradictory considering that in some earlier publications authors claim that there are detrimental effects of NaBr in the solution at concentrations as low as 6 ppm ^[39]. Those findings for Au-Pd catalysts correspond to findings of Samanta et al. for a Pd-catalyst ^[42]. They also reported an optimum bromide loading onto the catalyst of up to 1wt%, based on reduction in decomposition rate and increase in hydrogen peroxide yield. At higher bromide loadings the hydrogen conversion is dropping significantly, which is probably the consequence of non-selective poisoning of catalytic sites. Considering that the Au atoms present 'dilute' the Pd surface, it is reasonable to assume that due to a lower number of higher energy sites less bromide will be required to promote the direct formation of hydrogen peroxide

Chapter 1: Introduction

over decomposition and/or hydrogenation. It is important to stress that the promotional effect of Br is much more pronounced in case of a MgO supported catalyst in comparison to carbon. This means that with choosing the more suitable support or tuning the properties of the support, the addition of bromides can be avoided, which further results in a lower environmental impact and lower corrosiveness of liquid medium.

1.4. Solvent

The direct synthesis is a three-phase process which involves a H₂-O₂ mixture as gas-phase, a solvent and the solid catalyst phase. The role of the liquid phase used is to collect and solubilize the hydrogen peroxide formed, since pure hydrogen peroxide is highly unstable and decomposes to water and oxygen on the catalyst surface. Besides water, short chain alcohols or mixtures of alcohols and water are typically used in the direct synthesis as a liquid phase. Water is most often applied as a solvent in the direct synthesis considering that it is non-flammable and non-toxic, allowing the safest operation. However, it has been reported that organic solvents such as methanol, ethanol or acetone show a far better performance in direct synthesis [27,45]. The low solubility of reacting gases in the water phase in comparison to organic media is most often emphasized as the motivation to employ alcohols as solvents or co-solvents in the direct synthesis [28,41,46]. Krishnan et al. ascribed the higher concentration of H₂O₂ in acetone or methanol compared to water to a higher mass transfer mainly on gas-liquid interface, which they identify as the rate determining step [45]. The strong positive halide effect on the direct synthesis only in case of synthesis in an aqueous phase in contrast to organic solvents was underlined. In their calculation, authors showed that the mass transfer rate was 15 times higher in methanol than in water mainly due to the higher H₂ solubility. Still, when initial reaction rates observed in methanol and water with halides present are compared, the values seemed to be almost identical, meaning that the liquid film mass transfer does not play a crucial role after all. Certainly, the difference in the H₂ solubility in the liquid phase (O₂ is typically an order of magnitude more soluble than H₂ and thereby less likely to be limiting) in water and certain organic solvent might be crucial in achieving higher reaction rates. Addition of toluene and hexane, solvents which are known to increase the solubility of the reactants in comparison to pure water, proved not to be efficient in the direct synthesis reaction despite high conversions achieved [27], due to poor selectivity. In general, water miscible solvents such as different alcohols and acetone are identified as effective solvents for the direct synthesis in several industrial patents [47,48]. Alcohols are suitable solvents for the direct synthesis from the aspect of on-site application in epoxidation reactions as well [48].

Besides for epoxidations, hydrogen peroxide can also be used as an oxidant in a number of oxidation reactions involving different organic substrates, often water non-soluble.

As already emphasized in the introduction, the economic analysis presented in the recent review by García-Serna et al. suggests that H₂O₂ at the reactor outlet needs to reach a min of 15 wt% in case of an aqueous solution and 9 wt% in methanol ^[5] for the direct synthesis process to be competitive with AO process. Clearly, from an economical point of view methanol is a preferred solvent over water, considering that lower peroxide concentrations need to be directly generated in comparison to water. Advantageously, the reaction rates typically observed in methanol are much higher compared to in water, meaning that the targeted concentration can be achieved with lower amount of catalyst used. If required, a further downstream concentration of hydrogen peroxide solutions by means of distillation/vacuum distillation is less energy consuming in a methanol solution in comparison to in water.

1.5. Reactor concepts

Direct synthesis of hydrogen peroxide from its elements in a multiphase reaction involving liquid, gas and solid phase is typically studied in agitated vessels both in semi-batch^{[49][50]} or batch mode ^[51], fixed-bed reactors or trickle-beds ^[52–54] or slurry bubble columns ^[45,48]. Agitated vessels with the catalyst suspended in the form of powder in the liquid phase are successfully applied to study the catalyst performance or kinetics of the reaction. This type of vessels is particularly convenient considering that it allows to control the degree of mixing by adjusting the stirrer speed, and proper heat control. Applying the catalyst in the form of powder means it is possible to manipulate the particle size, which in combination with proper mixing, ensures that reaction can be done outside mass transfer limited regime. The advantage of the semi-batch operation is that pressure and the composition of the gas phase can be maintained constant, while only concentration of the peroxide in the liquid phase changes over time. Typically, under such conditions small amounts of peroxide are produced (except when higher amounts of catalyst are applied in combination with small liquid volumes), which results in lower rates of side reaction (hydrogenation and/or decomposition). When packed-bed or fixed-bed reactors are applied, it is necessary to pay attention to a proper catalyst dilution and a uniform bed packaging. By avoiding flow maldistribution, the potential formation of hot spots is avoided ^[53,55].

For a larger scale application of the direct synthesis reaction, fixed-bed reactors or slurry bubble columns represent more attractive options that allow for a continuous operation. In a series of patents ^[10,19,48] the direct synthesis reaction was performed in slurry bubble columns. This is not surprising if one has in mind that this type of reactor provides intense

Chapter 1: Introduction

agitation by bubbling, therefore efficient heat removal minimizing any possibility of hotspot formation or runaway reactions. However, besides the necessary catalyst separation, in order to achieve higher peroxide concentrations in the liquid phase, long residence times for the liquid phase might be required. Fixed-bed reactors are widely used in chemical industry in large scale heterogeneously catalyzed processes. They provide high surface area of solid catalyst, enabling high reaction rates per volume of the reactor. As already mentioned earlier, attention has to be paid on the hot spot formation especially if the trickle bed has dry spots to prevent possible runaways to occur, since heat removal might be a serious issue.

The important consideration that needs to be taken into account when operating those conventional reactor types is the flammability limit, which is defined as the range of concentrations of H₂ and O₂ in which flame propagation occurs. The lower flammability limit for hydrogen is typically around 4 vol%. This means that in order to operate the process safely, the reactive gas mixtures need to contain large excess of inert gas as a diluent. Reaction rates as a consequence of dilution will be lower. To compensate for the dilution, high total pressures have to be applied, which consequently increases the capital and operational costs. Typical pressures applied in such conventional reactors go up to 100 bar. Novel reactor concepts such as microreactors or membrane reactors overcome this problem. Due to extensively reduced dimensions in case of microreactors or selective feeding of one of the reacting gases in case of membrane reactors, conventionally explosive hydrogen and oxygen mixtures can be applied safely in the direct synthesis reaction. Membranes particularly attract a lot of attention considering that hydrogen and oxygen mixtures are mechanically separated. A Pd-Ag layer ^[56,56] or Pd-Pt ^[57,58] active catalytic layer is coated onto a ceramic membrane. Hydrogen diffuses through the membrane, dissociates on the catalyst surface and reacts with oxygen in the liquid phase. The reaction rate in this case is mainly limited by the hydrogen diffusion, which is rather poor. This can be improved by applying a thinner layer of palladium, but this can result in membrane mechanical failure.

The selectivity for hydrogen peroxide formation obtained in case of Ag-Pd membranes can be improved by coating the outer surface with pure Pd, or with a layer of hydrophobic polymer ^[56,56]. Hydrogen peroxide formed on the catalyst is repelled from hydrophobic surface, preventing its decomposition. Still, the major drawback associated with those membranes is the long term stability of these metallic films, despite improvements obtained in case of palladium alloying with metals such as Ag or Pt. The permeability of the membrane, and therefore reaction rates can be improved by applying higher

differential pressures. Pashkova et al. ^[59] showed that an increase in total pressure indeed leads to higher reaction rates, however the increase in differential pressure contrary to the expectation did not result in a higher reaction rate. . This unexpected finding was explained by lower thickness of liquid filled region and decrease in amount of Pd catalyzing the reaction as a consequence of increase in differential pressure. Therefore the increase in H₂ mass transfer rate is negatively compensated/ penalized with less catalyst participating in the reaction. The curiosity is that in this paper instead of thick dense Pd film, the authors deposited Pd nanoparticles inside the pores of the top layer of tubular membrane as a catalyst. The results achieved with methanol as a solvent show 7 times higher reactions rates in comparison to using water as solvent. Typically, the pressure of the gas phase as high as 6.9 MPa was applied.

1.5.1. Microreactors and the direct synthesis

The application of the microreactor concept into the direct synthesis reaction offers an opportunity to safely handle hydrogen and oxygen mixtures which would be explosive in conventional reactors. Potential safety concerns related to use of conventionally explosive hydrogen and oxygen mixtures in a wall-coated microchannel are discussed in detail by Chattopadhyay and Veser ^[60]. Generally, the safety of this reaction in a wall-coated microchannel is influenced by the combination of the temperature and pressure applied. Upon addition of the catalyst, the ignition point is shifted towards lower temperatures. Both the homogeneous high temperature dominated and the heterogeneous catalyst initiated ignition branch were taken into account. Simulations showed that a reactor diameter of 300 μm can be considered intrinsically safe (temperature independent) at 1 bar pressure. With increasing pressure in the system, the homogeneous reactions tend to accelerate, scaling with the square of reactor pressure, due to the dominance of bimolecular collisions, in contrast to surface reactions, which show linear dependence on pressure. However, at higher pressures, the surface reactions will be limited by diffusion of reacting species from the bulk face to catalytic surface, considering that $D \sim P^{-1}$. This means that consumption of reactants is accelerated near the catalytic wall, but delayed in the bulk phase. Chattopadhyay and Veser clearly show that for pressures as high as 10 bar, even in case of extremely small reactor diameters, ignition is dominated by the homogeneous reaction pathway. To operate a wall-coated catalytic reactor safely at higher pressures, it is crucial to stay below the critical ignition temperature, below which homogeneous ignition (explosion) can no longer occur for the desired channel diameter. Performing the reaction in a two phase gas–liquid flow additionally diminishes the possibility for radical or/and hot-spot formation. The liquid separates the gas in small bubbles and acts as a large heat sink. This positive general rule, that increase in pressure reduces flammability interval has been introduced by Piqueras et al. ^[61].

Chapter 1: Introduction

UOP announced in 2006 that they successfully demonstrated the use of microreactor technology in the direct synthesis of hydrogen peroxide achieving 75% selectivity at 80% conversion at $H_2:O_2$ ratio of 1:1 in methanol as a solvent.^[62] Later publications^[63] gave indications of the UOP process conditions; a pressure of 20 bars was applied instead of 100 bar required in conventional batch-type reactors, a selectivity as high as 85% was reached at 90% conversion at $H_2:O_2$ ratio of 1.5-3, with a space-time yield of $2 \text{ g}_{H_2O_2}/\text{g}_{cat}\cdot\text{h}$. Those laboratory tests were followed by pilot scale testing and basic engineering design for hydrogen peroxide production of 150 kt/year, as an demonstration example that microreactor technology is not only limited to a small scale, however the fate of this project is not known up to date.

A catalytic microreactor for direct synthesis can be realized as packed-bed column^[30,64-67], or the catalyst can be immobilized on the walls of the microchannel^[68-71]. Certainly, the most convenient route to incorporate the catalyst inside the microchannel and perform the direct synthesis reaction is to create a micro-packed bed. Inoue et al. published several papers applying micro packed-beds in the direct synthesis reaction^[30,65-67]. The major challenges associated with micro packed-beds were the high-pressure drop^[30,67] and poor catalyst wetting and contacting^[72]. Attention has to be paid on proper packing of the catalytic bed. Namely, due to the high catalyst concentration within the packed bed, a proper dilution of the catalyst bed with inert material as well as contacting of the catalyst with the liquid phase and wetting efficiency is critical to avoid high local heat generation and formation of hotspots. Inoue et al. reported that despite the small dimensions of glass chips applied in direct synthesis, explosions were still occurring if catalyst was maldistributed within reactor channels during packaging procedure^[30,67]. In the same publication, they reported the erosion of the catalytic bed and palladium elution within the first 48 h of operation most probably due to oxidative reaction conditions. The importance of a proper design of the gas and liquid inlet to ensure a proper gas-liquid flow distribution was stressed. The sizes of gas and liquid inlet channels need to be adjusted in such a way that the gas phase pressure drop is countered/compensated with increasing its superficial velocity, considering that liquid is typically 1000 times more viscous than gas. The flow regime observed is recognized as trickling flow regime. Recently, Inoue et al. reported that concentrations of hydrogen peroxide achieved over a Au-Pd/TiO₂ catalyst can reach as high as 11 wt% (at total gas flow rate 40 ccm (normal conditions) and liquid flow rate 0.01 ml/min) with a selectivity of around 20 %, which is tremendous improvement to initial 1 wt%^[66]. In addition, reaction was done in multichannel microreactor (8 parallel channels) with addition of sulfuric, phosphoric acid and NaBr as promoters. In comparison to Pd catalyst (Pd/Al₂O₃ and Pd/TiO₂) that showed palladium

loss with time as a consequence of PdO formation and elution under acidic conditions, the Au-Pd catalyst showed a stable performance over 100 h operation. This work is relying on the previously published study on the numbering up of micro packed-bed microchannels (4 in parallel) by introduction of microstructures in the upstream side of the channels that generates the pressure drop, which ensures proper gas-liquid flow distribution [65].

In the group of Voloshin et al. from Stevens Institute of Technology, micro-packed bed microreactors were successfully implemented to study the kinetics of the direct synthesis reaction [64,73,74]. Side reactions competing with direct synthesis, hydrogenation [74] and decomposition [73] were isolated and studied and modeled separately in order to obtain an overall kinetic model. Gas flow rates were kept high, 22 mL/min, with a liquid flow rate of 0.05 ml/min and residence times as low as 1.1 s. The flow regime observed was defined as slug flow (the liquid slugs continuously broken up by catalyst particles with long mist-like tails following the liquid slugs). The aqueous phase hydrogen peroxide was stabilized with addition of 1 wt% sulfuric acid and 10 ppm NaBr, which proved to block entirely decomposition of hydrogen peroxide formed [73]. The productivity values for Pd/SiO₂ catalyst prepared by sol-gel technique reached almost 4 mol_{H₂O₂}/g_{Pd}h under optimal conditions. The maximum hydrogen peroxide concentration reached in the liquid phase was approximately 1 wt%. High gas flow rates and high gas/liquid flow ratio ensures that flow pattern generated is consisting of alternating gas and liquid segments flowing over the catalyst. Segmented gas and liquid flow has been generated using a Teflon micromixer. However, no detailed study has been done on the flow pattern. An interesting observation made by authors while studying hydrogen peroxide hydrogenation and potential drawback in long-term application of such a catalyst was the partial catalyst deactivation after catalyst exposure to more concentrated solutions of hydrogen peroxide. The activity of the catalyst in this hydrogenation reaction dropped 3 times, after increasing the hydrogen peroxide concentration in the feed from approximately 0.5 to 3 wt% H₂O₂ solution, while the overall activity in direct synthesis reaction was 2 times lower after exposing the catalyst to a 3 wt% solution compared to initial value [74]. No new actions related to using this technology for the development of a new process have been reported after the latest publication in 2010.

The major advantages of microreactor application in multiphase reactions are the fast heat and mass transfer rates. It is well-known that in case of a reaction operated in Taylor flow in microchannels mass transfer of a gas component proceeds through following 3 steps: (1) From gas bubble directly to the solid catalyst through thin liquid film wetting the wall (gas-to-solid) (2) from the bubble caps to the liquid (gas-to-liquid) and (3) from the liquid to the catalyst for dissolved gas (liquid-to-solid). Mass transfer from gas-to-liquid and liquid-to-solid represent resistances in series and occur in parallel to mass transfer

Chapter 1: Introduction

directly from gas-to-solid. In case of a catalytic reaction occurring on the catalytic reactor wall, gas-to-solid mass transfer is the dominant step, often being considerably faster than the other two. Therefore, besides the advantage of the lower pressure drop that is expected if the catalyst is incorporated in a form of a wall-coated layer instead of a packed-bed, higher mass transfer rates can be achieved by utilization of the fast gas transfer through the thin liquid film layer between the wall and the gas bubble. In case of a micro-packed bed, no use is made of this fast gas-solid transfer step, since no Taylor flow is possible. For efficient catalyst usage, it is preferred to apply a thinner catalytic layer on the microchannel walls. Considering the fast mass gas to solid mass transfer rate (up to 100 s^{-1}), fast reaction can be often limited by slow diffusion of reactants through the thick catalytic layer. A thinner layer, on the other hand, lowers the catalyst hold-up, therefore an optimum thickness needs to be established balancing the amount of catalyst loaded per channel volume (catalyst layer thickness) and internal mass transfer limitations.

Maehara et al. introduced a compact system that consisted of a H_2 and O_2 generation unit and a microreactor for the direct formation of hydrogen peroxide [75]. Hydrogen and oxygen produced by water electrolysis in a flow through a solid polymer electrolyte (SPE) electrolyzer was supplied to the microreactor coated with Pd/C catalyst. The authors claim that the catalyst layer was coated on the wall by flushing the slurry of Pd/C catalyst and that the layer formed in such manner showed good adherence. Although this work represents an interesting approach from the point of compactness, the productivity achieved was not higher than approximately $0.02 \text{ mol}_{\text{H}_2\text{O}_2}/\text{g}_{\text{Pd}}\text{h}$. Wang et al. [69] reported reaction rates as high as $6.5 \text{ mol}_{\text{H}_2\text{O}_2}/\text{mol}_{\text{Pd}}\text{h}$ ($0.06 \text{ mol}_{\text{H}_2\text{O}_2}/\text{g}_{\text{Pd}}\text{h}$) over a heterogeneous zeolite supported Pd/Pt catalyst deposited on reactor wall at ambient pressure and at the highest liquid flow rate of 2 ml/h . The evaluated thickness of the wash-coat layer was around $100 \text{ }\mu\text{m}$. Kobayashi et al. [76] first introduced the method to deposit a colloidal solution of Pd encapsulated in copolymer micelles with polystyrene backbone on the walls of a microchannel creating thin layers covalently bonded to the glass surface and apply it in hydrogenation reaction. This approach was applied in the direct synthesis of hydrogen peroxide in the same group by Ng et al. [68] both in a single and a multichannel reactor system. However, the acidic conditions applied for the direct hydrogen peroxide synthesis are unfavorable for the stability of this kind of liquid film. The significant loss of catalytic activity was observed both in single and multichannel operation within first 10 h of the operation. It was reported that the wall-coated microchannel enabled sustainable production of 0.75 wt% of hydrogen peroxide in methanol (MeOH/HCl/KBr) this time, which corresponded to the productivity of $0.35 \text{ mol}_{\text{H}_2\text{O}_2}/\text{g}_{\text{Pd}}\text{h}$ for approximately 3 days, after which a drop in catalytic activity to 0.5 wt% was observed.

1.6. Objectives and outline

The objective of this thesis is the development and implementation of a three-phase capillary microreactor with a catalyst coated on the reactor walls in the direct synthesis of hydrogen peroxide. This technology should provide the basis for a modular unit for the production of hydrogen peroxide from its elements, combining directly hydrogen and oxygen. The microchannel size of 320 μm is chosen to allow for safe operation when using conventionally explosive hydrogen and oxygen mixtures. However, the prerequisite for a successful operation of such a unit with channels numbered-up is to be able to demonstrate the selective production of hydrogen peroxide in a single wall-coated channel. To achieve this, it is necessary to find a right combination of catalyst and reaction conditions.

The deposition of the catalyst on the reactor wall starts with the depositing of a support material. *Chapter 2* deals with methodologies used to coat channels with a support layer and challenges mainly associated with obtaining uniform and well adhered wash-coat layers. *Chapter 3* focuses further on the catalyst development suitable for the direct synthesis reaction and catalyst testing. The comparison of the reactor performance between the microchannel and the standard slurry system is done under conventionally non-explosive conditions. The benefits of the possibility to use concentrated hydrogen and oxygen mixtures safely in a microchannel are demonstrated.

In *Chapter 4* the suitable operating window was established for the direct synthesis reaction in a microchannel and to determine the range of concentrations of hydrogen peroxide that can be generated in liquid phase.

Chapter 5 is related to a detailed study of the overall kinetics of the hydrogen peroxide synthesis reaction in water as a liquid phase. In parallel to the direct synthesis of hydrogen peroxide, hydrogen peroxide decomposition and hydrogenation over a Au-Pd/SiO₂ catalyst are investigated in detail.

Chapter 6 focuses on understanding the catalyst performance in the presence of different solvents. Here we show that the solvent choice can have a tremendous influence on both conversion and selectivity towards hydrogen peroxide.

Finally, *Chapter 7* summarizes the results and discusses possibilities for further improvements.

Chapter 1: Introduction

References:

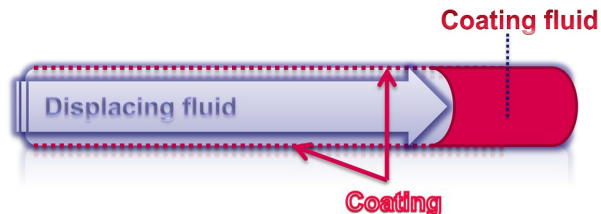
- [1] P. Bassler, H.-G. Goebbel, M. Weidenbach, *Chem. Eng. Trans.* **2010**, *21*, 571–576.
- [2] C. L. Hill, *Catal. Met. Complexes* **1992**, *9*, 253–280.
- [3] W. K. and O. W. G. Goor, *Ullmann's Encyclopedia of Industrial Chemistry*, , Vol. A13, Wiley-VCH Verlag GmbH & Co. KGaA, Weinheim, Germany, **1989**.
- [4] A. Willson, *Plant for Hydrogen Peroxide Production and a Process Using It*, **2013**, EP002639200A1.
- [5] J. García-Serna, T. Moreno, P. Biasi, M. J. Cocero, J.-P. Mikkola, T. O. Salmi, *Green Chem.* **2014**, *16*, 2320–2343.
- [6] C. Samanta, *Appl. Catal. A Gen.* **2008**, *350*, 133–149.
- [7] P. Landon, P. J. Collier, A. J. Papworth, C. J. Kiely, G. J. Hutchings, *Chem. Commun.* **2002**, 2058–2059.
- [8] P. Landon, P. J. Collier, A. F. Carley, D. Chadwick, A. J. Papworth, A. Burrows, C. J. Kiely, G. J. Hutchings, *Phys. Chem. Chem. Phys.* **2003**, *5*, 1917–1923.
- [9] J. K. Edwards, B. Solsona, E. N. N, A. F. Carley, A. Herzing, C. J. Kiely, G. J. Hutchings, *Science* **2009**, *323*, 1037–41.
- [10] M. Rueter, B. Zhou, S. Parasher, *Process for Direct Catalytic Hydrogen Peroxide Production*, **2006**, US 7144565.
- [11] Z. Zhihua, W. Zhihua, C. Zhang, B. Zhou, *Methods for Manufacturing Bi-Metallic Catalysts Having a Controlled Crystal Face Exposure*, **2008**, US 2008/0081017 A1.
- [12] Z. Zhou, Z. Wu, B. Zhou, *Methods for Manufacturing Supported Catalyst from a Porous Support and a Nanocatalyst Solution*, **2008**, US2008/0166288 A1.
- [13] Z. Wu, Z. Zhou, M. Rueter, B. Zhou, *Supported Nanocatalyst Particles Manufactured by Heating Complexed Catalyst Atoms*, **2008**, US2008/0193368 A1.
- [14] G. Li, J. Edwards, A. F. Carley, G. J. Hutchings, *Catal. Commun.* **2007**, *8*, 247–250.
- [15] H. Henkel, W. Weber, *Manufacture of Hydrogen Peroxide*, **1913**, US Patent 1108752.
- [16] P. P. Olivera, E. M. Patriito, H. Sellers, *Surf. Sci.* **1994**, *313*, 25–40.
- [17] J. K. Edwards, G. J. Hutchings, *Angew. Chem. Int. Ed. Engl.* **2008**, *47*, 9192–8.
- [18] F. Gao, D. W. Goodman, *Chem. Soc. Rev.* **2012**, *41*, 8009–20.
- [19] M. Rueter, *Direct Hydrogen Peroxide Production Using Staged Hydrogen Addition*, **2006**, US 7067103 B2.
- [20] R. Todorovic, R. J. Meyer, *Catal. Today* **2011**, *160*, 242–248.
- [21] J. Li, A. Staykov, T. Ishihara, K. Yoshizawa, *J. Phys. Chem. C* **2011**, *115*, 7392–7398.
- [22] E. Ntainjua N., J. K. Edwards, A. F. Carley, J. A. Lopez-Sanchez, J. A. Moulijn, A. A. Herzing, C. J. Kiely, G. J. Hutchings, *Green Chem.* **2008**, *10*, 1162–1169.
- [23] J. K. Edwards, A. Thomas, B. E. Solsona, P. Landon, A. F. Carley, G. J. Hutchings, *Catal. Today* **2007**, *122*, 397–402.

- [24] S. J. Freakley, M. Piccinini, J. K. Edwards, E. N. Ntainjua, J. A. Moulijn, G. J. Hutchings, *ACS Catal.* **2013**, *3*, 487–501.
- [25] S. Melada, R. Rioda, F. Menegazzo, F. Pinna, G. Strukul, *J. Catal.* **2006**, *239*, 422–430.
- [26] V. R. Choudhary, C. Samanta, P. Jana, *Appl. Catal. A Gen.* **2007**, *332*, 70–78.
- [27] R. Burch, P. R. Ellis, *Appl. Catal. B Environ.* **2003**, *42*, 203–211.
- [28] Q. Liu, J. H. Lunsford, *Appl. Catal. A Gen.* **2006**, *314*, 94–100.
- [29] V. R. Choudhary, Y. V Ingole, C. Samanta, P. Jana, *Ind. Eng. Chem. Res.* **2007**, 8566–8573.
- [30] T. Inoue, M. A. Schmidt, K. F. Jensen, *Ind. Eng. Chem. Res.* **2007**, *46*, 1153–1160.
- [31] G. Blanco-Brieva, M. P. de Frutos Escrig, J. M. Campos-Martin, J. L. G. Fierro, *Green Chem.* **2010**, *12*, 1163.
- [32] J. Lunsford, *J. Catal.* **2003**, *216*, 455–460.
- [33] T. A. Pospelova, N. I. Kobozev, *Russ. J. Phys. Chem.* **1961**, *35*, 584–587.
- [34] *INTEROX® Technical Grade, 35%, 50%, 70%, Technical Data Sheet, 2005.*
- [35] V. R. Choudhary, C. Samanta, P. Jana, *Appl. Catal. A Gen.* **2007**, *317*, 234–243.
- [36] V. R. Choudhary, C. Samanta, T. V. Choudhary, *Appl. Catal. A Gen.* **2006**, *308*, 128–133.
- [37] V. Choudhary, C. Samanta, *J. Catal.* **2006**, *238*, 28–38.
- [38] V. R. Choudhary, Y. V Ingole, C. Samanta, P. Jana, *Ind. Eng. Chem. Res.* **2007**, *46*, 8566–8573.
- [39] J. K. Edwards, A. Thomas, A. F. Carley, A. A. Herzing, C. J. Kiely, G. J. Hutchings, *Green Chem.* **2008**, *10*, 388.
- [40] E. Ntainjua N, M. Piccinini, J. C. Pritchard, J. K. Edwards, A. F. Carley, J. A. Moulijn, G. J. Hutchings, *ChemSusChem* **2009**, *2*, 575–80.
- [41] F. Menegazzo, P. Burti, M. Signoretto, M. Manzoli, S. Vankova, F. Boccuzzi, F. Pinna, G. Strukul, *J. Catal.* **2008**, *257*, 369–381.
- [42] C. Samanta, V. R. Choudhary, *Catal. Commun.* **2007**, *8*, 73–79.
- [43] V. Choudhary, P. Jana, *J. Catal.* **2007**, *246*, 434–439.
- [44] E. Ntainjua N., M. Piccinini, J. Pritchard, Q. He, J. Edwards, A. Carley, J. Moulijn, C. Kiely, G. Hutchings, *ChemCatChem* **2009**, *1*, 479–484.
- [45] V. V. Krishnan, A. G. Dokoutchaev, M. E. Thompson, *J. Catal.* **2000**, *196*, 366–374.
- [46] Y. Han, J. Lunsford, *J. Catal.* **2005**, *230*, 313–316.
- [47] G. Blanco-Brieva, M. M. J. Campos, J. L. Garcia Fierro, M. Argai Montiel, R. Garaffa, F. Janssens, *Patenten Process to Obtain Hydrogen Peroxide , and Catalyst Supports for the Same Process*, **2013**, WO 2013010835 A1.
- [48] T. Haas, R. Jahn, *Process for the Production of Hydrogen Peroxide*, **2008**, US 7364718.

Chapter 1: Introduction

- [49] F. Menegazzo, M. Signoretto, G. Frison, F. Pinna, G. Strukul, M. Manzoli, F. Boccuzzi, *J. Catal.* **2012**, *290*, 143–150.
- [50] T. M. Rueda, J. G. Serna, M. J. C. Alonso, *J. Supercrit. Fluids* **2011**, *61*, 119–125.
- [51] N. Gemo, Engineering the Catalytic Batchwise Synthesis of H₂O₂ from Its Elements, Università degli Studi di Padova, **2012**.
- [52] P. Biasi, J. García-Serna, A. Bittante, T. Salmi, *Green Chem.* **2013**, *15*, 2502.
- [53] P. Biasi, P. Canu, F. Menegazzo, F. Pinna, T. O. Salmi, *Ind. Eng. Chem. Res.* **2012**, *51*, 8883–8890.
- [54] P. Biasi, F. Menegazzo, F. Pinna, K. Era, P. Canu, *Ind. Eng. Chem. Res.* **2010**, *49*, 10627–10632.
- [55] M. H. Al-dahhan, M. P. Dudukovii, *AIChE J.* **1996**, *42*, 2594–2606.
- [56] V. R. Choudhary, A. G. Gaikwad, S. D. Sansare, *Angew. Chem. Int. Ed. Engl.* **2001**, *40*, 1776–1779.
- [57] S. Melada, F. Pinna, G. Strukul, S. Perathoner, G. Centi, *J. Catal.* **2006**, *237*, 213–219.
- [58] S. Abate, S. Melada, G. Centi, S. Perathoner, F. Pinna, G. Strukul, *Catal. Today* **2006**, *117*, 193–198.
- [59] A. Pashkova, K. Svajda, R. Dittmeyer, *Chem. Eng. J.* **2008**, *139*, 165–171.
- [60] S. Chattopadhyay, G. Veser, *AIChE J.* **2006**, *52*, 2217–2229.
- [61] C. M. Piqueras, J. García-Serna, M. J. Cocero, *J. Supercrit. Fluids* **2011**, *56*, 33–40.
- [62] K. Vanden Bussche, in *Micro Technol. Large Scale Appl. Direct Synth. Hydrog. Peroxide*, **2006**.
- [63] H. Pennemann, V. Hessel, H. Löwe, *Chem. Eng. Sci.* **2004**, *59*, 4789–4794.
- [64] Y. Voloshin, R. Halder, A. Lawal, *Catal. Today* **2007**, *125*, 40–47.
- [65] S. Murakami, K. Ohtaki, S. Matsumoto, T. Inoue, *Jpn. J. Appl. Phys.* **2012**, *51*, 06FK11.
- [66] T. Inoue, K. Ohtaki, J. Adachi, M. Lu, S. Murakami, *Catal. Today* **2014**, DOI 10.1016/j.cattod.2014.03.065.
- [67] T. Inoue, Y. Kikutani, S. Hamakawa, K. Mawatari, F. Mizukami, T. Kitamori, *Chem. Eng. J.* **2010**, *160*, 909–914.
- [68] J. F. Ng, Y. Nie, G. K. Chuah, S. Jaenicke, *J. Catal.* **2010**, *269*, 302–308.
- [69] X. Wang, Y. Nie, J. L. C. Lee, S. Jaenicke, *Appl. Catal. A Gen.* **2007**, *317*, 258–265.
- [70] V. Paunovic, V. Ordonsky, M. F. Neira, D. Angelo, J. C. Schouten, T. A. Nijhuis, *J. Catal.* **2014**, *309*, 325–332.
- [71] V. Paunovic, J. C. Schouten, T. A. Nijhuis, *Catal. Today* **2014**, doi:10.101, DOI 10.1016/j.cattod.2014.04.007.
- [72] D. van Herk, P. Castaño, M. Makkee, J. A. Moulijn, M. T. Kreutzer, *Appl. Catal. A Gen.* **2009**, *365*, 199–206.

- [73] Y. Voloshin, J. Manganaro, A. Lawal, *Ind. Eng. Chem. Res.* **2008**, *47*, 8119–8125.
- [74] Y. Voloshin, A. Lawal, *Appl. Catal. A Gen.* **2009**, *353*, 9–16.
- [75] S. Maehara, M. Taneda, K. Kusakabe, *Chem. Eng. Res. Des.* **2008**, *86*, 410–415.
- [76] J. Kobayashi, Y. Mori, K. Okamoto, R. Akiyama, M. Ueno, T. Kitamori, S. Kobayashi, *Science* **2004**, *304*, 1305–8.



Catalyst coating on prefabricated capillary microchannels for the direct synthesis of hydrogen peroxide

2

This chapter has been accepted for publication as:

V. Paunovic, V. Ordonsky, M. F. Neira d'Angelo, J. C. Schouten, T. A. Nijhuis, Catalyst coating on prefabricated capillary microchannels for the direct synthesis of hydrogen peroxide. Ind. Eng. Chem. Res. 2015, 54, 2919.

ABSTRACT

The geometric surface area of capillary microchannels is insufficient by large for the direct deposition of a catalyst active phase to reach a sufficient level of activity of the microreactor. For this reason it is necessary to coat a porous layer of a catalyst support on the channel wall prior to the deposition of the active metallic species. This work addresses the challenges related to the preparation of well-adhered and uniform silica coatings inside closed capillary channels suitable for catalyst deposition for the direct synthesis of hydrogen peroxide. The method used to deposit a layer of coating suspension, which upon solvent evaporation and heating is transformed into a solid film, is known as dynamic gas displacement. Variation of coating parameters and properties of the coating solution could be used to produce microreactors coated with different silica loadings. The most critical aspect of coating is maintaining the film regularity during and after displacement of the coating fluid. The uniformity of the coating thickness is greatly affected by the ability to maintain the coating parameters constant, such as the coating velocity, temperature and the solvent evaporation rate, during and after displacement of the coating solution, but also

by the rheological properties of the coating fluid. Advantages and disadvantages of different coating techniques such as colloidal coating, sol-gel and slurry coating are discussed in detail. Finally, we demonstrate that silica wall-coated layers with embedded Au-Pd colloidal alloy nanoparticles are active in catalyzing the direct synthesis of hydrogen peroxide.

2.1. Introduction

Microstructured reactors are particularly suitable for fast and exothermic reactions. The main advantage of microstructured reactors is a high surface to volume ratio which varies between 10000-50000 m²/m³, in comparison to conventional reactors which reach up to 1000 m²/m³ [1]. The direct synthesis of hydrogen peroxide out of hydrogen and oxygen is one of the reactions most suitable to be executed in microstructured reactors, considering the explosiveness of hydrogen-oxygen mixtures in a wide range of concentrations (4-96% H₂). Due to extensively reduced dimensions of the microchannels, direct synthesis of hydrogen peroxide can be performed using concentrated hydrogen and oxygen mixtures, which would be impossible due to the risk of explosion in conventional reactors. To safely operate conventionally explosive gas-mixtures [2,3], a channel diameter of ≤ 300 μm should be used. Heterogeneously catalyzed reactions, such as the hydrogen peroxide direct synthesis, require the inclusion of the solid catalyst phase in the microchannels. Microreactors for heterogeneously catalyzed reactions can be designed either as “micro-packed beds” or wall-coated microchannels. Micro-packed beds are often applied in catalyst testing [4] or kinetic studies of heterogeneously catalyzed reactions [5-7] due to the possibility to simply incorporate already optimized or conventional catalysts available on the market. Typically, catalyst particles used are in a range of 50–150 μm [4,7]. Such randomly packed structures often result in a high pressure drop and flow maldistribution as a consequence of packaging non-uniformity throughout different channels. In case of specific reactions, such as direct synthesis of hydrogen peroxide, due to improper bed dilution with inert material, hot spots can be formed followed by explosions [4]. By coating the catalyst on the reactor wall, a high pressure drop can be avoided as well as poor catalyst wetting and contacting [8] typical for micro-packed beds. Karim et al. showed that temperature gradients present in micro packed-beds during methanol steam reforming can be eliminated by coating the catalyst on the reactor wall, thus resulting in higher catalytic activity [9]. In addition, it has been reported that simply switching from a packed-bed to a wall-coated microreactor can lead to a significant difference in selectivity, as a result of difference in distribution of reactant concentration [10]. Still, to ensure a proper flow distribution during channel parallelization or numbering up, attention has to be given both to fabrication of the reactor and to the coating of the catalytic layers inside each individual microchannel. The effect of flow maldistribution on selectivity depends on both the reaction kinetics and mass

Chapter 2

transfer^[11]. The deviation in selectivity with flow distribution is generally greater in case of mass transfer limited regime.

Different methods can be applied to coat microstructures, depending on the properties of the surface that is used and the catalyst itself. Reviews available on coating monoliths^[12] or in general structured surfaces^[13] are already discussing procedures used to deposit the catalyst inside structures including pre-treatment of the support, properties of coating phases and/or deposition of active metal when necessary^[12]. Three-phase reactions in wall-coated microchannels are typically performed in Taylor flow because of the high mass transfer rates that can be achieved. A particularly fast step in Taylor flow operation is the transfer of the gas to the solid catalyst through the thin liquid film present between the bubble and the wall (gas-to-solid)^[14,15]. Typically, the amount of catalyst deposited on the wall (the thickness of the catalytic layer) needs to be carefully adjusted in such a way that the reactions kinetics can keep up with the fast external mass transfer, while at the same time in order to efficiently use all the catalyst available, diffusion limitations through the layer deposited need to be minimized. The amount of catalyst can be increased by increasing the length of the channel if the thickness of the catalytic layer is a limiting factor. Control of the amount of catalyst per reactor volume can be achieved also via adjustment of the channel diameter. Fast reactions in comparison to slow reactions require less catalyst to achieve the desired conversions and at the same time a thinner catalytic layer means a more efficient catalyst utilization. In the process of fine-tuning of the layer thickness, the presence of random thickness non-uniformities along the channel length or cross-section means that in some sections of the reactor the reaction could be limited by diffusion, thus it would not be possible to precisely predict the reactor performance. In addition, in case of more severe restrictions along the channel caused by coating non-uniformity, the difference in pressure drop along the parallel reaction channels would potentially lead to gas-liquid flow maldistribution or channeling when channels are numbered-up^[16]. For example, the study performed by Conant et al.^[17] on methanol steam reforming showed that the non-uniformity in coating thickness along parallel microchannels could lead to a variation in the flow rates over the channels and a decrease in the overall reactor performance. Stable, uniform and reproducible coatings are therefore a prerequisite for the reproducible operation on the level of single-channel, as well as for stable and uniform multichannel operation. The stability of coatings is determined by the adherence of the catalytic layer to the wall of the microchannel and the stability of the active metallic phase towards leaching and/or deactivation. While leaching and deactivation are a general characteristic of the catalyst, adherence is influenced by the characteristics of the coating phase and the surface that is coated. The adhesion of the wash-coat is typically dependent on the substrate porosity^[12]. Methods used to coat flat surfaces, such as spin or dip coating, are performed

prior to reactor assembly. In this case assembling of the coated microchannel plates often results in sealing problems considering that coating solution gets in contact with the entire surface of the plate, including the flat surfaces around the channels. Coating non-porous reactor walls with a catalyst after its assembly requires a different approach. The present work is dedicated to catalyst coating of closed capillary microchannels intended for use in direct synthesis of hydrogen peroxide. The main goal is to optimize relevant coating parameters to produce a porous and stable silica support layer of desired and uniform thickness along the channel length and cross-section. Finally, the performance of the wall-coated microchannel reactor with deposited Au-Pd catalyst will be demonstrated in the direct synthesis reaction.

2.2. Experimental

Fused silica capillaries were chosen as a suitable reactor configuration for coating experiments considering that they allow for relatively easy characterization. Glass capillaries are low cost and it is possible to cut a piece of the catalyst coated capillary for characterization purposes, while still retaining sufficient reactor length for catalytic testing, something which is not possible with chip type reactors. Glass as a material is also known to be inert to hydrogen peroxide, by non-catalyzing its decomposition. They are able to withstand the high pressures and flexible, allowing easy handling. The standard channel diameter used of 320 μm is stipulated by the safety requirements in order to be able to work with conventionally explosive hydrogen and oxygen mixtures in direct synthesis. The capillaries were typically coated with support material using the gas displacement method.

2.2.1. Deposition of the catalytic layer on capillary wall- Coating procedure

The active catalytic phase inside the microchannel can be deposited either by deposition of active metal on a pre-coated support layer or by directly coating a ready-made catalyst ^[12]. Unlike for example monolith structures, the walls of fused silica capillaries are almost non-porous. To create a surface area for deposition of the active metallic phase, it is necessary to first deposit a porous layer of support material such as silica. The support material should not play a role in the reaction itself except providing sufficient surface area to achieve a proper dispersion of the active catalytic phase. The choice of AuPd metal does not require a particular type of silica support or *vice versa*. Considering the possibility that some of the binder material present might close the catalyst pores containing active metal if a ready-made catalyst is directly coated onto the microchannel walls, the active phase should preferably be deposited afterwards on the coated catalyst support layer, allowing full accessibility of the active phase to reactant molecules.

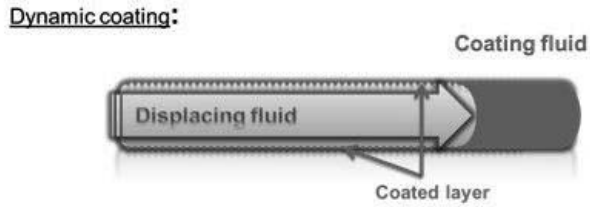


Figure 2.1. Dynamic coating method.

The dynamic coating involves displacement of the coating fluid by means of another fluid, typically a gas (Fig. 2.1). After a solution is forced through the microchannel, a thin liquid film remains on the wall. Continuous flushing of the gas after displacement allows the film to dry, resulting in a solid layer. Eventually, the capillary can be heated to provide additional bonding of the deposited solid phase to the material of the channel wall.

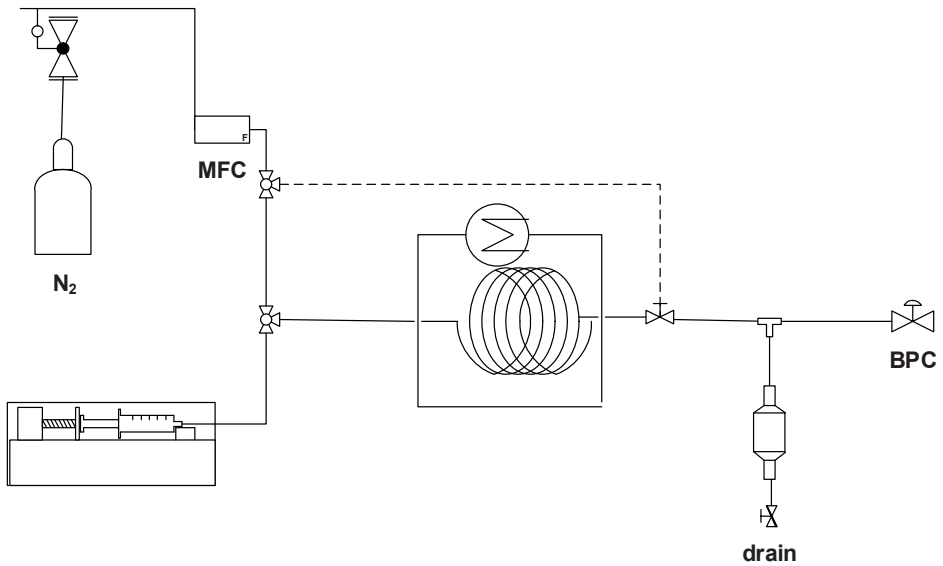


Figure 2.2. Coating set-up scheme.

Catalyst coating on prefabricated capillary microchannels

The scheme of the set-up used to control the dynamic coating process is depicted in Fig. 2.2. A silica composed coating fluid supplied to a capillary by means of a syringe pump is displaced using a flow of N₂ gas which is fed through the mass flow controller. The capillary was typically filled up to approximately one half of its length with silica coating slurry. It was estimated that this length of the plug can provide a sufficient amount of the suspension for coating the whole length of the capillary. In case of a shorter plug, a significant amount of the plug would be consumed particularly at higher displacement velocities. The most critical aspect of coating is maintaining a film uniformity during and after displacement of the coating fluid (See Results and Discussion). In order to prevent an increase in the velocity of the liquid plug leaving the capillary due to a decreasing backpressure as soon as the coating solution would leave the capillary, the pressure at the capillary end was maintained constant using a back-pressure controller. After the plug is displaced, the nitrogen flow was doubled and maintained throughout the drying process. To avoid changes in temperature along the capillary length, the capillary was kept in a thermostated oven or thermostated water-bath.

2.2.2. Preparation of the silica wash-coat solution and capillary pretreatment

Fused silica capillaries (Agilent, ID 320 μm) were pretreated with 1M NaOH solution and 1M HCl solution to increase the surface roughness and to clean the surface. Silica was chosen as a support material for the Au-Pd catalyst in direct synthesis considering the previous work done by Hutchings et al. ^[18,19], which emphasized the role of the isoelectric point of support in subsequent hydrogenation or decomposition of hydrogen peroxide. In addition, a good compatibility is expected between the glass surfaces of the capillary wall with a coated silica layer. Initially, a colloidal solution of silica was used to coat the washcoat layer on the fused silica surface. Colloidal silica solutions are readily available. In our experiments Ludox AS30 (Sigma Aldrich) was used. The silica content of this solution is 30% in water, with an average surface area of 230 m²/g and pH of around 9.1. The average particle size is around 12 nm. This makes the Ludox silica an excellent silica based binder material.

For the sol-gel coating procedure a sodium silicate solution was used as a silica sol (Sigma-Aldrich, SiO₂~26.5 wt%, Na₂O, ~10.6%). In order to avoid instant gelation which causes blockage of the capillary during the coating procedure (typically observed with the addition of acid), formamide (10%) was used as a gelation agent. Addition of formamide as a gelation agent gives much better control over the gelation rate, since hydrolysis of formamide leads only to a slight decrease in the pH. To remove sodium and to increase the porosity of the deposited layer, after heat treatment capillaries were flushed with 1 M solution of ammonium-nitrate followed by 1M solution of HCl and water, dried and calcined at 300 °C.

Chapter 2

The slurry coating methodology, as already applied for example for coating monoliths ^[12], results in thick(er) layers deposited on the channel wall, compared to coating with a colloidal solution. In this case, the slurry suspension contains large particles and smaller binder particles, typically two orders of magnitude smaller in size. Those colloidal small binder particles act as a “glue” between large particles improving the contact and cohesion. The slurries used for coating our capillaries typically contained Ludox AS 30 colloidal silica and sodium silicate solution (Sigma-Aldrich, SiO₂ ~26.5 wt%, Na₂O, ~10.6%) as binders, fumed silica (~4wt%, Sigma Aldrich) and larger particles in a form of Davisil silica gel (8wt%, 10-14 µm particle size). Fumed silica has a very small individual particle size (of only 7 nm), however in solution it tends to polymerize or agglomerates resulting in larger grouped particles. Addition of a sodium silicate solution (~10 wt% of solution) was necessary to improve the adherence of the coated layer, considering that upon heating at temperatures as high as 150 °C for 1.5h, Si-O-Si bonds are formed improving the layer adherence by chemical bonding. In this way sodium silicate acts as a “glue”. After Si-O-Si bonds are formed, sodium can be removed without damaging the layer cohesion. The second type of silica powder added (Davisil silica gel) was used as supplied.

2.2.3. Coating analysis

To determine the integrity and thickness of coating layers deposited Scanning Electron Microscopy (SEM) was used. In order to study the layer thickness uniformity along the capillary length and cross-section, point analyses were performed. Film thicknesses were measured at a number of points on a given capillary cross-section along the length. Initially, the adhesion of the coatings was also estimated via SEM analysis. In addition, to investigate the coating stability and adherence, capillaries were subjected to ultrasound test and/or exposed to liquid flow under nitrogen pressure. The pressure drop along the capillary length is often a good indication of possible blockages or restrictions present in the capillary. The porosity of the coated layers was determined using the nitrogen physisorption method.

The adherence of the coating layer greatly determines the long-term stability of the overall catalytic layer. Initial tests done to determine quality of the adherence involved ultrasonic testing of capillary section. Nevertheless, taking into account that the reaction is performed at high pressures using acidic aqueous phase, besides mechanical a chemical stability of the coated layer needs to be ensured. The ultimate analysis performed to assure the durability of coated layers was exposing the wall-coated channels to typical reaction conditions for a number of hours. The appearance of the layer determined by applying SEM analysis to different capillary section was used as an indication of quality of adherence. Absence of the coated layer on some capillary sections was not considered acceptable/satisfactory.

2.2.4. Deposition of Au-Pd catalyst

Capillaries wash-coated using the slurry method were used to deposit the Au-Pd catalyst to be tested in direct synthesis of hydrogen peroxide. The stability and uniformity of these wash-coats was satisfactory. The typical relative deviation in coating thickness was $\leq 20\%$. After capillary exposure to conditions applied in direct synthesis, there was no indication of coating loss. Different Au-Pd catalysts were used as active metallic phase. In order to achieve better control over Au and Pd metal phases mixing pattern, the method known as a two-phase synthesis was applied to prepare Au-Pd alloy nanoparticles. Colloidal nanoparticles with two different Au/Pd ratio in this case were generated in dichloromethane as a solvent. The application of dichloromethane in the catalyst preparation enables a fast evaporation of solvent, thus making the catalyst preparation process faster and more efficient. In general the two-phase synthesis approach involves dissolution of required amounts of anionic Au and Pd precursors in a water phase (HAuCl_4 and K_2PdCl_4 respectively), after which they are transferred to an organic phase by means of a phase-transfer agent. For the preparation of alloyed Au-Pd nanoparticles, separate dichloromethane solutions containing tetrachloropalladate and tetrachloroaurate anions in a desired ratio are mixed prior to reduction with NaBH_4 . The exact protocol for synthesis of Au-Pd alloy nanoparticles is described by Serpell et al. ^[20]. For deposition of these nanoparticles, the capillary is filled with the colloidal solution of Au-Pd nanoparticles in the required concentration to achieve approximately 5 wt% loading relative to the wash-coat material and the solvent is slowly evaporated. After deposition of Au-Pd alloy nanoparticles inside the wash-coated capillary and solvent removal, the capillary was dried at 120 °C for 12 h and calcined at 380 °C for 4 h. Nevertheless, solvent removal via evaporation needs to be performed rather carefully avoiding even small temperature gradients over the microchannel. Overheating of a capillary section would be followed by the development of the gas bubbles in the liquid and expansion with a pressure rise, which would lead to discharge of the suspension with colloidal nanoparticles at the capillary ends. For this purpose, during solvent evaporation procedure capillary ends are kept inside the small volume glass vials with a perforated cap to collect and quantify (for AuPd) if necessary suspension discharged.

Please note that more details on the characterization of Au-Pd catalyst is given in Chapter 3 (TEM analysis) and Chapter 6 (XPS analysis and CO adsorption).

2.2.5. Microchannel catalyst testing

A wall-coated catalytic capillary was placed in a thermostated oven (Fig. 2.3). The liquid phase is supplied to the system by means of a syringe pump (Teledyne ISCO 500D). The total gas flow through capillary is set at 5 ml N/min, keeping the H₂/O₂ ratio always 1:1. In order to maintain a constant pressure at 20 bar, a back-pressure regulator is placed downstream after a gas–liquid separation unit (Fig. 2.3). Considering that pure H₂/O₂ mixtures are used, the gas flow is diluted with N₂ gas at the capillary outlet to assure a non-explosive gas mixture in the larger tubing downstream of the capillary reactor. The pressure in the system was monitored before the inlet and after the microchannel outlet (Fig. 2.3), since the pressure drop over the capillary was used as an indirect indication of quality of coating procedure. Defects in the coatings would lead to a higher pressure drop, and such capillaries would not be used for catalytic performance testing. Gas samples were analyzed with online compact GC (column: Molsieve plot 5m 0.32 mm) equipped with a TCD detector. Liquid samples were collected and immediately titrated with a standard solution of cerium (IV) sulfate to a blue end-point to determine to concentration of hydrogen peroxide. Typically the capillary length used throughout experiments is in a range of ~0.5-1.3 m. Although the amount of the catalyst can be correlated with the length of the microchannel, the exact loading of the active metal(s) needs to be determined. In general, the loading (which eventually determines the conversion) depends on both nanoparticle preparation and deposition procedure inside the microchannel (see preparation and deposition of AuPd colloidal nanoparticles). The exact length of the capillary was adjusted in order to tune the H₂ conversion to desired level.

2.2.5.1. Flow pattern

Considering the influence that flow pattern has on the performance of the multiphase reactors, flow visualization was conducted prior starting microchannel experiments. With deposition of coatings on the channel walls, capillary channels become rather opaque, complicating the flow visualization. For this reason, a transparent empty fused silica capillary of the same dimensions as the reactive capillary was used to observe the flow pattern inside the microchannel. Under reaction conditions considered to be applied in catalyst testing, Taylor flow with alternating gas and liquid slugs was observed. For gas-liquid-solid reactions in microchannels, Taylor flow has been shown to enhance mass transfer significantly ^[15,21]. With consumption of gas along the channel length, the size of gas bubbles is expected to decrease. Nevertheless, at lower conversion levels used throughout our experiments, the change in the length of gas bubbles won't affect the flow pattern significantly. However, if one would operate reactor at high conversion level, due

to high degree of gas phase consumption along the capillary, changes in the gas-liquid hydrodynamics as approaching to the channel end would be obvious.

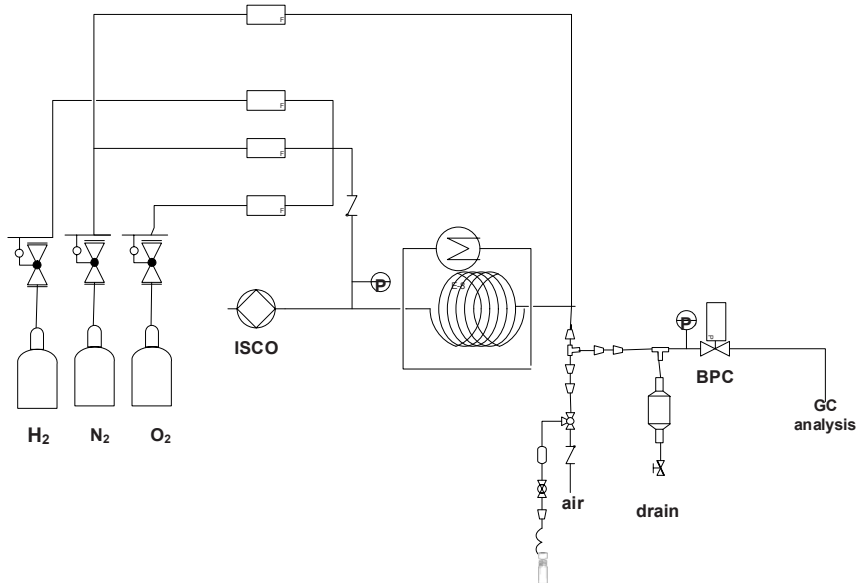


Figure 2.3. Scheme of the microchannel set-up used in direct synthesis of hydrogen peroxide.

2.3. Results

The main goal presented in this work is to prepare well adhered, porous silica layers of uniform thickness, desirably in a range of 1-10 μm . Important aspects that need to be taken into account when coating a catalyst support layer on microchannel walls is its layer adherence and stability under reaction conditions, porosity and thickness. Two major variables used to tailor the coating thickness were the coating displacement velocity and the composition of the coating fluid (which further reflects on viscosity and surface tension). Unlike porous monoliths used as catalytic converters, microreactors are often fabricated using non-porous inert glass materials, as fused silica capillaries. Considering the low porosity of this glassy material, issues with adherence of the coatings might be expected. The surface pre-treatment described in the experimental section is used to etch the glass surface in order to enhance the adhesion. In addition, the composition of coating slurry greatly affects the adherence and layer stability under reaction conditions.

2.3.1. Colloidal silica coatings

Initially, the fused silica capillaries were coated with a layer of readily available colloidal silica solution (Ludox AS30). Application of colloidal silica solutions is straightforward considering that those are readily available. The major drawback observed initially with coatings obtained after applying this procedure was non-uniformity of the layer thickness in different portions of the capillary when the free release gas displacement technique was used [22]. Large deviations in coating thickness need to be avoided in order to ensure equal catalyst effectiveness along the entire microchannel, which is directly influenced by the catalytic layer thickness. Therefore, an attempt was made to identify and control the variables associated with the development of layer non-uniformity.

2.3.1.1. Dynamic coating of capillary microchannels - coating uniformity

Experimentally, the increase of the velocity of the displacing plug was observed as soon as some of the fluid would leave the capillary due to the gas expansion. The change in velocity along the length of a 2 m long capillary was quantified experimentally while blowing out the coating fluid. The capillary was divided in 8 sections of 25 cm length over which displacement velocity was averaged (Fig. 2.4.). The first half of the capillary was filled with the coating solution (Ludox AS30). The movement of the plug between the marked sections of the capillary can be easily observed visually, since capillaries are transparent. The time needed for the displacing plug to bypass the given section was recorded.

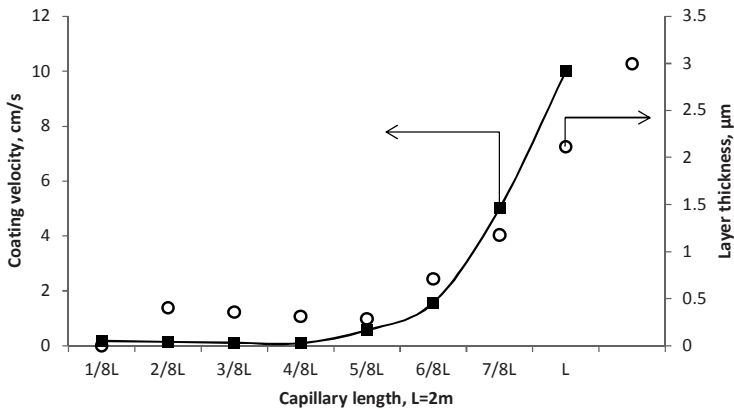


Figure 2.4. Increase of coating velocity in the capillary end section during free release gas-displacement and its effect on coating thickness along the capillary channel (capillary length L=2m; plug length 1m, coating fluid LudoxAS30 colloidal silica).

Catalyst coating on prefabricated capillary microchannels

It is clear that with the first half of the capillary length displacement speed remained unchanged, while with the clearance of the coating fluid from the microchannel a tremendous increase in velocity was observed, reaching from 0.2 cm/s almost 10 cm/s in the last portion (section) of the capillary. This finding is correlated with the fact that capillary was initially filled with the coating suspension up to half of its length. If instead only first $\frac{1}{4}$ of capillary length would be filled with coating suspension prior to displacement, in such a case more or less consistent displacement velocity would be observed in up to $\frac{3}{4}$ of capillary length. When shorter coating plugs are used, the considerable consumption of the coating suspension as the plug passes the capillary leads again to a higher linear velocity. According to Fairbrother and Stubbs [23], who studied displacement of the Newtonian fluids in tubes by means of gas, the fraction of coated m fluid can be directly correlated to the capillary number $m = Ca^{1/2}$ ($Ca = \mu U / \sigma$, where μ is the fluid viscosity, U is the displacing velocity and σ is the surface tension). Taylor's analysis, however, showed that the amount of liquid deposited on the wall increases with the interface speed and that m reaches asymptotically to a value of 0.56 as Ca approaches 2 [24]. Polynkin et al. [25] extended the Taylor model for predicting the maximum fraction coated for shear-thinning fluids. This in general means that with an increase of the coating velocity in the second half of the capillary, the layer thickness will increase resulting in non-uniform thickness along the capillary length (Fig. 2.4).

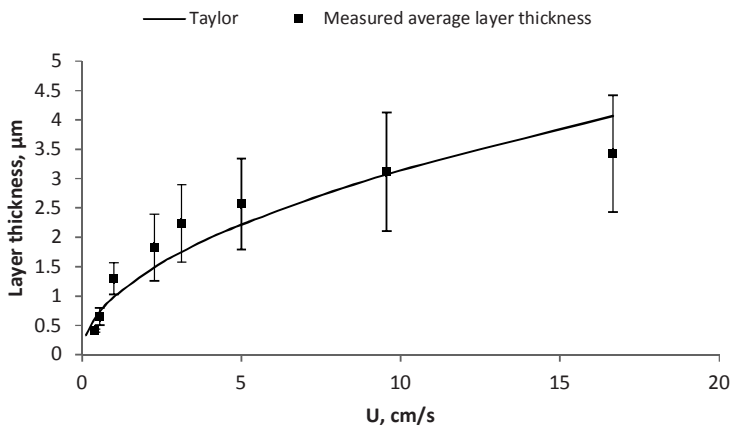


Figure 2.5. Average layer thickness (SEM) with standard error and predicted layer thickness from Taylor correlation as a function of displacement speed (coating fluid colloidal silica solution Ludox AS30, constant coating velocity values given on X-axis obtained using coating set-up presented in Fig. 2.2).

Chapter 2

It is clear that with a free release of the coating fluid one can end up with almost an order of magnitude difference in thickness compared to the first half and the end of the capillary if typically one half of the capillary is filled with the coating fluid. This problem of the increase in the coating velocity can be tackled by introducing the restriction at the capillary outlet to control the displacement velocity. Techniques to coat long capillary columns for gas chromatography and to control displacement velocity has been proposed by van Dalen and Levy et al. [26,27]. The syringe pump in van Dalen's method is applied as a brake to adjust the velocity of the meniscus, in contrast to the relatively complex liquid brake system introduced by Levy et al. The withdrawal speed of the pump needs to be adjusted to obtain desired displacement velocity. In a similar fashion, our coating set-up is provided with a back pressure controller at the outlet of the capillary to provide backpressure significantly higher than a pressure drop over the capillary and thereby significantly reduce the effect of the gas expansion with drop in resistance to the gas flow with the solution clearance (Fig. 2.2). More details on set-up parts and operation are given in the experimental section.

The effect of displacement velocity on the remaining layer thickness at constant displacement velocity (achieved using coating set-up on Fig. 2.2), both predicted by the Taylor correlation and experimentally measured by SEM, is presented in Fig. 2.5. It is clear from Fig. 2.5 that after introduction of a back pressure regulator at the microchannel outlet to control the linear velocity of displacing plug, the coating thickness uniformity is dramatically improved in comparison to Fig. 2.4 particularly in case of thinner layers ($\leq 1 \mu\text{m}$), nevertheless coating thickness is still not ideally uniform. It is clear that increase in layer thickness is accompanied by higher degree of non-uniformity. In addition to the coating procedure itself, the drying step is also often a source of irregularity in thickness of the deposited film if not performed carefully [28,29]. Namely, temperature fluctuations along the capillary length might cause that some of the solvent evaporated condenses in downstream cooler parts of capillaries creating a restriction to the gas flow used to dry the capillary [30]. Restrictions create a pressure difference leading to the transport of some of the liquid film towards the outlet. In addition, as observed by Conant et al. [17], in case of thick coatings large stresses during drying as a consequence of substantial loss of the volume (75% of slurry is water) can lead to cracks and loss of cohesion, resulting in severe coating non-uniformity. Gravity is an additional source of coating non-uniformity, mainly responsible for the difference in thickness observed along the cross-section [31,32]. Under the influence of gravity the deposited liquid film tends to drain from the walls resulting in thicker coating on the bottom. A less viscous coating fluid is more susceptible to drainage induced by gravity. The gravity effect is especially pronounced in case of thicker coatings and lower viscosity slurries. From Fig. 2.5 it is obvious that the degree of thickness non-uniformity is dependent on the layer thickness.

The liquid film on the microchannel wall is affected by rearrangement after deposition and before it is completely dry. This phenomenon, known as Rayleigh instability^[32] is independent of wall wettability with coating fluid. The instability of the coated film is the consequence of the decrease in interfacial energy on the gas-liquid interface and results in a wavelength of the disturbance which is independent of surface tension and viscosity, and equals to $2\pi r_{ch}/0.7$. The logarithmic growth rate of Rayleigh instabilities, as given by Bartle et al.^[33], is proportional to the surface tension (σ) and to the third power of the film thickness (d_f), and inversely to the viscosity (μ) and to the fourth power of the capillary diameter (r_{ch}):

$$\ln\left(\frac{b}{b_0}\right) = \frac{\sigma d_f^3 t}{12\mu r_{ch}^4} \quad (1)$$

Where b and b_0 are the amplitudes of the wave at time t and 0 respectively. So the time needed to double the disturbance calculated from this formula for low viscosity coating fluid, such as Ludox AS30, is already less than 10 min for coatings as thin as $1 \mu\text{m}$. In principle, this implies that either the fast film drying or fixation should be applied in order to avoid film perturbations or the rheological properties of the coating fluid (viscosity) should be tailored.

SEM images of deposited colloidal silica layers are given in Fig. 2.6. Due to the low viscosity of these colloidal silica solutions, to achieve higher thicknesses it was necessary to coat the capillary at high displacement velocities. From Fig. 2.5. it is clear that at high gas velocities ($>10 \text{ cm/s}$), the colloidal film thickness reaches $\sim 3 \mu\text{m}$, however a higher degree of thickness non-uniformity has to be taken into account as well. The general rule applies, that if a thicker coating layer is required, the concentration of the solution (or viscosity) rather than the coating speed should be increased. This is related to the fast development of drainage under the influence of gravity and wave disturbances after displacement in case of low viscosity coating fluids and therefore a higher degree of layer non-uniformity along the cross-section is expected. The relative deviation in the coating thickness increases from $\leq 10\%$ for a lower range of thicknesses, obtained at low coating speeds, to approximately 35% for coatings of $\sim 3 \mu\text{m}$ thickness. At the velocities typically applied in coating procedure of around 1 cm/s , the layer thickness was around $1 \mu\text{m}$. Larger layer thicknesses can be also achieved through multiple coatings or multiple layers, however in that case the adherence of the colloidal silica layers was problematic. After attempted application of the second or the third layer or in general when flowing liquid through the capillary under high pressure, resulted in part of the coated layer(s) being lost from some sections of the capillary. For this reason, the adherence of the coating had to be improved to make sure that no deposited

Chapter 2

layer detaches from the wall during the reaction. As will be discussed on in this paper, this can be achieved by the addition of small amounts of sodium silicate to the coating fluid.

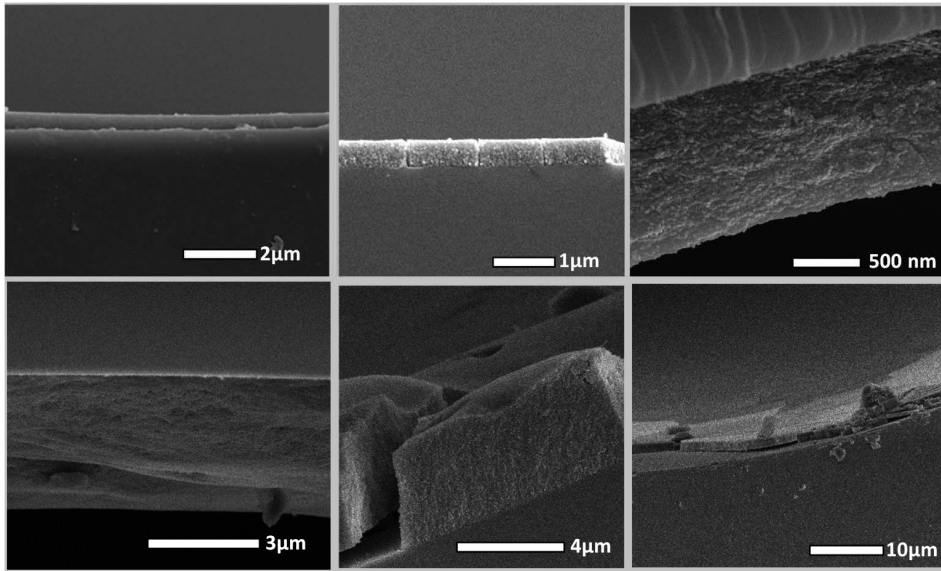


Figure 2.6. SEM images of colloidal silica coatings obtained using the gas displacement method.

To summarize, application of colloidal silica solutions such as Ludox although is rather straight forward has several disadvantages. Due to low viscosity, those fluids are prone to drainage under influence of gravity and at the same time give thinner layers in comparison to higher viscosity fluids. Besides viscosity modification, in order to ensure durability of those layers, it is necessary to further improve their binding properties (adherence).

2.3.2. Slurry coatings

Application of slurry coatings offers the possibility to increase the viscosity and enhance layer cohesion. To increase the viscosity of the colloidal silica coating solution, fumed silica was added to create a slurry. Fumed silica is a well-known rheology modifier used in industry. It is produced by high temperature hydrolysis of silicon tetrachloride in an oxygen–hydrogen flame and results in a primary particle size of only 7 nm. However, due to high surface area, those particles are not stable and they fuse together giving agglomerates of around 100-250 nm, which further grow to micron size agglomerates due to physical-chemical interactions^[34]. Due to a high surface area and a high number of silanol groups on

the surface, fumed silica is able to bond with other materials through hydrogen bonding including neighboring silica particles. If the fumed silica particles are suspended in water or an aqueous solution, hydrogen bonds are formed between the water molecules and the -OH groups on the surface of the silica particles. When the fumed silica particles are wetted with solvent molecules, the particles tend to float in the medium rather independent of each other resulting in an increase in viscosity to a certain extent. In cases where the molecules of the liquid cannot adsorb onto the surface of the fumed silica, particles tend to cling each other forming a randomly distributed grid. Mechanical stress applied temporarily disturbs the silica nano-particle aggregates or three-dimensional networks formed between the particles as a consequence of hydrogen bonding. Macroscopically, the system becomes free-flowing (thixotropic effect). When the force stops, three-dimensional aggregates are re-formed and the material becomes viscous to solid again. Overall, the thixotropic effect is much more evident when fumed silica is suspended in non-polar liquids than in polar liquids (water). The percentage of fumed silica added was optimized experimentally. Namely, at a fumed silica content typically higher than 6 wt%, the slurry prepared was too viscous, which reflected in the inability to fill the capillary with the coating fluid. In order to avoid capillary blockage, the content of fumed silica in the solution was adjusted to ≤ 4 wt%. In addition to fumed silica, silica slurries contained silica gel particles in micrometer range (Davisil silica) and a small amount of sodium silicate as an additional binder ensuring the good adherence of the coating to the glass microchannel wall. It is believed that upon heating silicate molecules lead to formation of Si-O-Si bonds with glass surface. Spin coating of a sodium silicate solution (7-10 wt%) followed by annealing at 90°C is used for glass-glass bonding in the production of microchip devices ^[35]. Without sodium silicate added, it was observed that after flowing liquid under pressure through the coated capillary, the pressure drop would increase, which was an indication of poor coating stability. SEM images also indicated the absence of the layer in some sections of the capillary. In addition, Zwinkels et al. reported that the addition of water glass to the colloidal silica slurry facilitates drying, since it leads to formation of larger pores reducing the stress caused by surface tension during evaporation of the solvent ^[36].

The principle of slurry coating is very clear. The bigger particles of silica gel in this case represent the mainframe or “skeleton” of the support layer. The small binder particles provide the interaction between those particles acting as glue. Therefore, without the binder particles the layer would not be coherent, while the pore size obtained with a layer consisting only of particles in nanometer range would be very small, limiting eventually their accessibility. The average thickness of the layer obtained when coating this type of slurry using the coating set-up (Fig. 2.2) was varied in the range of approximately 3µm to maximum 10µm. SEM micrographs of slurry wash-coats are presented in Fig. 2.7. Those

Chapter 2

values were corresponding to the desired range of values for coating thickness of the catalyst support layer, calculated to ensure the absence of internal mass transfer limitations. The reaction rate (constant) with Au-Pd catalyst was assumed to be at least twice higher than the one reported for Pd catalyst^[4]. In the relevant literature dealing with Au-Pd catalysts for the direct synthesis of hydrogen peroxide, it is reported that the addition of Au to Pd results typically in a 2-10 times higher productivity in comparison to the productivity observed with Pd catalysts only^[19,37,38]. The relative deviation in thickness uniformity was typically $\leq 20\%$. The surface area of slurry coatings was determined before and after post-treatment. Post-treatment of coatings with a 1M solution of ammonium nitrate and 1M HCl for several hours resulted in a BET surface area increase from 94.5 m²/g to approximately 207 m²/g.

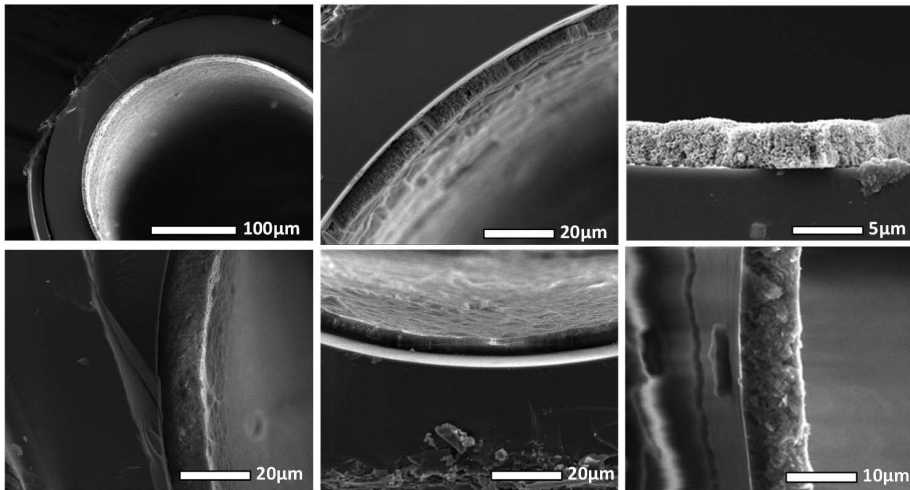


Figure 2.7. SEM images of slurry coatings deposited inside fused silica capillary.

2.3.3. Sol-gel coatings

An additional technique applied to deposit a silica layer inside fused silica microchannels is known as a sol-gel method. This technique offers the possibility to influence the viscosity by influencing the degree of gelation. In principle, the silica material introduced into the microchannel should be in form of a clear solution, containing no silica particles. Water glass or sodium silicate solution is a silica sol that is commercially available. In addition, silicate containing coating fluids showed good adherence to the non-porous fused silica surface, which makes this material suitable for a coating. The mechanism of sol transformation to gel is based on the change of pH. By lowering the pH of the sodium silicate solution, a gel can be formed. Initially, the formation of gel has been attempted by adding a HCl solution

Catalyst coating on prefabricated capillary microchannels

to sodium silicate. However, soon after lowering the pH of the solution to the desired value, the solution would become very viscous indicating that gelation is occurring fast. As already mentioned earlier, filling the capillary with such a viscous solution was often very difficult, even impossible if gelation already proceeded. The more desired scenario is that gelation is triggered after the layer of coating is deposited on the channel walls (in-situ gelation i.e. upon heating). Addition of formamide as a gelation agent gives much better control over the gelation rate. In the presence of alkali, formamide undergoes hydrolysis with formation of ammonium and formate ions in the solution and a slight decrease in pH (below 11). This pH already leads to polymerisation of di-silicate ions. However, in comparison to the direct addition of those ions, high local concentration and local gelation is avoided.

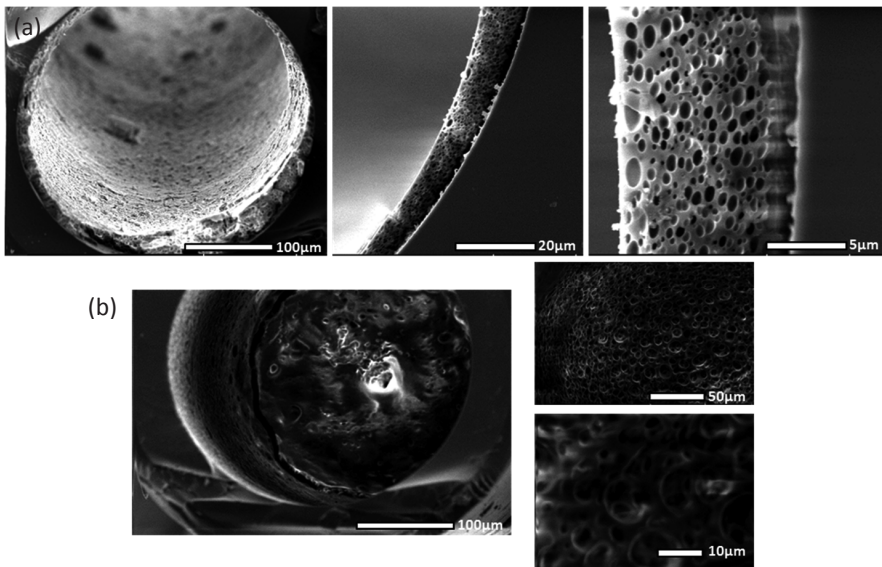


Figure 2.8. SEM images of sol-gel coatings prepared from sodium silicate solution (a) heating applied after plug displacement (b) blocked capillary as a consequence of plug gelation (heating applied during displacement).

The process can be further stimulated by heating. Immersing the capillary with the layer of sol deposited after the displacement procedure into the water-bath heated up to 80°C results in rapid transformation of the sol to gel preventing the fluid to drain from the walls. The SEM images of the coatings obtained applying sol-gel method, are presented on Fig. 2.8a.

Similar to slurry coating, sol-gel coatings were post-treated with a solution of ammonium nitrate and HCl. Although the coating thickness that can be reached was large ($\approx 10 \mu\text{m}$), the

Chapter 2

variation in coating thickness along the capillary cross-section was rather significant. On the example shown in Fig. 2.8a, the average thickness of the layer observed varied between ~ 4 μm on the top of the cross-section to approximately 13 μm at the bottom. This is a consequence of significant drainage of the liquid film prior gelation under influence of gravity. The influence of gravity can be minimized with instant polymerisation of the coated liquid film. However, if heating of the capillary was applied parallel to the coating (displacement) procedure, plug of displacement fluid would gel fast resulting easily in blockage of the microchannel (Fig. 2.8b). Due to instantaneous gelation triggered by heat, heating needs to be applied after the coating plug leaves the capillary in order to avoid blockage of the microchannel. Nevertheless, this leaves a certain time frame for development of coating non-uniformities.

Coating method	Adherence	Maximum coating thickness obtained (μm)	Coating thickness (μm) at recommended displacement velocity ($\sim 2 \text{ cm/s}$)
Colloidal silica coatings	Poor/not satisfying	3.5	1.3 ± 0.3
Slurry coating	Good	10	4 ± 0.8
Sol-gel coating	Good	$\sim 11^*$	7^*

*High degree of non-uniformity

Table 2.1. Comparison between different coating techniques used to create porous silica layer on microchannel walls.

To summarise (Table 2.1), different coating precursors/fluids were tested in order to obtain a coated silica layer which fulfils the process requirements i.e. a range of desired layer thickness and coating uniformity as well as a proper adherence under reaction conditions. Among the three different silica coating precursors, the slurry coating achieves the most promising results in terms of adherence of the deposited silica layer, thickness at the recommended/lower range of coating velocity and thickness uniformity. At lower range of displacement velocities, colloidal silica solutions give thinner layers. To increase the layer thickness, which would be desirable for the catalytic application in the direct synthesis, the colloidal silica solution needs to be displaced at high velocities. This results in a higher

degree of non-uniformity. In addition, in case of colloidal silica coatings the long term adherence and coating stability were considered an issue. In contrast, sol-gel coatings despite the good adherence and higher layer thickness, have a high degree of coating non-uniformity. The thicker the layer, the higher the catalyst hold-up in the microchannel. However a too thick catalytic layer means a less efficient catalyst usage as a consequence of internal diffusion limitations. To prevent that the direct synthesis reaction is diffusion limited, the estimated thickness of the catalytic layer should remain below 10 μm , preferably even not more than 5 μm . The extent of coating thickness non-uniformity obtained with the sol-gel technique makes them not suitable to be applied in the direct synthesis of hydrogen peroxide, since the reaction might be limited by reactant diffusion in some sections of the microchannel. Considering all the requirements above, the slurry coatings were only considered to be further applied as a catalyst support in the direct synthesis of hydrogen peroxide. Although, our goal was to develop the silica coatings to be used in the direct synthesis of hydrogen peroxide, their application can be extended. Still, it is difficult to give general recommendation on most suitable coating type without knowing specific requirements such as reaction conditions (chemical stability), desired level of uniformity and properties of substrate to be coated. The methodology to deposit a silica layer inside the microchannel can be extended to steel capillaries or glass chips. Wall-coated microchannel reactors were applied successfully within our group in reactions such as aqueous phase reforming^[39], propylene oxide production^[40] or in selective hydrogenation reactions^[41].

2.3.4. Activity of Au-Pd catalyst supported on SiO₂ wash-coats in a microchannel in the direct synthesis of hydrogen peroxide

In order to obtain the active catalyst for the direct synthesis of hydrogen peroxide, the silica wash-coated layer was embedded with Au-Pd bimetallic nanoparticles prepared using a two-phase synthesis procedure. Silica layers with embedded Au-Pd (1:2) colloidal nanoparticles were tested in the direct synthesis of hydrogen peroxide in different liquid mediums (Fig. 2.9). The stable catalytic activity after several hours operation was a good indication of the coating stability under reaction conditions. It is clear that if the aqueous phase is replaced by methanol, at H₂ conversions of around 30%, the selectivity achieved in methanol with the addition of acid as a liquid phase is significantly higher than in the acidic aqueous phase and the peroxide concentration observed in the liquid phase is around 1.5 wt%. However, if pure methanol is used, the selectivity is much lower at approximately the same conversion level. The direct formation of hydrogen peroxide is always followed by consecutive reactions, hydrogenation and decomposition, which result in the transformation of peroxide into water lowering the overall selectivity. In the presence of promoters (halides, mineral acids), the decomposition reaction is known to be inhibited^{[42-}

Chapter 2

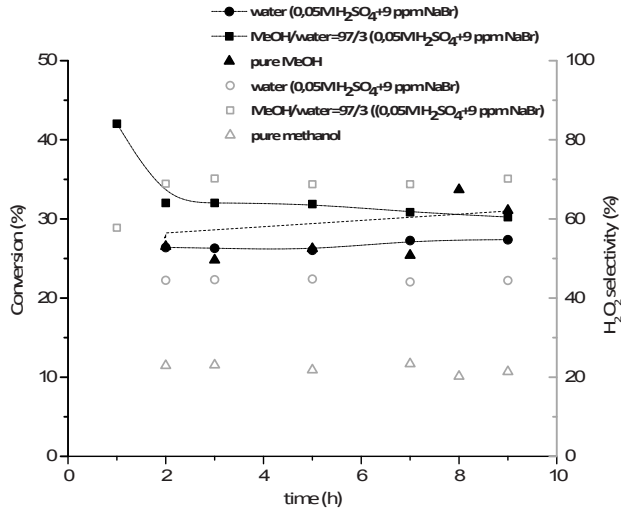
^{45]}. Therefore, the lower selectivity observed in the absence of H⁺ ions in a pure methanol liquid phase is a consequence of a base catalysed peroxide decomposition. It is believed that differences in selectivity observed between water and methanol as a solvent can relate to nature of the solvent.

In our publication dealing with the direct synthesis of hydrogen peroxide over a Au-Pd catalyst ^[31] and chapter 3, a performance comparison between conventional semi-batch slurry reactor with AuPd nanoparticles supported on silica powder and slurry-wash-coated microchannel with embedded AuPd nanoparticles under conventionally diluted conditions (gas mixtures contained 4 vol% of H₂ and O₂) is given. Considering that gas phase is continuously fed, the WHSV in semi-continuous and microreactor was adjusted to achieve comparable values in both reactors (~20 g_{H₂}/g_{cat}h). At the correspondent conversion (~10%), the initial productivity and selectivity values observed in the autoclave in the absence of mass transfer limitations show similar values to the steady-state productivity and selectivity obtained in a microchannel at a given LHSV under similar reaction conditions. This result indicates that we are able to successfully prepare an active catalyst in a microchannel which exerts identical activity to a conventional powder catalyst.

This is not surprising if one has in mind that nanoparticles are deposited on pre-coated silica layer, meaning that active metallic phase is readily accessible to reactant molecules. If a ready-made catalyst Au-Pd/SiO₂ would be coated on microchannel, the use of binder in coating procedure could cover some of the metal nanoparticles making them inaccessible for reactants. It is also known in literature that a catalyst supported on silica produced from different natural sources or using different procedures can exert a different catalytic activity to a certain extent. Nevertheless, in case of wall-coated microchannels or monoliths in order to preserve catalytic activity, the active metallic phase should be preferably deposited onto pre-coated support layer avoiding enclosure of the nanoparticles by binder material. Advantageously, in a continuous process in microchannel, productivity and selectivity values are maintained rather constant, while in autoclave decrease is observed as a consequence of consumption of accumulated peroxide to water (via decomposition or hydrogenation route).

Catalyst coating on prefabricated capillary microchannels

a)



b)

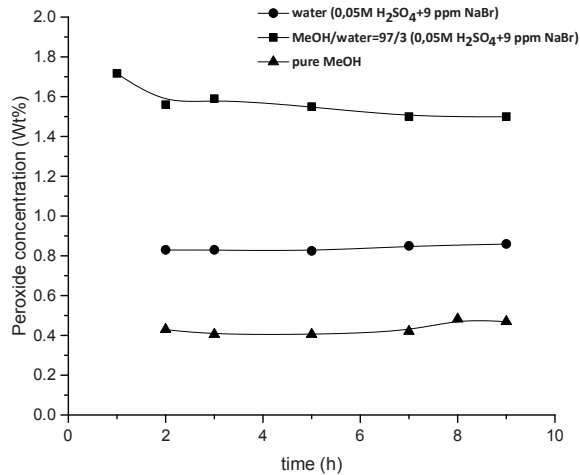


Figure 2.10. (a) H₂ conversion and H₂O₂ selectivity (b) Peroxide concentration observed in different liquid phases over Au-Pd alloy (1:2) supported on silica slurry wash-coat over time (Capillary internal diameter 320 μm; P=20 bar; T=42°C; Gas flow rate 5 ml/min (H₂/O₂=1:1); Liquid flow rate 0.05 ml/min.

2.4. Conclusions

Coating of a catalyst support material on walls of closed channels by the dynamic method was successfully accomplished. The uniformity of the remaining layer along the channel after the coating plug has left the column is mainly affected by the ability to successfully control the coating velocity within the channel length. A sharp increase in coating velocity is evident as soon as the coating solution is discharged from the end of the capillary which results in a thicker film at one channel end. Beside the coating velocity, a precise control of temperature and eventually evaporation rate of the solvent is critical for achieving a uniform coating thickness inside closed microchannels. Later rearrangement of the deposited liquid film can occur as a consequence of a gravity effect and Rayleigh instability of a long cylindrical column of liquid. In terms of silica precursor used as a coating fluid, different techniques were applied: colloidal coating, slurry coating and sol-gel technique. Generally, colloidal coating is resulting in thinner layers in comparison to the other two techniques at the similar displacement velocities. Although, the coating thickness can be increased by simply applying multiple layers, the stability of the colloidal silica layer under given reaction conditions was brought in question. The major disadvantage of the sol-gel approach was layer non-uniformity as a result of gravity induced drainage. Theoretically, the effect of gravity can be minimized by rotating the capillary around its horizontal axis. Nevertheless, this is not technically practical particularly if one has in mind coating long(er) capillary pieces or rectangular glass chips with sine-shaped microchannels. Considering all the above, slurry coating gave a satisfactory uniformity and stability (adherence) to be further applied as a catalyst support in direct synthesis of hydrogen peroxide. As a proof of concept, the direct synthesis reaction was successfully performed over bimetallic Au-Pd catalyst supported on silica slurry wash-coats in an acidified aqueous phase and in methanol. The catalytic coatings prepared are stable in the acidic environment applied. Peroxide concentrations observed in acidified aqueous phase under given condition reach 0.8wt%, while addition of methanol leads to almost twice higher peroxide concentrations in the liquid phase. A detailed discussion and experimental study of the wall-coated microchannel performance is presented elsewhere ^[46], including more details on achievable peroxide concentrations and long-term stability of catalytic layer.

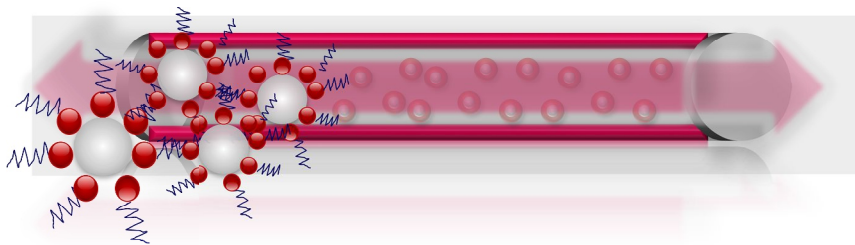
References:

- [1] M. N. Kashid, L. Kiwi-Minsker, *Ind. Eng. Chem. Res.* **2009**, *48*, 6465–6485.
- [2] M. T. Janicke, H. Kestenbaum, U. Hagendorf, F. Schüth, M. Fichtner, K. Schubert, *J. Catal.* **2000**, *191*, 282–293.
- [3] S. Chattopadhyay, G. Veser, *AIChE J.* **2006**, *52*, 2217–2229.
- [4] T. Inoue, M. A. Schmidt, K. F. Jensen, *Ind. Eng. Chem. Res.* **2007**, *46*, 1153–1160.
- [5] Y. Voloshin, J. Manganaro, A. Lawal, **2008**, 8119–8125.
- [6] Y. Voloshin, A. Lawal, *Appl. Catal. A Gen.* **2009**, *353*, 9–16.
- [7] Y. Voloshin, R. Halder, A. Lawal, *Catal. Today* **2007**, *125*, 40–47.
- [8] D. van Herk, P. Castaño, M. Makkee, J. A. Moulijn, M. T. Kreutzer, *Appl. Catal. A Gen.* **2009**, *365*, 199–206.
- [9] A. Karim, J. Bravo, D. Gorm, T. Conant, A. Datye, *Catal. Today* **2005**, *110*, 86–91.
- [10] K. Yube, M. Furuta, K. Mae, *Catal. Today* **2007**, *125*, 56–63.
- [11] M. Saber, J. M. Commenge, L. Falk, *Chem. Eng. Sci.* **2010**, *65*, 372–379.
- [12] T. A. Nijhuis, A. E. W. Beers, T. Vergunst, I. Hoek, F. Kapteijn, J. A. Moulijn, *Catal. Rev.* **2001**, *43*, 345–380.
- [13] V. Meille, *Appl. Catal. A Gen.* **2006**, *315*, 1–17.
- [14] M. T. Kreutzer, P. Du, J. J. Heiszwolf, F. Kapteijn, J. A. Moulijn, *Chem. Eng. Sci.* **2001**, *56*, 6015–6023.
- [15] M. T. Kreutzer, F. Kapteijn, J. A. Moulijn, *Catal. Today* **2005**, *105*, 421–428.
- [16] M. Al-Rawashdeh, L. J. M. Fluitsma, T. A. Nijhuis, E. V. Rebrov, V. Hessel, J. C. Schouten, *Chem. Eng. J.* **2012**, *181-182*, 549–556.
- [17] T. Conant, A. Karim, A. Datye, *Catal. Today* **2007**, *125*, 11–15.
- [18] E. Ntainjua N., J. K. Edwards, A. F. Carley, J. A. Lopez-Sanchez, J. A. Moulijn, A. A. Herzing, C. J. Kiely, G. J. Hutchings, *Green Chem.* **2008**, *10*, 1162–1169.
- [19] J. K. Edwards, A. Thomas, B. E. Solsona, P. Landon, A. F. Carley, G. J. Hutchings, *Catal. Today* **2007**, *122*, 397–402.
- [20] C. J. Serpell, J. Cookson, D. Ozkaya, P. D. Beer, *Nat. Chem.* **2011**, *3*, 478–83.
- [21] T. A. Nijhuis, F. M. Dautzenberg, J. A. Moulijn, **2003**, *58*, 1113–1124.
- [22] J. Bravo, A. Karim, T. Conant, G. P. Lopez, A. Datye, *Chem. Eng. J.* **2004**, *101*, 113–121.
- [23] E. J. Soares, M. S. Carvalho, P. R. S. Mendes, *Int. J. Heat Fluid Flow* **2006**, *27*, 95–104.
- [24] G. I. Taylor, *Fluid Mech.* **1960**, *10*, 161–165.
- [25] A. Polynkin, J. F. T. Pittman, J. Sienz, *Chem. Eng. Sci.* **2004**, *59*, 2969–2982.
- [26] J. P. J. Van Dalen, *Chromatographia* **1972**, *5*, 354–356.
- [27] R. L. Levy, D. A. Murray, H. D. Gesser, F. W. Hougen, *Anal. Chem.* **1968**, *40*, 459–461.
- [28] G. Redant, P. Sandra, M. Verzele, *Chromatographia* **1982**, *15*, 13–14.
- [29] L. Blomberg, *Chromatographia* **1975**, *8*, 324–326.

Chapter 2

- [30] J. Roeraade, *Chromatographia* **1975**, *8*, 511–516.
- [31] V. Paunovic, V. Ordonsky, M. F. Neira, D. Angelo, J. C. Schouten, T. A. Nijhuis, *J. Catal.* **2014**, *309*, 325–332.
- [32] T. Funada, D. Joseph, *J. Nonnewton. Fluid Mech.* **2003**, *111*, 87–105.
- [33] K. D. Bartle, C. L. Woolley, K. E. Markides, M. L. Lee, R. S. Hansen, *J. High Resolut. Chromatogr. Chromatogr. Commun.* **1987**, *10*, 128–136.
- [34] J.-N. Paquien, J. Galy, J.-F. Gérard, A. Pouchelon, *Colloids Surfaces A Physicochem. Eng. Asp.* **2005**, *260*, 165–172.
- [35] H. Y. Wang, R. S. Foote, S. C. Jacobson, J. H. Schneibel, J. M. Ramsey, *Sensors Actuators B* **2008**, *45*, 199–207.
- [36] M. F. M. Zwinkels, S. G. Jaras, P. Govind Menon, I. Assen Knut, *J. Mater. Sci.* **1996**, *31*, 6345–6349.
- [37] P. Landon, P. J. Collier, A. F. Carley, D. Chadwick, A. J. Papworth, A. Burrows, C. J. Kiely, G. J. Hutchings, *Phys. Chem. Chem. Phys.* **2003**, *5*, 1917–1923.
- [38] J. K. Edwards, B. Solsona, E. N. Ntainjua, A. F. Carley, A. A. Herzing, C. J. Kiely, G. J. Hutchings, *Science* **2009**, *323*, 1037–1041.
- [39] M. F. Neira D'Angelo, V. Ordonsky, V. Paunovic, J. van der Schaaf, J. C. Schouten, T. A. Nijhuis, *ChemSusChem* **2013**, *6*, 1708–16.
- [40] L. A. Truter, D. M. Perez Ferrandez, J. C. Schouten, T. a. Nijhuis, *Appl. Catal. A Gen.* **2015**, *490*, 139–145.
- [41] L. N. Protasova, E. V. Rebrov, H. E. Skelton, a. E. H. Wheatley, J. C. Schouten, *Appl. Catal. A Gen.* **2011**, *399*, 12–21.
- [42] Y. Han, J. Lunsford, *J. Catal.* **2005**, *230*, 313–316.
- [43] C. Samanta, *Appl. Catal. A Gen.* **2008**, *350*, 133–149.
- [44] V. R. Choudhary, Y. V Ingole, C. Samanta, P. Jana, *Ind. Eng. Chem. Res.* **2007**, 8566–8573.
- [45] V. R. Choudhary, C. Samanta, T. V. Choudhary, *J. Mol. Catal. A Chem.* **2006**, *260*, 115–120.
- [46] V. Paunovic, J. C. Schouten, T. A. Nijhuis, *Catal. Today* **2014**, *doi:10.101*, DOI 10.1016/j.cattod.2014.04.007.

Catalyst coating on prefabricated capillary microchannels



Direct synthesis of H₂O₂ over Au-Pd catalyst in a wall-coated microchannel

3

This chapter is published in:

*V. Paunovic, V. Ordonsky, M. F. Neira d'Angelo, J. C. Schouten, T. A. Nijhuis,
Direct synthesis of hydrogen peroxide over Au-Pd catalyst in a wall-coated
microchannel. J. Catal. 2014, 309, 325.*

ABSTRACT

Hydrogen peroxide production via direct hydrogenation of molecular oxygen offers many challenges for both catalyst and reactor development to have a high selectivity. An important advantage of using a capillary channel microreactor is the possibility to use H₂/O₂ concentrations that would be considered explosive in traditional reactors. Au-Pd bimetallic catalysts prepared by impregnation or two-phase synthesis procedure were deposited in a form of thin catalytic film in a capillary microchannel. This coated catalyst performed identical to a comparable slurry catalyst tested in a classical batch autoclave. Operating the microreactor within what would have been the explosive regime in a conventional reactor results in a higher selectivity and productivity.

3.1. Introduction

Efforts to make chemistry “greener” and more sustainable require innovation in chemical processes and chemicals used. Hydrogen peroxide is considered as an environmentally friendly oxidant, since water is the only byproduct remaining after its degradation.

Direct synthesis of H₂O₂ over Au-Pd catalyst in a wall-coated microchannel

However, the anthraquinone auto-oxidation (AO) process that is currently used for large-scale production of hydrogen peroxide cannot be listed as green. Besides its complexity, the main disadvantage of the AO process is waste generation which occurs during the hydrogenation step and results in the formation of hydroanthrahydroquinones, oxantrones and anthrones^[1]. Its green alternative, the direct synthesis method, offers many challenges for both catalyst and reactor development to have a high selectivity to the desired peroxide, since conditions suitable for the synthesis of hydrogen peroxide are the same leading to its decomposition or to a non-selective formation of H₂O. The development of a small scale on demand direct synthesis process for production of ultrapure grade hydrogen peroxide in desirable concentrations without addition of stabilizers and preservatives is of significant interest for fine chemical industry^[2,3]

Direct synthesis of hydrogen peroxide is a complex three-phase process which uses solid catalyst, H₂/O₂ mixtures supplied in a gas state and a solvent. An obvious drawback for the direct formation of hydrogen peroxide from H₂ and O₂ is the very wide explosive region. Reactor miniaturization provides an opportunity to safely handle the direct hydrogenation of molecular oxygen. The safety of this reaction in a wall-coated microchannel is influenced by the combination of temperature and pressure applied. The safety considerations of working with potentially explosive hydrogen and oxygen mixtures in a wall-coated microchannel are discussed in detail by Chattopadhyay and Veser^[4]. Upon addition of the catalyst ignition is shifted towards lower temperatures. Both the homogeneous high temperature dominated, and the heterogeneous catalyst initiated ignition branch were taken into account. Simulations showed that a reactor diameter of 300 μm can be considered intrinsically safe (temperature independent) at 1 bar pressure. With increasing pressure in the system homogeneous reactions tend to accelerate, scaling with the square of reactor pressure, due to the dominance of bimolecular collisions, in contrast to surface reactions, which show linear dependence on pressure. However, at higher pressures surface reactions will be limited by diffusion of reacting species from the bulk face to catalytic surface, considering that $D \sim P^{-1}$. This means that consumption of reactants is accelerated near the catalytic wall, but delayed in the bulk phase. Chattopadhyay and Veser clearly show that for pressures as high as 10 bar, even in case of extremely small reactor diameters, ignition is dominated by the homogeneous reaction pathway. To operate a wall-coated catalytic reactor safely at higher pressures, it is crucial to stay below the critical ignition temperature, below which homogeneous ignition (explosion) can no longer occur for the desired channel diameter. Performing the reaction in a two-phase gas-liquid flow additionally diminishes the possibility for radical or/and hot-spot formation. The liquid separates the gas in small bubbles and acts as a large heat sink.

Chapter 3

A catalytic microreactor for direct synthesis can be realized as packed-bed column^[5-7] or the catalyst can be immobilized on the walls of the microchannel^[8]. Catalyst deposition in the form of a catalytic film on the walls of gas-liquid microreactors is preferred over a catalyst bed due to the high pressure-drop^[5,6] and poor catalyst wetting and contacting^[9] associated with a packed-bed. Kobayashi et al.^[10] first introduced the method to deposit a colloidal solution of Pd encapsulated in copolymer-micells with polystyrene backbone on the walls of a microchannel creating thin layers covalently bonded to the glass surface. However, the acidic conditions applied in the direct hydrogen peroxide synthesis are unfavourable for the stability of this kind of liquid film.

In this work the focus is on the preparation of well-adhered and uniform catalytic layers inside closed capillary channels which are embedded subsequently with bimetallic Au-Pd nanoparticles. Supports with a low isoelectric point, such as SiO₂, are favourable for peroxide formation as this results in lower subsequent hydrogenation rates^[11]. For this reason, we used silica wash-coat layer as support. The main benefit of the application of porous films with a large internal surface area as a catalyst support in general is the considerably enhanced surface available for catalyst deposition compared to the geometric surface area of the microchannel wall only. The reaction rate per unit volume of microchannel in case of heterogeneously catalyzed reactions is directly determined by the available catalytic surface area^[12] since microchannels possess excellent mass and heat transfer properties.

3.2. Materials and Methods

3.2.1. Preparation of microchannel wash-coats

Uncoated fused silica capillaries 320 μm in diameter were wash-coated by displacing a plug of the coating slurry using N₂. The coating slurry contains fumed silica, silica gel and sodium-silicate and colloidal silica as binders. The most critical aspect of the coating is maintaining the film uniformity during and after displacement of the coating fluid. The uniformity of the coating thickness is greatly affected by the ability to maintain the coating parameters such as coating velocity, temperature and solvent evaporation rate constant during and after displacement of the coating solution. Disregarding those parameters often results in severe coating non-uniformity with often an order of magnitude high variation in layer thickness along the capillary length. To accurately control those critical coating parameters and prevent formation of layer non-uniformities, coating set-up was built (Chapter 2, Fig. 2.2). The layer thickness and uniformity were assessed using scanning electron microscopy (SEM). Additional ultrasonic adherence tests were performed to ensure mechanical stability of the wash-coated layer under reaction conditions. No loss of coating layer was observed after ultrasonic testing or after reaction performed.

3.2.2. Catalyst preparation

A gold-palladium catalyst was chosen for the direct hydrogen peroxide synthesis, since Pd alloyed with Au shows an enhanced activity to peroxide formation compared to the traditionally employed Pd catalyst [13–16]. The silica layer coated on the reactor walls or dried wash-coat powder material was functionalized with active Au-Pd metallic species by impregnation with aqueous solutions of $HAuCl_4$ and $PdCl_2$ or deposition of stabilized Au-Pd nanoparticles prepared using a two-phase synthesis method. Au-Pd nanoparticles were synthesized in dichloromethane following the protocol described elsewhere [17]. This two-phase synthesis approach, originally introduced by Brust and co-workers [18] involves transfer of tetrachloropalladate and tetrachloroaurate ions from water to the organic phase by means of tetraoctylammonium chloride as a phase transfer agent and subsequent reduction using $NaBH_4$. The layer of the phase transfer agent stabilizes nanoparticles sterically in the organic solvent.

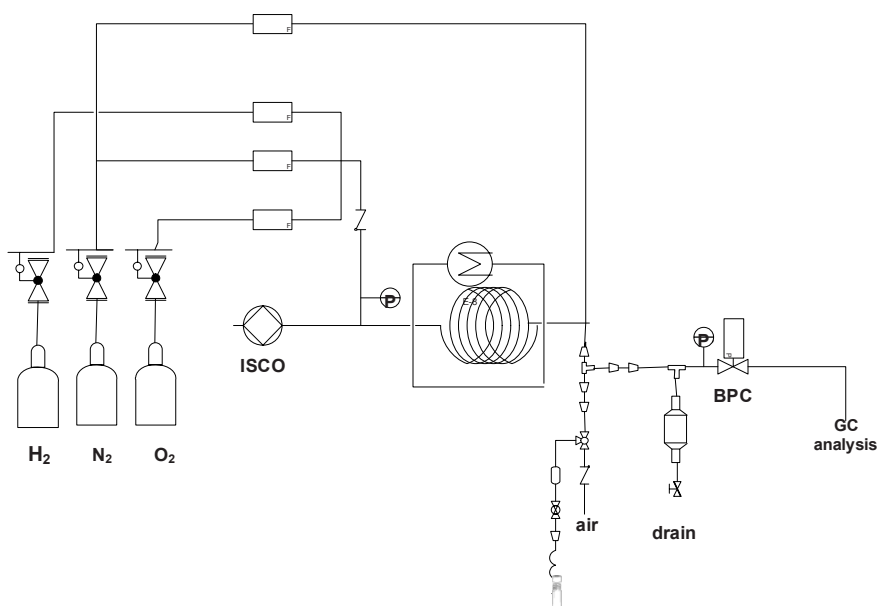


Figure 3.1. Scheme of micro-capillary set-up for direct synthesis of hydrogen peroxide

The application of dichloromethane in the catalyst preparation enables a fast evaporation of solvent, thus making the catalyst preparation process faster and more efficient. The concentrations of the metal precursors were adjusted to give an approximately 5 wt%

Chapter 3

total loading of the bimetallic catalyst with a variable Au/Pd molar ratio with respect to SiO₂ wash-coat material. The catalytic layers were dried at 120 °C for 12 h and calcined at 380 °C for 4h, since this is the upper temperature limit for the protective polymer film on the outside of the capillary.

Catalysts prepared by traditional wet impregnation were prepared by impregnating SiO₂ coated layer with a solution containing dissolved the required amounts of HAuCl₄ and PdCl₂ to achieve an approximately 5 Wt% loading calculated on the amount of support coated. After water removal the capillary was dried at 120 °C and calcined at 380 °C. Subsequently, the impregnated catalyst was reduced in a H₂ flow at 300 °C prior to use.

Deposition of active metallic species onto the pre-formed silica layer ensures that the catalyst remains accessible on the silica surface. A capillary filled with the solution containing Au and Pd was placed in an oven and the solvent was evaporated slowly avoiding temperature gradients. Both ends of the capillary were placed in a glass vial with perforated cap in order to collect and quantify the excess solution that might leave the capillary during the drying process.

The silica powder used as catalyst support in semi-batch experiment was obtained by drying the coating slurry. Upon drying, silica particles were stirred with 1M solution of NH₄NO₃ overnight, dried and sieved prior to addition of the Au-Pd nanoparticles.

The metal loadings were verified by Inductively Coupled Plasma (ICP).

3.2.3. Catalyst characterization

The thickness of the washcoat layer was determined with a XL30-ESEM-FEG scanning electron microscope (SEM) operated at 10 kV, with a working distance of 10 mm from the sample. Gold sputtering was used to coat the samples making them more conductive. The coating thickness was measured at three different cross-sections along the capillary length. Au-Pd particle size was examined by using TEM with a FEI Tecnai G2 Sphera transmission electron microscope at an acceleration voltage of 200 kV.

TGA analysis was done to determine the temperature required to remove the tetraoctylammonium species used as a phase transfer agent and stabilizer in two-phase removal was heated up to 750°C, with a temperature ramp of 5 °C/min. The weight of the sample was monitored as a function of temperature. No weight loss was observed at a temperature higher than 330 °C, which indicates that stabilizer molecules are not present on the catalyst after calcination at 380°C.

ICP analysis was performed to determine actual amount of Au and Pd present in the microchannel. Au-Pd samples were dissolved in aqua regia (HCl : HNO₃=1:3) and diluted

Direct synthesis of H₂O₂ over Au-Pd catalyst in a wall-coated microchannel

with distilled water. The instrument was calibrated using standard gold (Merck, 999 mg/L \pm 2 mg/L Au) and palladium (Merck, 999 mg/L \pm 2 mg/L Pd) solutions.

3.2.4. Catalytic testing

Catalytic testing was done in a conventional Titanium batch autoclave reactor and in a microcapillary set-up. The catalyst performance in the microchannel was investigated using both pure and diluted hydrogen –oxygen mixtures in order to study the effect of higher reactant partial pressures.

3.2.4.1. Slurry catalyst testing

The Au-Pd catalyst used in autoclave testing was immobilized on dried and sieved SiO₂ slurry particles in order to have an identical silica support in both types of experiments. The total loading of Au and Pd was approximately 5 wt%. The direct H₂O₂ synthesis is a three-phase process which involves H₂/O₂ mixtures as a gas phase, a solvent and the solid catalyst phase. The role of the liquid phase supplied is to collect and solubilize hydrogen peroxide formed, since pure hydrogen peroxide is highly unstable and decomposes to water and oxygen. To additionally minimize hydrogen peroxide decomposition, a water solution containing 0.05 M of sulfuric acid containing approximately 9 ppm of NaBr was used in all experiments as a liquid phase. Acids such as sulfuric or phosphoric decelerate based-catalyzed decomposition of peroxide, while bromide ions even at very low concentrations poison catalytic sites that promote O₂ dissociation and direct formation of water [19,20].

Semi-batch experiments were carried out in a 300 ml Titanium Gr2 autoclave. The reactor is equipped with magnetic impeller designed to stir up to a maximum 3000 rpm and electrical heating. The pressure in reactor is controlled by back pressure controller (BPC). Gas mixture containing 4 vol% of H₂ and O₂ was supplied through the stirrer shaft. Typically, 1/3 of the total autoclave volume was filled with the liquid phase containing catalyst powder. All experiments were done at 30°C, while pressure was maintained at 20 bar. After the desired temperature and pressure were reached, stirring was started. The rotation speed was varied in a range 800-1500 rpm to determine the optimum agitation speed. Both gas and liquid phase analysis were conducted using on-line GC equipped with TCD detector and hydrogen peroxide titration with standard solution of cerium (IV) sulphate respectively. Productivity and selectivity values in the semi-batch experiments are calculated using the following expressions:

$$\text{Productivity} = \frac{\Delta C_{\text{H}_2\text{O}_2} \times V_{\text{liquid}} \times M \left(\frac{\text{g}}{\text{mol}} \text{H}_2\text{O}_2 \right)}{\Delta t \times m_{\text{cat}}}$$

Chapter 3

$$\text{Selectivity} = \frac{\Delta C_{\text{H}_2\text{O}_2} \times V_{\text{liquid}}}{\text{moles H}_2 \text{ reacted}}$$

These correlations provide the productivity and selectivity at a certain moment in time in the reactor, rather than giving the cumulative numbers. In case if at the certain time more peroxide is decomposed than produced, this will therefore result in negative productivity and selectivity.

3.2.4.2. Microchannel catalyst testing

Microchannel experiments were performed feeding both pure and diluted H₂ and O₂ mixtures, while in semi-batch experiments only diluted mixtures were used due to explosion concerns. A catalytic capillary was placed in a thermostated oven. The water phase is supplied to the system by means of a syringe pump (Teledyne ISCO 500D). The total gas flow through capillary is set at 5 mlN/min, keeping the H₂/O₂ ratio always 1:1. In case of a diluted mixture, H₂ and O₂ content is set to be identical to the semi-batch process (4 vol%). In order to maintain a constant pressure at 20 bar, back pressure regulator is placed downstream after a gas/liquid separation unit. When pure H₂/O₂ mixtures are used, the gas is diluted with N₂ at the capillary outlet. The flow pattern observed under those reaction conditions was segmented gas-liquid flow (Taylor slug flow). A piece of empty 320 μm glass capillary was connected before the capillary coated with catalytic layer to be able to visually observe the flow pattern. The catalytic layer coated is relatively thin, thus it is expected that the same flow regime is retained in the wall-coated microchannel. The pressure in the system was monitored before the inlet and after the microchannel outlet. Pressure drop over the capillary was used as an indirect indication of the quality of the coating procedure. Typically, capillary length used in the experiments was in a range of 0.5-1 m. Defects in coatings would lead to a higher pressure drop and such capillaries would not be considered to be used in reaction. Gas samples were analyzed with compact GC (column: Molsieve plot 5m*0.32mm) equipped with TCD detector. Liquid samples were collected each 30 min and immediately titrated with a standard solution of cerium (IV) sulphate. Productivity and selectivity values are calculated in time using the regular expressions for a continuously operated reactor:

$$\text{Productivity} = \frac{\text{Liquid flow rate} \times C_{\text{H}_2\text{O}_2} \times M \left(\frac{\text{g}}{\text{mol}} \text{H}_2\text{O}_2 \right)}{m_{\text{cat}}}$$

$$\text{Selectivity} = \frac{\text{moles H}_2\text{O}_2 \text{ formed}}{\text{moles H}_2 \text{ reacted}}$$

3.3. Results and Discussion

3.3.1. Catalyst characterization

The average particle size of catalysts prepared using two-phase synthesis protocol or impregnation was determined by means of TEM. Approximately 20 micrographs were recorded for each sample and for the most representative pictures particle sizes were analyzed. In order to analyze the catalyst immobilized inside the fused silica capillaries, silica capillaries with catalyst deposited were crushed to give a powder which can be observed under microscope.

Sample	Average particle size (nm)	Standard deviation (nm)	Sample size
Au-Pd alloy (1:2)/CH ₂ Cl ₂	4.14	0.57	98
Au-Pd alloy (1:2)/capillary	4.24	1.95	111
Au-Pd alloy (1:2)/SiO ₂ slurry	3.98	1.52	95
Au-Pd alloy (1:1)/capillary	5.59	2.40	110
Au-Pd impregnated (1:1)/capillary	1.81 ^a	0.22 ^a	91

Table 3.1. Average particle size and particle size distribution derived from TEM data.

^a) Randomly present particle agglomerates noticed on 5 out of 20 TEM images were not taken into account when calculating average particle size.

Although the impregnation method produced particles of approximately 2 nm in diameter, randomly present large particle agglomerates are evident (Fig. 3.2.e, Table 3.1). For comparison, micrographs of Au-Pd colloidal nanoparticles suspended in dichloromethane, immobilized on dried and sieved silica wash-coat powder or nanoparticles deposited on wash-coat layer inside the microchannels were recorded (Fig. 3.2 a, b and c). TEM analysis revealed that the synthesized Au-Pd colloidal nanoparticles are almost monodisperzed with an average particle size of approximately 4 nm (Fig 3.2a).

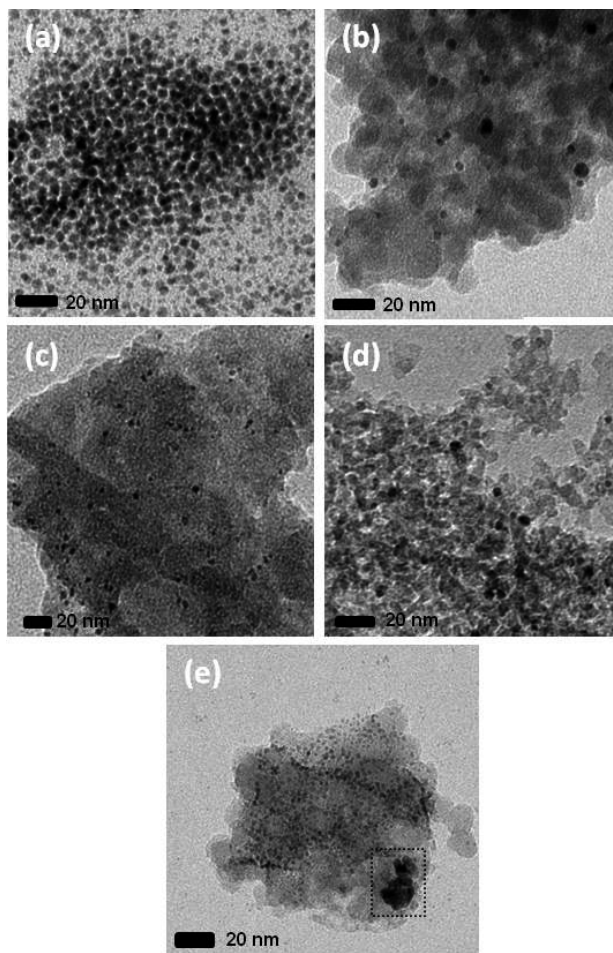


Figure 3.2. TEM data for (a) Au-Pd colloidal alloy (1:2) nanoparticles suspended in dichloromethane (b) capillary with deposited Au-Pd (1:2) alloy nanoparticles (c) Au-Pd alloy (1:2) nanoparticles immobilized on dried SiO₂ slurry powder (d) capillary with deposited Au-Pd (1:1) alloy nanoparticles (e) capillary impregnated with HAuCl₄ and PdCl₂ and reduced in H₂ flow (Au:Pd=1:1); Black dashed square shows particle agglomerates observed on TEM micrographs.

However, when the nanoparticles were deposited on silica support, the average particle size remained around 4 nm, but the particle size distribution broadened (Table 3.1). The

Direct synthesis of H₂O₂ over Au-Pd catalyst in a wall-coated microchannel

average particle size and particle size distribution of the Au-Pd nanoparticles immobilized inside the SiO₂ coated channel or on dried silica slurry support are in agreement (see Table 3.1).

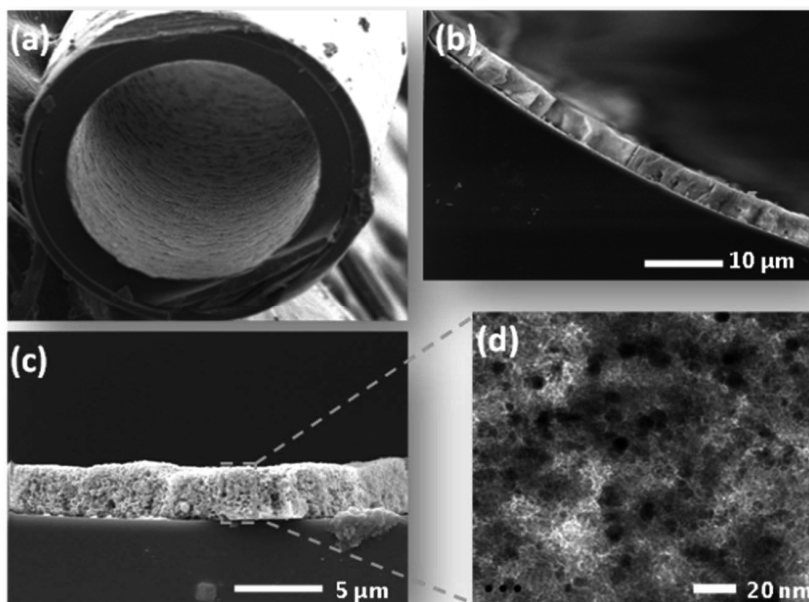


Figure 3.3. 320 μm ID capillary wash-coated with porous SiO₂ layer (a) cross-section of SiO₂ coated capillary (b) and (c) Magnified SEM image of SiO₂ wash-coat (d) TEM image of Au-Pd alloy nanoparticles deposited on the SiO₂ layer.

Please note that data on XPS analysis of Au, Pd and Au-Pd colloidal nanoparticles supported on silica are given in Chapter 6 as well as FTIR spectra of adsorbed CO.

In order to determine the uniformity of layer thickness along the capillary length and cross section, the coating thickness of each sample was measured at 3 different positions along the capillary. The variance of these data is used to assess the uniformity of the wash-coat layer. The average thickness of a single coated layer used further for catalyst testing in a microchannel was estimated to be approximately $4 \mu\text{m} \pm 0.8 \mu\text{m}$. Uniformity of the Au-Pd loading along the capillary length was difficult to determine directly. The loading of Au and Pd per capillary length is rather low, meaning that the amount of metal extracted from short capillary sections by dissolving it in aqua regia would be below the measuring range of ICP. The sections of the capillary with high(er) metal content would result in a darker colour shade after the calcination step in contrast to less loaded sections. This visual criterion provided a rough estimate of metal loading uniformity.

3.3.2. Catalytic testing

In order to obtain stirrer speed beyond which mass transfer effects can be neglected, reaction rate was studied as a function of agitation speed. The agitation speed in semi-batch reactor was varied in a range of 800-1500 rpms (rotations per minute). It was observed that the maximum initial productivity is already reached at 1300 rpms, therefore this stirring speed was used in subsequent experiments. Fig. 3.4 shows peroxide yield, H₂ conversion and selectivity versus time at optimum stirring speed. The data reveal that hydrogen peroxide formation rate and selectivity towards peroxide decrease as reaction proceeds. As the peroxide concentration in liquid phase becomes higher, the rates of peroxide conversion reactions (decomposition and hydrogenation) increase until the rate of the hydrogen peroxide conversion reactions becomes identical to the peroxide formation rate resulting in a levelling off of the peroxide concentration 4 h after the reaction start as shown in the Fig. 3.4. Since effectively no additional quantity of peroxide is generated, at this point the apparent selectivity of reaction drops to zero, as shown on the graph.

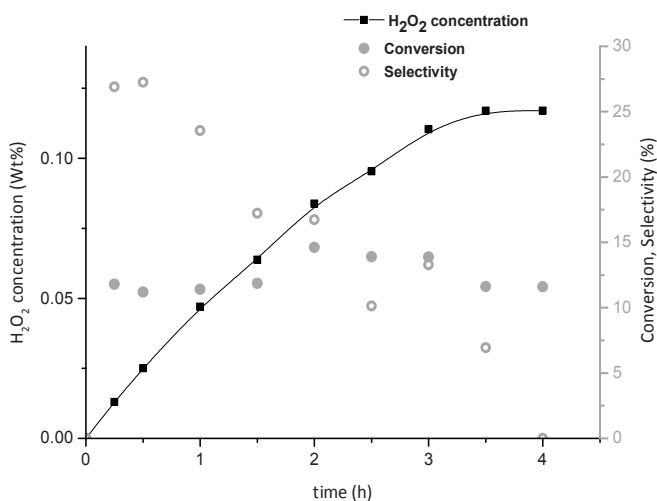


Figure 3.4. H₂O₂ synthesis experiment in autoclave set-up at optimal stirring speed (1300 rpms); T=30°C, p=20 bar, liquid phase 0.05 M H₂SO₄, 9 ppm NaBr; gas-phase 4 vol % H₂ and O₂; Catalyst Au-Pd (1:2) colloidal nanoparticles supported on sieved and dried silica slurry particles, X-axis designates time from experiment initiation.

The constant H₂ conversion throughout the semi-batch reaction and the constant productivity and selectivity observed with the same type of catalyst in the flow system

Direct synthesis of H₂O₂ over Au-Pd catalyst in a wall-coated microchannel

(Fig. 3.5) indicate that at these reaction times the catalyst does not deactivate. The decrease in the rate of direct peroxide formation in autoclave is not a consequence of catalyst deactivation or leaching, but a kinetically controlled increase in the rate of side reactions (hydrogenation and/or decomposition) with accumulation of peroxide in the liquid phase. Moreover, no loss of activity was observed even after operating the catalyst for three weeks in the microchannel.

The use of stabilizing agents in nanoparticle synthesis might be disadvantageous for its catalytic activity ^[21]. Therefore both dried and calcined Au-Pd colloidal nanoparticles supported on silica were tested in autoclave in order to observe the effect of heat treatment applied to the catalyst on its performance. Both calcined catalysts showed higher productivity values compared to their dried analogues (see Table 3.2).

Catalyst	Initial conversion, %	Initial productivity, gH ₂ O ₂ /g _{cat} h	Initial selectivity, %
Au-Pd alloy (1:2)/SiO ₂ /dried	2.4	1.032	16.21
Au-Pd alloy (1:2)/SiO ₂ /calcined	11.8	11.06	26.9
Au-Pd alloy (1:1)/SiO ₂ /dried	2.5	1.41	18.8
Au-Pd alloy (1:1)/SiO ₂ /calcined	15.3	10.46	20.1

Table 3.2. Effect of heat treatment on catalyst performance.

Additionally, thermogravimetric analysis (TGA) was done to detect carbon species possibly present on the catalyst surface. Analysis confirmed that after the calcination heat treatment the protective tetraoctylammonium layer is removed and the particle surface is accessible.

A comparison between semi-batch and microchannel experiments when diluted gas mixtures were used containing 4 vol% of H₂ and O₂ is given in Fig. 3.5. The initial productivity and selectivity values observed in the autoclave in the absence of mass transfer limitations show similar values to the steady-state productivity and selectivity obtained in a microchannel under similar reaction conditions. This observation demonstrates that the use of microchannel is not necessarily beneficial when compared to well-stirred slurry reactor systems. Furthermore, it is a good indication that we successfully prepared an active catalyst in a microchannel which performs identical to a

Chapter 3

conventional powdered catalyst. A clear benefit for the usage of a continuous microreactor is already visible in Fig. 3.5, as the high productivity is maintained and selectivity does not decrease in time.

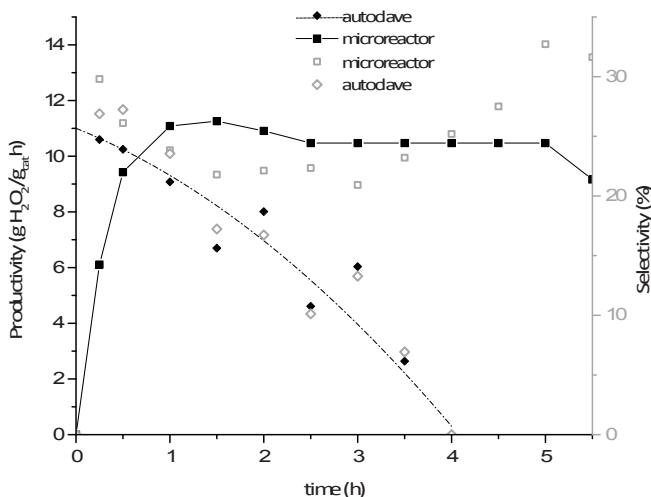


Figure 3.5. Comparison of productivity and selectivity values in autoclave and microchannel under diluted conditions (4 vol% of H₂ and O₂); T=30°C, p=20 bar, liquid phase 0.05 M H₂SO₄, 9 ppm NaBr; Catalyst Au-Pd (1:2) colloidal nanoparticles; microchannel total gas flow rate 5 ml/min with liquid flow rate 0.1 ml/min; X-axis designates time from reaction initiation (residence time for liquid phase in autoclave only, time on stream in microchannel experiment and for gas phase in autoclave).

A method to increase the peroxide production rate is to apply pure H₂/O₂ mixtures, which can be safely handled in the microchannel reactor system. Fig. 3.6. shows that switching the feed composition from non-explosive to explosive H₂/O₂ compositions (50:50, v/v) results in a major increase in both the productivity as well as the selectivity.

As discussed earlier, at concentrations as low as 4 vol% H₂ productivities observed in a microreactor are in the absence of mass transfer effects. However, with higher H₂ and O₂ partial pressures, the rate of peroxide formation is reaching higher values and in this regime mass transfer limitations cannot be excluded. The observed productivity of the Au-Pd alloy catalyst under conventionally explosive conditions is almost an order of magnitude higher than observed productivity under non-explosive conditions. This

Direct synthesis of H_2O_2 over Au-Pd catalyst in a wall-coated microchannel

possibility to operate under these conditions and thereby have this excellent performance makes the microreactor a highly attractive option.

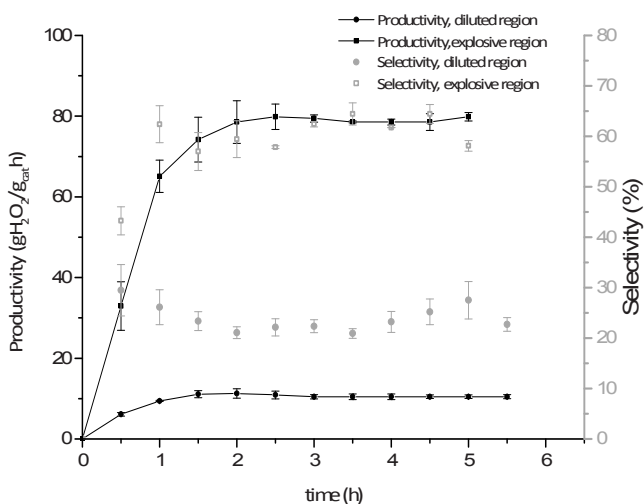


Figure 3.6. H_2O_2 synthesis using Au-Pd alloy catalyst at non-explosive vs. explosive H_2/O_2 ratio in a microchannel; total gas flow rate 5ml/min, liquid flow rate 0.1 ml/min, $T=30^\circ C$, $p=20$ bar, liquid phase 0.05 M H_2SO_4 , 9 ppm NaBr; capillary ID $320\mu m$; X-axis designates time on stream.

Although, non-selective formation of water seems to be substantial at lower H_2 and O_2 partial pressures, a significant decrease is observed when the reaction is performed in the explosive regime. This increase in selectivity can be explained by a previously proposed surface reaction mechanism for hydrogen peroxide and water formation^[11,22] which indicates that hydrogen peroxide formation proceeds only via hydrogenation of adsorbed O_2 . If dissociative adsorption of O_2 occurs due to the presence of the neighbouring active site, only water is generated. The results suggest that with higher partial pressures of reactants resulting in a higher surface coverage, dissociation of adsorbed oxygen is suppressed by a lower number of available neighbouring vacant dissociation sites leading to an almost factor of 3 higher selectivity.

Chapter 3

To study the effect of the overall pressure on the selectivity and productivity, the direct synthesis reaction was performed varying the pressure between 15 and 25 bar. Fig. 3.7. confirms that an increase in the partial pressures of H₂ and O₂ results in both higher reaction rates and a higher selectivity toward peroxide. To reach high selectivity and productivity values, lower concentrations of hydrogen and oxygen in the gas phase can be compensated by applying a higher pressure. However, the possibility to handle conventionally explosive mixtures within microchannels eliminates the need for high pressure conditions and allows a better reactor performance at the same total pressure.

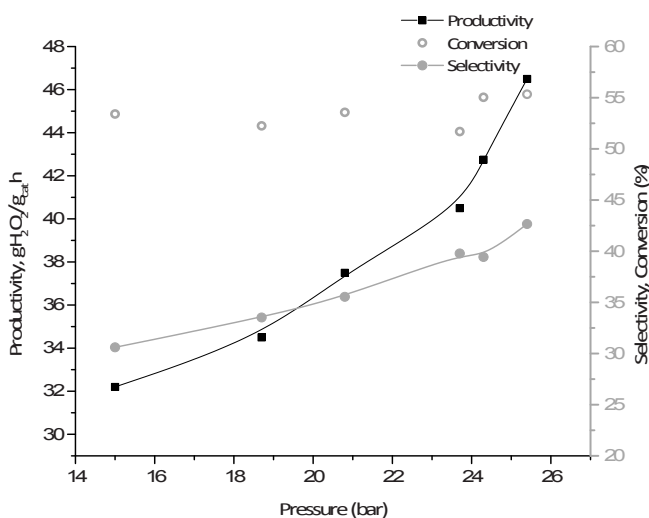


Figure 3.7. Effect of total pressure on the direct synthesis in a microchannel; T=42°C, liquid phase 0.05 M H₂SO₄, 9 ppm NaBr; liquid flow rate 0.05 ml/min; catalyst Au-Pd (1:2) colloidal nanoparticles, 20 vol% of H₂ and O₂, total gas flow rate 5ml/min.

Practising direct synthesis reaction using concentrated hydrogen-oxygen mixtures needs to be done cautiously. Inoue et al. reported that despite small dimensions of glass chips applied in direct synthesis, explosions were still occurring if catalyst was maldistributed within reactor channels during packaging procedure [6]. Due to high catalyst concentration within packed bed, proper dilution of the catalyst bed with inert material as well as contacting of the catalyst with the liquid phase and wetting efficiency are critical to avoid high local heat generation and formation of hotspots. However, in case of wall-coated microchannel, amount of catalyst per channel volume is relatively small and catalyst is continually wetted with thin liquid layer preventing the possibility of local overheating and

Direct synthesis of H₂O₂ over Au-Pd catalyst in a wall-coated microchannel

chain-branching reactions. In practise, wall-coated microchannel proved to be safe, since no explosions or capillary breakages were observed while performing direct synthesis reaction under conventionally explosive conditions.

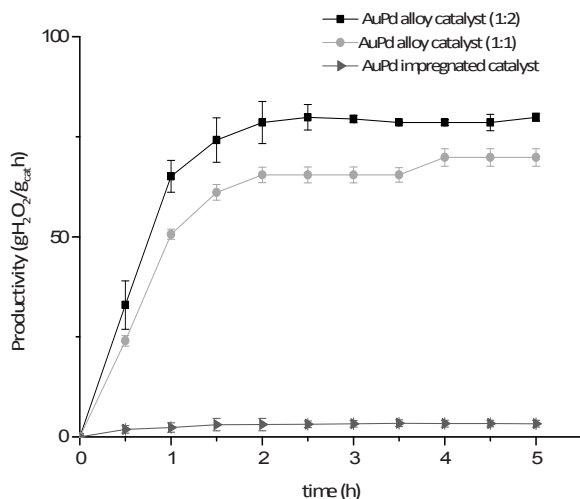


Figure 3.8. Au-Pd catalyst performance in microreactor tests in explosive conditions; total gas flow rate 5ml/min (50:50 v/v), liquid flow rate 0.1 ml/min, T=30°C, p=20 bar, liquid phase 0.05 M H₂SO₄, 9 ppm NaBr; 320µm ID capillary; X-axis designates time on stream.

Three different Au-Pd catalysts supported on a microchannel wall were tested in the direct synthesis of hydrogen peroxide using a 50:50 v/v H₂/O₂ mixture. A comparison of the activities of the catalysts prepared using colloidal particles or directly impregnated in the capillary microchannel (Fig. 3.8.) shows a superior activity for the nanoparticles. Impregnation, as the most routinely used method in catalyst preparation produces catalysts with low activity for H₂O₂ production. This low activity is associated with the presence of inactive large agglomerates or poor dispersion [23,24]. In contrast, the enhanced performance of bimetallic nanoparticles synthesized in a non-polar organic solvent via two-phase synthesis method can be attributed to better particle size control due to steric stabilization via alkyl groups present [25] and uniform alloying [17]. A comparison of the catalytic activities of nanoparticles with a different Au:Pd molar ratio shows that decreasing the Au content from 1:1 to 1:2 results in a higher reaction rate. Earlier it was suggested that Au-Pd catalysts exhibit a maximum synthesis activity when the Au:Pd ratio

Chapter 3

is in a range of 1:1.85 to 1:2 ^[15]. A further increase in the gold content proved to be disadvantageous for catalysis.

For operating the direct synthesis reaction in a continuous mode catalyst stability under reaction conditions is an imperative. Exposure to acidic conditions and reductive and oxidative environment might influence catalyst performance over time. Stability of the Au-Pd alloy catalyst (1:2) was studied in detail under continuous operation using gas feed with 1:1 H₂ to O₂ ratio. No loss of activity was observed after three weeks operation.

3.4. Conclusions

The direct synthesis of hydrogen peroxide over Au-Pd catalyst was performed in a single wall coated microchannel. Uniform and stable catalytic films were prepared inside a closed capillary. The desired uniformity and reproducibility of the deposited film was achieved by controlling the displacement velocity of coating plug during coating process and subsequent drying.

Catalytic tests done in a slurry reactor and microchannel under diluted hydrogen-oxygen mixtures show that the microchannel does not outperform conventional slurry reactor. However, we have demonstrated that it is possible to achieve an order of magnitude higher reaction rates when operating the same catalyst under conventionally explosive conditions in the microchannel. Even more important, higher hydrogen and oxygen partial pressures proved to be highly beneficial for the selectivity as well resulting in less water formed in the explosive regime.

A significant improvement in the peroxide production rate was achieved with using a two phase synthesis of nanoparticles. Better control over alloying and particle size associated with those nanoparticles is crucial for its catalytic activity. The calcination step applied during catalyst preparation ensures removal of the nanoparticle protective layer, which could limit the availability of reactants on the catalytic surface during the reaction. The activity is very much dependent on the Au:Pd ratio and for maximizing the production rate of peroxide it is necessary to determine the optimum ratio. Important aspect for continuous production of hydrogen peroxide is certainly stable catalyst performance over time. Supported Au-Pd nanoparticles remained equally active in direct synthesis under continuous operation over several weeks.

References:

- [1] W. K. and O. W. G. Goor, *Ullmann's Encyclopedia of Industrial Chemistry*, , Vol. A13, Wiley-VCH Verlag GmbH & Co. KGaA, Weinheim, Germany, **1989**.
- [2] C. W. Jones, *Application of Hydrogen Peroxide and Derivatives*, The Royal Society Of Chemistry, Cambridge, UK, **1999**.
- [3] R. Noyori, M. Aoki, K. Sato, *Chem. Commun. (Camb)*. **2003**, 1977–86.
- [4] S. Chattopadhyay, G. Veser, *AIChE J.* **2006**, *52*, 2217–2229.
- [5] T. Inoue, Y. Kikutani, S. Hamakawa, K. Mawatari, F. Mizukami, T. Kitamori, *Chem. Eng. J.* **2010**, *160*, 909–914.
- [6] T. Inoue, M. A. Schmidt, K. F. Jensen, *Ind. Eng. Chem. Res.* **2007**, *46*, 1153–1160.
- [7] Y. Voloshin, R. Halder, A. Lawal, *Catal. Today* **2007**, *125*, 40–47.
- [8] J. F. Ng, Y. Nie, G. K. Chuah, S. Jaenicke, *J. Catal.* **2010**, *269*, 302–308.
- [9] D. van Herk, P. Castaño, M. Makkee, J. A. Moulijn, M. T. Kreutzer, *Appl. Catal. A Gen.* **2009**, *365*, 199–206.
- [10] J. Kobayashi, Y. Mori, K. Okamoto, R. Akiyama, M. Ueno, T. Kitamori, S. Kobayashi, *Science* **2004**, *304*, 1305–8.
- [11] E. Ntainjua N., J. K. Edwards, A. F. Carley, J. A. Lopez-Sanchez, J. A. Moulijn, A. A. Herzing, C. J. Kiely, G. J. Hutchings, *Green Chem.* **2008**, *10*, 1162–1169.
- [12] S. R. a de Loos, J. van der Schaaf, M. H. J. M. de Croon, T. a. Nijhuis, J. C. Schouten, *Chem. Eng. J.* **2011**, *167*, 671–680.
- [13] P. Landon, P. J. Collier, A. F. Carley, D. Chadwick, A. J. Papworth, A. Burrows, C. J. Kiely, G. J. Hutchings, *Phys. Chem. Chem. Phys.* **2003**, *5*, 1917–1923.
- [14] J. K. Edwards, B. Solsona, E. N. Ntainjua, A. F. Carley, A. A. Herzing, C. J. Kiely, G. J. Hutchings, *Science* **2009**, *323*, 1037–1041.
- [15] J. Pritchard, L. Kesavan, M. Piccinini, Q. He, R. Tiruvalam, N. Dimitratos, J. a Lopez-Sanchez, A. F. Carley, J. K. Edwards, C. J. Kiely, et al., *Langmuir* **2010**, *26*, 16568–77.
- [16] E. N. Ntainjua, M. Piccinini, S. J. Freakley, J. C. Pritchard, J. K. Edwards, A. F. Carley, G. J. Hutchings, *Green Chem.* **2012**, *14*, 170.
- [17] C. J. Serpell, J. Cookson, D. Ozkaya, P. D. Beer, *Nat. Chem.* **2011**, *3*, 478–83.
- [18] M. Brust, M. Walker, D. Bethell, D. J. Schiffrin, R. Whyman, *J.Chem.Soc.,Chem.Commun.* **1994**, 801–802.
- [19] Y. Han, J. Lunsford, *J. Catal.* **2005**, *230*, 313–316.
- [20] C. Samanta, *Appl. Catal. A Gen.* **2008**, *350*, 133–149.
- [21] A. Villa, D. Wang, D. S. Su, L. Prati, *ChemCatChem* **2009**, *1*, 510–514.
- [22] M. Piccinini, E. Ntainjua, J. K. Edwards, A. F. Carley, J. a Moulijn, G. J. Hutchings, *Phys. Chem. Chem. Phys.* **2010**, *12*, 2488–2492.

Chapter 3

- [23] J. K. Edwards, A. F. Carley, A. a. Herzing, C. J. Kiely, G. J. Hutchings, *Faraday Discuss.* **2008**, *138*, 225.
- [24] J. K. Edwards, S. F. Parker, J. Pritchard, M. Piccinini, S. J. Freakley, Q. He, A. F. Carley, C. J. Kiely, G. J. Hutchings, *Catal. Sci. Technol.* **2013**, *3*, 812.
- [25] D. I. Gittins, F. Caruso, *Angew. Chem. Int. Ed.* **2001**, *40*, 3001–3004.

Direct synthesis of H₂O₂ over Au-Pd catalyst in a wall-coated microchannel

Direct synthesis of H₂O₂ in a wall-coated microchannel over Au-Pd catalyst- microchannel performance study

4

This chapter is published as:

V. Paunovic, J. C. Schouten, T. A. Nijhuis, Direct synthesis of hydrogen peroxide in a wall-coated microchannel over Au-Pd catalyst- microchannel performance study. Cat. Today, 2014, 248, 160.

ABSTRACT

The direct synthesis of hydrogen peroxide out of hydrogen and oxygen has been studied in a wall-coated microchannel. A silica wash-coat layer embedded with Au-Pd colloidal nanoparticles served as an active catalyst for the direct synthesis reaction. The influence of different reaction variables has been evaluated in order to identify optimal process conditions and to maximize the concentration of peroxide produced in the liquid phase. The gas mixture used in this study contained hydrogen and oxygen concentrations that would be considered explosive in conventional reactors. The results presented here show that combining the active Au-Pd catalyst with microchannel technology can lead up to 5 wt% peroxide solutions at hydrogen conversions as high as 80 %.

4.1. Introduction

The direct synthesis of hydrogen peroxide is a green alternative to the current Anthraquinone autoxidation (AO) process. The major disadvantages of the AO process are its complexity and the waste generation caused by accumulation of permanently

hydrogenated alkylanthraquinone products hydroanthrahydroquinones, oxantrones and anthrones^[1]. In order to be economically viable, the process needs to run on a large scale of at least 40kt/year for each production unit. The world's largest plants situated in Antwerp and Thailand are designed to produce 230 and 330 kt/year of hydrogen peroxide respectively. Besides the complexity of such large scale processes, the transportation of concentrated peroxide solutions to the customer sites requires special precautions related to safety. For many application, such as in fine chemical industry^[2,3], the development of a small scale on demand direct synthesis process for production of ultra-pure grade hydrogen peroxide in desirable concentrations without the addition of stabilizers and preservatives is of significant interest, thus avoiding the risks of transportation and storage of hydrogen peroxide and possible effects of the stabilizers on the downstream process. The major challenges associated with the direct synthesis of hydrogen peroxide are the explosiveness of the hydrogen-oxygen mixtures over a very wide range of concentrations (4-96%) and the selectivity towards hydrogen peroxide as the desired product. All known catalysts, besides being active in direct synthesis of hydrogen peroxide are also active in the direct formation of water from H_2 and O_2 , and in the hydrogenation as well as the decomposition of the peroxide formed (Fig. 4.1).

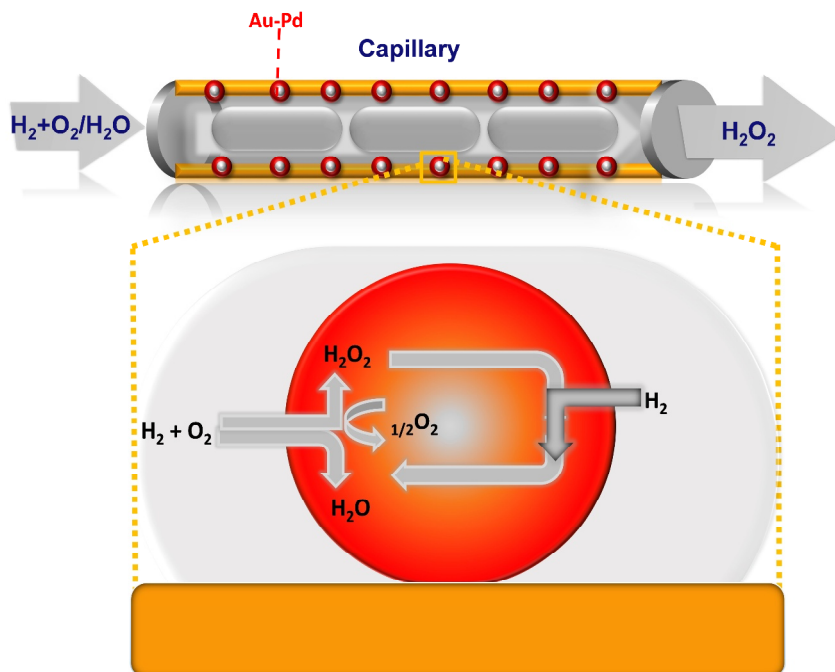


Figure 4.1. Schematic of a wall-coated microreactor for direct hydrogen peroxide synthesis.

The application of the microreactor concept into the direct synthesis reaction offers an opportunity to safely handle the hydrogen and oxygen mixtures which would be explosive in conventional reactors. Potential safety concerns related to the use of conventionally explosive hydrogen and oxygen mixtures in a wall-coated microchannel are discussed in detail by Chattopadhyay and Veser ^[4]. The safety aspects of the direct synthesis reaction in a microchannel coated with Au-Pd catalytic films are addressed in our previous publication ^[5]. Overall, the conclusion is that at higher pressure in a capillary microreactor an explosion is not physically impossible, but this reaction can be performed safe due to the absence of an ignition source and the difficulty for hot spot to appear. The high surface area of the microreactor makes heat removal very fast and the liquid additionally separates the gas in very small volume packages (approximately 0.1 μl for a typical 2 mm bubble size in 300 μm channel) preventing the possibility for propagation. In addition, the small volume of the microchannel makes it easy to design a reactor which can withstand the energy of an explosion within.

The direct synthesis of hydrogen peroxide has been performed earlier in both micro-packed beds ^[6-8] or in a wall-coated microchannel ^[5,9]. To avoid high pressure drop and poor catalyst wetting and contacting associated with micro packed-beds ^[10], it is beneficial to coat the catalyst on the reactor wall. The amount of catalyst per channel volume in a wall-coated microchannel is relatively small and the catalyst is continuously wetted with a thin liquid film preventing the possibility of local overheating and chain-branching reactions.

The catalyst coating in the microchannel can be deposited in a form of thin colloidal solution of Pd encapsulated in copolymer-micells with a polystyrene backbone ^[9,11], or as a catalytic wash-coat ^[5]. Wash-coats are generally preferred over colloidal catalytic films for this reaction considering their stability when exposed to the acidic environment in direct synthesis. This work focuses on application of well-adhered and uniform silica-wash-coats embedded with Au-Pd bimetallic nanoparticles as a catalyst for direct synthesis reaction inside the microchannels. As support with a low isoelectric point, SiO_2 is favourable for peroxide formation, since it shows lower hydrogen peroxide hydrogenation rates ^[12]. The main benefit of the application of porous films with a large internal surface area as a catalyst support in general is the considerably enhanced surface available for catalyst deposition compared to the geometric surface area of the microchannel wall only. The reaction rate per unit volume of microchannel in case of heterogeneously catalyzed reactions is directly determined by the available catalytic surface area ^[13], since microchannels possess excellent mass and heat transfer properties. A gold-palladium catalyst was chosen for the direct hydrogen peroxide synthesis, since Pd alloyed with Au shows an enhanced activity to peroxide formation compared to the traditionally employed Pd catalyst ^[14-17].

The main goal of this paper is to assess the possibility to apply a wall-coated microchannel for a small to medium scale on-site production of hydrogen peroxide considering the advantage of smaller pressure drops compared to a packed-bed microchannel. Considering that most of the applications of hydrogen peroxide require concentrations in a range of 1-15 wt%, it is necessary to determine if those values can be reached using a wall-coated microchannel technology.

4.2. Materials and Methods

4.2.1. Preparation of microchannel wash-coats

Fused silica capillaries 320 μm in diameter and 0.5-1.5 m in length, initially pre-treated for cleaning and surface roughening with 1M solution of NaOH followed by 1M HCl solution, were wash-coated by displacing a plug of the coating slurry using N_2 . The coating slurry contained 4 wt% fumed silica and 8 wt% silica gel (Davisil Grade 633, Sigma-Aldrich) with colloidal silica (Ludox AS30, Sigma-Aldrich) as a binder with addition of up to 8 wt% of sodium silicate solution (Sigma-Aldrich, $\text{SiO}_2 \sim 26.5$ wt%, Na_2O , $\sim 10.6\%$). In order to obtain uniform coating thickness along the capillary length and cross-section, the great attention has to be given to the control of the coating parameters such as coating velocity, temperature and solvent evaporation rate during and after displacement of the coating solution. Disregarding those parameters often results in severe coating non-uniformity with often an order of magnitude high variation in layer thickness along the capillary length. Following the drying of the deposited silica layer, the capillary was washed with 1M solution of NH_4NO_3 overnight at a flow rate of 0.2 ml/min and subsequently with water. The deposited silica layer was dried and calcined at 380 $^\circ\text{C}$ prior to deposition of Au-Pd catalyst.

More details on coating procedure is given in our previous publication ^[5].

4.2.2. Catalyst preparation

The silica layer coated on the reactor wall was functionalized with an active Au-Pd metallic species by deposition of stabilized Au-Pd (1:2) colloidal nanoparticles prepared using a two-phase synthesis method. This type of colloidal nanoparticles with a Au:Pd ratio of 1:2 proved to be both, most active and most selective when tested in the direct synthesis reaction ^[5]. The two-phase synthesis approach, originally introduced by Brust and co-workers^[18] involves transfer of tetrachloropalladate and tetrachloroaurate ions from water to the organic phase by means of tetraoctylammonium chloride as a phase transfer agent and subsequent reduction using NaBH_4 . The concentrations of the metal precursors HAuCl_4 and K_2PdCl_4 were adjusted to give an approximately 5 wt% total loading of the bimetallic catalyst with respect to a SiO_2 wash-coat material when deposited inside the wall-coated microchannel. To ensure complete reduction, excess of NaBH_4 was used. After the colloidal nanoparticles had been generated in the organic solvent, the aqueous and organic phase

are separated, followed by additional washing of the organic phase. The exact protocol used for synthesis of colloidal Au-Pd nanoparticles is described elsewhere ^[19].

After the bimetallic nanoparticles were prepared, they were deposited in the wash-coated microchannel by filling the channel with colloidal solution followed by slow evaporation of the solvent. The estimated thickness of the wash-coat layer is typically around 4 μm . The application of a solvent with a high vapour pressure such as dichloromethane in the catalyst preparation enables a fast evaporation of the solvent, making the preparation process faster and more efficient. After removal of the organic solvent, the catalytic layers were dried at 120 $^{\circ}\text{C}$ for 12 h and calcined at 380 $^{\circ}\text{C}$ for 4h. The calcination temperature is determined by the upper temperature limit for the protective polymer film on the outside of the capillary. The calcination step is critical for removal of the protective tetraoctylammonium layer.

4.2.3. Direct synthesis of hydrogen peroxide in a wall-coated microchannel

The direct synthesis reaction in the microchannel was investigated using both, pure and partially diluted hydrogen–oxygen mixtures. In case of diluted mixtures, nitrogen was used as an inert diluent gas. A catalytic capillary was placed in a thermostated water bath. The direct synthesis is a three-phase process which involves a $\text{H}_2\text{-O}_2$ mixture as gas-phase, a solvent and the solid catalyst phase. The role of the liquid phase supplied is to collect and solubilize the hydrogen peroxide formed, since pure hydrogen peroxide is highly unstable and decomposes to water and oxygen. To additionally minimize the hydrogen peroxide decomposition, a water solution containing 0.05 M of sulfuric acid and 9 ppm of NaBr was used in all experiments as a liquid phase. Acids such as sulfuric or phosphoric decelerate base-catalyzed decomposition of peroxide, while bromide ions even at very low concentrations poison catalytic sites that promote O_2 dissociation and direct formation of water ^[20,21]. The water phase is supplied to the system by means of a syringe pump. The desired gas flow rates were controlled using mass flow controllers. In order to maintain a constant pressure at 20 bar, a back pressure regulator is placed downstream after a gas/liquid separation unit. Since conventionally explosive H_2/O_2 mixtures were used, the gas is diluted with N_2 at the capillary outlet to stay below the explosive H_2 and O_2 concentrations in the larger volume downstream equipment. To be able to visually monitor the flow pattern in a microchannel, a piece of empty 320 μm glass capillary was connected before the capillary coated with the catalytic film. The flow pattern observed was segmented gas-liquid flow (Taylor slug flow). The catalytic layer coated is relatively thin, thus it is expected that the same flow regime is retained in the wall-coated microchannel. At higher conversion levels the size of the gas bubbles will change along the microchannel, however, unless one runs at almost complete conversion, one will retain the desired Taylor-flow throughout the

channel. The pressure in the system was monitored before the inlet and after the microchannel outlet. The pressure drop over the capillary was used as an indirect indication of quality of the coating procedure (typically varying between 0.1-0.2 bar from the gas inlet to the outlet). Defects in the coating would lead to a higher pressure drop and such capillaries would not be considered to be used in the reaction. All experiments were performed with 320 μm in diameter fused silica capillaries initially coated with the layer of catalyst. The length of those capillaries used in the experiments ranged from approximately 0.3 m to 1.5 m.

Gas samples were analyzed online with an InterScience Compact GC (column: Molsieve plot 5m*0.32mm) equipped with TCD detector. Liquid samples were collected manually at the liquid sampling point and immediately titrated with a standard solution of cerium (IV) sulphate. The productivity and selectivity values are calculated in time using the regular expressions for a continuously operated reactor:

$$\text{Productivity} = \frac{\text{Liquid flow rate} \times C_{\text{H}_2\text{O}_2} \times M \left(\frac{\text{g}}{\text{mol}} \text{H}_2\text{O}_2 \right)}{m_{\text{cat}}}$$

$$\text{Selectivity} = \frac{\text{moles H}_2\text{O}_2 \text{ formed}}{\text{moles H}_2 \text{ reacted}}$$

4.3. Results and Discussion

The experimental results presented below give an overview of the influence of different operating conditions on the amount of peroxide produced by the direct combination of hydrogen and oxygen over the Au-Pd colloidal nanoparticles deposited on the SiO₂ wash-coat layer inside the capillary microchannel. The direct combination of H₂ and O₂ involves two parallel reactions which give H₂O₂ and H₂O as the main products. The hydrogen peroxide formed can be further converted to water through consecutive hydrogenation and decomposition reactions. It is a well-known fact that in order to minimize the occurrence of those consecutive reactions, the hydrogen peroxide concentration in the reactor should be kept as low as possible. This is the case even in the conventional AO process. The produced hydrogen peroxide solutions are concentrated to commercially available grades in downstream processing by applying unit operations such as vacuum distillation. Producing the lower concentration units of hydrogen peroxide in a small scale production facility might not be as cost effective as in the large scale process. In case of small scale production, the process needs to be optimized for producing directly a more concentrated peroxide solution with a potential direct utilization even at the expense of selectivity. The goal of this study is to investigate the range of peroxide concentrations expressed in wt% that can be generated using this type of microreactor technology.

4.3.1. Effect of operating conditions on the catalyst performance in a microchannel

In our previous work^[5] we were testing the performance of colloidal Au-Pd (1:2) nanoparticles in an autoclave and a microreactor using a 4 vol% H₂ and O₂ mixture. A comparison of the initial productivity and selectivity values in the autoclave with steady state values in the microchannel at the same hydrogen conversion level showed that both reactors perform the same, as the same catalyst obviously should if it is operated under identical conditions in the absence of mass transfer limitations. However, the advantage of using a continuous operation compared to semi-batch was reflected in the fact that in the continuous flow microreactor productivity and selectivity values could be maintained with time on stream, due to the continuous removal of the liquid phase and the short residence times of the hydrogen peroxide generated. The performance of the catalyst could be further improved by switching from non-explosive to pure hydrogen-oxygen mixtures. Besides the productivity increase, the selectivity towards the peroxide was three times higher. We assume that according to the suggested mechanism^[22,23], higher partial pressures and thereby surface coverages with H₂ and O₂ might lead to blocking of the available neighbouring decomposition sites. If dissociative adsorption of O₂ occurs due to the presence of the neighbouring active site, only water is generated (Table 4.1). Dissociation of already formed peroxide species on the catalyst surface leads as well to formation of water. Being able to block those vacant dissociation sites suppresses both, O-O and H-O-O-H bond cleavage and therefore increases the selectivity towards the peroxide.

According to this hypothesis it might have been expected that increasing the partial pressure of reactants by increasing the total pressure in the system while maintaining H₂ and O₂ concentration in the feed constant will have a similar effect on the selectivity. The effect of total pressure on reaction rate and selectivity was studied by varying the pressure in a range between 15 and 25 bar while keeping the H₂ and O₂ content at 20 vol%. The results obtained confirmed that an increase in the partial pressures of H₂ and O₂ results in both higher reaction rates or higher concentrations of peroxide generated in liquid phase and a higher selectivity toward peroxide. The same effect of total pressure on selectivity was observed earlier by Voloshin et al.^[8]. To reach high selectivity values and high peroxide concentration in the liquid phase, lower concentrations of hydrogen and oxygen in the gas phase can be compensated by applying a higher pressure. However, the possibility to handle conventionally explosive mixtures within microchannels eliminates the need for high pressure conditions and allows for a better reactor performance at the same total pressure.

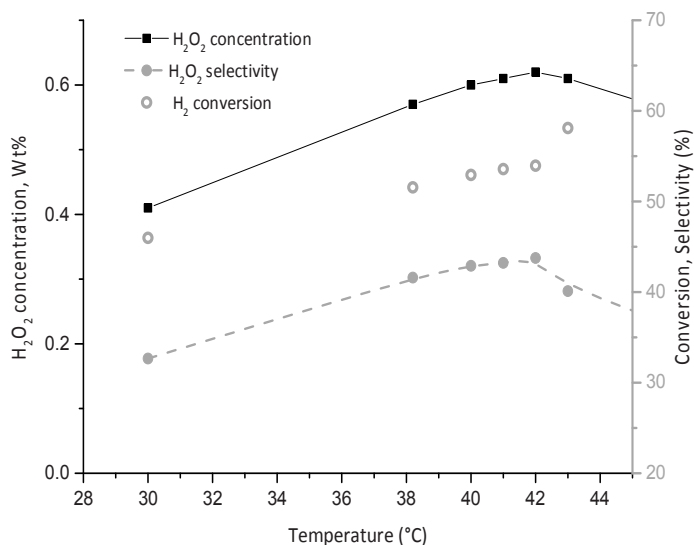


Figure 4.2. Effect of temperature on direct synthesis reaction; $p=25$ bar, channel diameter $320\ \mu\text{m}$, liquid phase $0.05\ \text{M}\ \text{H}_2\text{SO}_4$, $9\ \text{ppm}\ \text{NaBr}$; liquid flow rate $0.05\ \text{ml/min}$; catalyst Au-Pd (1:2) colloidal nanoparticles, $20\ \text{vol\%}$ of H_2 and O_2 , total gas flow rate $5\ \text{ml/min}$.

Besides the H_2 and O_2 partial pressures as controlling parameters, the concentration of hydrogen peroxide at the reactor outlet will also be highly dependent on a combination of the following parameters: temperature, gas and liquid flow rates and the amount of catalyst or microchannel length applied. The overall rate of peroxide formation is, in general, affected by the reactant/product residence time. It is expected that with longer residence times, the chance of peroxide transformation into water is increasing. In order to determine the influence of each of these parameters on the overall reaction rate and concentration of peroxide generated in liquid phase and define suitable operating window for direct synthesis, a decision was made to vary each parameter separately, one at the time.

One of the first questions that needs to be answered when designing a set-up for the hydrogen peroxide direct synthesis reaction is if cooling or heating of the microchannel reactor should be applied in order to maximize the concentration of peroxide in the liquid phase. Literature survey gives a variety of optimum temperature conditions reported for the direct synthesis reaction. Some authors suggest that reaction optimally should be performed at low temperatures close to 0°C due to the fact that at higher temperatures

decomposition and hydrogenation reactions are faster leading to less peroxide generated at higher temperatures ^[24,25], while others claim that optimal temperature value for direct synthesis might lie well above this value ^[8]. In fact, the overall rate of reaction will increase with temperature as long as the rate of peroxide formation for a given temperature under given conditions is faster than the rate of side reactions, which all lead to water formation. This is highly dependent on the catalyst type used and presence or absence of promoters, which determine the surface reaction mechanism and kinetics of each of the reaction steps involved. The effect of temperature on the hydrogen peroxide concentration in liquid phase, the hydrogen conversion and selectivity was investigated for Au-Pd colloidal nanoparticles supported on a silica-wash coated microchannel in order to obtain the temperature range suitable for direct synthesis reaction. Our results show that when using partially diluted H₂ and O₂ mixtures (20 vol%) the reaction rate increases up to around 40 °C for given gas and liquid flow rates. Under the reaction conditions applied, the peroxide concentration in the liquid phase and the selectivity are almost levelling off in a range of 41-43 °C reaching the maximum values, after which a decline in the peroxide concentration is observed. At higher temperatures, water formation is favoured, since side reactions (hydrogenation and/or decomposition) prevail over the peroxide synthesis.

The effect of the H₂/O₂ molar ratio at constant overall gas flow rate can be studied in two ways. Considering the fact that undiluted H₂-O₂ mixtures produce hydrogen peroxide more selectively, the application of pure H₂-O₂ mixtures throughout the study would be justified. However, this also means that in order to vary the H₂/O₂ ratio at constant overall gas flow rate, it is necessary to vary both H₂ and O₂ flow rates at the same time. Therefore, partial pressures as well as residence times of both reactants are manipulated in parallel. To avoid this, the decision has been made to maintain the flow rate, concentration and residence time of reactant in excess constant and to use nitrogen to compensate for the decrease in the flow rate of limiting reactant. The gas mixtures used throughout the experiments still remain fairly concentrated considering the reactant content is $\geq 60\%$. All experiments presented in Fig. 4.3 were performed using a total gas flow through capillary of 5 mlN/min. The experiments are done in such a manner that the flow rate of the reactant in excess was maintained at 2.5 mlN/min. For H₂/O₂<1, the O₂ flow rate was kept at 2.5 ml/min, while decrease in H₂ flow rate was compensated by adding inert (N₂) to keep the total gas flow rate through the capillary constant at 5 mlN/min. In contrast, for H₂/O₂>1 the H₂ flow was maintained at 2.5 mlN/min while decreasing the O₂ flow rate. In case of H₂/O₂=1 pure hydrogen-oxygen mixtures were used containing 50 vol % of both reactants.

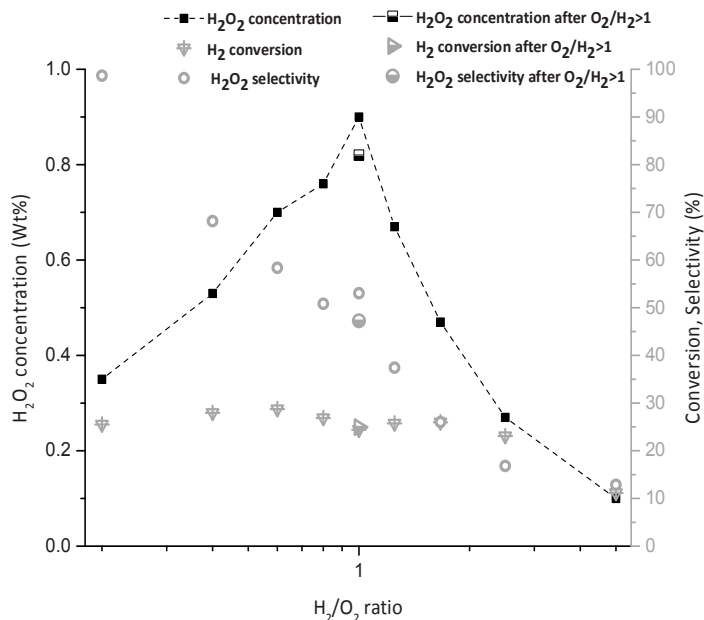


Figure 4.3. Effect of H₂/O₂ ratio on direct synthesis; T=42°C, p=20bar, channel diameter 320 μm, liquid phase 0.05 M H₂SO₄, 9 ppm NaBr; liquid flow rate 0.05 ml/min; catalyst Au-Pd (1:2) colloidal nanoparticles, total gas flow rate 5 mlN/min.

From Fig. 4.3 we can conclude that the optimum H₂/O₂ ratio in terms of concentrations of peroxide produced in a solution is 1. A decrease in the O₂ content leads to decrease in both, peroxide yield and selectivity. The selectivity drop can be explained by the potential surface reaction mechanism shown in Table 4.1. The reduction of the selectivity towards the peroxide is determined by two major surface reactions which lead to water formation-decomposition of hydrogen peroxide by disproportionation to water and oxygen and hydrogenation of peroxide either direct as shown in Table 4.1 or via hydrogenation of the two OH groups. This indicates that with higher H₂ partial pressures the hydrogenation reaction is accelerating leading to loss of peroxide formed on the catalyst surface. In contrast, lowering the H₂ content at constant O₂ content in the system is beneficial for selectivity, since less H atoms on the surface are available for the hydrogenation reaction. A lower H₂ partial pressure is accompanied by less H₂O₂ generated in the liquid phase meaning that both, hydrogenation and decomposition will be reduced by lower hydrogen peroxide content for H₂/O₂ < 1. As shown in Fig. 4.3, 100% selectivity towards the peroxide

can be reached by running the reaction using very low H₂/O₂ ratios. Unfortunately, such a high selectivity has to be traded off for lower catalytic activity and low concentration of hydrogen peroxide generated in the liquid phase.

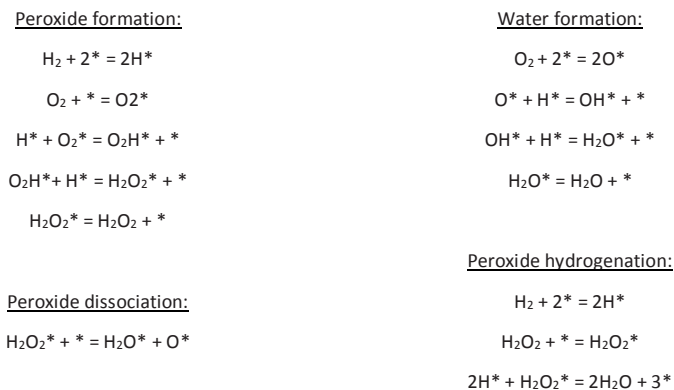


Table 4.1: Reactions occurring on Au-Pd surface during direct combination of H₂ and O₂.

A drawback observed after exposure of the catalyst to higher O₂ concentration for a longer period of time is partial catalyst deactivation. A catalyst that has been subjected to H₂/O₂<1 shows a lower selectivity and peroxide yield when later exposed to initial H₂/O₂=1, although the H₂ conversion remains the same. Nevertheless, it was observed that after exposure of the catalyst to H₂, the initial catalytic activity can be restored. Therefore, the idea of palladium elution as a consequence of its oxidation to PdO observed in micro-packed bed reactor^[5] can be ruled out. A potential explanation for this phenomenon lies in the oxidation state of the catalyst and moreover, changes of the oxidation state of Pd under different reaction conditions. The XPS analysis of freshly prepared Au-Pd bimetallic particles supported on silica indicates presence of Au⁰, Pd⁰ and PdO phases. Namely, the role of Au added to Pd in this kind of bimetallic catalyst is to “dilute” the Pd surface and to isolate Pd sites. It is believed that significant isolation of Pd sites in bimetallic alloy catalyst prevents O₂ dissociation and increases the selectivity towards the peroxide ^[26]. However, the important parameter that might influence the catalytic activity of Au-Pd bimetallic catalysts is the oxidation state of the palladium under reaction conditions, considering the presence of both reductive and oxidative species in the direct synthesis. It is well known that the oxidation state of Pd catalysts switches between metallic and oxide depending on the temperature and oxygen concentration. Deactivation of Pt-group of metals (Pt, Pd, Rh) as a

consequence of the metal oxide phase formation under high pressures and high O₂ partial pressures has been already reported for CO oxidations^[27,28]. The influence of the PdO phase formation on the direct synthesis reaction is still under discussion. Some studies suggest that supported PdO catalysts show lower hydrogenation/decomposition rates when compared to their metallic analogues^[29], while some authors made contradictory conclusion that metallic palladium is responsible for high activity and selectivity^[30]. Moreover, it has been shown that the formation of bulk PdO proceeds via several intermediate steps^[31]. Those intermediate surface oxygen phases might exert different catalytic properties in the direct formation of hydrogen peroxide. Further detailed investigations are needed to understand the influence of different oxide phases of Pd on catalyst activity and selectivity in direct synthesis reaction. An attempt was made to determine the catalyst oxidation state inside the microchannel. In order to do XPS analysis capillary samples were crashed, but due to a very low metal to inert content in the sample, the analysis failed. Considering that the direct synthesis reaction is a three phase reaction, involving besides the solid catalyst both, a gas and a liquid phase, the influence of gas and liquid flow rates, as well as catalyst loading on hydrogen conversion, selectivity and yield was assessed. All the experiments were performed at 20 bar pressure and a temperature of 42 °C. The liquid flow rate was varied in a range of 0.01 ml/min to 0.1 ml/min, while maintaining the total gas flow rate at 5 mlN/min. The gas phase used contained 20 vol% of hydrogen and oxygen.

The data presented in Fig. 4.4 show that in this range of liquid flow rates the hydrogen conversion somewhat decreases with an increase in the liquid flow rate, but not significantly. The liquid slug length, which has a strong impact on gas to liquid mass transfer increases with an increase in the liquid flow rate. For a longer liquid slug the mass transfer from the gas to the liquid is slower^[32–34]. The Sherwood number decreases with increase in dimensionless slug length^[32,35], thus the liquid to catalyst mass transfer will be enhanced with generation of shorter slugs as well. Decreasing the liquid flow results in higher concentrations of peroxide generated in the liquid phase (as shown on Fig. 4.4). However, from Fig. 4.4 we can conclude that a decrease of the liquid flow below 0.05 ml/min results in a tremendous drop in the selectivity towards the peroxide. This selectivity drop is attributed to reaction kinetics.

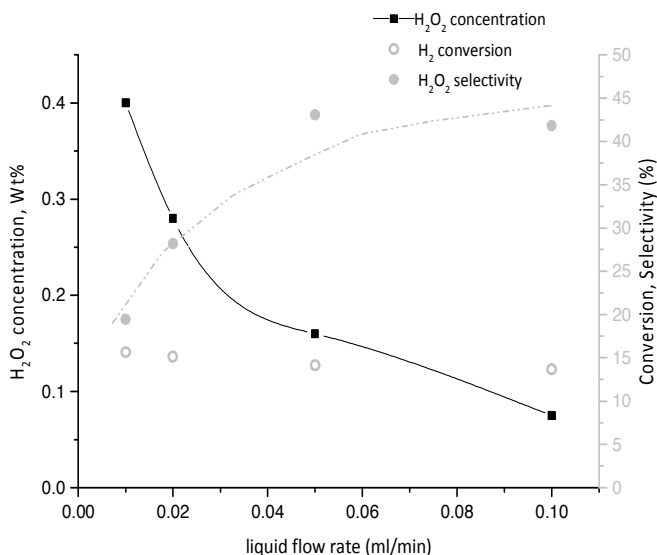


Figure 4.4. Effect of liquid flow rate; T=42°C, p=20 bar, channel diameter 320 μm , liquid phase 0.05 M H_2SO_4 , 9 ppm NaBr; catalyst Au-Pd (1:2) colloidal nanoparticles, 20 vol% of H_2 and O_2 , total gas flow rate 5 mlN/min,

A higher peroxide concentration at a lower liquid flow rates accompanied with a higher concentration of hydrogen in shorter liquid slugs leads to a high peroxide hydrogenation and/or decomposition rates, which as a consequence has a significantly lower selectivity. In a very simplistic manner, the effect of liquid phase velocity can be interpreted through “removal” of hydrogen peroxide generated from catalyst surface - at low liquid flow rates, the gas plugs are comparatively too long and too much peroxide builds up in the liquid film wetting the catalyst until a new liquid slug passes. Fast refreshment of the catalyst surface with the aqueous phase means shorter contact time for dissociation or further hydrogenation of peroxy species formed.

To study the effect of the gas flow rate, the total gas flow was varied in a range of 5-15 mlN/min, while the liquid flow rate was set to 0.05 ml/min. The gas phase used contained 20 vol% of H_2 and O_2 . Higher gas flow rates at a constant liquid flow rate result in longer gas bubbles and catalytic shorter liquid slugs. In case of the absence of a reaction on the wall it has been shown that gas bubble length in fact does not have significant impact on gas to

liquid mass transfer ^[32,33], since the layer close to the wall is saturated with gas contributing no further to mass transfer. In the presence of the reaction, absorbed H₂ and O₂ in liquid phase are consumed thus maintaining the concentration gradient needed for the transport to occur. It is expected based on Fig. 4.4 that with higher gas to liquid flow rates (G/L), shorter liquid with a higher interfacial area, more H₂ and O₂ will be transferred to liquid within a certain time period. However, with an increase of the gas flow rate, the residence time of the gas phase reactants in the microchannel shortens resulting in fact in lower hydrogen conversions as indicated on Fig. 4.5. This means that changing the gas flow rate at a constant liquid flow rate affects both the slug to bubble length and the residence time considering that higher amount of reactants is fed per amount of catalyst in the same time interval (higher WHSV value). Lower hydrogen conversions at higher gas flow rates are accompanied by a higher amount of hydrogen peroxide generated in the liquid phase, since a lower percentage of H₂ converted is compensated by a higher throughput of the reactants.

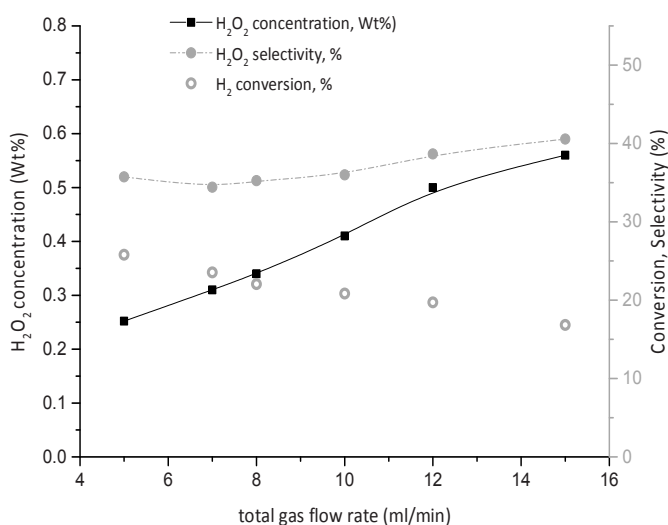


Figure 4.5. Effect of gas flow rate; T=42°C,p=20 bar, channel diameter 320 μm, liquid phase 0.05 M H₂SO₄, 9 ppm NaBr; liquid flow rate 0.05 ml/min; catalyst Au-Pd (1:2) colloidal nanoparticles, gas phase 20 vol% of H₂ and O₂.

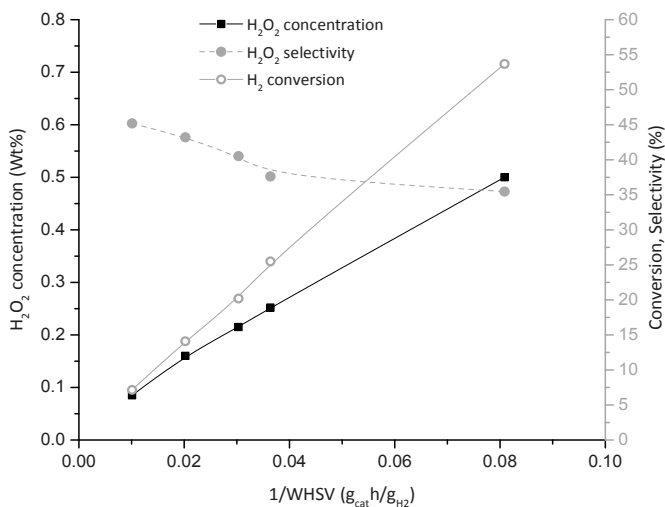


Figure 4.6. Effect of 1/WHSV (residence time) on reactor performance based on catalyst loading; T=42°C, p=20 bar, channel diameter 320 μm, liquid phase 0.05 M H₂SO₄, 9 ppm NaBr; liquid flow rate 0.05 ml/min; catalyst Au-Pd (1:2) colloidal nanoparticles, 20 vol% of H₂ and O₂, total gas flow rate 5 mlN/min.

Fig. 4.5 also indicates that in terms of peroxide concentration achieved it is beneficial to run the reaction at the higher gas to liquid flow ratios. In addition, Kreutzer et al. showed that contrary to the expectations, higher gas velocities are not beneficial for mass transfer rates [34] as would be the case in a fixed bed reactor. External mass transfer in a microchannel improves with decreasing the velocity, which can be correlated with the fact that liquid film thickness, which represents the major resistance to mass transfer, is decreasing with lower Capillary numbers [34]. The weight hourly space velocity (WHSV) was additionally varied by using different amounts of catalyst. The effect of 1/WHSV (residence time) on the hydrogen conversion and selectivity is given in Fig. 4.6. In all experiments the gas and liquid flow rates were maintained at 5 mlN/min and 0.05 ml/min respectively. As it can be expected, the hydrogen conversion increases proportional to the 1/WHSV or catalyst loading, while the selectivity decreases. A higher concentration of peroxide generated in the liquid phase when using a higher catalyst amount in the reactor has the adverse effect on the peroxide

selectivity since it accelerates its subsequent hydrogenation and decomposition reactions that consume peroxide.

4.3.2. Effect of external and internal mass transfer effects

To verify the conclusions related to effect of studied process parameters on reaction kinetics, the potential influence of mass transfer has to be evaluated. It is known that in case of the Taylor flow in microchannels mass transfer of a gas component proceeds through following 3 steps: (1) From gas bubble directly to the solid catalyst through thin liquid film (gas-to-solid) (2) from the bubble caps to the liquid (gas-to-liquid) and (3) from the liquid to the catalyst for dissolved gas (liquid-to-solid). Mass transfer from gas-to-liquid and liquid-to-solid represent resistances in series and occur in parallel to mass transfer directly from gas-to-solid. In case of a catalytic reaction occurring on the reactor wall, gas-to-solid mass transfer is the dominant step, being considerably faster than the other two. Calculation of the mass transfer coefficient from gas-to solid $k_{GS}a_{GS}$ was performed using well established correlations available in literature [35]. For the range of gas and liquid flow rates used throughout the experiments the $k_{GS}a_{GS}$ values are approximately in a range of 23 to 45 s^{-1} . The criterion used to evaluate if the overall volumetric reaction rate $R_{v,ov}$ is fully determined by external mass transfer rate is following:

- External mass transfer is not significant if $R_{v,ov} \leq 0.1 k_{GS}a_{GS} C_{H_2}^{sat}$
- Reaction is mass transfer limited if $R_{v,ov} \geq 10 k_{GS}a_{GS} C_{H_2}^{sat}$

Calculated values of mass transfer rates show to be already more than an order of magnitude higher than observed overall volumetric reaction rates, indicating that external mass transfer is not the limiting step.

To determine whether mass transfer limitations within the catalyst layer might be significant, the Weisz modulus was calculated:

$$\Phi = \frac{L^2 R_{v,coating}}{D_{H_2,eff} C_{H_2}^{sat}} < 0.15$$

$R_{v,coating}$ represents the reaction rate per unit volume of the catalytic layer. For calculation of the effective diffusivity $D_{H_2,eff}$ typical values for porosity of coating layer of 0.4 and tortuosity value of 6 were used. The thickness of catalyst layer L is 4 μm , which is the average thickness of wash-coat layer estimated by SEM [5]. For the highest reaction rates observed in the above experiments, values obtained for Weisz modulus are in a range of 0.2 to 0.3, indicating that pore diffusion effects are present, but still not significant considering that

for those values the catalyst effectiveness η is not lower than 0.9. However, according to Weisz-Prater criterion, pore diffusion effects can be considered absent only if $\Phi \leq 0.15$, meaning that somewhat thinner catalyst layer should be introduced in capillary to ensure that catalyst effectiveness is equal to 1. The calculated values of k_{GSaGS} indicate a very fast gas-to-solid mass transfer rate in a wall-coated microchannel, meaning that the transfer of gas to the catalyst surface is not a rate limiting step in the reaction. With the estimated catalytic layer thickness of 4 μm , the direct synthesis reaction is partially limited by diffusion of reactants through the catalytic layer.

4.3.3. Towards the application of direct synthesis

We have shown that it is possible to perform the direct synthesis of hydrogen peroxide safely in a wall-coated microchannel using undiluted hydrogen-oxygen mixtures. A highly beneficial effect of higher hydrogen and oxygen concentrations in reaction mixtures (higher partial pressures) besides higher observed reaction rates was the selectivity enhancement. In order to bring microreactor technology closer to application, it is necessary to estimate the potential concentration range of hydrogen peroxide solutions produced using this concept of wall-coated microchannel with colloidal Au-Pd nanoparticles. The study was performed to evaluate to which extent it is possible to increase the peroxide concentration in the solution when using pure hydrogen and oxygen mixtures in the synthesis, taking into account the discussed effects of gas and liquid flow rates. Considering that a change in gas flow rate at constant liquid phase flow rate influences both, the residence time and the G/L ratio, and thereby the slug to bubble length, in this study gas and liquid flow rates were increased proportionally, always keeping the same G/L ratio while decreasing residence time. The concentration of peroxide, hydrogen conversion and selectivity for two different G/L ratios are plotted with respect to WHSV. It is clear from Fig. 4.7 that in terms of selectivity it is beneficial to maintain higher WHSV values. Short contacting time for both reactants and hydrogen peroxide formed with the catalyst seems to result in fewer “dissociation” events on the catalyst surface. It is indicative that water formation reactions which typically involve dissociation step of either oxygen molecules or hydrogen peroxide itself (Table 4.1) require longer contacting times. At lower WHSV values (accompanied with lower liquid space velocities), both hydrogen conversion and hydrogen peroxide concentration increase, but selectivity drops as a consequence of slower peroxide “stripping” from the catalyst surface. An increase in peroxide concentration also means an increase in productivity, considering that the amount of catalyst and capillary length remain the same throughout the experiment.

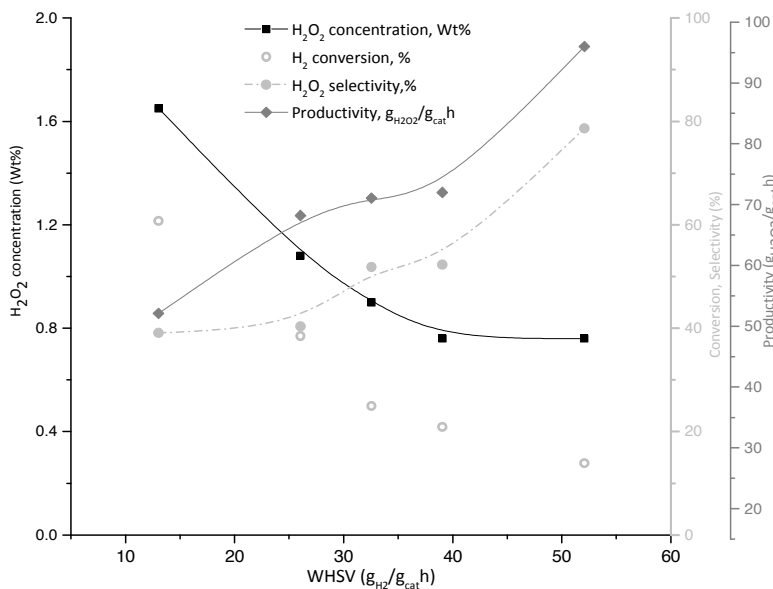


Figure 4.7. Effect Of WHSV on peroxide concentration, productivity, selectivity and H_2 conversion, $T=42^\circ\text{C}$, $p=20$ bar, channel diameter $320\ \mu\text{m}$ liquid phase $0.05\ \text{M}\ \text{H}_2\text{SO}_4$, $9\ \text{ppm}\ \text{NaBr}$; catalyst Au-Pd (1:2) colloidal nanoparticles, $50\ \text{vol}\%$ of H_2 and O_2 , $F_{\text{gas}}/F_{\text{liquid}}=5$.

If we want to increase further the concentration of peroxide, it is necessary to decrease the flow of liquid phase relative to gas phase (Fig. 4.8). As already expected based on results presented in Fig. 4.4 this will lead to conversion increase, but further reduction in the selectivity. However, concentrations as high as $5\ \text{wt}\%$ of peroxide can be achieved if G/L ratio is increased to 20. This value is significantly higher compared to the maximum reported in literature for a wall-coated microchannel^[9] and similar to the values of Inoue et al.^[6,36] reported in a micro packed-bed with an advantage of an order of magnitude lower pressure drop and better catalyst stability. Inoue et al.^[6] chose to operate the reactor using a higher oxygen concentration relative to hydrogen, which leads to erosion of the catalyst bed and palladium elution in oxidative atmosphere within the first 48 h of operation. The productivity loss in case of a wall-coated microchannel^[9] is attributed to the catalyst leaching due to corrosive conditions. Similar to our work, a tremendous selectivity drop^[6] is

observed when peroxide concentrations as high as 3 wt% are generated in the liquid phase, even though reaction was done under oxygen-rich conditions.

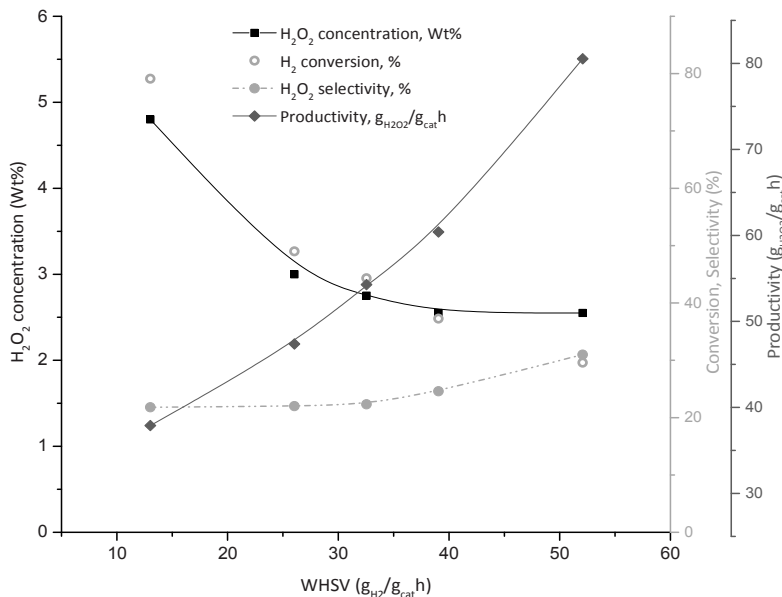


Figure 4.8. Effect Of WHSV on peroxide concentration, productivity, selectivity and H_2 conversion, $T=42^\circ\text{C}$, $p=20$ bar, channel diameter $320\ \mu\text{m}$, liquid phase $0.05\ \text{M}\ \text{H}_2\text{SO}_4$, $9\ \text{ppm}\ \text{NaBr}$; catalyst Au-Pd (1:2) colloidal nanoparticles, $50\ \text{vol}\%$ of H_2 and O_2 , $F_{\text{gas}}/F_{\text{liquid}}=20$.

The conclusion is that a significant selectivity loss in the direct synthesis reaction associated with an increasing peroxide concentration cannot be disregarded. The application of solvents such as methanol, ethanol or isopropanol^[30] might be a good solution for achieving higher reaction rates, thus higher peroxide concentrations in liquid phase, but the partial conversion of valuable peroxide to water is difficult to avoid. One of the process options would certainly be to operate the reactor at low hydrogen peroxide concentration in order to retain high selectivity and to concentrate solutions subsequently by means of distillation

^[37]. This implies that in the final process optimization the costs of concentrating dilute hydrogen peroxide solutions vs. the costs of peroxide and H₂ consumed in side reactions, if concentrated hydrogen peroxide solutions are synthesized directly, need to be evaluated. It is necessary to keep in mind that for a variety of applications hydrogen peroxide concentrations used are in a range of 1-15 wt%. The diluted solutions of hydrogen peroxide produced via two-stage cyclic AO process are mainly concentrated by distillation for the logistic purposes and transportation costs to 50 or 70 wt%. In this lower range of peroxide concentrations the selectivity of this direct synthesis route is quite high.

4.3.4. Hydrogen peroxide direct synthesis - Potential and challenges

An interesting alternative to retain the high selectivity observed with a lower peroxide concentration in the liquid phase even at higher residence times might be the in-situ consumption of peroxide formed in a coupled oxidation reaction. This would mean that one reactive microchannel would be used for performing at least two consecutive reactions, one of which is direct formation of hydrogen peroxide. Attempts to use in-situ formed hydrogen peroxide species for direct oxidation of benzene to phenol ^[38-40] or propene to propene-oxide (PO) ^[41,42] instead of liquid phase hydrogen peroxide have been already made. Considering the high price of hydrogen peroxide mostly, in-situ generated peroxide from H₂-O₂ is cheaper alternative for bulk chemical production. In case of benzene hydroxylation, it has been shown that in-situ generated hydrogen peroxide can be even more selective compared to hydrogen peroxide added directly by syringe-pump ^[40]. However, some reports show that the rate of water formation is often an order of magnitude higher than rate of phenol formation ^[39] or PO formation ^[41]. Synthesis of PO using propene, hydrogen and oxygen mixtures often suffers from poor selectivity due to fast propene hydrogenation to propane ^[42].

Application of hydrogen peroxide in the fine chemical and pharmaceutical industry is especially interesting due to process economics that allow the application of more expensive oxidants. In contrast to oxygen, hydrogen peroxide is a mild oxidant, thereby more suitable for performing selective oxidations. In addition, lower temperatures are required for oxidations using peroxide as an oxidant. A number of liquid phase oxidations with hydrogen peroxide reported in the fine chemical industry are homogeneously catalysed, often due to the fact that homogeneous catalysts are more selective. However, the application of heterogeneous catalysts such as zeolites and non-crystalline heterogeneous catalyst types (amorphous metallosilicalites, heteropolyacids) is known as well ^[43]. Preferably, "oxidation" processes considered to be linked to direct synthesis of hydrogen peroxide should be homogeneously catalysed if the same type of catalyst is retained for hydrogen peroxide synthesis (Au-Pd nanoparticles supported on silica). The advantages of the application of microreactors in homogeneous and phase-transfer

catalysis related to enhancement of reaction rates and better heat management compared to standard reactor types are well known ^[44,45]. Liquid phase oxidation reactions performed in microreactors using hydrogen peroxide as an oxidant ^[46–48] confirm this proposition. Heterogeneously catalysed liquid phase oxidations, such as propene oxide production process that uses TS-1 as an active catalyst can be considered, although this would require design of a bi-functional catalyst able to catalyse both peroxide synthesis and propene epoxidation. However, for a bulk process like the propene oxide production, microreactor technology might be too expensive. The most facile approach in that case would be deposition of Au-Pd colloidal nanoparticles on TS-1 layer grown directly inside the microchannel.

One of the factors that has to be considered when linking the direct synthesis of hydrogen peroxide with a subsequent chemical reaction is the effect of acid and halogen ions fed in the liquid phase. In some cases such as propene epoxidation, an acidic environment results in an epoxy-ring opening lowering the selectivity toward desired product. Only if the rate of coupled oxidation reaction would be faster than the peroxide hydrogenation and decomposition under given conditions, the use of such additives could be avoided. However, this is often not the case, therefore the influence of stabilizers on the overall process needs to be assessed. Removal of those components, if necessary, would represent an additional step in the overall process. Separation could be achieved through the application of ion exchange resins. Sodium ions can be removed by contacting the peroxide containing solution with acidic cation exchange resin. Bringing the solution further into contact with basic type ion exchange resin ensures exchange of anions SO_4^{2-} and Br^- for hydroxide ions and neutralization of acid thereby ($2\text{R}^+\text{OH}^- + \text{H}_2\text{SO}_4 = \text{R}_2^+\text{SO}_4^{2-} + 2\text{H}_2\text{O}$ and $\text{R}^+\text{OH}^- + \text{HCl} = \text{R}^+\text{Cl}^- + \text{H}_2\text{O}$). Ion exchange technology has been already applied in preparation of purified aqueous peroxide solutions ^[49]. In case of anion exchange resins, preference is given to a carbonate or a bicarbonate ion type, since the peroxide can be decomposed in contact with a strongly basic OH^- type anion exchange resin.

An interesting alternative to avoid usage of acidic solutions is the application of the solid acid as catalyst support through functionalization of coated silica support with sulfonic groups. The effect of halide addition on selectivity was not part of this study. However, there are indications that the role of halides is similar to the role of Au or Pt. Therefore, it is not quite clear if addition of halides additionally enhances selectivity towards the peroxide when a bimetallic catalyst is used, since the mechanism of halide action is not fully understood yet. Some experiments recently done in our group show that halide addition can be completely avoided, at least under conventionally explosive synthesis conditions.

One of the factors that still limits the application of this technology is the channel “numbering-up” in order to extend the capacity. The work previously done in our group on developing the design protocols to control gas-liquid distribution inside the parallel microchannels under Taylor flow regime which is a prerequisite for microreactor scale-up brings the multiphase microreactor technology closer to its industrial application [50–52]. An important issue that has to be considered when applying the concept of modular microreactors in direct synthesis of hydrogen peroxide with concentrated H₂-O₂ mixtures is that the dimensions of all the mini-plant (set up) elements in contact with such a mixture have to be of certain diameter that allows for safe operation. Otherwise, it is necessary to dilute the gas mixture before it comes into contact with parts of the equipment of larger dimensions or environment. In practise this can be prevented by operating the overall process at full conversions. The design of microreactor units would need to include a micro gas-liquid separator at the end of each microchannel. The unreacted gas phase collected from parallel channels containing undiluted H₂-O₂ mixtures can be utilized in a secondary reactor operating at somewhat lower pressure placed downstream allowing full consumption of the residual H₂.

To completely optimize the direct synthesis reaction and describe microchannel performance with corresponding mathematical model, detailed kinetic study needs to be performed. The kinetic model of the overall reaction besides the direct synthesis has to include the kinetics of hydrogenation and/or decomposition reaction involved in transformation of hydrogen peroxide into water. Further understanding and quantification of kinetics of direct synthesis reaction is desired for estimating potential applications of in-situ generated peroxide.

4.4. Conclusions

The potential of the wall-coated capillary microchannel to be applied in direct synthesis of hydrogen peroxide as a reactor system was evaluated. The effect of the gas and liquid flow rates as well as the catalyst loading on the hydrogen conversion and the concentration of hydrogen peroxide in liquid phase were studied. This allowed us to optimize the reaction conditions and to assess the range of peroxide concentrations that can be generated inside the microchannel. A decrease in the liquid flow rate leads to higher peroxide concentrations generated in the liquid phase. However, the generation of higher peroxide concentrations is accompanied by a faster peroxide conversion due to the subsequent hydrogenation and decomposition under those conditions and low selectivity. An increase in catalyst amount has a very similar effect. A decrease in the gas flow rate on the other hand results in higher conversions due to longer residence times, but lower hydrogen peroxide concentrations compared to higher flow rates. Although less hydrogen peroxide is converted at shorter residence times, the overall concentration of hydrogen peroxide in liquid phase is higher

due to the higher throughput of reactants. The maximum hydrogen peroxide concentration in liquid phase is accomplished when H_2 and O_2 ratio in the gas phase is equal to 1. Increase in oxygen content leads to higher selectivity due to suppression of peroxide hydrogenation reaction, reaching even 100 % selectivity at low H_2/O_2 ratios. Nevertheless, the exposure of the catalyst to $O_2/H_2 > 1$ over a longer period of time leads to a partial loss of the selectivity, although the hydrogen conversion remains the same. Higher H_2 partial pressures compared to O_2 result in a loss of selectivity and a drop in the hydrogen peroxide content as a consequence of the hydrogenation of the desired product.

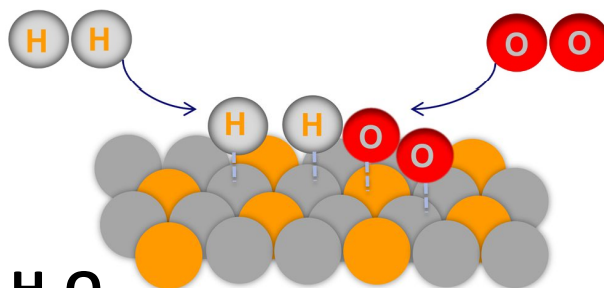
The final goal of this study was to assess the advantages and drawbacks of a microchannel as a reactor system for producing concentrated solutions of hydrogen peroxide that could be consumed on site in a specific local application. The dependence of H_2O_2 concentration in liquid phase and H_2 selectivity on WHSV was studied for two different G/L ratios. The results show a tremendous selectivity loss if one decides to operate the direct synthesis reaction at high H_2 conversions and high H_2O_2 concentrations in liquid phase. This implies that coupling the direct synthesis of hydrogen peroxide with consecutive reaction in which peroxide is consumed is necessary in order to prevent peroxide conversion to water.

References

- [1] W. K. and O. W. G. Goor, *Ullmann's Encyclopedia of Industrial Chemistry, Vol. A13*, Wiley-VCH Verlag GmbH & Co. KGaA, Weinheim, Germany, **1989**.
- [2] C. W. Jones, *Application of Hydrogen Peroxide and Derivatives*, The Royal Society of Chemistry, Cambridge, UK, **1999**.
- [3] R. Noyori, M. Aoki, K. Sato, *Chem. Commun. (Camb)*. **2003**, 1977–86.
- [4] S. Chattopadhyay, G. Veser, *AIChE J.* **2006**, *52*, 2217–2229.
- [5] V. Paunovic, V. Ordonsky, M. F. Neira, D. Angelo, J. C. Schouten, T. A. Nijhuis, *J. Catal.* **2014**, *309*, 325–332.
- [6] T. Inoue, Y. Kikutani, S. Hamakawa, K. Mawatari, F. Mizukami, T. Kitamori, *Chem. Eng. J.* **2010**, *160*, 909–914.
- [7] T. Inoue, M. A. Schmidt, K. F. Jensen, *Ind. Eng. Chem. Res.* **2007**, *46*, 1153–1160.
- [8] Y. Voloshin, R. Halder, A. Lawal, *Catal. Today* **2007**, *125*, 40–47.
- [9] J. F. Ng, Y. Nie, G. K. Chuah, S. Jaenicke, *J. Catal.* **2010**, *269*, 302–308.
- [10] D. van Herk, P. Castaño, M. Makkee, J. A. Moulijn, M. T. Kreutzer, *Appl. Catal. A Gen.* **2009**, *365*, 199–206.
- [11] J. Kobayashi, Y. Mori, K. Okamoto, R. Akiyama, M. Ueno, T. Kitamori, S. Kobayashi, *Science* **2004**, *304*, 1305–8.
- [12] E. Ntainjua N., J. K. Edwards, A. F. Carley, J. A. Lopez-Sanchez, J. A. Moulijn, A. A. Herzing, C. J. Kiely, G. J. Hutchings, *Green Chem.* **2008**, *10*, 1162–1169.
- [13] S. R. A. de Loos, J. van der Schaaf, M. H. J. M. de Croon, T. A. Nijhuis, J. C. Schouten, *Chem. Eng. J.* **2011**, *167*, 671–680.
- [14] P. Landon, P. J. Collier, A. F. Carley, D. Chadwick, A. J. Papworth, A. Burrows, C. J. Kiely, G. J. Hutchings, *Phys. Chem. Chem. Phys.* **2003**, *5*, 1917–1923.
- [15] J. K. Edwards, B. Solsona, E. N. N., A. F. Carley, A. A. Herzing, C. J. Kiely, G. J. Hutchings, *Science (80-.)*. **2009**, *323*, 1037–1041.
- [16] J. Pritchard, L. Kesavan, M. Piccinini, Q. He, R. Tiruvalam, N. Dimitratos, J. a Lopez-Sanchez, A. F. Carley, J. K. Edwards, C. J. Kiely, et al., *Langmuir* **2010**, *26*, 16568–77.
- [17] J. K. Edwards, S. F. Parker, J. Pritchard, M. Piccinini, S. J. Freakley, Q. He, A. F. Carley, C. J. Kiely, G. J. Hutchings, *Catal. Sci. Technol.* **2013**, *3*, 812.
- [18] M. Brust, M. Walker, D. Bethell, D. J. Schiffrin, R. Whyman, *J.Chem.Soc., Chem.Commun.* **1994**, 801–802.
- [19] C. J. Serpell, J. Cookson, D. Ozkaya, P. D. Beer, *Nat. Chem.* **2011**, *3*, 478–83.
- [20] Y. Han, J. Lunsford, *J. Catal.* **2005**, *230*, 313–316.
- [21] C. Samanta, *Appl. Catal. A Gen.* **2008**, *350*, 133–149.
- [22] M. Piccinini, E. Ntainjua, J. K. Edwards, A. F. Carley, J. a Moulijn, G. J. Hutchings, *Phys. Chem. Chem. Phys.* **2010**, *12*, 2488–2492.

- [23] E. N. Ntainjua, M. Piccinini, S. J. Freakley, J. C. Pritchard, J. K. Edwards, A. F. Carley, G. J. Hutchings, *Green Chem.* **2012**, *14*, 170.
- [24] M. Piccinini, J. K. Edwards, J. a. Moulijn, G. J. Hutchings, *Catal. Sci. Technol.* **2012**, *2*, 1908.
- [25] P. Biasi, P. Canu, F. Menegazzo, F. Pinna, T. O. Salmi, *Ind. Eng. Chem. Res.* **2012**, *51*, 8883–8890.
- [26] F. Gao, D. W. Goodman, *Chem. Soc. Rev.* **2012**, *41*, 8009–20.
- [27] S. M. McClure, D. W. Goodman, *Chem. Phys. Lett.* **2009**, *469*, 1–13.
- [28] E. Ozensoy, E. I. Vovk, *Top. Catal.* **2013**, *56*, 1569–1592.
- [29] V. R. Choudhary, C. Samanta, P. Jana, *Appl. Catal. A Gen.* **2007**, *317*, 234–243.
- [30] R. Burch, P. R. Ellis, *Appl. Catal. B Environ.* **2003**, *42*, 203–211.
- [31] H. H. Kan, J. F. Weaver, *Surf. Sci.* **2009**, *603*, 2671–2682.
- [32] G. Berčić, A. Pintar, *Chem. Eng. Sci.* **1997**, *52*, 3709–3719.
- [33] M. T. Kreutzer, P. Du, J. J. Heiszwolf, F. Kapteijn, J. A. Moulijn, *Chem. Eng. Sci.* **2001**, *56*, 6015–6023.
- [34] M. T. Kreutzer, F. Kapteijn, J. a. Moulijn, J. J. Heiszwolf, *Chem. Eng. Sci.* **2005**, *60*, 5895–5916.
- [35] M. T. Kreutzer, F. Kapteijn, J. A. Moulijn, *Catal. Today* **2005**, *105*, 421–428.
- [36] S. Murakami, K. Ohtaki, S. Matsumoto, T. Inoue, *Jpn. J. Appl. Phys.* **2012**, *51*, 06FK11.
- [37] P. Biasi, J. García-Serna, A. Bittante, T. Salmi, *Green Chem.* **2013**, *15*, 2502.
- [38] S. Niwa Si, M. Eswaramoorthy, J. Nair, A. Raj, N. Itoh, H. Shoji, T. Namba, F. Mizukami, *Science* **2002**, *295*, 105–7.
- [39] T. Miyake, M. Hamada, Y. Sasaki, M. Oguri, **1995**, *131*, 33–42.
- [40] J. E. Remias, T. a. Pavlosky, A. Sen, *J. Mol. Catal. A Chem.* **2003**, *203*, 179–192.
- [41] J. Chen, S. J. A. Halin, J. C. Schouten, T. A. Nijhuis, *Faraday Discuss.* **2011**, *152*, 321.
- [42] R. Meiers, U. Dingerdissen, W. F. Hoelderich, **1998**, *386*, 376–386.
- [43] C.W. Jones, *Applications of Hydrogen Peroxide and Derivatives*, Royal Society Of Chemistry, **1999**.
- [44] T. Wirth, *Microreactors in Organic Synthesis and Catalysis*, Wiley –VCH Verlag GmbH&Co., KGaA , Weinheim, Weinheim, **2008**.
- [45] J. Jovanovic, *Liquid-Liquid Microreactors for Phase Transfer Catalysis*, Eindhoven University of Technology, **2011**.
- [46] K. Yube, K. Mae, *Chem. Eng. Technol.* **2005**, *28*, 331–336.
- [47] M. Shang, T. Noël, Q. Wang, V. Hessel, *Chem. Eng. Technol.* **2013**, *36*, 1001–1009.
- [48] M. Damm, B. Gutmann, C. O. Kappe, *ChemSusChem* **2013**, *6*, 978–982.
- [49] T. Fujio, S. Ichiro, A. Takashi, M. Kazuhisa, *Process for Producing a Purified Aqueous Hydrogen Peroxide Solution*, **2005**, 6896867.

- [50] M. Al-Rawashdeh, Barrier-Based Micro / Milli Channels Reactor, PhD thesis, Eindhoven University of Technology, **2013**.
- [51] M. Al-Rawashdeh, L. J. M. Fluitsma, T. A. Nijhuis, E. V. Rebrov, V. Hessel, J. C. Schouten, *Chem. Eng. J.* **2012**, *181-182*, 549–556.
- [52] M. Al-Rawashdeh, F. Yu, T. A. Nijhuis, E. V. Rebrov, V. Hessel, J. C. Schouten, *Chem. Eng. J.* **2012**, *207-208*, 645–655.



Direct synthesis of H₂O₂ over Au-Pd catalyst- Kinetic study

5

This chapter is submitted for publication as:

V. Paunovic, J. C. Schouten, T. A. Nijhuis, Direct synthesis of hydrogen peroxide in a wall-coated microchannel over Au-Pd catalyst- Kinetic study, Appl. Cat. A: General, 2015, accepted.

ABSTRACT

The kinetics for direct synthesis of hydrogen peroxide out of hydrogen and oxygen has been studied over AuPd colloidal nanoparticles, which were prepared using a two-phase synthesis protocol. Reactions of direct formation of peroxide and peroxide reduction in the presence of hydrogen were studied separately to obtain the overall kinetic model, which was suitable to predict peroxide concentration at the outlet of the wall-coated microchannel reactor. The decomposition reaction was eliminated by the addition of sulfuric acid. The kinetic model of the direct formation of hydrogen peroxide from hydrogen and oxygen assumes hydrogen adsorption, pairwise dissociation, but not spill-over of H-species over the bimetallic AuPd surface. Peroxide concentration values predicted with an overall kinetic model and values experimentally measured at the outlet of the microchannel with a catalytic layer deposited on the wall are in acceptably good agreement.

5.1. Introduction

Hydrogen peroxide is one of the most important and versatile commercial chemicals today with application in the paper and pulp industry as a bleaching agent, disinfectant, in semiconductors for surface cleaning and in production of chemicals (peroxy compounds, oxidations, epoxidation, hydroxylation agent)^[1-3]. Such a wide variety of applications is influenced by the green nature of the chemical. Water is the only by-product of the peroxide decomposition, making the hydrogen peroxide an environmentally friendly reagent. Hydrogen peroxide is generated as a side product via the oxidation of hydroquinone suspended in organic solvent, followed by the extraction to the aqueous phase containing stabilizers in a process known as Anthraquinone autooxidation process (AO). Recently built AO plants for H₂O₂ production reach an annual production capacity of 300kt. The economic feasibility of the AO process requires large scale operations if one has in mind the complexity of the process and the number of downstream unit operations (extraction, distillation) used to concentrate acidified aqueous peroxide solutions to commercial grades (50 or 70 wt%) suitable to be transported over large distances. End users of hydrogen peroxide typically require concentrations in a range of 1-10 wt%. Considering the end-user requirements and safety hazards associated with transport and storage of peroxide solutions, the development of small scale on-demand process for hydrogen peroxide production is of significant interest ^[4]. Among the alternatives, the direct synthesis of hydrogen peroxide has been recognized as the best option. In contrast to the AO process, the direct synthesis combines directly hydrogen and oxygen gas in one reaction step. The major setback for the direct synthesis to be operated using conventional reactor technology (semi-continuous stirred tanks, fixed-bed and slurry bubble columns) relates to the safety requirements, which dictate that the H₂ and O₂ concentrations in the gas stream stay below the explosive limits. In practise this means less than 4 vol% of hydrogen in the gas feed. Novel reactor technologies, such as membranes or microreactors diminish the safety risks associated with reacting directly H₂ and O₂. Although the main advantage of membranes is to keep reacting gasses separate, their cost is rather high. The reduction in dimensions of reactive channels in case of microreactors and high heat dissipation allow for direct synthesis of hydrogen peroxide to be operated safely using concentrated hydrogen and oxygen mixtures. Extensive calculations performed by Chattopadhyay and Vesper ^[5], indicated that channel diameters below 300 µm are intrinsically safe. Still, taking into account that reaction is performed at elevated pressures, the safety margin for this particular channel diameter will be shifted towards lower temperatures. The modular nature of microreactors makes them applicable for on-site on demand production of chemicals. In addition, considering fast heat and mass transfer rates, associated with a high surface to volume ratio which varies between 10000-50000 m²/m³, in comparison to

Chapter 5

conventional reactors which reach up to $1000 \text{ m}^2/\text{m}^3$ ^[6], makes them suited for fast and exothermic reactions.

Micro-packed beds are nowadays commonly used in catalyst testing^[7] or kinetic studies of heterogeneously catalyzed reactions^[8–10], since they simply allow application of already optimized or conventional catalysts available on the market. Typically, catalyst particles used are in a range of $50\text{--}150 \text{ }\mu\text{m}$ ^[7,10]. Those randomly packed structures often result in a high pressure drop and flow maldistribution as a consequence of packaging non-uniformity throughout different channels. In case of specific reactions, such as direct synthesis of hydrogen peroxide, due to improper bed dilution with inert material, hot spots can be formed followed by explosions^[7]. By deposition of a catalytic layer on the reactor wall, a high pressure drop can be avoided as well as poor catalyst wetting and contacting^[11] typical for micro-packed beds. Karim et al. showed that temperature gradients present in micro packed-beds during methanol steam reforming can be eliminated by coating the catalyst on the reactor wall, thus resulting in higher catalytic activity^[12]. In addition, it has been reported that simply switching from a packed-bed to a wall-coated microreactor can lead to a significant difference in selectivity, as a result of difference in distribution of reactant concentration^[13]. In comparison to micro-packed beds, three-phase reaction in wall-coated microchannels can be operated in conventional Taylor flow. Three-phase reactions in wall-coated microchannels are typically performed in Taylor flow because of the high mass transfer rates that can be achieved. A particularly fast step that coexists with other G-L and L-S mass transfer steps in Taylor flow operation is the transfer of the gas to the solid catalyst through the thin liquid film present between the bubble and the wall (gas-to-solid)^[14,15]. In micro-packed bed liquid slugs are continuously broken by the solid particles present in the channel, therefore Taylor flow as such does not exist in micro packed-beds^[10,16]. Still, this flow regime is known to enhance G-L mass transfer^[17].

A number of publications by Inoue et al. report the successful application of microreactor technology in the production of H_2O_2 by direct synthesis reaction in the required range (1–10wt%)^[7,18–20]. The highest peroxide concentrations observed are achieved using Au-Pd supported catalyst in a form of a micro-packed bed^[19]. Their earlier publications also hinted to potential concerns in relation with direct synthesis in packed-bed microreactors. Beside elimination of hot-spots via proper catalyst loading along the channel bed, potential catalyst elution as a consequence of overoxidation of the active catalytic phase at higher oxygen content also needs to be excluded^[7]. This is a prerequisite for safe and long-term operation. Voloshin et al. studied in detail the kinetics of direct synthesis of hydrogen peroxide over a Pd catalyst by isolating and separately studying direct synthesis^[10], hydrogenation^[9] and decomposition^[8] reaction in a packed-bed microchannel. Their work also indicated that the catalyst activity is highly influence by the reaction environment. They showed that exposure

of the catalyst to higher peroxide concentrations (1.02 mol/L) modified the catalyst resulting in both lower hydrogenation and hydrogen peroxide formation rates ^[9]. This observations were in agreement with results observed in decomposition of H₂O₂ (0.2wt%) solutions over Pd/C catalyst which indicated 6-8% lower catalytic activity after each successive use of the catalyst ^[21].

Our approach was to apply a wash-coated silica layer embedded with Au-Pd colloidal nanoparticles as a catalytic layer for the direct synthesis of hydrogen peroxide inside a wall-coated microchannel ^[22,23]. We demonstrated that a concentration as high as 5 wt% of hydrogen peroxide can be generated in an acidified aqueous phase using a pure H₂ and O₂ at 1:1 ratio. Moreover, these catalytic layers proved to be stable even after several weeks of operation under the given reaction conditions.

An increase in reactant concentration in the gas phase or a high(er) reactant partial pressure proved to be highly beneficial for the selectivity ^[22]. The effect of addition of Au to Pd is often assigned to the dilution of the Pd surface and blockage of O₂ or H₂O₂ dissociation sites. It is believed that ensembles of Pd active sites are needed to dissociate oxygen bond forming water non-selectively ^[24–26]. The increase in selectivity towards peroxide at higher H₂ and O₂ partial pressures is associated with the blockage of side reactions on the catalyst surface at high surface coverage with reacting gas molecules. In general, with higher reactant concentration and higher fraction of active sites occupied, adsorption effects are becoming increasingly important. To account for the effect of adsorption, the L-H type of kinetic models are more accurate (appropriate). Considering all the above, to understand the direct synthesis reaction, our goal was to isolate the reactions involved in the peroxide formation and determine the kinetic expressions taking into account that adsorption of reactants on the catalyst surface might play an important role in the overall kinetics of peroxide formation.

5.2. Materials and Methods

The AuPd catalytic phase inside the microchannel can be deposited either by deposition of active metal on a pre-coated support layer or by directly coating a ready-made catalyst ^[27]. To create a surface area for deposition of the active metallic phase (wall material is non-porous), it is necessary to first deposit a porous layer of support such as silica. Knowing that some of the binder material used in preparation of coating slurry might close the pores with active metal if a ready-made catalyst is directly coated onto the microchannel walls, the active phase was deposited afterwards on the coated catalyst support layer, allowing full accessibility of the active phase to reactant molecules.

5.2.1. Deposition of silica layer

The silica layer used to support the catalyst nanoparticles inside the microchannel was deposited using a dynamic displacement procedure. The dynamic coating involves displacement of the coating fluid by means of another fluid, typically a gas. After a solution is forced through the microchannel, a thin liquid film remains on the wall. A silica composed coating fluid supplied to a capillary by means of a syringe pump is displaced using a flow of N_2 gas which is fed through the mass flow controller. The slurries used for coating our capillaries typically contained Ludox AS 30 colloidal silica and sodium silicate solution (Sigma-Aldrich, $SiO_2 \sim 26.5$ wt%, Na_2O , $\sim 10.6\%$) as binders, the silica slurry typically contained fumed silica (~ 4 wt%, Sigma Aldrich) and larger particles in a form of Davisil silica gel (8wt%, 10-14 μm particle size). The slurry suspension contains large particles and smaller binder particles (typically two orders of magnitude smaller in size), which act as a “glue” between large particles improving the contact and cohesion. Details on the coating procedure and coating set-up used are given in our earlier publication ^[22].

5.2.2. Deposition of Au-Pd catalyst

Capillaries wash-coated using the slurry method or silica powder (Davisil) were used to deposit the Au-Pd colloidal nanoparticles active in direct synthesis of hydrogen peroxide. Au-Pd nanoparticles were used as active metallic phase in both the direct synthesis and hydrogen peroxide hydrogenation kinetic experiments. Colloidal nanoparticles with a 1:2 Au/Pd ratio in this case were generated in dichloromethane as a solvent. The application of dichloromethane in the catalyst preparation enables a fast evaporation of solvent, thus making the catalyst preparation process particularly in a microchannel faster and more efficient. In general the two-phase synthesis approach involves the dissolution of required amounts of anionic Au and Pd precursors in a water phase ($H AuCl_4$ and K_2PdCl_4 respectively), after which they are transferred to an organic phase by means of a phase-transfer agent. Separate dichloromethane solutions containing tetrachloropalladate and tetrachloroaurate anions in a desired ratio are mixed prior to reduction with $NaBH_4$. The exact protocol for synthesis of Au-Pd alloy nanoparticles is taken from Serpell et al. ^[28]. The dichloromethane solution containing stabilized Au-Pd colloidal nanoparticles was subsequently used to impregnate the silica support either in a form of a layer deposited inside the microchannel or as silica powder. For the deposition of these nanoparticles, the capillary is filled with the colloidal solution of Au-Pd nanoparticles and the solvent is slowly evaporated. After deposition of the Au-Pd alloy nanoparticles inside the wash-coated capillary and solvent removal, the capillary was calcined at 380 °C for 4 hours in static air. The same calcination/heating procedure was applied on Au-Pd nanoparticles supported on silica powder.

5.2.3. Direct synthesis of hydrogen peroxide in a microchannel–kinetic experiments

The scheme of the microchannel set-up used to conduct the kinetic experiments is given in Fig. 5.1. A wall-coated catalytic capillary was placed in a thermostated water bath. The liquid phase is supplied to the system by means of a syringe pump (Teledyne ISCO 500D) typically at a flow rate of 0.05 ml/min. The total gas flow through the capillary is set at 5 mlN/min, while the flow of reactant in excess was always kept at 2.5 mlN/min.

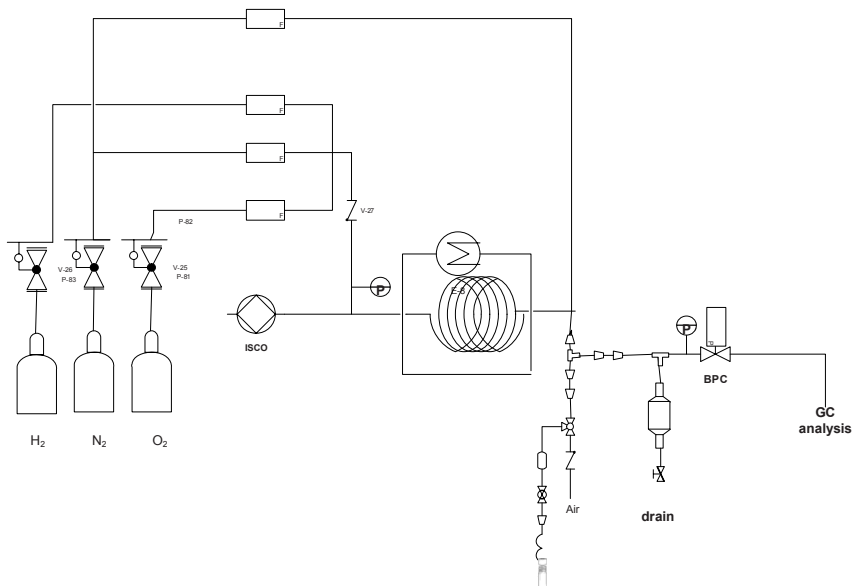


Figure 5.1. Scheme of the microchannel set-up used in direct synthesis of hydrogen peroxide.

Partial pressure of limiting reactant was varied by adjusting limiting reactant flow rate and flow rate of nitrogen. In order to maintain a constant pressure at 20 bar, a back-pressure regulator is placed downstream after a gas–liquid separation unit. Considering that concentrated H_2/O_2 mixtures are used, the gas flow is diluted with N_2 gas at the capillary outlet to assure a non-explosive gas mixture in the larger tubing downstream of the capillary reactor. The pressure in the system was monitored before the inlet and after the microchannel outlet. The pressure drop during the kinetic experiments was not exceeding 0.1 bar, which is a typical value observed when non-coated silica capillary of the same diameter is placed in the set-up. Gas samples were analyzed with an online compact GC (column: Molsieve plot 5m 0.32 mm) equipped with a TCD detector to calculate the conversion of hydrogen and oxygen. Liquid samples were collected and immediately titrated with a standard solution of cerium (IV) sulfate to determine to concentration of

Chapter 5

hydrogen peroxide. Typically, 2-3 drops of ferroin indicator are added to the ice cold solution of sulphuric acid (1:19 v/v) and titrated dropwise to a pale blue color prior sample addition. Upon addition of the weighed sample the solution turns red. The solution is stirred during the course of titration. A cerium sulphate standard solution is added until the blue end point appears.

Knowing that the hydrodynamics affect the performance of the multiphase reactor, flow visualization experiments were conducted prior to starting the kinetic experiments. For this purpose, an empty fused silica capillary of the same dimensions as reactive capillary was used. Under the reaction conditions applied in the kinetic study, Taylor flow with alternating gas and liquid slugs was observed. For gas-liquid-solid reactions in microchannels, Taylor flow has been shown to enhance mass transfer significantly^[15,29].

5.2.4. Hydrogenation of hydrogen peroxide in semi-batch reactor-kinetic experiments

The reduction of hydrogen peroxide in the presence of H₂ was investigated using semi-continuous operation with a titanium Gr2 300 ml autoclave (i.e. as batch for the liquid phase with a continuous gas flow, Fig. 5.2). The gas mixture used in these experiments contained H₂ in nitrogen as an inert and was fed by means of mass flow controllers. The autoclave is equipped with an overhead stirrer which provides stirring in a range of 0-3000 rpms. Typically, 150 ml of the liquid phase containing Au-Pd supported catalyst, promoters (H₂SO₄ and NaBr) and water was charged in the autoclave. Gas is supplied to the liquid phase through the stirrer shaft (gas inducing stirrer) at a total flow rate of 500 ml/min. After charging the liquid phase and the catalyst, the autoclave was purged with N₂ and thermostated at the desired temperature before adding hydrogen peroxide and starting pressurization with the reaction gas mixture. Temperature control of the slurry reactor is achieved using a heating jacket. The desired gas flow rates were controlled using mass flow controllers. In order to maintain a constant pressure at 20 bar, a back pressure regulator was used at the gas outlet just before the GC. Liquid samples were collected manually at the liquid sampling point and titrated with a standard solution of cerium (IV) sulphate to a blue end-point. Samples collected were weighed to account for a decrease in liquid volume in the reactor over time. As soon as the desired pressure was reached, the stirrer was started designating the start of the reaction and the first sample was collected to determine the initial concentration of peroxide (at t=0).

The effect of acids and halides was investigated by Liu and Lunsford^[30] as well as by the group of Choudhary^[31] concluding that there will be hydrogenation and decomposition at the same time in the reactor immediately after exposure of hydrogen to hydrogen peroxide in the absence of acid. In the absence of halide or the presence of fluoride anions, decomposition reaction is pronounced whereas in the presence of chloride or bromide

anions, the hydrogenation reaction is prominent. For this reason the decision was made to add 0.05M H_2SO_4 and 10ppm NaBr to the liquid reactants in the experiments in order to suppress the decomposition reaction during peroxide hydrogenation experiments. Under these conditions, it was experimentally verified that the decomposition reaction is entirely suppressed.

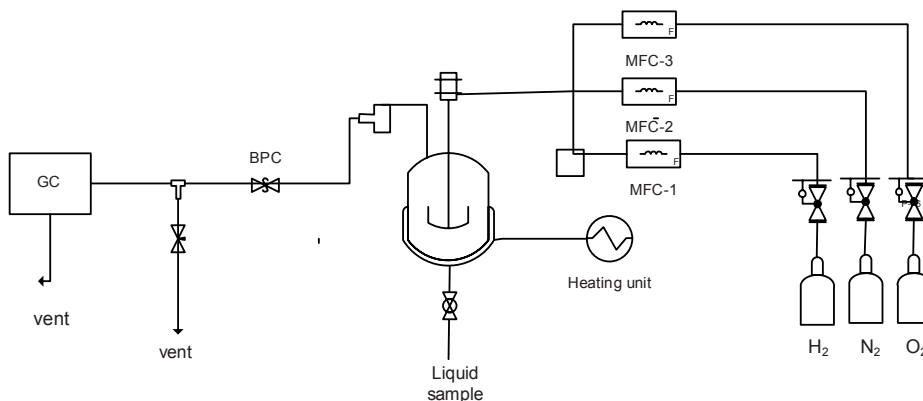


Figure 5.2. Scheme of the semi-batch set-up used in hydrogenation of hydrogen peroxide.

5.2.5. Parameter determination

Values of kinetic parameters are obtained by applying non-linear regression analysis. The fit functions are derived assuming different elementary reaction steps on the surface (see Appendix). To reduce the number of constants fitted, surface reaction mechanisms are somewhat simplified. The software iterated through values for the constants until it obtained values that minimized the sum of the squares of the residuals. Hydrogenation rate data were fitted using Polymath 6.10, while oxygen conversion rates were fitted in Matlab using the NLINFIT function with the confidence intervals calculated from the residuals and Jacobian using the NLPARCI function. For calculation of the activation energy (E_a) and adsorption enthalpies (ΔH) linearized Arrhenius plots were used ($\ln(k)$ vs. $1/T$).

5.3. Results and Discussion

5.3.1. Characterization of Au-Pd catalysts

In order to determine the surface composition of the freshly calcined Au-Pd (1:2) nanoparticles supported on silica material, XPS analysis was performed. Analysis revealed that 38% of surface atoms are Au, which corresponds to an initial molar ratio used in the

synthesis procedure. It is evident that the Au-Pd nanoparticles are alloys. In addition, 74.7 % of surface Pd is in a form of PdO.

The nature of the metal sites for the silica supported catalysts was investigated by FTIR spectroscopy of adsorbed CO. Carbon monoxide is a well-established probe molecule for the characterization of the metal state in solid catalysts^[32]. CO was gradually adsorbed until a complete saturation of active sites was reached. The saturation point is accompanied by the appearance of a band at ca. 2140 cm^{-1} , characteristic of physically adsorbed CO. For comparison purposes, the CO adsorption experiments were performed over reference Au and Pd nanoparticles supported on silica. The results obtained are shown in Fig. 5.3a. The appearance of bands at ca. 2156, 2138, 2108, 2000, 1976 and 1888 cm^{-1} (Fig. 5.3a) observed with adsorption of CO on Pd/SiO₂, is typical for Pd supported on silica samples^[33]. The band at 2138 cm^{-1} is assigned to physically adsorbed CO, while the band at 2156 cm^{-1} can be attributed to the vibrations of CO adsorbed on the Si-OH surface groups of the support. Bands at 2108 and 2000 cm^{-1} correspond to linear and bridging carbonyls of the Pd⁺ surface species, correspondingly, whereas bands at lower frequencies (1976 and 1888 cm^{-1}) can be ascribed to the adsorption of CO over metal Pd sites with the formation of (Pd₂)⁰CO and (Pd₃)⁰CO surface species.

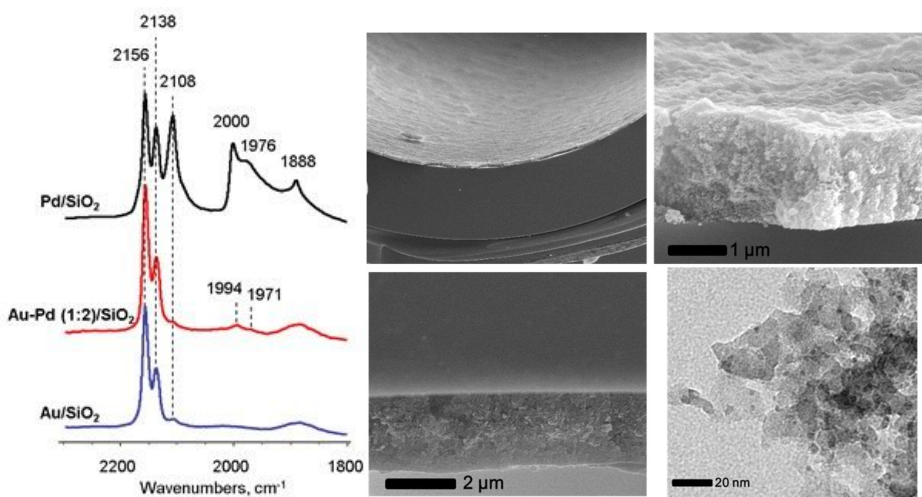


Figure 5.3. a) IR bands resulting from CO adsorption at 100 K on Pd/SiO₂, Au-Pd/SiO₂ and Au/SiO₂ (Chapter 6, Fig. 6. 11) **b)** SEM image of silica wash-coated layer and TEM of silica layer embedded with Au-Pd (1:2) nanoparticles.

The Au/SiO₂ catalyst reveals a simpler spectrum: bands at 2156 and 2138 cm⁻¹, similar to Pd/SiO₂ and a band at 2108 cm⁻¹, which corresponds to the adsorption of CO over Au⁺ defects [34].

In the case of the Au-Pd/SiO₂ sample, new bands at 1994 and 1971 cm⁻¹ were detected. These bands can be attributed to the interaction of CO with Au-Pd sites in surface alloys, which can be formed during the synthesis of bimetallic particles. CO adsorption results indicate a strong interaction between Au and Pd. Comparison of the spectra for Pd/SiO₂ and Au-Pd/SiO₂ shows that the addition of gold leads to a disappearance of the bands corresponding to (Pd₂)⁰CO and (Pd₃)⁰CO species, pointing to the presence of Au atoms in the Pd environment. In fact, the results imply that Pd is strongly diluted by Au on the surface, since there are almost no Pd-Pd centers (no bridged CO over Pd). This observation is in line with the XPS data, which showed that the surface Au/Pd ratio is close to that of the bulk, calculated from the synthesis procedure (Chapter 6).

Due to the high external mass transfer rates in microchannels, fast reactions might be limited by diffusion of reactants through the support layer. The thicker the layer, the higher the catalyst hold-up in the microchannel. In contrast, thinner layer ensures a more efficient catalyst usage. In order to ensure that the kinetic data are collected under in kinetically limited regime, it is necessary to ensure that the catalyst efficiency η is equal to 1 meaning that 100 % of the catalyst deposited inside the microchannel is utilized. Knowing that thickness of the coating plays a significant role, the silica layer thickness was estimated from SEM images of coated capillaries. The typical thickness of the layer used in the kinetic experiments is estimated to be around 2 μm (Fig. 5.3b).

5.3.2. Reaction

The direct synthesis of hydrogen peroxide involves a two-step reaction series (Fig. 5.4), with two parallel reactions in each step. Oxygen, in the presence of hydrogen, is directly converted either to hydrogen peroxide or to water. Hydrogen peroxide formed in the first step is an intermediate product, which can be easily decomposed or hydrogenated to water.

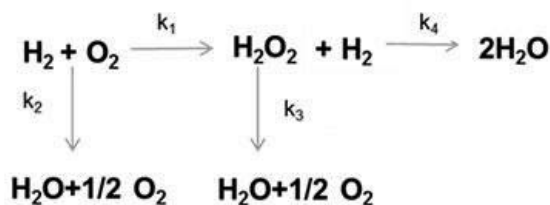


Figure 5.4. Direct synthesis of hydrogen peroxide-reaction scheme.

Chapter 5

The problem of peroxide decomposition, which easily occurs even in the absence of catalyst as a consequence of base catalyzed decomposition^[35], can be successfully eliminated by introducing acid and/or halides^[30,36–39]. It has been confirmed that besides the proton, the associated anion of the mineral acids also has an influence on observed reaction rate and selectivity. Typically non-coordinating anions, such as sulfate, phosphate, nitrate, etc., are assumed not to block the catalytically active sites in the direct synthesis^[36,40], while coordinating anions, such as chloride, bromide and iodide are responsible for catalyst poisoning^[41]. Although phosphoric acid is suitable due to the low corrosiveness and low leaching in case of Pd catalysts^[42], there are reports claiming a deteriorating inhibiting effect of the phosphate anion in the direct synthesis of hydrogen peroxide over Au-Pd catalyst^[43]. We observed that at a sulfuric acid content of 0.05M and a NaBr content of approximately 10 ppm, the decomposition reaction is completely inhibited. The water produced upon addition of acid and halide at the required concentration during the direct synthesis can originate either from peroxide reduction by hydrogen or direct formation of water from H₂ and O₂. In our earlier publication^[23] it was observed that at high oxygen and low hydrogen partial pressures, the selectivity towards H₂O₂ is reaching 100%. This means that the water formation over a Au-Pd catalyst during the direct combination of H₂ and O₂ is a result of peroxide reduction by H₂, leading to a significant simplification of the reaction scheme considered.

The simplified reaction scheme implies that all the oxygen reacts in the first step with hydrogen to form hydrogen peroxide, which is, in the second step, in the excess of H₂ reduced to water. So following expressions are considered in the rate analysis:

$$\begin{aligned}
 -R_{O_2} &= R_{H_2O_2, \text{formation}} \\
 R_{H_2O_2} &= R_{H_2O_2, \text{formation}} - R_{H_2O_2, \text{hydrogenation}} \\
 -R_{H_2} &= R_{H_2O_2, \text{formation}} + R_{H_2O_2, \text{hydrogenation}}
 \end{aligned}$$

As already discussed in the introduction, exposure of the Pd catalyst to hydrogen peroxide even at low concentrations of hydrogen peroxide might result in catalyst deactivation^[9,21] ascribed to the oxidation of Pd. Due to an undesired gradual loss of activity in continuous operation, the hydrogen peroxide hydrogenation reaction was isolated and studied in semi-batch reactor using initial rate analysis. The initial reaction rates were determined by a differential method with Δt of 1-2 min within the first 5-10 min from the reaction start (≤ 15 % peroxide converted).

5.3.3. Catalyst oxidation state alternation and activity

In general, the overoxidation of Pd and potential loss of catalytic activity can occur when operating the catalyst under prevailing oxidative conditions. Inoue et al.^[7] reported that at higher oxygen contents in the gas phase the activity of Pd catalyst is gradually decreasing as a consequence of oxidation and leaching. To measure the intrinsic kinetics of the direct synthesis reaction, one needs to ensure a stable catalyst performance. Au-Pd nanoparticles deposited on a silica wash-coated layer do not show signs of deactivation even after several weeks of operation when using a 1:1 H₂:O₂ ratio. However, the alteration of catalytic activity is observed after exposing the catalyst to a higher H₂ and/or higher O₂ content for a longer period of time (Fig. 5.5). Fig. 5.5a. Illustrates that exposure of the Au-Pd catalyst to a low H₂/O₂ ratio for over 100 h results in a partial loss of activity. To further investigate if the loss of activity is reversible or not, the catalyst was reduced in a H₂ flow. Considering that the catalytic activity was completely restored when comparing to the initial values obtained with 1:1 H₂:O₂ mixtures, it was concluded that the most likely cause of such behavior is the change in the oxidation state of Pd. In addition, leaching of Pd was excluded.

In contrast, catalyst exposure for a number of hours to a higher H₂ content improves the catalytic activity (Fig. 5.5b). However, after applying an equimolar H₂/O₂ ratio again, with time on stream the catalytic activity as determined from the peroxide concentration is decreasing towards the initially observed value. The alteration of the catalyst activity with catalyst exposure to different oxidant/reductant ratios has a significant influence in case of long term reaction/reactor performance and in our case was mainly observed when limiting reactant content was in depletion. Nevertheless, it is difficult to say if similar effect would occur for any O₂/H₂ ratio for longer reaction times than considered in our study. Knowing that higher selectivity values are observed at O₂/H₂>1, one would possibly choose to operate direct synthesis using higher oxygen content in the gas phase with cyclic catalyst reduction to avoid permanent catalyst deactivation. Our goal was to determine the intrinsic kinetics of reaction without taking into account kinetics of deactivation or reactivation. Considering all the above, the kinetics of direct synthesis reaction was studied avoiding the long catalyst exposure to either H₂ or O₂ rich environment. Hydrogen and oxygen flow rates were alternated, using 1:1 H₂:O₂ mixture intermittently between the two measurements as a standard to detect any changes in catalyst performance typically overnight.

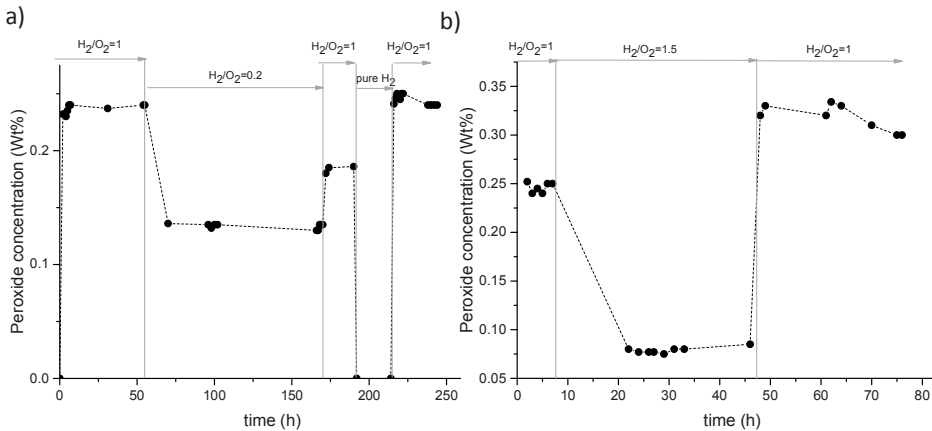


Figure 5.5. Changes in catalyst activity with H₂/O₂ ratio a) effect of catalyst exposure to H₂/O₂ < 1 b) effect of catalyst exposure to H₂/O₂ > 1 (Total gas flow rate 5 ml/min, liquid flow rate 0.05 ml/min, aqueous phase 0.05M H₂SO₄ and 10 ppm bromide; total pressure 20 bar).

5.3.4. External and internal mass transfer in microchannel

To verify the conclusions related to the effect of the studied process parameters on the reaction kinetics, the potential influence of mass transfer has to be evaluated. It is known that in case of Taylor flow in microchannels mass transfer of a gas component proceeds through the following 3 steps: (1) From gas bubble directly to the solid catalyst through thin liquid film (gas-to-solid) (2) from the bubble caps to the liquid (gas-to-liquid) and (3) from the liquid to the catalyst for dissolved gas (liquid-to-solid). Mass transfer from gas-to-liquid and liquid-to-solid proceeds via resistances in series and occur in parallel to mass transfer directly from gas-to-solid. In case of a catalytic reaction occurring on the reactor wall such as direct synthesis of hydrogen peroxide, gas-to-solid mass transfer is the dominant step. In comparison to $k_{GS}a_{GS}$, under the given operating conditions for direct synthesis reaction contribution of other two steps to overall mass transfer rate is negligible. Calculation of mass transfer coefficient from gas-to solid $k_{GS}a_{GS}$ was performed using well established correlations available in literature [15,29]. For gas and liquid flow rates used in kinetic experiments the $k_{GS}a_{GS}$ value is approximately reaching 50 s^{-1} (46.7). To evaluate if the overall volumetric reaction rate $R_{v,ov}$ is fully determined by external mass transfer rate the following criterion was established which corresponds to criteria widely used in literature [44,45] :

- External mass transfer is not significant if $R_{v,ov} \leq 0.1 k_{GS}a_{GS}C_{H_2}^{sat}$

- Reaction is mass transfer limited if $R_{v,ov} \geq 10 k_{GS} a_{GS} C_{H_2}^{sat}$

The saturated concentration of H_2 is considered limiting, since oxygen typically exerts an order of magnitude higher solubility than hydrogen. Calculated values of the mass transfer rates show that these are already more than an order of magnitude higher than highest observed overall volumetric reaction rates (at 50°C), indicating that external mass transfer is not the limiting step.

To determine whether mass transfer limitations within the catalyst layer might be significant, the Wheeler –Weisz modulus was calculated:

$$\Phi = \frac{L^2 R_{v,coating}}{D_{H_2,eff} C_{H_2}^{sat}} < 0.15$$

$R_{v,coating}$ represents the reaction rate per unit volume of the catalytic layer. For calculation of the effective diffusivity $D_{H_2,eff}$ and $D_{O_2,eff}$ typical values for porosity of coating layer of 0.4 and tortuosity value of 6 were used. The thickness of the catalyst layer L is estimated to be close to 2 μm . For the highest reaction rates observed in the above experiments, calculated values for Weisz modulus are $\Phi < 0.15$. According to Weisz-Prater criterion^[46], this is a good indication that pore diffusion effects are absent and that the catalyst effectiveness $\eta = 1$.

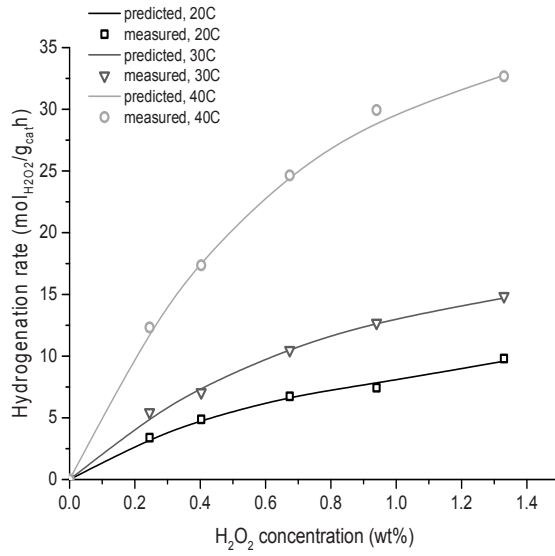
5.3.5. Hydrogenation kinetics

Initially considering the reports related to the potential deactivation of the catalyst in the presence of higher H_2O_2 concentration observed in hydrogenation reaction by Voloshin et al.^[9], the decision was made to evaluate kinetics of H_2O_2 hydrogenation in an autoclave using the initial rate method.

A series of tests has been performed to determine the operating conditions in kinetically limited regime and to ensure absence of both external and internal mass transfer limitations. External mass transfer limitations were determined by variation in the stirring speed and catalyst amount or loading while keeping all the other parameters constant such as concentration of hydrogen peroxide and partial pressure of hydrogen. As the reaction rate remains unchanged at the stirring speed of 1600 rpms or higher for the upper range of H_2 partial pressures and H_2O_2 concentrations, a stirrer speed of 1600 rpms was required to reduce the external mass transfer limitations.

Chapter 5

a)



b)

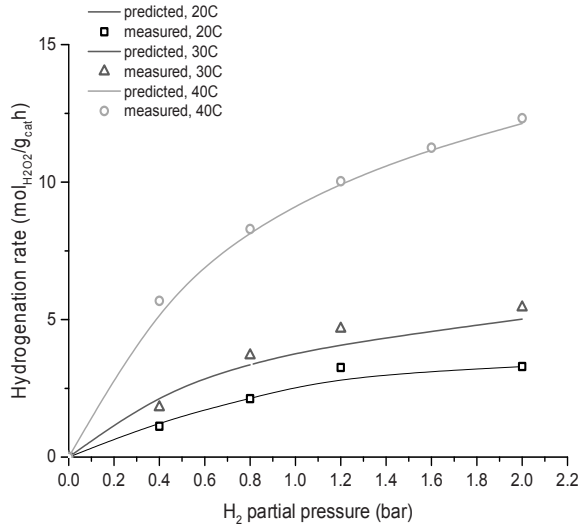


Figure 5.6. Hydrogenation kinetics (a) Effect of the H₂O₂ concentration (at constant p_{H₂}=2bar) (b) Effect of hydrogen partial pressure (at constant H₂O₂ concentration of 0.25 wt%).

The set of experiments carried out with different support particle sizes was used to investigate the presence of internal mass transfer limitations. The absence of the rate change with decreasing particle size indicates the absence of diffusion limitations. The internal mass transfer limitations were eliminated for support particle sizes in the range tested ($\leq 72 \mu\text{m}$). Results obtained in the kinetic experiments (Fig. 5.6) by varying hydrogen partial pressure while using the same starting peroxide concentration or using different initial peroxide concentrations at the same H_2 partial pressure were fitted with the expression derived based on the mechanism proposed by Choudhary & Samanta^[41] (Table 5.1) assuming the surface reaction step as a rate determining (the rate is influenced both by hydrogen and peroxide concentration). This mechanism assumes a hydrogenation of an adsorbed peroxide species with a dissociated hydrogen species. The maximum partial pressure of hydrogen used is 2 bars, which corresponds to hydrogen concentration of 10 vol% in the gas feed.

Kinetic model	$\text{H}_2 + ** = 2\text{H}^*$ $\text{H}_2\text{O}_2 + * = \text{H}_2\text{O}_2^*$ $\text{H}_2\text{O}_2^* + 2\text{H}^* = 2\text{H}_2\text{O} + 3\text{H}^*$ $R = kK_{\text{H}_2\text{O}_2}C_{\text{H}_2\text{O}_2}K_{\text{H}_2}P_{\text{H}_2} \left(\frac{1}{1 + \sqrt{K_{\text{H}_2}P_{\text{H}_2}} + K_{\text{H}_2\text{O}_2}C_{\text{H}_2\text{O}_2}} \right)^3$		
Kinetic parameters	k (mol g ⁻¹ h ⁻¹)	K_{H_2} (bar ⁻¹)	$K_{\text{H}_2\text{O}_2}$ (mol dm ⁻³)
30°C	323 (±195*)	0.367 (±0.414*)	0.118 (±0.0323*)
40°C	498 (±190*)	0.383 (±0.25*)	0.122 (±0.030*)
50°C	1039 (±268*)	0.40 (±0.0.20*)	0.143 (±0.0165*)
Activation energy and enthalpies of adsorption	E_a (kJ/mol)	ΔH_{KH_2} (kJ/mol)	$\Delta H_{\text{KH}_2\text{O}_2}$ (kJ/mol)
	44.3 (±8.5)	3.3 (±0.1)	7.1 (±3.3)

* Parameter confidence intervals are computed using the inverse of Student's t cumulative distribution function.

Table 5.1. Surface reaction mechanism describing hydrogen peroxide hydrogenation reaction with rate expression, values of kinetic constants fitted using non-linear regression analysis by minimizing the residual sum of squares with 95% confidence intervals and Arrhenius parameters.

Chapter 5

The parameter values obtained after applying non-linear regression are presented in Table 5.1, including 95% confidence intervals for parameter estimates. In addition, the values of activation energy and enthalpy of adsorption are determined assuming validity of Arrhenius relationship for kinetic parameters. Although the goodness of fit was comparable with the mechanism suggested by Choudhary & Samanta, the mechanism involving both hydrogen and hydrogen peroxide dissociation was disregarded taking into account that fitted values of hydrogen and oxygen adsorption coefficients showed a maximum and a minimum respectively at 40°C.

5.3.6. Kinetics of direct formation reaction

Kinetic data for the direct formation reaction is presented in Fig. 5.7. The oxygen conversion was monitored as a function of the hydrogen and oxygen partial pressure applied at differential conditions. The partial pressure of the limiting reactant was varied, while maintaining the pressure of the reactant in excess and at constant total pressure. The variation of the partial pressure is achieved by changing the flow rate of the limiting reactant using nitrogen as make-up gas, keeping the gas flow through microchannel constant. As discussed earlier, the direct formation of water from hydrogen and oxygen can be disregarded as a side reaction (H_2 selectivity at high O_2 and low H_2 content is ~100%), meaning that all the oxygen is converted initially to hydrogen peroxide and further to water only in a consecutive hydrogenation step. For fitting the oxygen conversion rates, many expressions derived on the bases of L-H and E-R reaction mechanisms were considered. Most of the considered mechanisms in literature starting with the mechanism proposed by Pospelova et al. ^[47] in 1960 assume dissociation and spill-over of hydrogen on the catalyst surface to react with non-dissociatively adsorbed oxygen. Both one-site and two- catalytic site mechanisms were analyzed assuming reaction step as rate determining (see Appendix 5B). Dissociative adsorption and “splitting” of hydrogen on the surface implies that there should be a square root dependence for the oxygen conversion rate on the hydrogen partial pressure. Although satisfactory fittings were obtained assuming different mechanisms involving hydrogen dissociation and migration over AuPd surfaces to react with oxygen adsorbed species, further analysis of activation energy and adsorption enthalpies indicates that the energy needed to dissociate H_2 would be higher than the activation energy, which disagrees with the rate determining step assumption. Therefore, it was concluded that such a mechanism would be highly unlikely. XPS and CO adsorption analysis (Fig. 5.3a) performed to characterize the surface of our AuPd alloy nanoparticles revealed that Pd surface is highly diluted by Au. The DFT calculations on H_2 adsorption and dissociation over Au-Pd alloy surfaces suggests that in the presence of neighboring Au atoms on Pd surface H_2 spill-over is impossible ^[48]. The formation of Pd ensembles is crucial for dissociative adsorption of hydrogen, considering that H_{ad} is the most stable on Pd_3 threefold hollow sites, less stable

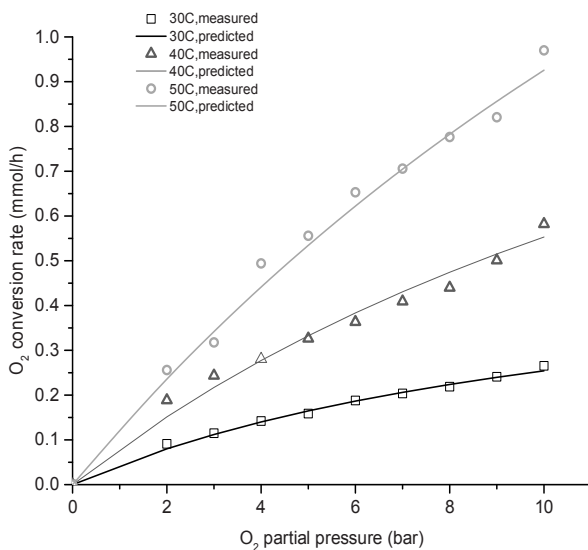
on Pd₂ bridge sites and least stable on Pd monomers [49]. Surface diffusion of H species between isolated Pd ensembles is inhibited considering the high energy of H_{ad} adsorbed on Au surface sites. This further implies that dissociative adsorption of H₂ molecules is only possible if both H species can be stably adsorbed on the same Pd ensemble, in a way that hydrogen adsorption occurs pairwise [49]. TPD and STM imaging studies show that H₂ uptake mainly occurs on Pd islands. In addition, the isotopic studies using deuterium/hydrogen exchange revealed that a small portion of the D₂ is able to dissociate on the H-precovered Pd–Au surface [50]. It is believed that in similar fashion continuous Pd sites are responsible for dissociative adsorption of oxygen [24,50]. In case of the direct synthesis, this results in non-selective formation of water. Therefore, it is widely accepted that “dilution” of Pd surface with Au is a cause of higher selectivities in the direct synthesis observed over Au-Pd catalysts in comparison to traditional Pd.

Kinetic model	$H_2 + ** = H**H$ $O_2 + \#\# = O_2\#\#$ $H**H + O_2\#\# = H_2O_2 + ** + \#\#$ $R = kK_{H_2}P_{H_2}K_{O_2}P_{O_2} \left(\frac{1}{(1 + K_{H_2}P_{H_2})(1 + K_{O_2}P_{O_2})} \right)$		
Kinetic parameters	k (mol g ⁻¹ h ⁻¹)	K _{H₂} (bar ⁻¹)	K _{O₂} (bar ⁻¹)
30°C	13.8 (±2.9*)	0.0682 (±0.0149*)	0.0838 (±0.0164*)
40°C	33.6 (±20.0*)	0.0908 (±0.0417*)	0.0507 (±0.0316*)
50°C	62.9 (±26.3*)	0.1404 (±0.0325*)	0.0336 (±0.0169*)
Pre-exponential factor	5.3*10 ¹¹	7.3*10 ³	3.2*10 ⁻⁸
Activation energy and enthalpies of adsorption	E _a (kJ/mol)	ΔH _{KH₂} (kJ/mol)	ΔH _{KH₂O₂} (kJ/mol)
	61.9 (±5.8)	23.9 (±4.6)	-39.7(±1.6)

*Parameter confidence intervals are computed using the inverse of Student's t cumulative distribution function.

Table 5.2. Surface reaction mechanism describing the hydrogen peroxide direct formation reaction with the best fitted rate expression, values of kinetic constants fitted using non-linear regression analysis by minimizing the residual sum of squares with 95% confidence intervals and Arrhenius parameter.

a)



b)

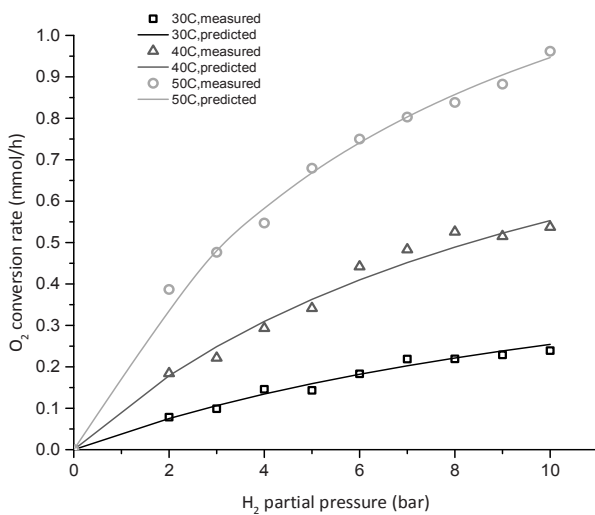
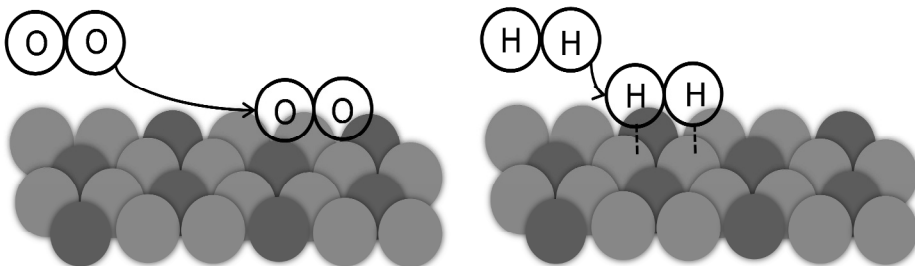


Figure 5.7. Kinetics of hydrogen peroxide direct formation reaction (a) Effect of the O₂ partial pressure at constant p_{H₂}=10 bar (b) Effect of H₂ partial pressure at constant p_{O₂}=10 bar (total gas flow rate 5 ml/min, total pressure 20 bar, aqueous phase (0.05 M H₂SO₄ + 10 ppm NaBr) at flow rate 0.05 ml/min).

The kinetic data presented in Fig. 5.7 are fitted with the proposed mechanism, which assumes the dissociative adsorption of H_2 without spill-over on the catalyst surface on one type of catalytic sites and non-dissociative adsorption of O_2 on different type of active site. It is believed that two metal surface atoms in contact (associated surface atoms) are involved in each adsorption step. Those two neighbouring sites represent one type of active site, since they are in close proximity. The positive enthalpy of adsorption for H_2 indicates that the process involves the dissociation of the hydrogen bond and formation of a H_{ad} species pairwise on two neighbouring surface atoms, which are accounted for as one active site. However those two hydrogen atoms are unable to spill over the surface in a random fashion in order to further react with O-O species, meaning that reaction rate is not inversely proportional to square root of hydrogen partial pressure. The positive enthalpy of adsorption in case of hydrogen is accompanied by the positive entropy change ($\Delta S=74$ J/molK). In cases of dissociative chemisorption, adsorption may be characterized by an increase in the translational freedom of the molecule and a positive entropy change. In contrast oxygen adsorption results in restriction in the translational freedom and a negative entropy change ($\Delta S=144$ J/molK).

The pairwise hydrogen dissociation mechanism indicated as is indicated by the good agreement with the experimentally collected kinetic data is in agreement with the conclusion made by Takehiro et al. ^[49] on hydrogen dissociation on AuPd surfaces. The enthalpy of adsorption is also influenced by the surface coverage i.e. at low surface coverage species adsorbing are attracted to the surface stabilizing it, however at high surface coverage molecules approaching to the surface repel each other leading to higher/positive enthalpy of adsorption (endothermic) ^[51].

In comparison to two-site L-H mechanism, non-linear regression analysis performed assuming only one type of active sites for hydrogen and oxygen adsorption on the catalyst surface does not give a satisfactory fitting (R^2).



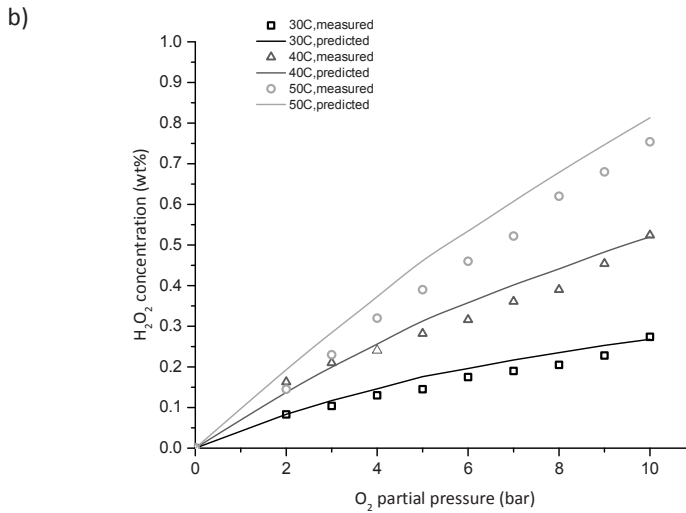
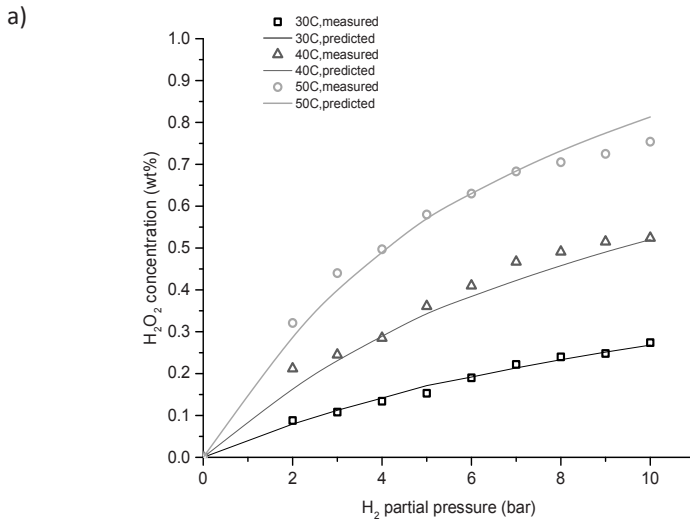


Figure 5.8. Influence of hydrogen and oxygen partial pressures on the hydrogen peroxide concentration at the reactor outlet (a) at constant $p_{O_2}=10$ bar (b) at constant $p_{H_2}=10$ bar (total gas flow rate 5 ml/min, total pressure 20 bar, aqueous phase (0.05 M H_2SO_4 +10 ppm NaBr) at flow rate 0.05 ml/min).

5.3.7. Hydrogen peroxide concentration –the validation of kinetic expressions

The concentration of hydrogen peroxide as an intermediate product was monitored at the reactor outlet during the direct synthesis experiments performed at 30, 40 and 50°C while varying the reactant partial pressures.

Fig. 5.8 shows the peroxide concentrations determined experimentally and the peroxide concentrations predicted by the overall kinetic model applying the kinetic rate expressions derived for direct formation and hydrogenation reaction. From Fig. 5.8a it can be concluded that a good agreement exists between the observed and predicted peroxide concentration values. The higher degree of disagreement between the experimental and predicted values is the most evident at high hydrogen partial pressure at 50°C (9-10 bar), however somewhat higher hydrogenation rates than expected by the model are observed also at lower temperatures (Fig. 5.8b) for a high hydrogen partial pressure. The peroxide concentration observed at the microchannel outlet is lower than predicted by kinetics.

The cause for this mismatch cannot be associated with the catalyst oxidation state under specific reactive conditions and corresponding activity. Typically the reaction was operated alternating high H₂ and O₂ partial pressures, using a 1:1 H₂ to O₂ ratio between the measurements as a reference gas mixture to avoid over-oxidation or over-reduction of the catalyst.

Kinetic data for the hydrogenation reaction were collected at 20, 30 and 40 °C at H₂ partial pressures up to 2 bar, which might result in the deviations observed at the H₂ partial pressure of 10 bar applied in direct synthesis of hydrogen peroxide in the microchannel reactor. The values of the reaction rate constants as well as adsorption constants for hydrogenation reaction at 50°C are extrapolated using Arrhenius plots from the those values obtained for lower H₂ partial pressures at lower temperature.

Therefore, the error in one of parameter estimates might lead to the observed level of discrepancy between predicted and measured data at 50°C. In addition, it is likely that at higher H₂ partial pressures and higher temperature reaction, the trace impurities present in the liquid phase, in the reactor material or downstream set-up parts are able to catalyze peroxide reduction to water, leading to lower peroxide concentration than expected based on the model prediction.

5.4. Conclusions

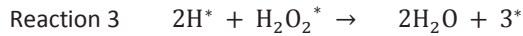
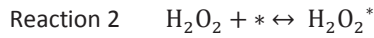
In this work, the expressions obtained in fitting separately reactions of direct formation of peroxide and peroxide reduction in the presence of hydrogen were combined to obtain the overall kinetic model suitable to predict peroxide concentration at the reactor outlet. The direct synthesis reaction is performed over Au-Pd nanoparticles prepared using two-phase

Chapter 5

synthesis protocol. Catalyst characterization revealed that the surface of those nanoparticles consist of a mixture of Au and Pd atoms, resulting in unique catalytic properties. CO adsorption experiments confirmed absence of Pd-Pd indicating strong interaction of Au with Pd. The rate of direct water formation from hydrogen and oxygen was *a priori* neglected, considering that observed H₂ selectivity in direct synthesis at high oxygen partial pressures was 100% in our previous study. The decomposition reaction was eliminated by the addition of sulfuric acid. Addition of acid is generally practiced in direct synthesis of hydrogen peroxide as well as in conventional AO process not only for preventing the decomposition catalyzed by the catalyst itself, but also hindering the decomposition caused by equipment material. As established by the kinetic model, direct formation of hydrogen peroxide from hydrogen and oxygen seems to involve hydrogen adsorption, dissociation, but not spill-over of H-species over the AuPd surface. It is most likely that reaction occurs between non-dissociated oxygen and hydrogen species adsorbed pairwise as suggested by several studies on hydrogen adsorption over AuPd surfaces [48,49]. The comparison of our results with kinetic studies earlier published for Pd catalysts [10] on direct formation of hydrogen peroxide indicate entirely different surface reaction mechanism on AuPd surfaces in comparison to Pd catalyst, ascribed to difference in surface properties of the two type of catalysts. The peroxide concentration values predicted with an overall model and experimentally measured are in acceptably good agreement. A somewhat larger discrepancy between the model and experiments in comparison to overall data is observed at high H₂ partial pressures at 50°C. This can be ascribed to the extrapolation of hydrogenation rate constants or presence of impurities able to catalyze peroxide reduction.

Appendix 5A: Derivation of L-H kinetic expressions for hydrogenation of hydrogen peroxide

Mechanism Proposed by Choudhary and Samanta [41]:



Reaction 1

$$r_1 = r_{-1}$$

$$k_1 P_{\text{H}_2} \theta^{*2} = k_{-1} \theta_{\text{H}}^2$$

$$\theta_{\text{H}}^2 = K_{\text{H}_2} P_{\text{H}_2} \theta^{*2}$$

Reaction 2

$$r_2 = r_{-2}$$

$$k_2 C_{\text{H}_2\text{O}_2} \theta^* = k_{-2} \theta_{\text{H}_2\text{O}_2}^*$$

$$\theta_{\text{H}_2\text{O}_2}^* = K_{\text{H}_2\text{O}_2} C_{\text{H}_2\text{O}_2} \theta^*$$

Site Balance

$$1 = \theta_{\text{H}_2\text{O}_2} + \theta_{\text{H}_2} + \theta^*$$

$$1 = \theta^* + \sqrt{K_{\text{H}_2} P_{\text{H}_2}} \theta^* + K_{\text{H}_2\text{O}_2} C_{\text{H}_2\text{O}_2} \theta^*$$

$$\theta^* = \frac{1}{1 + \sqrt{K_{\text{H}_2} P_{\text{H}_2}} + K_{\text{H}_2\text{O}_2} C_{\text{H}_2\text{O}_2}}$$

Reaction 3

This is the rate determining step

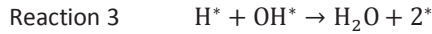
$$r_3 = k_3 \theta_{\text{H}_2}^{*2} \theta_{\text{H}_2\text{O}_2}^*$$

$$r_3 = \frac{k_3 K_{\text{H}_2\text{O}_2} C_{\text{H}_2\text{O}_2} K_{\text{H}_2} P_{\text{H}_2}}{(1 + \sqrt{K_{\text{H}_2} P_{\text{H}_2}} + K_{\text{H}_2\text{O}_2} C_{\text{H}_2\text{O}_2})^3}$$

Mechanism involving both hydrogen and hydrogen peroxide dissociation:



Chapter 5



Reaction 1	Reaction 2	Site Balance
$r_1 = r_{-1}$	$r_2 = r_{-2}$	$1 = \theta_{OH} + \theta_H + \theta^*$
$k_1 P_{H_2} \theta^{*2} = k_{-1} \theta_H^2$	$k_2 C_{H_2O_2} \theta^{*2} = k_{-2} \theta_{OH}^2$	$1 = \theta^* + \sqrt{K_{H_2} P_{H_2}} \theta^* + \sqrt{K_{H_2O_2} C_{H_2O_2}} \theta^*$
$\theta_H^2 = K_{H_2} P_{H_2} \theta^{*2}$	$\theta_{OH}^2 = K_{H_2O_2} C_{H_2O_2} \theta^{*2}$	$\theta^* = \frac{1}{1 + \sqrt{K_{H_2} P_{H_2}} + \sqrt{K_{H_2O_2} C_{H_2O_2}}}$

Reaction 3

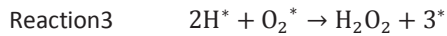
This is the rate determining step

$$r_3 = k_3 \theta_H \theta_{OH}$$

$$r_3 = \frac{k_3 (K_{H_2O_2} C_{H_2O_2} K_{H_2} P_{H_2})^{1/2}}{(1 + \sqrt{K_{H_2} P_{H_2}} + \sqrt{K_{H_2O_2} C_{H_2O_2}})^2}$$

Appendix 5B: Derivation of main L-H kinetic rate expressions for direct formation reaction

Mechanism 1: Non-dissociative adsorption of oxygen with dissociative adsorption of hydrogen on single type of active site



<u>Reaction 1</u>	<u>Reaction 2</u>	<u>Site Balance</u>
$r_1 = r_{-1}$	$r_2 = r_{-2}$	$1 = \theta_{O_2} + \theta_H + \theta^*$

$$k_{H_2} P_{H_2} \theta^{*2} = k_{-H_2} \theta_H^2$$

$$k_{O_2} P_{O_2} \theta^* = k_{-O_2} \theta_{O_2}^*$$

$$1 = \theta^* + \sqrt{K_{H_2} P_{H_2}} \theta^* + K_{O_2} P_{O_2} \theta^*$$

$$\theta_H^2 = K_{H_2} P_{H_2} \theta^{*2}$$

$$\theta_{O_2}^* = K_{O_2} P_{O_2} \theta^*$$

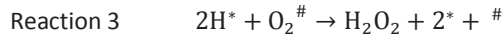
$$\theta^* = \frac{1}{1 + \sqrt{K_{H_2} P_{H_2}} + K_{O_2} P_{O_2}}$$

Reaction 3- the rate determining step

$$r_3 = k_3 \theta_H^{*2} \theta_{O_2}$$

$$r_3 = \frac{k_3 K_{O_2} P_{O_2} K_{H_2}^2 P_{H_2}}{(1 + \sqrt{K_{H_2} P_{H_2}} + K_{O_2} P_{O_2})^3}$$

Mechanism 2: Non-dissociative adsorption of oxygen with dissociative adsorption of hydrogen on two different types of active sites



Reaction 1

$$r_1 = r_{-1}$$

$$k_{H_2} P_{H_2} \theta^{*2} = k_{-H_2} \theta_H^2$$

$$\theta_H^2 = K_{H_2} P_{H_2} \theta^{*2}$$

Reaction 2

$$r_2 = r_{-2}$$

$$k_{O_2} P_{O_2} \theta^\# = k_{-O_2} \theta_{O_2}^\#$$

$$\theta_{O_2}^\# = K_{O_2} P_{O_2} \theta^\#$$

Site Balance(s)

$$1 = \theta_H + \theta^* \text{ and } 1 = \theta_{O_2}^\# + \theta^\#$$

$$1 = \theta^* + \sqrt{K_{H_2} P_{H_2}} \theta^* \text{ and}$$

$$1 = \theta^\# + K_{O_2} P_{O_2} \theta^\#$$

$$\theta^* = \frac{1}{1 + \sqrt{K_{H_2} P_{H_2}}}$$

$$\theta^\# = \frac{1}{(1 + K_{O_2} P_{O_2})}$$

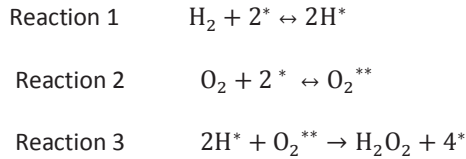
Chapter 5

Reaction 3-rate determining step

$$r_3 = k_3 \theta_H^{+2} \theta_{O_2}^{\#}$$

$$r_3 = \frac{k_3 K_{O_2} P_{O_2} K_{H_2} P_{H_2}}{(1 + K_{O_2} P_{O_2})(1 + \sqrt{K_{H_2} P_{H_2}})^2}$$

Mechanism 3: Non-dissociative adsorption of oxygen on two active sites with dissociative adsorption of hydrogen (single type of active site)



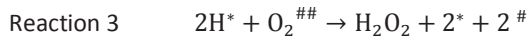
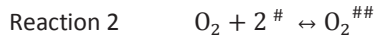
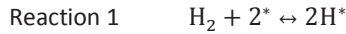
<u>Reaction 1</u>	<u>Reaction 2</u>	<u>Site Balance</u>
$r_1 = r_{-1}$	$r_2 = r_{-2}$	$1 = 2\theta_{O_2} + \theta_H + \theta^*$
$k_{H_2} P_{H_2} \theta^{*2} = k_{-H_2} \theta_{H^*}^2$	$k_{O_2} P_{O_2} \theta^{*2} = k_{-O_2} \theta_{O_2^{**}}$	$1 = \theta^* + \sqrt{K_{H_2} P_{H_2}} \theta^* + 2K_{O_2} P_{O_2} \theta^{*2}$
$\theta_H^2 = K_{H_2} P_{H_2} \theta^{*2}$	$\theta_{O_2^{**}} = K_{O_2} P_{O_2} \theta^{*2}$	$\theta^* = \frac{-(1 + \sqrt{K_{H_2} P_{H_2}}) \pm \sqrt{((1 + \sqrt{K_{H_2} P_{H_2}})^2 + 8K_{O_2} P_{O_2})}}{4K_{O_2} P_{O_2}}$

Reaction 3-rate determining step

$$r_3 = k_3 \theta_H^{+2} \theta_{O_2}^{**}$$

$$r_3 = k_3 K_{O_2} P_{O_2} K_{H_2} P_{H_2} \left(\frac{-(1 + \sqrt{K_{H_2} P_{H_2}}) \pm \sqrt{\left((1 + \sqrt{K_{H_2} P_{H_2}}) \right)^2 + 8K_{O_2} P_{O_2}}}{4K_{O_2} P_{O_2}} \right)^4$$

Mechanism 4: Non-dissociative adsorption of oxygen on two active sites with dissociative adsorption of hydrogen (two different types of active site)



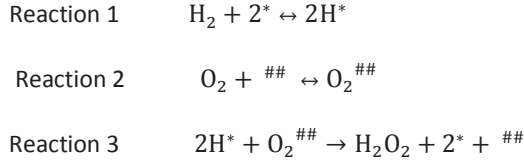
<u>Reaction 1</u>	<u>Reaction 2</u>	<u>Site Balance</u>
$r_1 = r_{-1}$	$r_2 = r_{-2}$	$1 = \theta_H + \theta^*$ and $1 = 2\theta_{O_2}^{##} + \theta^{\#}$
$k_{H_2} P_{H_2} \theta^{*2} = k_{-H_2} \theta_H^2$	$k_{O_2} P_{O_2} \theta^{##2} = k_{-O_2} \theta_{O_2}^{##}$	$1 = \theta^* + \sqrt{K_{H_2} P_{H_2}} \theta^*$ and
		$1 = \theta^{\#} + 2K_{O_2} P_{O_2} \theta^{\#2}$
		$\theta^* = \frac{1}{1 + \sqrt{K_{H_2} P_{H_2}}}$
$\theta_H^2 = K_{H_2} P_{H_2} \theta^{*2}$	$\theta_{O_2}^{##} = K_{O_2} P_{O_2} \theta^{##2}$	$\theta^{\#} = \frac{-1 \pm \sqrt{1 + 8K_{O_2} P_{O_2}}}{4K_{O_2} P_{O_2}}$

Reaction 3-rate determining step

$$r_3 = k_3 \theta_H^{*2} \theta_{O_2}^{##}$$

$$r_3 = k_3 K_{O_2} P_{O_2} K_{H_2} P_{H_2} \left(\frac{1}{1 + \sqrt{K_{H_2} P_{H_2}}} \right)^2 \left(\frac{-1 \pm \sqrt{1 + 8K_{O_2} P_{O_2}}}{4K_{O_2} P_{O_2}} \right)^2$$

Mechanism 5: Non-dissociative adsorption of oxygen on two neighbouring active sites with dissociative adsorption of hydrogen (two different types of active sites for H₂ and O₂ adsorption)



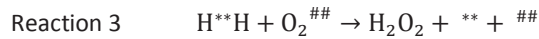
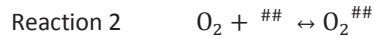
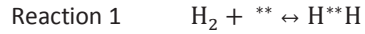
<u>Reaction 1</u>	<u>Reaction 2</u>	<u>Site Balance(s)</u>
$r_1 = r_{-1}$	$r_2 = r_{-2}$	$1 = \theta_H + \theta^*$ and $1 = \theta_{O_2}^{##} + \theta^{##}$
$k_{H_2} P_{H_2} \theta^{*2} = k_{-H_2} \theta_H^2$	$k_{O_2} P_{O_2} \theta^{##} = k_{-O_2} \theta_{O_2}^{##}$	$1 = \theta^* + \sqrt{K_{H_2} P_{H_2}} \theta^*$ and
		$1 = \theta^{##} + K_{O_2} P_{O_2} \theta^{##}$
$\theta_H^2 = K_{H_2} P_{H_2} \theta^{*2}$	$\theta_{O_2}^{##} = K_{O_2} P_{O_2} \theta^{##}$	$\theta^* = \frac{1}{(1 + \sqrt{K_{H_2} P_{H_2}})^2}$
		$\theta^{##} = \frac{1}{(1 + K_{O_2} P_{O_2})}$

Reaction 3-rate determining step

$$r_3 = k_3 \theta_H^{*2} \theta_{O_2}^{##}$$

$$r_3 = \frac{k_3 K_{O_2} P_{O_2} K_{H_2} P_{H_2}}{(1 + K_{O_2} P_{O_2})(1 + \sqrt{K_{H_2} P_{H_2}})^2}$$

Mechanism 6: Non-dissociative adsorption of oxygen on two neighbouring active sites with pairwise dissociative adsorption of hydrogen on two neighbouring active sites (two different types of active sites for H₂ and O₂ adsorption)



<u>Reaction 1</u>	<u>Reaction 2</u>	<u>Site Balance(s)</u>
$r_1 = r_{-1}$	$r_2 = r_{-2}$	$1 = \theta_{H_2^{**}} + \theta^{**}$ and $1 = \theta_{O_2^{##}} + \theta^{##}$
$k_{H_2} P_{H_2} \theta^{*2} = k_{-H_2} \theta_H^2$	$k_{O_2} P_{O_2} \theta^{##} = k_{-O_2} \theta_{O_2}^{##}$	$1 = \theta^{**} + K_{H_2} P_{H_2} \theta^{**}$ and
		$1 = \theta^{##} + K_{O_2} P_{O_2} \theta^{##}$
$\theta_H^2 = K_{H_2} P_{H_2} \theta^{*2}$	$\theta_{O_2}^{##} = K_{O_2} P_{O_2} \theta^{##}$	$\theta^{**} = \frac{1}{(1 + K_{H_2} P_{H_2})}$
		$\theta^{##} = \frac{1}{(1 + K_{O_2} P_{O_2})}$

Reaction 3-rate determining step

$$r_3 = k_3 \theta_{H_2^{**}} \theta_{O_2}^{##}$$

$$r_3 = \frac{k_3 K_{O_2} P_{O_2} K_{H_2} P_{H_2}}{(1 + K_{O_2} P_{O_2})(1 + K_{H_2} P_{H_2})}$$

References:

- [1] C. W. Jones, *Application of Hydrogen Peroxide and Derivatives*, The Royal Society Of Chemistry, Cambridge, UK, **1999**.
- [2] W. K. and O. W. G. Goor, *Ullmann's Encyclopedia of Industrial Chemistry*, , Vol. A13, Wiley-VCH Verlag GmbH & Co. KGaA, Weinheim, Germany, **1989**.
- [3] G. Blanco-Brieva, M. M. J. Campos, J. L. Garcia Fierro, M. Argaiz Montiel, R. Garaffa, F. Janssens, *Patenten Process to Obtain Hydrogen Peroxide , and Catalyst Supports for the Same Process*, **2013**, WO 2013010835 A1.
- [4] A. Willson, *Plant for Hydrogen Peroxide Production and a Process Using It*, **2013**, EP002639200A1.
- [5] S. Chattopadhyay, G. Veser, *AIChE J.* **2006**, *52*, 2217–2229.
- [6] M. N. Kashid, L. Kiwi-Minsker, *Ind. Eng. Chem. Res.* **2009**, *48*, 6465–6485.
- [7] T. Inoue, M. A. Schmidt, K. F. Jensen, *Ind. Eng. Chem. Res.* **2007**, *46*, 1153–1160.
- [8] Y. Voloshin, J. Manganaro, A. Lawal, **2008**, 8119–8125.
- [9] Y. Voloshin, A. Lawal, *Appl. Catal. A Gen.* **2009**, *353*, 9–16.
- [10] Y. Voloshin, R. Halder, A. Lawal, *Catal. Today* **2007**, *125*, 40–47.
- [11] D. van Herk, P. Castaño, M. Makkee, J. A. Moulijn, M. T. Kreutzer, *Appl. Catal. A Gen.* **2009**, *365*, 199–206.
- [12] A. Karim, J. Bravo, D. Gorm, T. Conant, A. Datye, *Catal. Today* **2005**, *110*, 86–91.
- [13] K. Yube, M. Furuta, K. Mae, *Catal. Today* **2007**, *125*, 56–63.
- [14] M. T. Kreutzer, P. Du, J. J. Heiszwolf, F. Kapteijn, J. A. Moulijn, *Chem. Eng. Sci.* **2001**, *56*, 6015–6023.
- [15] M. T. Kreutzer, F. Kapteijn, J. A. Moulijn, *Catal. Today* **2005**, *105*, 421–428.
- [16] Y. Voloshin, A. Lawal, *Chem. Eng. Sci.* **2010**, *65*, 1028–1036.
- [17] K. F. J. M.W. Losey, M.A.Schmidt, *Ind.Eng.Chem.Res.* **2001**, *40*, 2555–2562.
- [18] S. Murakami, K. Ohtaki, S. Matsumoto, T. Inoue, *Jpn. J. Appl. Phys.* **2012**, *51*, 06FK11.
- [19] T. Inoue, K. Ohtaki, J. Adachi, M. Lu, S. Murakami, *Catal. Today* **2014**, DOI 10.1016/j.cattod.2014.03.065.
- [20] T. Inoue, Y. Kikutani, S. Hamakawa, K. Mawatari, F. Mizukami, T. Kitamori, *Chem. Eng. J.* **2010**, *160*, 909–914.
- [21] V. R. Choudhary, C. Samanta, T. V. Choudhary, *J. Mol. Catal. A Chem.* **2006**, *260*, 115–120.
- [22] V. Paunovic, V. Ordonsky, M. F. Neira, D. Angelo, J. C. Schouten, T. A. Nijhuis, *J. Catal.* **2014**, *309*, 325–332.
- [23] V. Paunovic, J. C. Schouten, T. A. Nijhuis, *Catal. Today* **2014**, doi:10.101, DOI 10.1016/j.cattod.2014.04.007.

- [24] F. Gao, D. W. Goodman, *Chem. Soc. Rev.* **2012**, *41*, 8009–20.
- [25] E. Ntainjua N., J. K. Edwards, A. F. Carley, J. A. Lopez-Sanchez, J. A. Moulijn, A. A. Herzing, C. J. Kiely, G. J. Hutchings, *Green Chem.* **2008**, *10*, 1162–1169.
- [26] M. Piccinini, J. K. Edwards, J. a. Moulijn, G. J. Hutchings, *Catal. Sci. Technol.* **2012**, *2*, 1908.
- [27] T. A. Nijhuis, A. E. W. Beers, T. Vergunst, I. Hoek, F. Kapteijn, J. A. Moulijn, *Catal. Rev.* **2001**, *43*, 345–380.
- [28] C. J. Serpell, J. Cookson, D. Ozkaya, P. D. Beer, *Nat. Chem.* **2011**, *3*, 478–83.
- [29] T. A. Nijhuis, F. M. Dautzenberg, J. A. Moulijn, **2003**, *58*, 1113–1124.
- [30] Q. Liu, J. H. Lunsford, *Appl. Catal. A Gen.* **2006**, *314*, 94–100.
- [31] V. R. Choudhary, Y. V Ingole, C. Samanta, P. Jana, *Ind. Eng. Chem. Res.* **2007**, 8566–8573.
- [32] K. I. Hadjiivanov, G. N. Vayssilov, *Adv. Catal.* **2002**, *47*, 307–511.
- [33] Y. Lokhov, A. Davydov, *Kinet. Catal.* **1980**, *21*, 1515–1522.
- [34] J. Grunwaldt, A. Baiker, *J. Phys. Chem.* **1999**, *103*, 1002–1012.
- [35] T. A. Pospelova, N. I. Kobozev, *Russ. J. Phys. Chem.* **1961**, *35*, 584–587.
- [36] V. R. Choudhary, C. Samanta, P. Jana, *Appl. Catal. A Gen.* **2007**, *332*, 70–78.
- [37] V. R. Choudhary, C. Samanta, P. Jana, *Appl. Catal. A Gen.* **2007**, *317*, 234–243.
- [38] V. Choudhary, P. Jana, *J. Catal.* **2007**, *246*, 434–439.
- [39] Y. Han, J. Lunsford, *J. Catal.* **2005**, *230*, 313–316.
- [40] V. R. Choudhary, C. Samanta, T. V. Choudhary, *Appl. Catal. A Gen.* **2006**, *308*, 128–133.
- [41] V. Choudhary, C. Samanta, *J. Catal.* **2006**, *238*, 28–38.
- [42] J. Lunsford, *J. Catal.* **2003**, *216*, 455–460.
- [43] J. K. Edwards, A. Thomas, A. F. Carley, A. A. Herzing, C. J. Kiely, G. J. Hutchings, *Green Chem.* **2008**, *10*, 388.
- [44] P. L. Mills, R. V. Chaudhari, *Catal. Today* **1997**, *37*, 367–404.
- [45] Ramachandran, P. A., Chaudhari, R. V., *Three-Phase Catalytic Reactors*, Gordon And Breach Science Publishrs Inc, London, **1983**.
- [46] P. W. N. M. Van Leeuwen, R. A. Van Santen, B. A. Averill, J. A. Moulijn, Eds. , *Catalysis: An Integrated Approach*, Elsevier Science, Amsterdam, **2002**.
- [47] T. A. Pospelova, N. I. Kobozev, *Russ. J. Phys. Chem.* **1961**, *35*, 262–265.
- [48] A. E. Baber, H. L. Tierney, T. J. Lawton, E. C. H. Sykes, *ChemCatChem* **2011**, *3*, 607–614.
- [49] N. Takehiro, P. Liu, A. Bergbreiter, J. K. Nørskov, R. J. Behm, *Phys. Chem. Chem. Phys.* **2014**, *16*, 23930–43.
- [50] W. Yu, G. M. Mullen, C. B. Mullins, *J. Phys. Chem. C* **2013**, 19535–19543.
- [51] L. Jewell, B. Davis, *Appl. Catal. A Gen.* **2006**, *310*, 1–15

Direct synthesis of H₂O₂ over Au-Pd catalyst- Effect of co-solvent addition

6

This chapter is accepted for publication as:

V. Paunovic, V. Ordonsky, V. Sushkevich, J. C. Schouten, T. A. Nijhuis, Direct synthesis of hydrogen peroxide over Au-Pd catalyst- Effect of co-solvent addition. ChemCatChem, 2015, 7, 1161.

ABSTRACT

The direct synthesis is a realized highly attractive novel green route for hydrogen peroxide production. This reaction is performed as a three-phase reaction, which besides solid catalyst and gas reactants involves a liquid phase to collect hydrogen peroxide formed from the catalyst surface. The choice of solvent and/or addition of promoters has a significant effect on the reaction rates observed as well as selectivity towards peroxide. Besides water, as the greenest solvent, short chain alcohols are very attractive due to good solubility of reacting gases. Here we report an extensive study on the influence that different groups of solvents have on the direct synthesis reaction when applied alone or as a co-solvent under non-explosive and conventionally explosive reaction conditions.

6.1. Introduction

Hydrogen peroxide is one of the most important chemicals produced worldwide with a market of around 3000 kt/year constituting to 12-15% of global chemical revenues. It is mainly consumed in paper and pulp industry as a bleaching agent, as a disinfectant in

pharmaceutical and cosmetic industry, oxidant in water treatment or selective oxidant in chemical synthesis^[1,2]. The state of the art process to produce hydrogen peroxide is a two-stage cyclical anthraquinone auto-oxidation process (AO), which involves the hydrogenation of an anthraquinone working solution over a hydrogenation catalyst and thereafter the oxidation of the anthraquinone working solution giving the hydrogen peroxide in the organic phase containing the anthraquinone. The major disadvantages of the AO process are its complexity and the waste generation caused by accumulation of permanently hydrogenated alkylanthraquinone products hydroanthrahydroquinones, oxantrones and anthrones^[3]. For these reasons, in order to be economically viable, the process needs to run on a large scale of at least 40kt/year for each production unit. The world's largest plants situated in Antwerp and Thailand are designed to produce 230 and 330 kt/year of hydrogen peroxide respectively. Besides the complexity of such a large scale process, the transportation of concentrated peroxide solutions to the customer sites requires special precautions related to safety. For safe handling, the concentration of hydrogen peroxide is lowered to 50 wt% in water, while 70 wt% is used if transported over the large distances due to reduction of transportation costs. Eventually, the various application of hydrogen peroxide on the customer site requires a concentration in a range of 1-10 wt%.

The direct synthesis of hydrogen peroxide in a single catalytic reactor from hydrogen and oxygen is a green alternative for the current Anthraquinone autoxidation (AO) process. The major challenges associated with the direct synthesis of hydrogen peroxide (DS) are the explosiveness of the hydrogen-oxygen mixtures over a very wide range of concentrations (4-96%) and the selectivity towards hydrogen peroxide as the desired product. To achieve a high selectivity towards peroxide, it is necessary to design a catalyst that favours the direct synthesis reaction over the thermodynamically favoured direct formation of water from H₂ and O₂. In addition, the catalyst should catalyse as little as possible the further transformation of the hydrogen peroxide to water through a hydrogenation or a decomposition reaction. A major step forward made in this direction was the introduction of alloyed noble metal catalysts. It has been shown that addition of Au to Pd leads to a significant enhancement in the selectivity compared to Pd catalysts only^[4], which is most often attributed to a reduction in the O-O bond dissociation on the catalytic surface. Nevertheless, the effect of gold is not fully understood yet. Unfortunately, depending on the type of support, Au-Pd catalysts might show the tendency to enhance hydrogenation of hydrogen peroxide as well^[5].

The direct synthesis is a three-phase process which involves a H₂-O₂ mixture as gas-phase, a solvent and the solid catalyst phase. The role of the liquid phase used is to collect and solubilize the hydrogen peroxide formed, since pure hydrogen peroxide is highly unstable

Chapter 6

and decomposes to water and oxygen. Besides water, short chain alcohols or mixtures of alcohols and water are typically used in the direct synthesis as a liquid phase. In a recent review on direct synthesis, the authors ^[6] discuss the cost analysis/economics of the AO and the DS process, concluding that the DS process can compete with the AO process only if it is able to reduce CAPEX by avoiding the typically applied concentration steps in the AO process (extraction, distillation) and produce hydrogen peroxide solutions directly in a concentrations required for further applications. It was estimated that the H₂O₂ concentration required would be 15 wt% of H₂O₂ in case of aqueous solutions and 9 wt% for methanol/alcohol solutions. They further emphasize that the reactor technology needs to provide high conversions (>99%) with a selectivity over 20 %. In our previous publication ^[7], we have shown that an increase in the hydrogen peroxide concentration in a microreactor system from 0.8 to approximately 5 wt % leads to a tremendous selectivity drop (down to 20 %), which leads to the conclusion that the in-situ consumption of peroxide produced is highly desired in order to prevent consumption of peroxide through hydrogenation and/or decomposition and maintain selectivity values high. On the other hand, it can also be argued that if one designs a direct synthesis process in which the hydrogen peroxide concentration produced in the reactor is lower (say about 1 wt%) at much higher selectivities, one can afford to add concentration steps to the process and still be competitive with the AO process. The overall economics will very much depend on the needs of the application. For applications requiring a low peroxide concentration aiming for a DS process producing high concentrations at the expense of selectivity does not make much sense. For this reason, in our research we focus primarily on obtaining the highest possible peroxide selectivities and have a high peroxide concentration only as the secondary objective.

Water is most often applied as a solvent in direct synthesis considering that it is non-flammable and non-toxic, allowing the safest operation. However, it has been reported that organic solvents such as methanol, ethanol or acetone show far better performance in direct synthesis^[8,9]. The low solubility of reacting gasses in the water phase in comparison to organic media is most often emphasized as the motivation to employ alcohols as solvents or co-solvents in the direct synthesis ^[10-12]. Krishnan et al. ascribed the higher concentration of H₂O₂ in acetone or methanol compared to water to a higher mass transfer mainly on the gas-liquid interface, which they identify as the rate determining step ^[8]. In addition, they show a strong positive halide effect on the direct synthesis only in the case of synthesis in an aqueous phase in contrast to organic solvents. Addition of toluene or hexane, solvents which are known to increase the solubility of the reactants in the liquid phase, proved not to be efficient in the direct synthesis reaction despite high conversions achieved ^[9], due to poor selectivity. The authors explained that the cause of

the poor catalytic performance lies in the inability of those water non-miscible solvents to wet the hydrophilic catalyst surface. Poor wettability of the catalyst with the organic phase limits the benefits of a high hydrogen concentration in the organic phase. Application of a hydrophobic instead of a hydrophilic support would allow an efficient contact of the catalyst with the water immiscible solvent, however the problem that might arise is associated with promoters soluble in the aqueous phase and as such unable to reach the catalyst and stabilize the peroxide formed on the catalyst surface. In general, water miscible solvents such as different alcohols and acetone are identified as effective solvents for the direct synthesis in several industrial patents^{[13][14]}. Alcohols are suitable solvents for the direct synthesis from the aspect of on-site application in epoxidation reactions as well^[13]. In general, besides for epoxidations, hydrogen peroxide can also be used as an oxidant in a number of oxidation reactions involving different organic substrates, often water non-soluble. Considering the scenario which involves its in-situ or on-site application, it is clear that hydrogen peroxide should be preferably produced in a desired organic solvent for its consecutive usage instead of aqueous phase. Here we report the study on the influence of the solvent on the direct synthesis reaction performed using bimetallic Au-Pd catalysts both in a slurry reactor and in a wall-coated microchannel.

6.2. Materials and Methods

6.2.1. Catalyst preparation

For testing the effect of solvent on the direct synthesis of hydrogen peroxide in a slurry reactor, hydrophobic carbon or silica (Davisil) support were functionalized with an active Au-Pd metallic species by impregnating the support with stabilized Au-Pd (1:2), Pd or Au colloidal nanoparticles prepared using a two-phase synthesis method. For microchannel experiments, the silica wash-coat layer was embedded with the same type of active metallic species.

The metal precursors used in catalyst preparation were HAuCl_4 and K_2PdCl_4 . Their concentrations were adjusted to give approximately 5 wt% total loading of Au, Pd or bimetallic Au-Pd in a given molar ratio with respect to a support used (carbon, silica, SiO_2 wash-coat material). Those compounds were dissolved in the aqueous phase separately. Tetrachloropalladate and tetrachloroaurate ions from water were extracted with dichloromethane by means of tetraoctylammonium chloride as a phase transfer agent. Separated organic phases containing gold and palladium precursors in case of bimetallic nanoparticles were mixed together and reduced using NaBH_4 . The phase transfer agent provides in addition stabilization of nanoparticles formed in the organic phase. To ensure complete reduction, excess of NaBH_4 was used. After colloidal nanoparticles had been

Chapter 6

generated in the organic solvent, the aqueous and organic phase are separated, followed by additional washing of the organic phase. The exact protocol used for the synthesis of colloidal Au-Pd nanoparticles is known in literature as a two-phase synthesis of nanoparticles^[48]. This type of colloidal nanoparticles with a Au:Pd ratio of 1:2 proved to be both, most active and most selective when tested in the direct synthesis reaction^[35]. Pre-formed Au-Pd colloidal nanoparticles are supported on carbon or silica support. In case of a powder catalyst, support material was impregnated with a suspension of nanoparticles. In case of the microchannel, the channel initially coated with a silica layer, was filled with a nanoparticle suspension followed by evaporation of the solvent. After solvent removal, both types of the prepared supported catalyst (wash-coated silica layer or powder) were additionally dried and calcined at 380 °C in static air. More details on the microchannel wash-coating procedure is given in our previous publication^[35]

6.2.2. Catalyst characterization

Supported Au, Pd and Au-Pd catalysts were characterized using X-ray photoelectron spectroscopy (XPS) and FTIR adsorption of CO, CD₃CN and CH₃OH. To understand the surface composition of Au, Pd and Au-Pd catalysts supported on C or SiO₂, XPS was used. The characterization has been performed ex-situ on freshly prepared catalyst. The powder samples were supported on conductive carbon type. The spectra were recorded using a Thermo Scientific K-Alpha spectrometer with monochromatic Al K α sources. Analysis and quantification of the measured data was performed using CasaXPS software.

IR spectra were recorded with a Nicolet Protégé 380 FT-IR spectrometer with a 4 cm⁻¹ optical resolution. Prior to the measurements, the catalysts were pressed in self-supporting discs and activated in the IR cell attached to a vacuum line at 523 K for 4h. Adsorption of CO was carried out in a low-temperature cell at 100 K. In the experiments of acetonitrile adsorption, deuterated CD₃CN was dosed to the cell with a catalyst sample at 298 K to attain the pressure of 1 torr, afterwards the physisorbed molecules were desorbed at 298 K for 40 min. Methanol was adsorbed in the same way with subsequent evacuation with an increase of the temperature. The pressure was measured by a Barocell gauge. Difference spectra were obtained by the subtraction of the spectra of the activated catalyst samples from the spectra of the samples with adsorbate. The subtraction was carried out using OMNIC 7.3 package

6.2.3. Direct synthesis of hydrogen peroxide and peroxide decomposition experiments

The direct synthesis reaction in the presence of an organic co-solvent was investigated using both a titanium Gr2 300 ml autoclave and a wash-coated microchannel reactor. The autoclave experiments were operated as half batch, i.e. as batch for the liquid phase with a continuous gas flow. The gas mixture used in these experiments contained 4 vol% of H₂

and O₂ in nitrogen as an inert and was fed by means of mass flow controllers. The autoclave is equipped with an overhead stirrer which provides stirring in a range of 0-3000 rpms. Typically a stirring rate of 1300 rpms was used. Typically, 125 ml of the liquid phase containing catalyst, promoters (H₂SO₄ and NaBr) and water or a water/co-solvent mixture was charged in the autoclave. Gas is supplied to the liquid phase through the stirrer shaft at a total flow rate of 500 ml/min. After charging the liquid phase, the autoclave is normally purged with N₂ before starting pressurization with the reaction gas mixture. In case of the microchannel experiments, the reactor is operated using pure hydrogen and oxygen mixtures at a 1:1 ratio. The catalyst was deposited in the form of a thin catalytic film on the reactor wall (320 μm in diameter fused silica capillary). The diameter of capillary is carefully chosen taking into account safety considerations, which were discussed in our previous publications^[7,35] To additionally minimize the hydrogen peroxide decomposition, sulphuric acid was added to the liquid phase (0.05 M) if not stated differently. Acids such as sulfuric or phosphoric decelerate base-catalyzed decomposition of peroxide, while bromide ions even at very low concentrations poison catalytic sites that promote O₂ dissociation and direct formation of water^[11,49].

Temperature control of the slurry reactor is achieved using a heating jacket, while the catalytic capillary was placed in a thermostated water bath. The desired gas flow rates were controlled using mass flow controllers. In order to maintain a constant pressure at 20 bar, a back pressure regulator was used in both systems at the gas outlet just before the GC. Since in some of the experiments conventionally explosive H₂/O₂ mixtures were used in the microchannel, for this reactor the gas is diluted with N₂ at the capillary outlet to stay below the explosive H₂ and O₂ concentrations avoiding any safety risks. The flow pattern typically observed in a microchannel was segmented gas-liquid flow (Taylor slug flow). Gas samples were analysed online using GCs equipped with TCD detector. Liquid samples were collected manually at the liquid sampling point and immediately titrated with a standard solution of cerium (IV) sulphate to a blue end-point. Typically, 2-3 drops of ferroin indicator are added to the ice cold solution of sulphuric acid (1:19 v/v) and titrated dropwise to pale blue color prior sample addition. Upon addition of a weighed sample the solution turns red. The solution is stirred during the course of titration. A cerium sulphate standard solution is added to the blue end point appearance.

Decomposition experiments performed with hydrogen peroxide were done in the titanium autoclave, the same which was used in direct synthesis experiments. After introduction of the liquid phase with the catalyst suspended, the reactor was purged with N₂ gas and thermostated at the desired temperature. The reaction was started upon H₂O₂ addition to the liquid phase. When testing the decomposition kinetics in water over the Au-Pd/C catalyst, with or without co-solvent (acetonitrile and methanol) added, no promoters

Chapter 6

were added to the liquid phase. Although the titanium grade 2 material of the autoclave should be inert towards hydrogen peroxide, decomposition of hydrogen peroxide in pure water phase was still observed. The decomposition was most probably caused by reactor material or impurities. In order to quantify the decomposition caused by material itself, blank experiments were done in addition to decomposition experiments with a Au-Pd supported catalyst. Typically, an amount of catalyst used in kinetic experiments was 0.025g.

6.3. Results and Discussion

6.3.1. Catalyst characterization

In order to determine the surface composition of the calcined Au-Pd, Pd and Au catalysts, XPS analysis was performed. The analysis revealed the presence of a PdO phase in the Au-Pd catalysts, both supported on carbon and on silica, while the surface of the catalysts prepared by support impregnation with Pd colloidal nanoparticles after calcination consisted purely of PdO. It is also evident that Au-Pd nanoparticles are alloys (Table 1). The surface composition of carbon supported nanoparticles shows a higher Au content in comparison to the silica supported catalyst, and a lower PdO content.

Catalyst	Au/Pd surface ratio	PdO content, %
Au-Pd (1:2)/C	0.48	66
Pd/C	0	100
Au/C	1	0
Au-Pd (1:2)/SiO ₂	0.38	74.7
Pd/SiO ₂	0	100
Au/SiO ₂	1	0

Table 6.1. Surface composition of Au-Pd, Pd and Au catalysts determined by XPS analysis

6.3.2. Direct synthesis of hydrogen peroxide in presence of a co-solvent

Considering the negative effect that the consecutive hydrogenation and decomposition reactions have on the hydrogen peroxide yield, the initial strategy to improve the reactor performance was to carry out the direct synthesis reaction in a two-phase liquid medium, with the catalyst suspended in a water non-miscible phase and hydrogen peroxide extracted to the aqueous phase during the course of reaction. Au-Pd bimetallic

nanoparticles were supported on hydrophobic carbon in order to ensure that the catalyst remains suspended only in organic solvent.

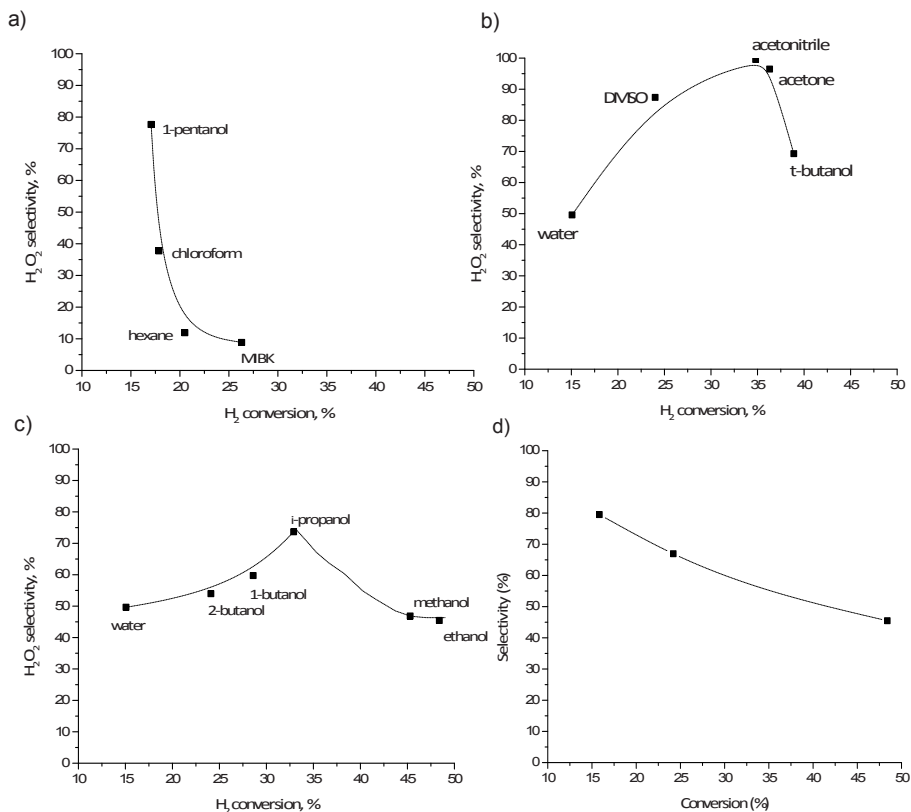


Figure 6.1. Effect of co-solvent addition in direct synthesis of hydrogen peroxide over Au-Pd catalyst supported on hydrophobic carbon in (a) water non-miscible co-solvents (b) water miscible protic solvents (c) water miscible aprotic solvents (d) conversion vs. selectivity relationship with for liquid phase containing methanol as a co-solvent (gas phase: 4 vol% of H₂ and O₂, total gas flow rate 50 ml/min; p=20 bar, T=30 °C, liquid phase: water, 0.05 M H₂SO₄, 9 ppm NaBr, 20 vol% organic co-solvent, stirring speed 1300 rpm).

The hydrogen peroxide generated during the course of reaction would be repelled from the hydrophobic support and transferred to the water phase, thus its consecutive decomposition and/or hydrogenation on the catalyst surface would be disabled. The

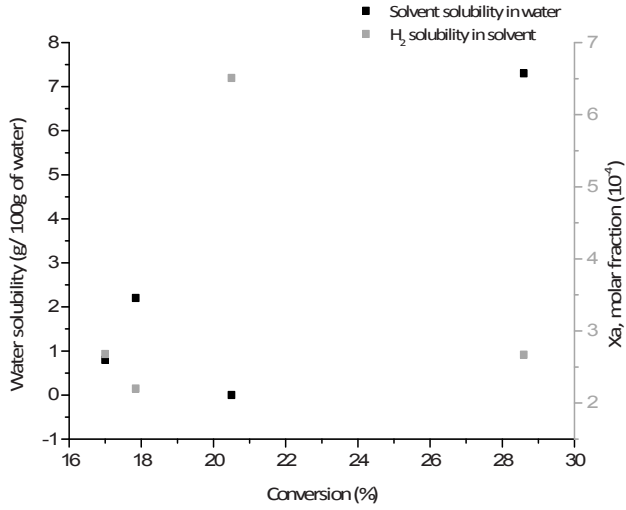
Chapter 6

solubility of H_2 and O_2 is often higher in organic solvents, such as hexane, in comparison to water, allowing the higher hydrogen conversion, reaction rates or hydrogen peroxide yields. A range of solvents with different polarities and miscibility with water were tested as a co-solvent in the direct synthesis reaction. Typically the reaction mixture contained 20 vol% of organic solvent.

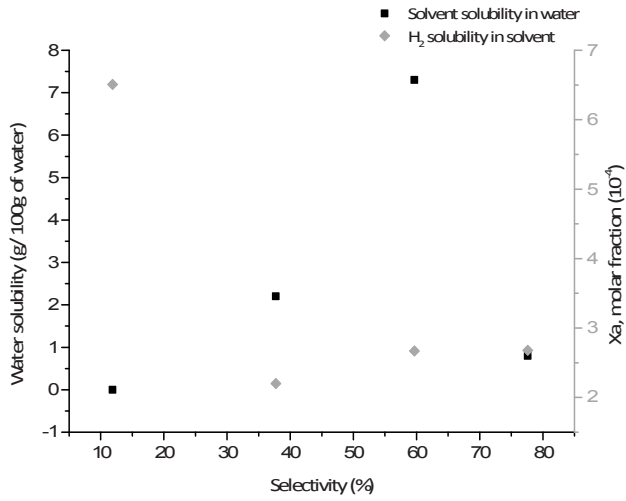
Fig. 6.1. displays the initial conversion against selectivity relationship and productivities achieved with a Au-Pd bimetallic catalyst supported on hydrophobic carbon in an aqueous phase or a mixture of aqueous phase and different co-solvents, including water non-miscible (Fig. 6.1a), water miscible protic (Fig. 6.1b) and aprotic (Fig. 6.1c) solvents under identical operating conditions. With water non-miscible solvents added to the aqueous phase, two-phases are present in the liquid medium. The catalyst, since it is supported on hydrophobic carbon, is in that case suspended in the organic phase solely. It is clear from the results shown that the H_2 conversion in water non-miscible solvents MIBK, chloroform and hexane is somewhat higher than in the aqueous phase, but opposite to our expectations, the catalyst performance in terms of selectivity is rather poor. Among the given water non-miscible solvents, H_2 solubility is highest in hexane (molar fraction of H_2 - $X_{A,H_2}=0.000699$ at 1 atm), almost 3 times higher than in chloroform or 4.5 times higher than in 1-pentanol. Nevertheless, the selectivity is significantly lower compared to other two water non-miscible solvents, although H_2 conversion is only slightly higher. A similar observation with addition of hexane as a co-solvent was made by Burch et al. ^[9], although a hydrophilic catalyst was used. The low selectivity, in this case, could have been a consequence of a poor contact of the aqueous phase with the catalyst and the organic phase in general due to low miscibility with water. The extraction of hydrogen peroxide formed during the course of reaction from the organic to the water phase is evidently rather poor. In addition, acid added to the liquid phase is not able to reach the peroxide in the organic phase and stabilize it against decomposition on the catalyst surface. If the productivity, H_2 conversion and selectivity towards H_2O_2 are plotted for water non-miscible or partially miscible co-solvents against H_2 solubility in pure solvent and solvent solubility in aqueous phase, the following trends are observed (Fig. 6.2); The co-solvent with the highest solubility in water (1-butanol) and low H_2 solubility shows the highest productivity at relatively high conversions with still relatively high selectivity. In contrast, the addition of a co-solvent which exerts a high H_2 solubility with a low solubility in water results in a low selectivity and a productivity at moderate hydrogen conversions.

Effect of co-solvent addition

a)



b)



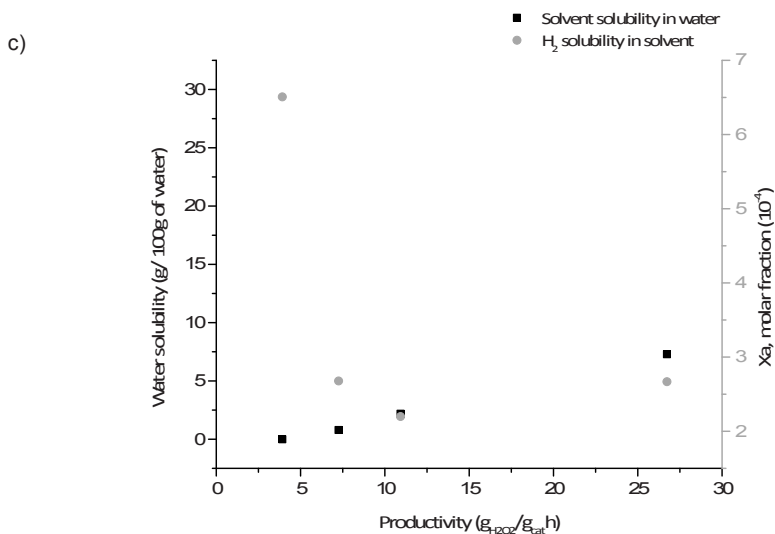


Figure 6.2. a) H_2 conversion, b) H_2O_2 selectivity and c) productivity vs. H_2 solubility in pure co-solvent and co-solvent solubility in water (gas phase: 4 vol% of H_2 and O_2 , total gas flow rate 500 ml/min; $p=20$ bar, $T=30$ °C, liquid phase: water, 0.05 M H_2SO_4 , 9 ppm NaBr, 20 vol% organic co-solvent water non-miscible and partially miscible, hydrophobic Au-Pd/C; stirring speed 1300 rpms).

Despite the expectations, experimental results given here indicate that in order to achieve higher rates of hydrogen peroxide formation it is necessary for the co-solvent to be water miscible. Transport of peroxide from the organic to the water phase and accessibility of promoters that stabilize peroxide formed is crucial for achieving a higher selectivity and indirectly higher reaction rates. A high hydrogen conversion, if not accompanied by a fast peroxide removal from the catalyst surface or its stabilization, is not necessarily beneficial.

The results presented in Fig. 6.1 confirm the conclusion made previously by several other authors that water soluble alcohols are good solvents for the direct synthesis reaction [9,14]. Among the given alcohols, the best performance in terms of conversion and selectivity is observed with *i*-propanol. Methanol and ethanol under identical operating conditions give a lower selectivity than *i*-propanol, but at higher H_2 conversion. From the initial conversion-selectivity relationship (Fig. 6.1d) it is clear that at lower H_2 conversion levels, the selectivity observed after addition of methanol as a co-solvent can be much higher. In fact, the selectivity observed in the aqueous phase only is almost twice lower

Effect of co-solvent addition

compared to for the aqueous/methanol (4:1) mixture at the same H₂ conversion level (~15 %).

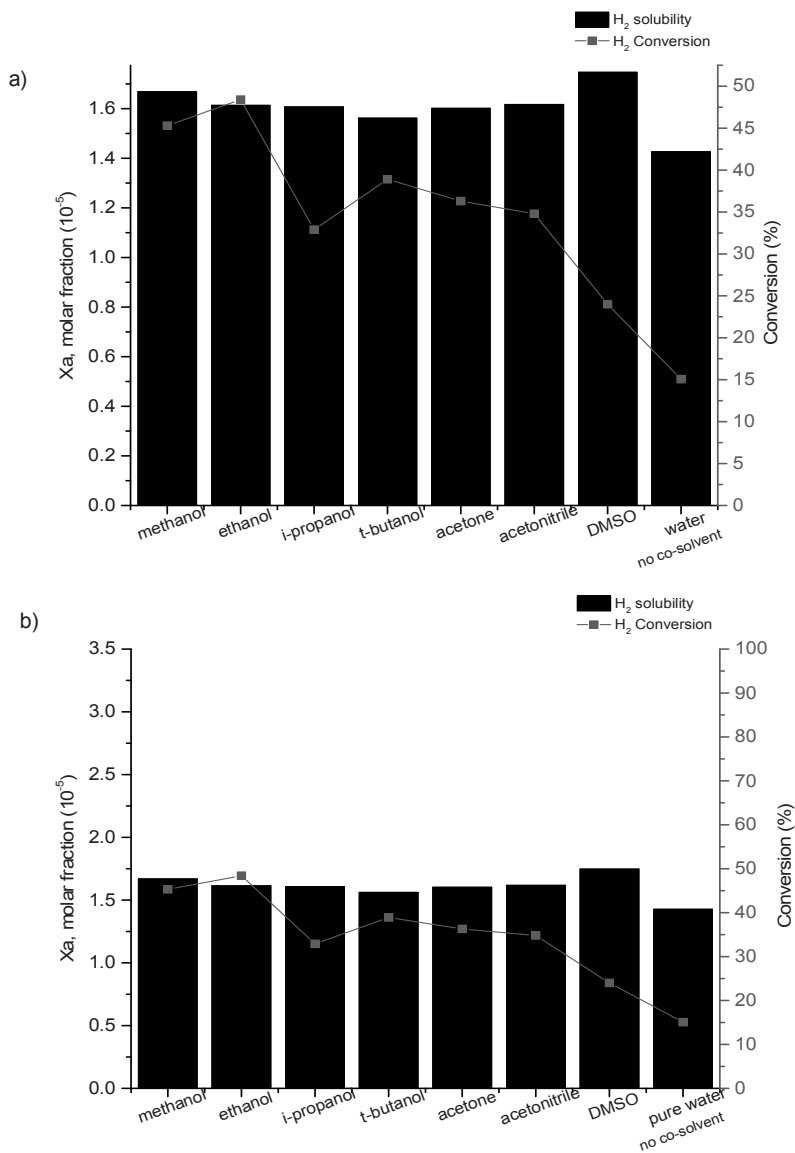


Figure 6.3. Initial H₂ conversion as a function of (a) solubility of H₂ in different solvents; (b) solubility of H₂ in water/co-solvent mixtures (20 vol% of co-solvent; the co-solvent is indicated on the X-axis).

Chapter 6

The highest selectivity values, in addition to a high conversion, were obtained after adding acetone, acetonitrile or DMSO as a co-solvent to the aqueous phase (Fig. 6.1c). Benefits of addition of acetone ^[15] and acetonitrile ^[16] as a co-solvent in the liquid phase used in the direct synthesis reaction were recognized in several earlier publications as well. As already mentioned in the introduction, a higher H₂ solubility in organic solvents in comparison to water is often used to explain higher rates of hydrogen peroxide formation or to justify the application of solvents different as water in the direct synthesis reaction.

In Fig. 6.3a and 6.3b the solubility of H₂ in pure solvents and the co-solvent/water mixture used in the experiments is given respectively. Strictly considering the H₂ solubility in pure solvents, acetone, followed by isopropanol or tert-butanol would be chosen as the best solvent for the direct synthesis reaction. Still, the highest H₂ conversion is observed with methanol and ethanol as a co-solvent. However, it is well known according to the 'solubility theory' that the gas solubility in solvent mixtures is influenced by the solvent-co-solvent interaction through the solubility parameter ^[17]. In order to account for this interaction, the solubility of H₂ in the solvent-co-solvent mixture was calculated (Fig. 6.3b) ^[17-19].

Fig. 6.3b indicates that acetone is actually as good co-solvent as i-propanol, ethanol or acetonitrile for the direct synthesis reaction on the bases of the H₂ solubility in the solvent/co-solvent mixture. The mixture of DMSO and water can be considered ideal, since it is resulting in the highest H₂ solubility, followed by methanol-water solvent mixture. However, if we observe the H₂ consumption obtained experimentally with the addition of the above mentioned co-solvents, DMSO gives a lower H₂ conversion than methanol, ethanol, acetone, t-butanol, isopropanol or acetonitrile, while the conversion observed with tert-butanol is somewhat higher compared to isopropanol, acetone or acetonitrile as well, despite the lower H₂ solubility. In addition, exceptionally high selectivity values exceeding 95% were obtained after addition of acetonitrile or acetone in comparison to other co-solvents tested. The superior behaviour of those two aprotic solvents in terms of yield cannot be simply explained by the solubility of reacting gases.

6.3.2.1. Reactant-co-solvent interaction

To further understand the effect of the co-solvent and the results obtained, the solvent dipole moment (μ) and dielectric constants (ϵ) (Fig. 6.4) were considered. Those properties often determine the ability of the solvent to dissolve or provide a suitable reaction media for the corresponding solute. Some authors have attempted to make a correlation between the hydrogenation rates and solvent polarity, μ or ϵ ^[20-22]. The effect of the nature of the solvent (protic/aprotic) and polarity (dielectric constant) on the reaction rate

and selectivity has been recognized in oxidation reactions with H_2O_2 over Ti-containing zeolites^[23,24]. The influence of the external medium on the adsorption of olefins, alkanes and alcohols is related to the partition coefficient, defined as a ratio of intra-porous to extra-porous concentration, which is directly dependant on solvent polarity and for a given solvent, on hydrophobicity of the molecular sieve^[25].

In regard to this claim, the intra-porous concentration of olefins and other apolar reactants is higher inside TS-1, since TS-1 is more hydrophobic than Ti, Al- β . In a similar fashion, the concentration of more apolar compounds (gases dissolved in less polar solvent) is expected to be higher inside the pores of hydrophobic carbon. This effect of the solvent on the reaction was also reported by Corma et al, who showed that the initial rate of epoxidation of 1-hexene follows the trend of solvent polarity for a homogeneous series of solvents, however the rate is much higher in acetonitrile when compared to methanol as solvent, despite the very similar values for dielectric constants and the reported positive effect that protic solvents exert due to the stabilization of the Ti-peroxo complex through hydrogen bonding^[23]. In some cases, such as cyclohexanol oxidation, the solvent is tailoring the reaction rate mainly through competitive adsorption with reacting molecules on the catalyst surface.

The hydrogen conversion, hydrogen peroxide formation rate and selectivity are plotted against the values for the dielectric constant and the dipole moment of the solvent found in literature (Fig. 6.4). For water miscible solvents, the general trend that can be seen is that an increase in the dipole moment from protic to aprotic solvents seems to lead to a decrease in H_2 conversion, but to a higher selectivity and reaction rates, although this correlation is not very precise, since a group of alcohols with almost identical dipole moment is showing different catalytic performance. The dependence of H_2 conversion, the peroxide formation rate and the selectivity on the dielectric constant seems to be completely random and an apparent relation is missing, indicating that the solvent polarity is not determining the catalyst performance.

6.3.2.2. Solvent/co-solvent-catalyst interactions

Adsorption of the solvent or co-solvent molecule on a catalyst surface, either on the support or on the active metal, might alter the observed reaction rate. Beside solvent co-adsorption^[23], examples where the addition of non-reactive reaction modifiers, such as quinoline, lead to a selectivity improvement, due to co-adsorption on the catalyst surface are reported^[26]. The effect of quinoline co-adsorption is ascribed to the modification of adsorption frequency and the adsorption strength of reactants and products.

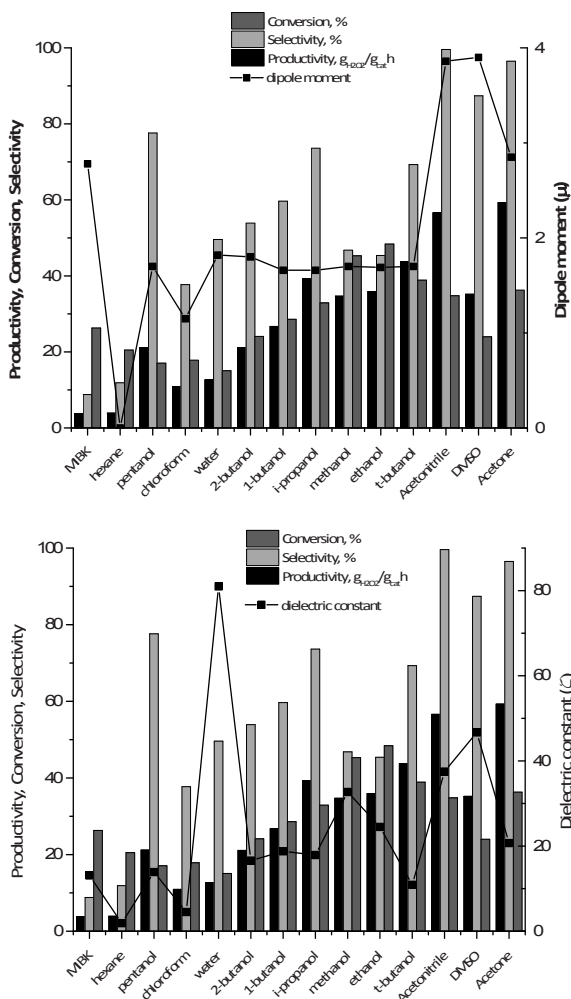


Figure 6.4. Initial H_2O_2 productivity, H_2 conversion and H_2O_2 selectivity as a function of dipole moment (μ) and dielectric constant (ϵ).

Among the small molecules, alcohols and acetone are known to be adsorbed by heterolytic dissociation at room temperature on transition metal oxide surfaces ^[27] p.66. Spitz et al. proved the hypothesis that the relative strength of adsorption of different solvent molecules on ZnO and MgO follows the same order as aqueous pKa values of considered solvents ^[27,28]. As a stronger acid, methanol was able to replace more pre-

adsorbed ethanol on MgO than vice versa, indicating a stronger interaction with the oxide surface. In those experiments the oxide ion served as a Bronsted base. It is expected that the same analogy applies in the case of hydroxyl groups as a Bronsted acid, since the same mechanism is involved in charge stabilization. Analogously, the relative adsorption strength of solvent molecules on the hydroxylated transition metal surface should follow the order of relative basicity in aqueous phase.

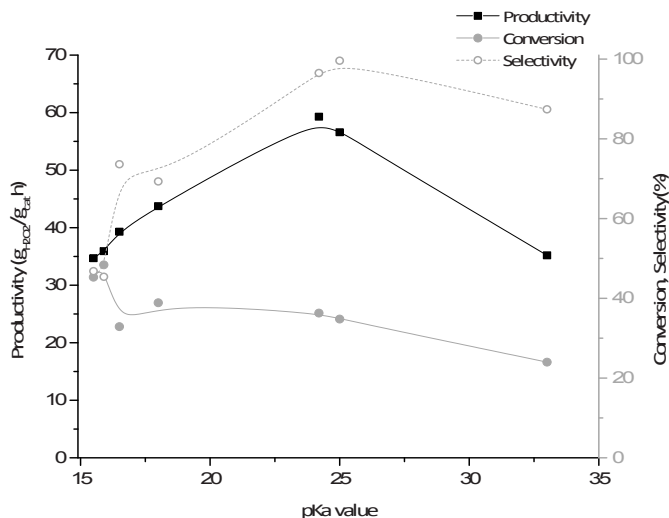


Figure 6.5. The effect of the pKa value of the co-solvent on productivity, conversion, selectivity (gas phase: 4 vol% of H₂ and O₂, total gas flow rate 500 ml/min; p=20 bar, T=30 °C, liquid phase :water, 0.05 M H₂SO₄, 9 ppm NaBr, 20 vol% of organic co-solvent in water, stirring speed 1300 rpms); solvents methanol (pKa=15.5), water (pKa=15.9), ethanol (pKa=16.5), i-propanol (pKa=18), acetone (pKa=24.2), acetonitrile (pKa=25) and DMSO (pKa=33) .

The role of the oxidation state of palladium in the direct synthesis reaction is not quite clear yet. Some studies suggest that supported PdO catalysts show lower hydrogenation/decomposition rates when compared to their metallic analogues [29], while some authors made a contradictory conclusion that metallic palladium is responsible for high activity and selectivity [9]. Considering that under those reaction conditions the catalyst is exposed to both an reductive and an oxidative environment, it is reasonable to assume that different palladium atoms have different oxidation states [30], which can be also dependant on the H₂/O₂ ratio applied [7]. Nyberg et al. [31] showed that when an

Chapter 6

oxygen pre-covered Pd (100) surface is exposed to water vapour hydroxyl (PdOH) is formed. XPS analysis performed confirmed that our fresh Au-Pd bimetallic catalyst, when supported on carbon, contains Au, Pd and PdO phases. Moreover, approximately 66% of Pd is in the form of PdO (Table 1), indicating that in the water medium the palladium surface might be covered with hydroxyl species, representing Bronsted acid type of sites on the actual active metal. Solvents such as acetonitrile or ethanol are recognized to be able of co-ordinating to palladium [9]. Therefore, in a potential solvent interaction, both acidic properties of the support as well as hydroxyl groups on the palladium surface may play a role, in addition to potential solvent co-ordination to the reduced metal surface.

The initial reaction rate, H₂ conversion and H₂O₂ selectivity plotted versus the co-solvent aqueous pKa value is presented in Fig. 6.5. With an increase of the pKa value of the co-solvent, the H₂ conversion is decreasing while the selectivity and productivity values are increasing reaching the apparent maximum. Presumably, the effect of the pKa of the co-solvent is a measure of its ability to coordinate/adsorb to the catalyst surface or of the strength of such an interaction. A drop in conversion is observed with solvents that show a more basic character (acetone, acetonitrile), which can be an indication that those solvents adsorb more strongly compared to more acidic lower alcohols. If, indeed, the co-solvent is coordinating to the active metal (Pd), the higher the pKa value of the co-solvent, the corresponding anion adsorbed on catalyst surface is more Bronsted basic and less electron withdrawing. This results in a lower electrophilicity of the surface metal (ion), which as a final consequence has a weaker adsorption and interaction with the reactant molecule. It is widely believed that the oxygen molecule has to be non-dissociatively adsorbed on the catalyst surface in order to form hydrogen peroxide. Should the O₂ molecule be dissociated on the catalyst, only water is generated. Therefore, it is expected that in case of a weaker interaction with molecular oxygen, less oxygen will be dissociatively adsorbed, meaning that hydrogen peroxide formation will be favoured over water. This is exactly the trend observed if we disregard the effect of DMSO. With an increase in pKa value, the selectivity is significantly increasing as well. However, it is also indicative that using a stronger base as a co-solvent, such as DMSO, results in a somewhat lower selectivity and productivity. It has been previously shown that in the presence of a strong base such as triethanolamine (TEA), the direct synthesis reaction can be even completely suppressed [9].

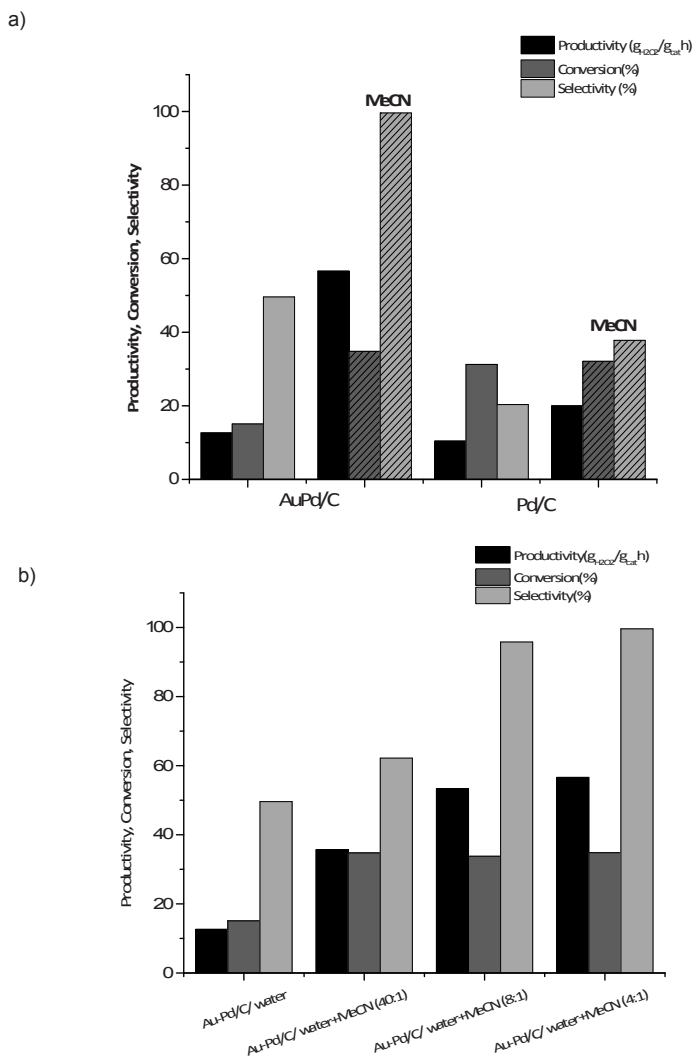


Figure 6.6. (a) The effect of co-solvent on initial productivity, conversion, selectivity on Pd and Au-Pd supported catalysts with and without addition of co-solvent (20 vol% of MeCN added) (b) effect of amount of acetonitrile on productivity, conversion, selectivity over Au-Pd supported catalysts (gas phase: 4 vol% of H_2 and O_2 ; total gas flow rate 500 ml/min; $p=20$ bar; $T=30$ °C; liquid phase: water, acetonitrile, 0.05 M H_2SO_4 , 9 ppm NaBr, stirring speed 1300 rpms).

Chapter 6

One of the potential explanations offered is that TEA is strongly coordinating to the transition metal catalyst. It seems that in case of stronger bases such as DMSO or TEA the interaction between the co-solvent and the catalyst is becoming rather more complex, leading eventually to this apparent maximum in productivity and selectivity observed in the direct synthesis. Generally speaking, the adsorption of a co-solvent molecule on a catalyst surface may influence the activity of metal active site(s) or intermediate complex formed in the reaction, modifying thereby the activation energy. However, the competitive adsorption of reactant and co-solvent is expected to modify the frequency of reactant adsorption on an active site or the pre-exponential factor in Arrhenius equation lowering the reaction rate.

Therefore, competitive adsorption of co-solvent on oxygen adsorption sites that participate in hydrogen peroxide formation would lead to a lower reaction rate and circumstantially to a lower selectivity. The situation becomes additionally complicated if we consider that hydrogen peroxide is in fact an intermediate product which undergoes hydrogenation and/or decomposition on the catalyst surface. The accurate interpretation of the results is difficult, considering that acidic properties of the support material may also play a role. It is not possible to exclude or distinguish the effect of co-solvent adsorption on the support material and decomposition sites potentially present on the support from co-solvent adsorption or co-ordination to active metal itself, and influence this might have on observed catalytic activity.

The phenomenon of potential selective poisoning and a modification of the electronic structure of the palladium surface was already suggested to explain the role of halides in the direct synthesis reaction^[32,33]. Samanta et al.^[32] attributed the strong poisoning effect of I⁻ ions to their strong affinity to Pd surface, while F⁻ is not-coordinating to the Pd surface. Among the halogen ion series, the highest reaction rate and selectivity in halogen group of ions was observed after addition of Br⁻, followed by Cl⁻^[33].

6.3.2.3. Type of metal affected and the amount of solvent

The direct synthesis reaction was tested in a slurry reactor using Au, Pd and Au-Pd nanoparticles supported on hydrophobic carbon as a support with and without the addition of 20 vol% of acetonitrile as a co-solvent to the aqueous phase. Unfortunately monometallic Au seemed to be very inactive in the direct synthesis reaction resulting in a very low peroxide concentration that was insufficient for a precise determination of the hydrogen peroxide. Addition of acetonitrile did not seem to make a difference. However, it is clear that the addition of acetonitrile has a tremendous effect on the selectivity and productivity both in case of Pd and Au-Pd nanoparticles (Fig. 6.6a). The XPS analysis

performed on the same type of catalyst used in the given experiments confirms the difference in catalyst surface composition in terms of the PdO phase. A fresh palladium catalyst used in the reaction is in fact 100% PdO, after calcination performed, while in case of Au-Pd catalyst approximately 66% of surface palladium is in the form of PdO (Table 1). Initial selectivity values observed in case of the Au-Pd catalyst supported on carbon after addition of acetonitrile reach almost 100% as given in Fig. 6.6a. Although both catalysts, Au-Pd and Pd, show a selectivity increase towards peroxide (which is not evident for the Au catalyst), Au-Pd catalyst additionally shows a higher H₂ conversion after the addition of acetonitrile. This might indicate that co-adsorption of acetonitrile on the Au-Pd surface alters the electronic properties of the active metal(s). The acetonitrile interaction with the catalyst is supported by a study of acetonitrile adsorption on evaporated palladium films by XPS which suggests that acetonitrile adsorbs onto the palladium surface via CN^[34]. Even a concentration of acetonitrile additive of a few vol% leads to a significant increase in conversion and yield (Fig. 6.6b), which implies strong interaction with the catalyst. A further increase in acetonitrile content in the liquid phase (to approx. 10 vol%) does not increase the conversion further, but the impact on the selectivity is tremendous. Increasing the amount of solvent on the other hand from 10 to 20 vol% does not seem to have a significant influence on the catalyst activity (Fig. 6.6b), so it is reasonable to assume that with this solvent content saturation of the effect is already achieved. In addition, the catalytic activity is not hampered with addition of higher amount of acetonitrile, meaning that the co-solvent does not poison the active sites needed to form hydrogen peroxide at higher concentrations when conventional diluted mixtures of H₂ and O₂ are used (4 vol% of each reactant).

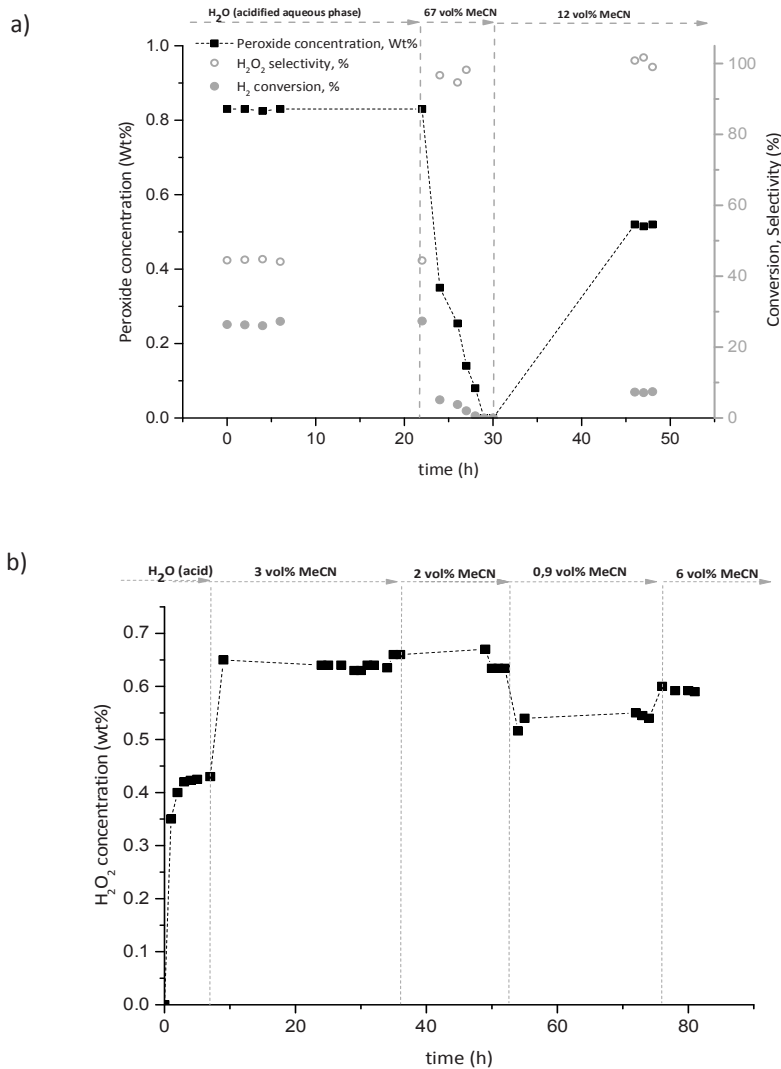
6.3.2.4. Direct synthesis of hydrogen peroxide in a wall-coated microchannel

Previously we showed that the major benefits of having the possibility to perform a direct synthesis reaction under conventionally explosive conditions, using pure H₂ and O₂ mixtures in a microchannel reactor, are significantly higher selectivity values observed in comparison to diluted H₂-O₂ mixtures as well as higher reaction rates^[35].

It is believed that at high surface coverage with reactant molecules, active sites that would be otherwise available for O₂ dissociation or peroxide decomposition on the catalyst surface are occupied, resulting in a higher selectivity. Having in mind the previously made conclusions that certain solvents added might show an interaction with the catalyst through adsorption or competitive adsorption on catalyst surface, the question can be raised if the solvent effect is similar under conventionally explosive conditions. Therefore, the direct synthesis reaction was performed in a wall coated microchannel with

Chapter 6

embedded Au-Pd nanoparticles using pure H₂ and O₂ mixtures with an addition of acetonitrile or methanol as a co-solvent to the aqueous phase containing promoters.



Addition of acetonitrile as a co-solvent to the aqueous phase in the direct synthesis reaction at a high concentration leads to gradual decrease in the H₂O₂ concentration in liquid phase with time on stream as well as to a drop in conversion, until the synthesis reaction is completely stopped (Fig. 6.7a). Lowering the acetonitrile concentration from the initial 67 to 12 vol% of acetonitrile as a co-solvent results in a recovery of the catalyst activity, however the concentration of peroxide observed in the liquid phase remains lower in comparison to the concentration observed using a pure aqueous phase, although the selectivity values reach almost 100%. In the second experiment performed using significantly lower concentrations of acetonitrile than in the initial experiment indicates that concentrations as high as 2-3 vol% of acetonitrile are needed to maximize the H₂O₂ production.

A somewhat higher or lower acetonitrile content as given in Fig. 6.7b gives a lower peroxide content in the liquid phase. The effect of the acetonitrile content on the peroxide productivity with pure H₂-O₂ mixtures is in accordance with the assumption that solvent molecules coordinate to active sites on the catalyst surface (Au-Pd) allowing no adsorption/dissociation of reactive molecules. At very high concentrations, acetonitrile inhibits the active catalytic sites unselectively by suppressing the direct synthesis reaction almost completely. At lower concentrations only the most active catalytic sites involved in O-O bond dissociation or H-O-O-H dissociation are blocked leading to a higher selectivity. It is likely that in order to dissociate the O-O bond, an ensemble of vacant sites is needed. With co-adsorption of solvent molecules and a somewhat higher surface coverage, fewer ensembles would be available to dissociate hydrogen peroxide leading to a higher selectivity. In general, at a higher reactant concentration and higher fraction of active sites occupied, adsorption effects are becoming rather relevant. This in principle also explains the higher selectivity observed with increasing H₂ and O₂ partial pressure^[35]. As mentioned earlier, with a high solvent content, all active sites on the catalyst surface, including those involved in O₂ and/or H₂ adsorption and dissociation are blocked by the solvent making the catalyst inactive.

Taking into account the fact that in case of microchannel Au-Pd nanoparticles are deposited on a SiO₂ wash-coat layer instead of on carbon, a comparison between performance of Au-Pd nanoparticles supported on silica and carbon with addition of acetonitrile as a co-solvent in the autoclave is given in Fig. 6.8. It is clear that despite the fact that Au-Pd catalyst supported on carbon gives less side reactions than for the same bimetallic catalyst supported on silica, after addition of acetonitrile to Au-Pd/SiO₂ the selectivity increase is tremendous reaching a selectivity of over 90%. We can conclude that in terms of selectivity enhancement acetonitrile as a co-solvent is even more effective in case of the catalyst supported on silica than on carbon. This finding can be correlated with

Chapter 6

the fact that XPS analysis of a freshly prepared Au-Pd (1:2) catalyst supported on SiO₂ shows that 75% of surface palladium is in the form of PdO in comparison with 66% for the carbon supported catalyst and/or with more surface hydroxyl groups expected on silica in comparison to carbon support. Interestingly, both silica and carbon supported Au-Pd catalysts besides higher selectivity, show an increase in H₂ conversion after acetonitrile addition, which definitely implies the interaction of co-solvent with the active metal(s), not only with the support.

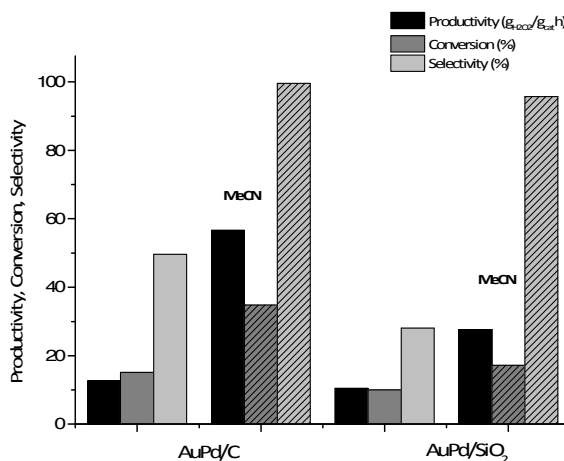


Figure 6.8. Direct synthesis in presence of Au-Pd/C and Au-Pd/SiO₂ with or without addition of acetonitrile in autoclave (gas phase: 4 vol% of H₂ and O₂; total gas flow rate 500 ml/min; p=20 bar; T=30 °C; liquid phase :water, 0.05 M H₂SO₄, 9 ppm NaBr, stirring speed 1300 rpms, with or without 20vol% of acetonitrile).

The same strategy was applied to test the effect of methanol which is often considered as a solvent of choice for the direct synthesis reaction besides water. Methanol is a solvent which is compatible with processes potentially considered to be directly linked to direct synthesis of hydrogen peroxide such as the HPPO process [1]. In addition, considering the application of the direct synthesis reaction in the oxidation of fine chemicals in -situ, methanol is an excellent solvent for many organic substrates that could be considered. In contrast to acetonitrile, addition of methanol at high concentrations does not have a detrimental effect on the direct synthesis reaction when pure H₂-O₂ mixtures are applied in the wall-coated microchannel reactor. The liquid phase applied in the direct synthesis

Effect of co-solvent addition

consisted of 97 vol% of methanol (Fig. 6.9). From Fig. 6.9 we can see that with methanol addition, almost the same selectivity is retained although the conversion and peroxide concentration clearly increased. In case of acetonitrile addition at concentration of 67 vol%, the hydrogen peroxide formation was entirely inhibited (Fig. 6.7a). Therefore, it is reasonable to assume that the strength of methanol interaction with the catalyst is weaker in comparison to acetonitrile, considering that methanol is not adsorbing competitively with reactants in high concentrations.

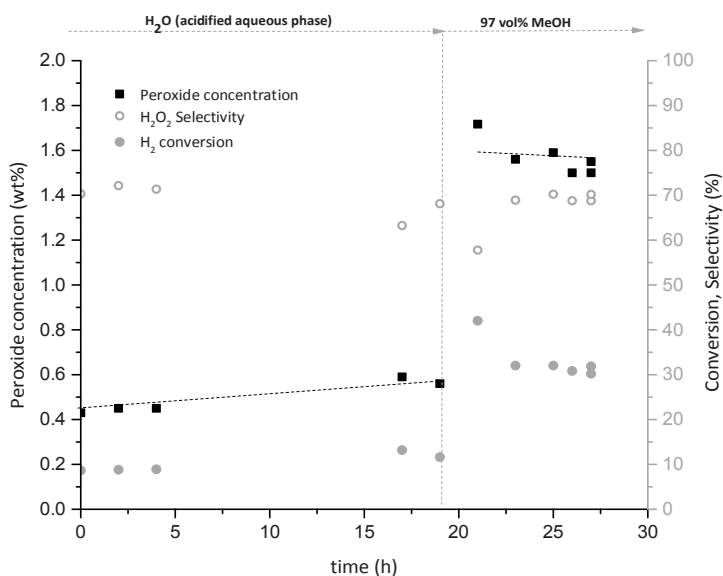


Figure 6.9. Direct synthesis of hydrogen peroxide in a microreactor using methanol/water(acid) as a solvent (gas phase: 50 vol% of H₂ and O₂; p=20 bar; T=30 °C; flow rate 5 ml/min; liquid phase: 0.05 M H₂SO₄, 9 ppm NaBr, water or methanol/water (97/3), flow rate 0.05 ml/min).

As mentioned earlier in the introduction, Krishnan et al. attributed the difference in rate of H₂O₂ formation in water and methanol to differences in the gas-liquid mass transfer rate^[8]. Their calculation showed that the mass transfer rate from gas to liquid was 15 times higher in methanol than in water mainly due to the higher H₂ solubility. In parallel, the resistance to solid-liquid mass transfer was calculated to be much lower compared to gas-liquid under their reaction conditions. The reaction rates in the liquid phase containing

Chapter 6

water with sulphuric acid was significantly lower than in a methanol/sulphuric acid medium. Still, initial reaction rates in methanol and water with halides present were almost identical, meaning that a liquid film mass transfer does not play a crucial role after all. Certainly, the difference in the H_2 solubility in the liquid phase (O_2 is typically an order of magnitude more soluble than H_2 and thereby less likely to be limiting) is the most obvious explanation for higher reaction rates obtained in methanol. However, microreactors are recognized for their very high mass transfer rates, primarily due to their higher surface to volume ratios. It is known that in case of the Taylor flow in microchannels mass transfer of a gas component proceeds through following 3 steps: (1) From gas bubble directly to the solid catalyst through thin liquid film (gas-to-solid) (2) from the bubble caps to the liquid (gas-to-liquid) and (3) from the liquid to the catalyst for dissolved gas (liquid-to-solid). Mass transfer from gas-to-liquid and liquid-to-solid represent resistances in series and occur in parallel to mass transfer directly from gas-to-solid. In case of a catalytic reaction occurring on the reactor wall, gas-to-solid mass transfer is the dominant step, being considerably faster than the other two. Typically, gas-to-solid mass transfer through the thin liquid film wetting the catalytic wall is so fast that the probability that reactions are affected by internal mass transfer is much higher. This fast mass transfer through this thin liquid film is enhanced further by the very high geometric surface area available for mass transfer in the microchannel ($12500 \text{ m}^2_{\text{catalyst external surface}}/\text{m}^3_{\text{reactor}}$). Calculation of the mass transfer coefficient from gas-to-solid k_{GS} performed using well established correlations available in literature [36], gives a value of approximately 40 s^{-1} , which is pretty close to a 45 s^{-1} calculated for the water phase. Values of mass transfer rates obtained in methanol and in water are more than an order of magnitude higher than observed overall volumetric reaction rates ($R_{V,ov_solvent} \leq 0.1k_{GS}a_{GS}C_{H_2,solvent}^{sat}$), indicating that the reaction supposedly is not limited by the H_2 transfer. In addition, it is clear that despite that the H_2 conversion is much higher than in case of aqueous solvent, the selectivity values are retained. Clearly, the biggest advantage achieved with methanol as a solvent is the high selectivity towards peroxide in respect to water with already remarkably high peroxide concentrations in the liquid phase. The hydrogen conversion in the water/methanol mixture observed in the experiments performed in the autoclave (Fig. 6.1) is more than twice higher than those in the water phase, which could not be expected based on the H_2 solubility values solely (Fig. 6.3 b).

For many applications, such as in fine chemical industry [37,38], the development of a small scale on demand direct synthesis process for production of ultra-pure grade hydrogen peroxide in desirable concentrations without the addition of stabilizers and preservatives is of significant interest, thus avoiding the risks of transportation and storage of hydrogen peroxide and possible effects of the stabilizers on the downstream processes. Detrimental

effects that the addition of acid and halides might have on equipment need to be considered, but also on the secondary reaction coupled to direct synthesis (HPPO process). Therefore we decided to perform the direct synthesis reaction over the Au-Pd bimetallic catalyst using pure methanol as a solvent in the absence of these additives in the microchannel reactor with pure H₂ and O₂ mixtures.

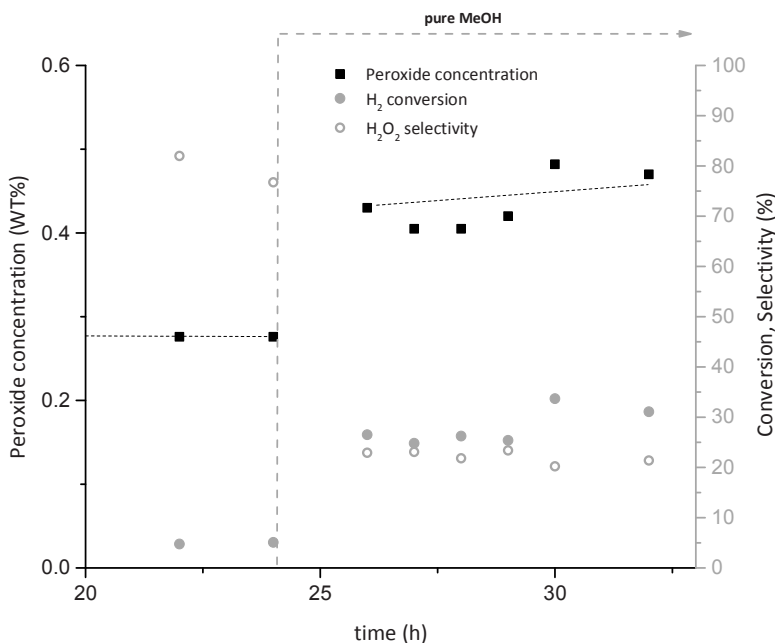


Figure 6.10. Direct synthesis of hydrogen peroxide in a microreactor using pure methanol as a solvent (gas phase: 50 vol% of H₂ and O₂; p=20 bar; T=30 °C; flow rate 5 ml/min; liquid phase: liquid phase: 0.05 M H₂SO₄, 9 ppm NaBr, water or pure methanol, flow rate 0.05 ml/min).

From Fig. 6.10. it is clear that H₂ conversion is approximately 5-6 times higher in pure methanol than in the aqueous phase with promoters added. The peroxide concentration is almost twice as high as in the aqueous phase, however the drop in selectivity in pure methanol towards peroxide is evident. The presence of promoters plays a very important role in the peroxide production, preventing hydrogen peroxide transformation to water.

6.3.3. FTIR adsorption of CO, acetonitrile and methanol over Au, Pd and Au-Pd catalysts supported on silica

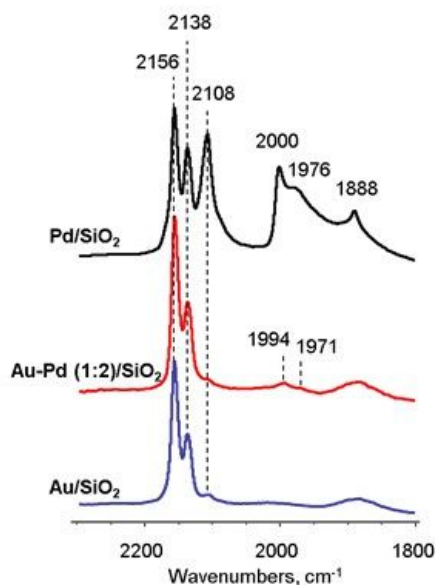


Figure 6.11. IR bands resulting from CO adsorption at 100 K on Pd/SiO₂, Au-Pd/SiO₂ and Au/SiO₂

The nature of the metal sites in silica supported catalysts was investigated by FTIR spectroscopy of adsorbed CO. Carbon monoxide was selected for this study, since it is a well-established probe molecule for the characterization of the metal state in solid catalysts^[39]. In a typical experiment, CO was gradually adsorbed dose by dose until a complete saturation of active sites was reached accompanied by the appearance of a band at ca. 2140 cm⁻¹, characteristic of physically adsorbed CO. The results obtained are shown in Fig. 6.11. The adsorption of CO on Pd/SiO₂ leads to the appearance of bands at ca. 2156, 2138, 2108, 2000, 1976 and 1888 cm⁻¹ (Fig. 6.11), typical for Pd supported on silica samples^[40]. The band at 2138 cm⁻¹ is due to physically adsorbed CO, while the band at 2156 cm⁻¹ can be attributed to the vibrations of CO adsorbed on the Si-OH surface groups of the support. Bands at 2108 and 2000 cm⁻¹ correspond to linear and bridging carbonyls of the Pd⁺ surface species, correspondingly, whereas bands at lower frequencies (1976 and 1888 cm⁻¹) can be assigned to the adsorption of CO over metal Pd sites with the formation of (Pd₂)⁰CO and (Pd₃)⁰CO surface species.

The Au/SiO₂ catalyst reveals a simpler spectrum: bands at 2156 and 2138 cm⁻¹, similar to Pd/SiO₂ and a band at 2108 cm⁻¹, which corresponds to the adsorption of CO over Au⁺ defects [41].

In the case of the Au-Pd/SiO₂ sample, new bands at 1994 and 1971 cm⁻¹ were detected. These bands can be attributed to the interaction of CO with Au-Pd sites in surface alloys, which can be formed during the synthesis of bimetallic particles. CO adsorption results indicate strong interaction between Au and Pd. Comparison of the spectra for Pd/SiO₂ and Au-Pd/SiO₂ shows that addition of gold leads to a disappearance of the bands corresponding to (Pd₂)⁰CO and (Pd₃)⁰CO species, pointing to the presence of Au atoms in the Pd environment. In fact, results imply that Pd is strongly diluted by Au on the surface, since there are almost no Pd-Pd centers (no bridged CO over Pd). This observation is in line with XPS data, which showed that the surface Au/Pd ratio is close to that of the bulk, calculated from the synthesis procedure.

Also, the addition of Au to Pd leads to a decrease of Pd⁺ cationic sites in the catalyst, which are most probably unselective in the H₂O₂ synthesis reaction.

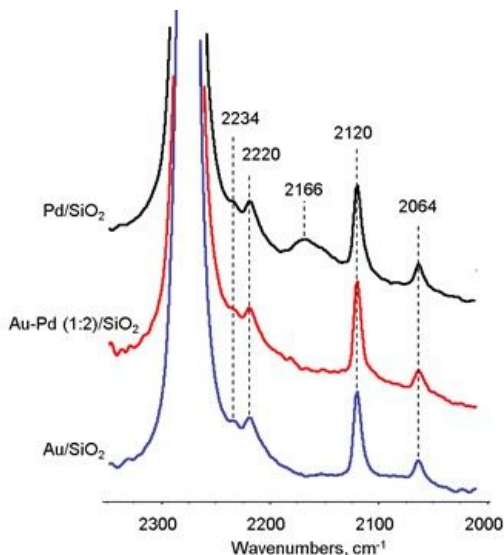


Figure 6.12. FTIR spectra of acetonitrile adsorption on Pd/SiO₂, Au-Pd/SiO₂ and Au/SiO₂ at r.t.

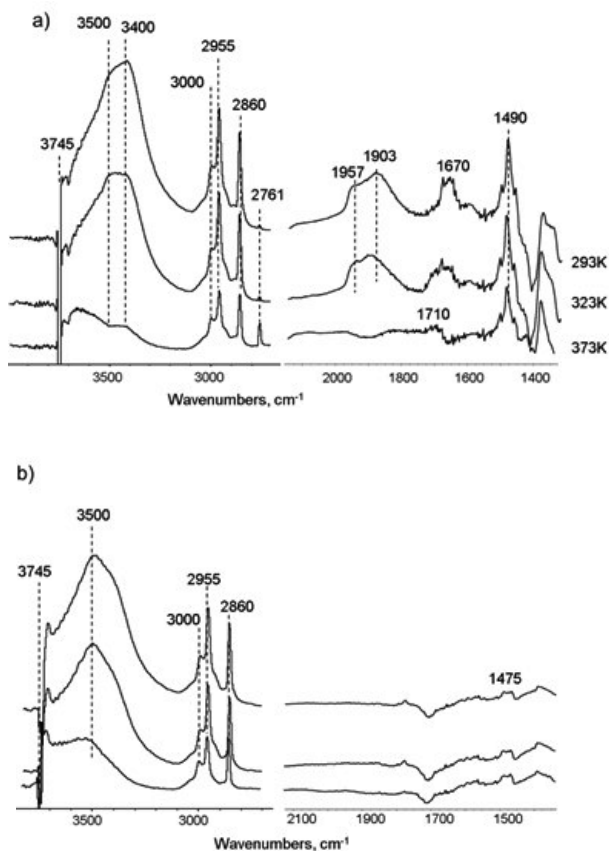


Figure 6.13. FTIR spectra of methanol adsorption on Pd/SiO₂ (a) and Au/SiO₂ (b) at different temperatures of evacuation.

6.3.3.1. FTIR of adsorbed CD₃CN

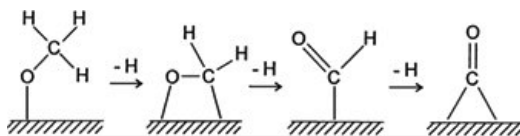
For the FTIR experiments deuterated acetonitrile was used to avoid the excitation of Fermi resonances of $\nu(\text{C-C})$ and $\delta_s(\text{CH}_3)$ vibrations, which overlap with the characteristic $\nu(\text{C-N})$ bands and impede the interpretation of the spectra. When deuterated acetonitrile was adsorbed on silica supported catalysts, several bands in the 2000-2300 cm⁻¹ IR region could be observed. For Au/SiO₂ and Au-Pd/SiO₂, five bands at ~2275, 2234, 2220, 2120 and 2064 cm⁻¹ are observed (Fig. 6.12). An intense band at 2275 cm⁻¹ is associated with acetonitrile coordinated with silanol groups of silica, a band at 2120 is due to the $\delta_s(\text{CD}_3)$

vibration. Weak bands at 2234, 2220 and 2064 cm^{-1} appears in liquid acetonitrile and can be attributed to nonspecifically bonded CD_3CN .

After the adsorption of acetonitrile on Pd/SiO_2 besides the above mentioned bands a new band at 2166 cm^{-1} appears. This band can be associated with the dissociation of acetonitrile on Pd particles with formation of Pd-CN adsorbed species ^[42]. Comparison of this data with FTIR of adsorbed CO shows that dissociation of CD_3CN occurs only over defect sites with the Pd environment. The FTIR results correlates with the catalytic data. It can be suggested, that acetonitrile can be adsorbed on unselective defect Pd sites, resulted in its blocking and increasing the selectivity of the H_2O_2 synthesis.

6.3.3.2. FTIR of adsorbed CH_3OH

The strong interaction of solvents with Pd has been supported by additional analysis of methanol adsorption over Pd/SiO_2 in comparison with Au/SiO_2 . Difference spectra of methanol adsorbed on Pd/SiO_2 and Au/SiO_2 are shown at Fig. 6.13. After MeOH adsorption over all catalysts the characteristic bands of molecularly adsorbed methanol appear ^[43]. An intense negative peak at 3745 cm^{-1} appears in the OH stretching region as a result of the interaction of the surface Si-OH groups with methanol. A broad band centered at approximately 3500 cm^{-1} is characteristic for the O-H stretching vibration of hydrogen-bonded Si-OH groups and suggests that MeOH molecules are hydrogen bonded to the surface. In the C-H bond vibration region, the following bands are observed: 3000 ($\nu''_{\text{as}}\text{CH}_3$), 2955 ($\nu'_{\text{as}}\text{CH}_3$), 2860 ($\nu'_s\text{CH}_3$). Evacuation of methanol at different temperatures leads to gradual decrease of the intensity of these bands, which point to a weak interaction of CH_3OH with the surface and confirms the suggestion of H-bonding of methanol with Si-OH groups. In case of methanol adsorbed over Pd/SiO_2 an additional band at 2761 cm^{-1} and a shoulder at 3400 appears in the spectra, at the intensity at 2761 increases upon evacuation. These bands clearly can be assigned to the development of a $\nu(\text{C-H})$ vibration in formate species ^[44], which can be formed via dissociation of methanol H-OCH_3 over Pd with subsequent dehydrogenation. This mechanism has been earlier proposed during methanol adsorption over Pd based catalysts ^[45,46]:



Scheme 6.1. Methanol adsorption with decomposition over Pd surface.

Chapter 6

Analysis of the region of lower wavenumbers supports this assumption (Fig. 6.13). Adsorption of methanol over Au/SiO₂ demonstrates only weak bands at 1475 cm⁻¹ attributed to deformation vibrations of adsorbed methanol $\delta_{as}(\text{CH}_3)$ and $\delta_s(\text{CH}_3)$ [46]. Methanol adsorption over Pd/SiO₂ at r.t. results in the appearance of intensive bands at 1957, 1903, 1670 and 1490 cm⁻¹. The bands at 1957 and 1903 cm⁻¹ can be assigned to strong adsorption of CO (Fig. 6.12) due to partial decomposition of methanol. The broad band at 1670 cm⁻¹ might be assigned to $\delta(\text{HOH})$ of adsorbed water most probably formed due to decomposition of methanol: $\text{CH}_3\text{OH} + \text{OH} = \text{CO} + \text{H}_2\text{O} + 3/2\text{H}_2$ [46]. The strong bands at 1490 cm⁻¹ are attributed to deformation vibrations of dissociated methanol [46]. Those bands are present both at 293 and 323 K, which is a range of temperatures typically intended to be applied in the direct synthesis. Temperatures of 303 K used in semi-batch synthesis experiments with a co-solvent applied pertains to this range. The bands assigned to water and CO adsorption disappear in the spectrum at 373 K due to desorption. The rest band at 1710 cm⁻¹ can be attributed to vibration of the carbonyl group of formyls chemisorbed onto the Pd metal [46] which correlates with appearance of a strong band C-H at 2761 cm⁻¹. Thus, these results show a strong interaction of Pd with adsorbed methanol with its dissociation, dehydrogenation with formation of formate species and decomposition with formation of CO and H₂O. The same sites can be responsible for the decomposition of hydrogen peroxide. Addition of methanol or forming an alloy with Au should lead to suppression of this activity according to the FTIR results.

6.3.4. Hydrogen peroxide decomposition in water/co-solvent mixture

Decomposition of hydrogen peroxide over the catalyst surface is, besides its hydrogenation, the main side reaction responsible for water formation from H₂O₂. Although the synthesis experiments presented were typically performed with the addition of acid if not stated differently to ensure that the decomposition of hydrogen peroxide is minimized, it is of importance to establish if this step can be avoided in the presence of the co-solvent. The decomposition of hydrogen peroxide was tested initially over a Au-Pd and a Pd catalyst supported on carbon with or without acetonitrile (20 vol%) added as a co-solvent (Fig. 6.14a).

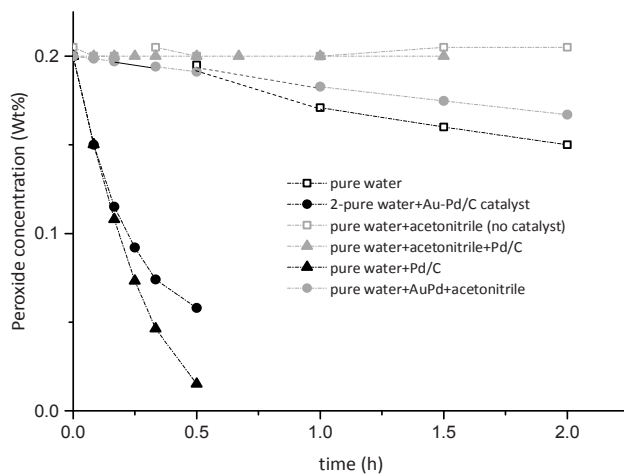
In general, decomposition of hydrogen peroxide in pure water is often caused by the presence of traces of ions or impurities and often dependent on slight changes in pH of the distilled water used, which is also observed in our experiments. After addition of acetonitrile as a co-solvent to pure water, the decomposition reaction over the Pd/C catalyst seems to be completely blocked. The decomposition reaction over the Au-Pd catalyst is also significantly inhibited after acetonitrile addition in comparison with pure water. Decomposition experiments performed separately with the Au/C catalyst, showed

no difference in decomposition curves obtained in pure water without catalyst added (blank) and after catalyst addition, proving that the monometallic Au/C catalyst was inactive both in the decomposition of hydrogen peroxide as well as in the synthesis reaction. We believe based on those decomposition experiments that solvent molecules indeed might adsorb on Pd or PdO sites blocking the O-O bond dissociation. The presence of water miscible alcohols as co-solvents (methanol, isopropanol, 1-butanol) seems to reduce the decomposition of hydrogen peroxide, however alcohols do not seem to be as efficient as acetonitrile (Fig. 6.14b.).

To test this hypothesis on a potential solvent interaction with the catalyst surface further, the kinetics of hydrogen peroxide decomposition over the Au-Pd catalyst was studied in pure water, water-methanol and water-acetonitrile mixtures (Appendix Fig.S1).

The solvent effects considered might be a consequence of solvent interaction with the solute, hydrogen peroxide in this case, or with the catalyst itself. The solvent-solute interaction can be quantified via an activity coefficient. When modelling the decomposition of hydrogen peroxide in a water/methanol liquid medium taking into account the activity coefficient (see supporting information), values of the activity coefficient obtained at 20 and 30 °C were 0.998 and 0.997 respectively. This confirms that methanol is not interacting (strongly) with the catalyst, but presumably with the solute itself. In contrast to methanol, it is evident that acetonitrile hinders the decomposition reaction even at a very small concentration, which is indicative for a competitive solvent adsorption on catalyst sites responsible for H₂O₂ decomposition. Kinetic fitting indicates that competitive adsorption of acetonitrile on the catalyst surface can explain the decomposition results, meaning that acetonitrile is indeed able to strongly interact with the catalyst altering therefore its activity in the decomposition reaction (Supporting Information). Taking into account the effect of acetonitrile on hydrogen peroxide decomposition and hindrance of the direct synthesis reaction under explosive conditions, it is reasonable to conclude that acetonitrile is able to interact strongly with the catalyst surface.

a)



b)

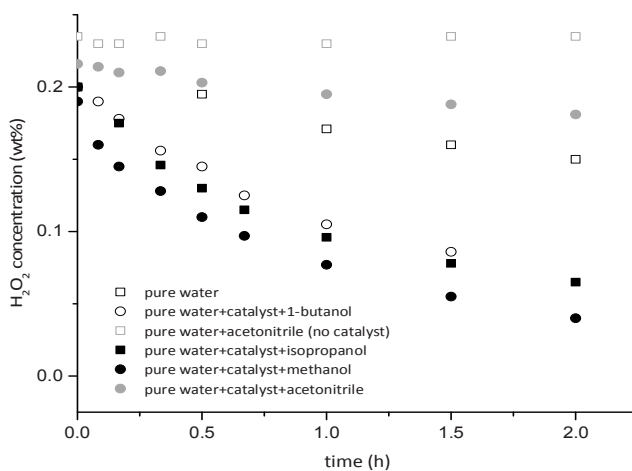


Figure 6.14. (a) Decomposition of hydrogen peroxide in an autoclave over a Au-Pd/C and a Pd/C catalyst with and without addition of 20 vol% of acetonitrile as a co-solvent (b) Decomposition of hydrogen peroxide in an autoclave over a Au-Pd/C catalyst with addition of various co-solvents ($T=30\text{ }^{\circ}\text{C}$; liquid phase: H_2O_2 , pure water, 20 vol% of co-solvent with or without 0.2 g catalyst added).

6.4. Conclusions

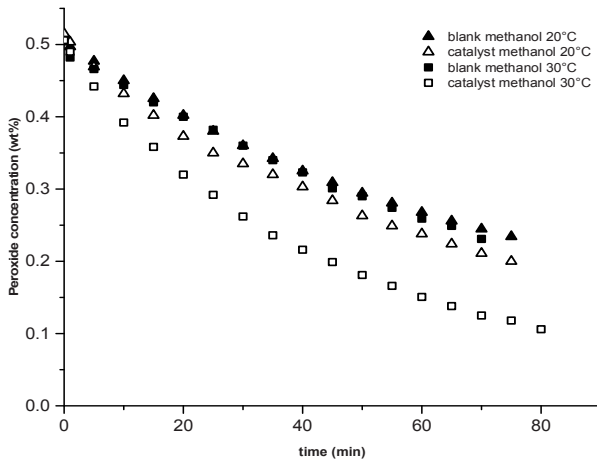
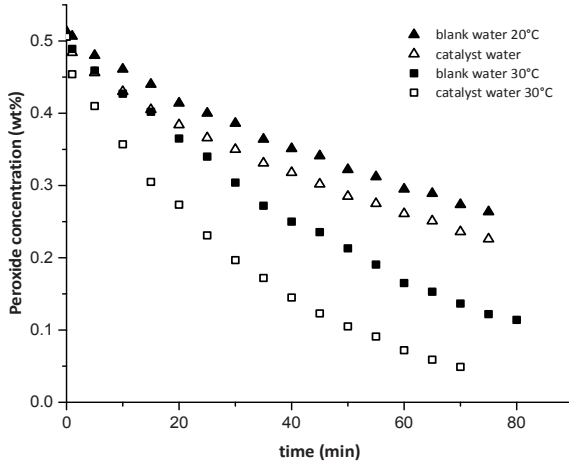
The solvent nature strongly affects the observed catalytic activity of the catalyst in the direct synthesis of hydrogen peroxide. Besides the effect on the H₂ conversion, some solvents added to typically used aqueous phase can significantly modify the selectivity towards peroxide. Despite the fact that some water non-miscible solvents show a high H₂ solubility, they are not suitable for the direct synthesis reaction. In fact, addition of hexane, the solvent with the highest H₂ solubility, results in poor selectivity. Our results suggest that suitable solvents for the direct synthesis are water miscible. Lower alcohols, among those show pretty high selectivity at moderate to high conversions, and as such are suitable for the direct synthesis reaction. With the group of aprotic polar solvents (acetone, acetonitrile, DMSO) a very high selectivity can be achieved, probably due to the solvent interaction with the catalyst surface. However, as is evident from the microreactor experiments, at high concentrations of the solvent and reacting gases, the aprotic solvent can completely poison the catalyst. The strength of solvent adsorption for the group of water miscible protic and aprotic solvents can be correlated with its pK_a value. With an increase in the pK_a value of the solvent, although the conversion slightly drops, the selectivity is increasing significantly. Still, the results suggest that solvents with a very high pK_a value are less selective poisons of the catalytic surface. The positive effect of acetonitrile on selectivity is even more pronounced with a silica supported catalyst, which can be ascribed to both higher PdO content in case of the silica supported Au-Pd catalyst, but also to higher amount of surface hydroxyl groups available on the silica surface. Considering that the Au-Pd catalyst both supported on carbon and silica, in addition to higher selectivity gives higher H₂ conversion upon addition of acetonitrile, a possibility of solvent coordination to the active metal seems to be likely. The FTIR measurements of adsorbed CO proves the strong interaction of Au and Pd through alloy formation resulting in the unique nature of a Au-Pd bimetallic catalyst. The CD₃CN adsorption experiments indicate that acetonitrile adsorbs on unselective defect Pd sites, which could be responsible for peroxide decomposition on the catalyst surface. Eventually, the selective poisoning of the catalyst surface with an aprotic solvent was confirmed via decomposition of hydrogen peroxide in the presence of a catalyst. Decomposition in the presence of co-solvent (acetonitrile) was either blocked (at higher acetonitrile content) or decelerated (lower acetonitrile content). Although FTIR studies of methanol adsorption show a strong interaction with Pd, the addition of methanol does not significantly affect the hydrogen peroxide decomposition kinetics over the Au-Pd catalyst itself in comparison with pure water. The effect of methanol addition on the hydrogen peroxide decomposition seems to correlate with the interaction of methanol with the peroxide, rather than with the catalytic sites responsible for cleavage of an O-O bond.

Chapter 6

In case of the application of microreactors with concentrated hydrogen and oxygen mixtures, the addition of only small amounts of aprotic solvents such as acetonitrile (up to a few percent) leads to a significant improvement in selectivity and yield, but high concentrations are detrimental for the catalytic activity assumingly due to a non-selective adsorption on active catalytic sites. Addition of methanol, however, as a solvent or co-solvent when using concentrated H₂ and O₂ gas feed does seem to be a much better option, considering that the yield observed can be several times higher than in aqueous solutions. Methanol is a suitable solvent from the aspect of direct consumption of peroxide produced in selective oxidations, considering that many organic substrates show a good solubility in methanol. Still, the addition of acid as a peroxide stabilizer which prevents its decomposition is difficult to avoid considering the impact on the selectivity. The presence of acid in peroxide solutions is not only needed during the course of the reaction, but during the post-processing, in contact with pipelines or storage. If the Au-Pd catalyst would be the only cause of its decomposition, reaction solutions could be simply neutralized after the reaction step. Specifications of commercially available standard grade peroxide solutions indicate that those are also acidified with the aim to prevent rapid decomposition. Addition of metal chelating agents as stabilizers is not sufficient to prevent peroxide decomposition, since it is believed that peroxide decomposition proceeds via formation of HO₂⁻ species^[47]. Having in mind that in an earlier publication we showed that it is possible to reach peroxide concentrations up to 5 wt% in aqueous media and that here we show that application of methanol as a solvent instead of water can improve the yield by factor of 3-4 (with acid present), it is reasonable to assume that the concentration of 9 wt% set as objective by economic evaluation is possible to attain.

Appendix 6A: Decomposition of H₂O₂ in the presence of co-solvent

a)



b)

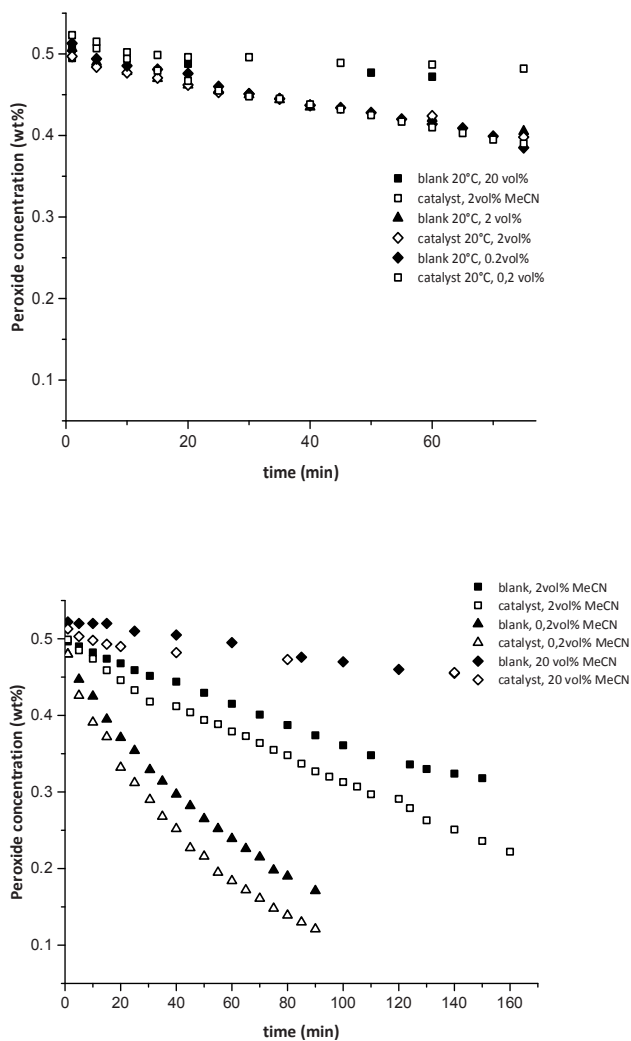
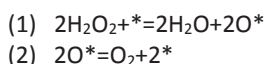


Figure S1. Kinetics of decomposition of hydrogen peroxide in autoclave over Au-Pd catalyst (a) In pure water at 20 and 30 °C (b) In water-methanol (20 vol%) mixtures at 20 and 30 °C (c) In water-acetonitrile mixtures (different acetonitrile content) at 20°C (d) In water-acetonitrile mixtures (different acetonitrile content) at 30°C

Blank experiments, involving the decomposition of hydrogen peroxide without catalyst, were performed before each of the catalytic experiment due to the sensitivity of the decomposition reaction on the presence of impurities or stabilizers in H₂O₂ solution, material of the autoclave itself or quality of distilled water used.

Comparing the H₂O₂ decomposition over time (Fig. S1) in the presence of catalyst in pure water, water/methanol (20 vol%) and water/acetonitrile mixtures suggests complete inhibition of peroxide decomposition after addition of 20 vol% of acetonitrile to the pure water, while decomposition in water/methanol compared to pure water is only slightly slower. Lowering the acetonitrile concentration in the liquid medium results in a faster peroxide decomposition as well. Interestingly, even at an acetonitrile content as low as 0.2 vol% in pure water, the decomposition rates are slower than in a pure water at a given temperature. The kinetics of hydrogen peroxide decomposition in a pure water over Au-Pd/C catalyst was modelled using the following surface reaction mechanism:



Constant	20°C	30°C
k (mol/dm ³ h)	0.049	0.1115
K _{ads} (dm ³ /mol)	24.2	8.99

The formation of O₂ molecule has been assumed to be the rate determining step. The expression obtained with this mechanism was describing accurately the experimental data observed. The values for the reaction rate and adsorption constants are given in Table.

$$R = k \left(\frac{K_{ads} C_{H_2O_2}}{1 + K_{ads} C_{H_2O_2}} \right)^2$$

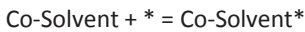
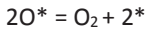
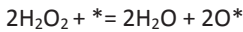
Several different predictive thermodynamic models are available for calculation of activity coefficients, among which UNIFAC-based method is particularly versatile and handy. Our attempt to assess activity coefficients for H₂O₂ in water-methanol or water-acetonitrile mixture was not successful, since specific parameters used to describe interaction between different functional groups of those molecules were not available. However, when decomposition of hydrogen peroxide in water/methanol mixture was modelled

Chapter 6

using the expression (2) with reaction rate and adsorption constants obtained for pure water and introducing the peroxide activity $a_{H_2O_2} = \gamma^* C_{H_2O_2}$ instead of concentration as follows:

$$R = k \left(\frac{K_{ads} \gamma^* C_{H_2O_2}}{1 + K_{ads} \gamma^* C_{H_2O_2}} \right)^2$$

the values obtained for γ at 20 and 30 °C were 0.998 and 0.997 respectively. In contrast to methanol, it is evident that acetonitrile hinders the decomposition reaction even at very small concentration, which is indicative for competitive solvent adsorption on catalysts sites responsible for H_2O_2 decomposition. Therefore, following mechanism was proposed to describe acetonitrile interaction with the catalyst and H_2O_2 in the liquid phase:



$$R = k \left(\frac{K_{ads} C_{H_2O_2}}{1 + K_{ads} C_{H_2O_2} + K_{co-sol} C_{co-sol}} \right)^2$$

Due to inability to distinguish between the decomposition of peroxide in water/acetonitrile phase in the presence and absence of the catalyst at 20°C, the decomposition results obtained at 30°C were used to test this hypothesis. After fitting the experimental results with corresponding expression, values for K_{co-sol} were 29.7 L/mol for 2 vol% MeCN and 37.4 L/mol_{MeCN} for 0.2 vol% MeCN added to the pure water. The discrepancy between the values observed could be ascribed to inaccuracy caused either by the blank experiments or acetonitrile dilution at very small concentrations.

References:

- [1] P. Bassler, H. G. Goebbel, M. Weidenbach, *Chem. Eng. Trans.* **2010**, *21*, 571–576.
- [2] C. L. Hill, *Catal. Met. Complexes* **1992**, *9*, 253–280.
- [3] W. K. and O. W. G. Goor, *Ullmann's Encyclopedia of Industrial Chemistry, Vol. A13*, Wiley-VCH Verlag GmbH & Co. KGaA, Weinheim, Germany, **1989**, p.393-423
- [4] J. K. Edwards, B. Solsona, E. N. N, A. F. Carley, A. Herzing, C. J. Kiely, G. J. Hutchings, *Science* **2009**, *323*, 1037–1041.
- [5] E. Ntainjua N., J. K. Edwards, A. F. Carley, J. A. Lopez-Sanchez, J. A. Moulijn, A. A. Herzing, C. J. Kiely, G. J. Hutchings, *Green Chem.* **2008**, *10*, 1162–1169.
- [6] J. García-Serna, T. Moreno, P. Biasi, M. J. Cocero, J.-P. Mikkola, T. O. Salmi, *Green Chem.* **2014**, *16*, 2320–2343.
- [7] V. Paunovic, J. C. Schouten, T. A. Nijhuis, *Catal. Today* **2014**, *i*, DOI 10.1016/j.cattod.2014.04.007.
- [8] V. V. Krishnan, A. G. Dokoutchaev, M. E. Thompson, *J. Catal.* **2000**, *196*, 366–374.
- [9] R. Burch, P. R. Ellis, *Appl. Catal. B Environ.* **2003**, *42*, 203–211.
- [10] Q. Liu, J. H. Lunsford, *Appl. Catal. A Gen.* **2006**, *314*, 94–100.
- [11] Y. Han, J. Lunsford, *J. Catal.* **2005**, *230*, 313–316.
- [12] F. Menegazzo, P. Burti, M. Signoretto, M. Manzoli, S. Vankova, F. Boccuzzi, F. Pinna, G. Strukul, *J. Catal.* **2008**, *257*, 369–381.
- [13] T. Haas, R. Jahn, *Process for the Production of Hydrogen Peroxide*, **2008**, US 7364718.
- [14] G. Blanco-Brieva, M. M. J. Campos, J. L. Garcia Fierro, M. Argai Montiel, R. Garaffa, F. Janssens, *Process to Obtain Hydrogen Peroxide, and Catalyst Supports for the Same Process*, **2013**, WO2013010835 A1.
- [15] J.S. Campbell, *Process for Producing Hydrogen Peroxide*, **1967**, Brit. Pat 1094804.
- [16] L. Kim, G.W. Schoenthal, *United States Patent*, **1977**, US 4007256.
- [17] R. L. S. J.H. Hildebrand, *The Solubility of Nonelectrolytes*, Reinhold, New York, 1950., **1950**, vol.17
- [18] M. Belmares, M. Blanco, W. A. Goddard, R. B. Ross, G. Caldwell, S.-H. Chou, J. Pham, P. M. Olofson, C. Thomas, *J. Comput. Chem.* **2004**, *25*, 1814–26.
- [19] A. F. M. Barton, *Chem. Rev.* **1975**, *75*, 731–753.
- [20] M.A. Aramendia, V. Borau, J.F. Gomez, A. Herrera, C. Jimenez, *J. Catal.* **1993**, *140*, 335–343.
- [21] M. Guisnet, J. Barrault, C. Bouchoule, D. Duprez, *Heterogeneous Catalysis and Fine Chemicals II*, **1991**, p.245-252.
- [22] B. Bachillerbaeza, A. Guerreroruiz, I. Rodriguezramos, *J. Catal.* **2005**, *229*, 439–445.
- [23] A. Corma, P. Esteve, A. Mart, *J. Cata* **1996**, *161*, 11–19.

Chapter 6

- [24] V. Hulea, E. Dumitriu, F. Patcas, R. Ropot, P. Graffin, P. Moreau, *Appl. Catal. A Gen.* **1998**, *170*, 169–175.
- [25] M.G.Clerici, *Metal Oxide Catalysis*, Wiley –VCH Verlag GmbH&Co., KGaA , Weinheim, **2009**, p.740-745.
- [26] T. A. Nijhuis, G. Van Koten, J. A. Moulijn, **2003**, *238*, 259–271.
- [27] H. H. Kung, *Transition Metal Oxides: Surface Chemistry and Catalysis*, Elsevier, Science Publishing Company B.V., Amsterdam, Amsterdam, **1989**,p.72-83.
- [28] R. N. Spitz, J. E. Barton, M. A. Barteau, R. H. Staley, *J. Phys. Chem.* **1986**, *90*, 4067–4075.
- [29] V. R. Choudhary, C. Samanta, P. Jana, *Appl. Catal. A Gen.* **2007**, *332*, 70–78.
- [30] J. M. Campos-Martin, G. Blanco-Brieva, J. L. G. Fierro, *Angew. Chem. Int. Ed. Engl.* **2006**, *45*, 6962–6984.
- [31] C. Nyberg, C. G. Tengstål, *J. Chem. Phys.* **1984**, *80*, 3463-3468.
- [32] C. Samanta, V. R. Choudhary, *Catal. Commun.* **2007**, *8*, 73–79.
- [33] V. Choudhary, P. Jana, *J. Catal.* **2007**, *246*, 434–439.
- [34] K.Kishi and S. Ikeda, *Surf. Sci.* **1981**, *107*, 405–416.
- [35] V. Paunovic, V. Ordonsky, M. F. Neira, D. Angelo, J. C. Schouten, T. A. Nijhuis, *J. Catal.* **2014**, *309*, 325–332.
- [36] M. T. Kreutzer, F. Kapteijn, J. A. Moulijn, *Catal. Today* **2005**, *105*, 421–428.
- [37] C. W. Jones, *Application of Hydrogen Peroxide and Derivatives*, The Royal Society Of Chemistry, Cambridge, UK, **1999**, p.80-267.
- [38] R. Noyori, M. Aoki, K. Sato, *Chem. Commun. (Camb)*. **2003**, 1977–1986.
- [39] K. I. Hadjiivanov, G. N. Vayssilov, *Adv. Catal.* **2002**, *47*, 307–511.
- [40] Y.Lokhov, A.Davydov, *Kinet. Catal.* **1980**, *21*, 1515–1522.
- [41] J. Grunwaldt, A. Baiker, *J. Phys. Chem.* **1999**, *103*, 1002–1012.
- [42] J. Raskó, J. Kiss, *Catal. Letters* **2006**, *109*, 71–76.
- [43] M. A. Natal-Santiago and J. A. Dumesic, *J. Catal.* **1998**, *175*, 252–268.
- [44] M. A. Babaeva, D. S. Bystrov, A. Y. Kovalgin, a. a. Tsyganenko, *J. Catal.* **1990**, *123*, 396–416.
- [45] J. Rasko, J. Bontovics, F. Solymosi, *J. Catal.* **1994**, *146*, 22–33.
- [46] G. C. Cabilla, A. L. Bonivardi, M. A. Baltanás, *J. Catal.* **2001**, *201*, 213–220.
- [47] J. Lunsford, *J. Catal.* **2003**, *216*, 455–460.
- [48] C. J. Serpell, J. Cookson, D. Ozkaya, P. D. Beer, *Nat. Chem.* **2011**, *3*, 478–83.
- [49] C. Samanta, *Appl. Catal. A Gen.* **2008**, *350*, 133–149.

Effect of co-solvent addition

Conclusions

& Outlook



7.1. Conclusions

The research done in this thesis focuses on development and testing of wall-coated capillary microchannels for the synthesis of hydrogen peroxide using the direct combination of hydrogen and oxygen over an Au-Pd heterogeneous catalyst as the most green and direct route. The most important aspect of microreactors that justifies their application in the direct synthesis of hydrogen peroxide is the elimination of potential explosive hazards of hydrogen and oxygen mixtures. Heat removal from microchannels is fast, while small channels diameters prevent the development of radical chain reactions (quenching). Channels with relatively small dimensions (i.e. 300 μm) are considered safe to work with pure hydrogen and oxygen mixtures, which would be explosive in conventional chemical reactors. In addition, microchannel operation in the gas-liquid Taylor flow regime improves safety additionally by compartmenting the gas phase between the liquid slugs.

Deposition of support layer and preparation of catalytic films inside microchannels

Deposition of the catalyst in the form of catalytic film on microchannel walls is advantageous because of lower pressure drops and better catalyst wetting and contacting. To increase the surface area to deposit the active catalyst on the microchannel wall it was necessary to coat the capillary with a stable and uniform layer of silica support material. The main factor controlling the uniformity of the deposited layer was the control over the velocity of the displacing plug during the wash-coating procedure. The initially estimated thickness of the catalytic film inside the microchannel that assumes an efficient catalyst usage was roughly in a range of 1-10 μm for a reaction performed in aqueous phase. Later calculations showed that at the reaction rates observed with our AuPd catalyst, the desired thickness of catalytic layer should remain below 4 μm for reaction in aqueous medium. This implies that a variation in the layer thickness over the channel length of higher than $\pm 1 \mu\text{m}$ would result in differences in diffusion of reacting molecules in different channel sections. The stability of the wash-coated layer under reaction conditions is essential for long term microchannel performance. The adherence of the silica layer is mainly influenced by surface and chemistry of coating fluid.

Testing catalyst performance

The second step in the development of catalytic coatings is to successfully implement the active phase, metallic Au and Pd in our case. In order to ensure that all AuPd is available for reacting molecules, the metallic phase is deposited on a pre-coated silica support layer. Various methods for catalyst preparation have been tested. In chapter 3 a comparison between conventional impregnation catalyst and colloidal nanoparticles is given, showing that nanoparticles are significantly more active than traditional impregnated catalysts under identical conditions. This was ascribed to the random presence of a bulk metal phase in case of impregnation due to poor dispersion. In addition, we were able to show that the activity of colloidal nanoparticles supported on silica powder and inside the microchannels is identical, meaning that the preparation procedure is successfully translated to microchannel. The possibility to apply pure instead of diluted hydrogen and oxygen mixtures in the microreactor proved to be not only beneficial in terms of productivity, but in terms of selectivity as well. Clearly, at higher reactant partial pressures adsorption effects on the catalyst surface become rather relevant. Due to less vacant sites available on the surface, less side reactions occurs (decomposition and hydrogenation). Reactant molecules adsorbed on neighbouring active sites responsible for catalyzing side reactions and non-selective peroxide transformation to water are blocked under those conditions, leading to observed selectivity enhancement.

Chapter 7

A wall-coated microchannel performance study

The performance of the wall-coated microchannel was investigated. This allowed us to assess the range of peroxide concentrations that can be generated inside the microchannel. The maximum hydrogen peroxide concentration in the liquid phase is accomplished when the H_2 and O_2 ratio in the gas phase is equal to 1. An increase in the oxygen content leads to a higher selectivity due to the suppression of the peroxide hydrogenation reaction, reaching even 100 % selectivity at low H_2/O_2 ratios. Nevertheless, the exposure of the catalyst to $O_2/H_2 > 1$ over a longer period of time leads to partial loss of the selectivity, although hydrogen conversion remains the same. This is ascribed to a change in the catalyst oxidation state and further on it has been shown that catalyst activity can be recovered upon reduction. Higher H_2 partial pressures compared to O_2 results in a loss of selectivity and a drop in hydrogen peroxide content as a consequence of the hydrogenation of the desired product.

The most important goal of this study was to assess the advantages and drawbacks of a microchannel as a reactor system for producing concentrated solutions of hydrogen peroxide that could be consumed on site in a specific local application. The dependence on WHSV of the concentration in the liquid phase and the H_2 selectivity was studied for two different G/L ratios. The results show a tremendous selectivity loss if one decides to operate the direct synthesis reaction at high H_2 conversions and high H_2O_2 concentrations in the liquid phase. By using the current set-up configuration, it is possible to achieve peroxide concentrations as high as 5 wt% at the reactor outlet, but with a selectivity drop to approximately 20%. This implies that coupling the direct synthesis of hydrogen peroxide with a consecutive reaction, in which peroxide is consumed in a desired reaction thus keeping its concentration low, is necessary in order to prevent peroxide conversion to water.

Kinetic study

To obtain the overall kinetic model suitable to predict the peroxide concentration at the reactor outlet, expressions obtained by fitting separately the reactions of direct formation of peroxide and peroxide reduction in the presence of hydrogen were combined. The addition of acid is generally practiced in the direct synthesis of hydrogen peroxide as well as in conventional AO process not only for preventing the H_2O_2 decomposition catalyzed by the catalyst itself, but also hindering the decomposition caused by equipment material. Catalyst characterization revealed that the surface of Au-Pd colloidal nanoparticles consist of a mixture of Au and Pd atoms, resulting in unique catalytic properties. CO adsorption experiments confirmed the absence of Pd-Pd indicating a strong interaction of Au with Pd. The rate of direct water formation from hydrogen and oxygen was a priori neglected, considering that the observed H_2 selectivity in the direct synthesis at high oxygen partial

pressures was 100% in our previous study. The decomposition reaction was eliminated by the addition of sulfuric acid. As established by the kinetic model, the direct formation of hydrogen peroxide from hydrogen and oxygen seems to involve hydrogen adsorption, dissociation, but not spill-over of H-species over the AuPd surface. It is most likely that the reaction occurs between non-dissociated oxygen and hydrogen species adsorbed pairwise as suggested by several studies on hydrogen adsorption over AuPd surfaces. The comparison of our results with kinetic studies earlier published for Pd catalysts on the direct formation of hydrogen peroxide indicate somewhat different surface reaction mechanism on AuPd surfaces in comparison to Pd catalyst, ascribed to difference in surface properties of the two type of catalysts. The peroxide concentration values predicted with an overall model and experimentally measured are in acceptably good agreement.

Application of organic solvents in direct synthesis of hydrogen peroxide

The coupling of the direct synthesis reaction with an oxidation reaction would often require the application of organic solvents instead of a pure aqueous phase. Therefore, the effect of different organic solvents on the direct synthesis was evaluated. The solvent nature strongly affects the observed catalytic activity of the catalyst in the direct synthesis of hydrogen peroxide. Besides the effect on the H₂ conversion, some solvents added to the typically used aqueous phase can significantly modify the selectivity towards peroxide. Despite the fact that some water non-miscible solvents show a high H₂ solubility, they are not suitable for the direct synthesis reaction. In fact, addition of hexane, the solvent with the highest H₂ solubility, results in a poor selectivity. Our results suggest that suitable solvents for the direct synthesis are water miscible. In particular, lower alcohols show a pretty high selectivity at moderate to high conversions, and as such are suitable for the direct synthesis reaction. With the group of aprotic polar solvents (acetone, acetonitrile, DMSO) a very high selectivity can be achieved, probably due to the solvent interaction with the catalyst surface. However, as is evident from the microreactor experiments, at high concentrations of the solvent and reacting gases, the aprotic solvent can completely poison the catalyst. CD₃CN adsorption experiments indicate that acetonitrile adsorbs on unselective defect Pd sites, which could be responsible for peroxide decomposition on the catalyst surface. Eventually, the selective poisoning of the catalyst surface with an aprotic solvent was confirmed via decomposition of hydrogen peroxide in the presence of a catalyst. Decomposition in the presence of co-solvent (acetonitrile) was either blocked (at higher acetonitrile content) or decelerated (lower acetonitrile content). Although FTIR studies of methanol adsorption show a strong interaction with Pd, the addition of methanol does not significantly affect the hydrogen peroxide decomposition kinetics over the Au-Pd catalyst itself in comparison with pure water. The effect of methanol addition on the hydrogen peroxide decomposition seems to correlate with the interaction of methanol with

Chapter 7

the peroxide, rather than with the catalytic sites responsible for cleavage of an O-O bond at the surface.

If the direct synthesis of hydrogen peroxide is performed in a conventional reactor system using diluted mixtures of reacting gases, addition of aprotic solvents such as acetonitrile or acetone can be highly beneficial in terms of yield and selectivity. Among the lower alcohols, isopropanol seems to be particularly suitable as a co-solvent/solvent. Researchers working on the direct synthesis reaction in conventional reactors besides traditional solvents, water and methanol, should also consider other lower alcohols or aprotic solvents such as acetonitrile. Particularly acetonitrile at higher content (20 vol%) is highly efficient in preventing peroxide decomposition. This implies that the required acidification of aqueous solutions used in the direct synthesis can be avoided if acetonitrile is applied as a solvent or co-solvent. Moreover, the role of solvent should be observed in a broader context, not only through solubility of reacting gases, but also the potential interaction of solvent functional groups with the catalyst as well.

In case of the application of microreactors with concentrated hydrogen and oxygen mixtures, the addition of only small amounts of aprotic solvents such as acetonitrile (up to a few percent) leads to a significant improvement in selectivity and yield, but high solvent concentrations are detrimental for the catalytic activity assumingly due to a non-selective adsorption on active catalytic sites. Addition of methanol, however, as a solvent or co-solvent when using concentrated H₂ and O₂ gas feed does seem to be a much better option, considering that the yield observed can be several times higher than in aqueous solutions. Methanol is a suitable solvent from the aspect of direct consumption of peroxide produced in selective oxidations, considering that many organic substrates show a good solubility in methanol. However, also with methanol as a solvent the addition of acid as a peroxide stabilizer which prevents its decomposition is difficult to avoid considering the impact on the selectivity.

The presence of acid in peroxide solutions is not only needed during the course of the reaction, but also during the post-processing, in contact with pipelines or storage. If the Au-Pd catalyst would be the only cause of its decomposition, reaction solutions could be simply neutralized after the reaction step. Specifications of commercially available standard grade peroxide solutions indicate that those are also acidified with the aim to prevent rapid decomposition. Addition of metal chelating agents as stabilizers is not sufficient to prevent peroxide decomposition, since it is believed that peroxide decomposition proceeds via formation of HO₂⁻ species. Considering we showed that it is possible to reach peroxide concentrations up to 5 wt% in aqueous media and that here we show that application of methanol as a solvent instead of water can improve the yield by factor of 3-4 (with acid

present), it is reasonable to assume that the concentration of 9 wt% set as objective by economic evaluation is attainable.

7.2. Outlook

The economic evaluation performed earlier ^[1] suggests that hydrogen peroxide by direct synthesis (DS) can compete with the conventional AO process only if it is possible to produce peroxide in the concentration range required by the user (1-10wt% typically) without applying additional concentration steps such as vacuum distillation. This reduction in concentration costs would compensate for the high CAPEX caused by high pressure equipment required assuming the case where direct synthesis is conducted in conventional reactors. Due to low H₂ content of gas phase, to increase its partial pressure high total pressures are required in the system (~several hundreds of bars). In contrast to conventional reactors, the possibility to use pure hydrogen and oxygen mixtures in a microchannel eliminates the need for high pressures (lower CAPEX), meaning that the production of hydrogen peroxide in microreactors even at concentrations lower than 10 wt% could be economically feasible if the costs of microreactor fabrication would be lower than that of the conventional high pressure equipment required in case of conventional DS. In general, the estimated CAPEX for a direct synthesis plant to be competitive with AO process is around 40-50 million US dollars for a plant capacity of 10 kt/year. To have better idea on the complexity and costs of microreactor units for the direct synthesis reaction on the small/medium scale, it is necessary to design a multichannel unit involving reaction channels, gas-liquid separators, manifolds for proper gas-liquid distribution integrated with heat-exchangers. The extensive research has been already done in our group in relation to (micro/mili) channel numbering up for applications in multiphase reactions ^[2]. Although process intensification generally reduces the size of equipment, costs per unite vessel volume are generally higher. The cost of microchannel fabrication is mainly influenced by channel sizes and fabrication tolerances. The channel sizes cannot be significantly manipulated in this case due to safety restrictions. One of the techniques considered for the massive production of microchannel plates is 3D printing, which is becoming more and more affordable and suitable for massive production.

Within the DEMIS project ^[3], successful microchannel scale-up (achieved through internal numbering up) from lab scale multi-channel modules with a production capacity of 1kg/h directly to 1000-2000kg/h has been already reported. This pilot plant is used to produce propylene oxide from propylene and liquid phase hydrogen peroxide over a wall-coated TS-1 catalyst. The channel diameter in this case is smaller than 1 mm, due to the safety requirements and the residence time reported is in the range of seconds. Modules are equipped with cross-flow heat exchangers using water as a cooling fluid. The direct synthesis process would potentially make savings in the manufacturing costs. Raw materials

Chapter 7

used are in essence the same in both the DS and AO processes as well as the additives needed, nevertheless due to a lower number of operations, the direct synthesis will lower labor costs. Direct synthesis in a microchannel reactor in comparison to conventional reactors does not require a high excess of oxygen. In addition, energy consumption (electricity) will be lower due to a lower total pressure required. This will lead to a further cost reduction and a higher competitiveness of the direct synthesis with the conventional AO process.

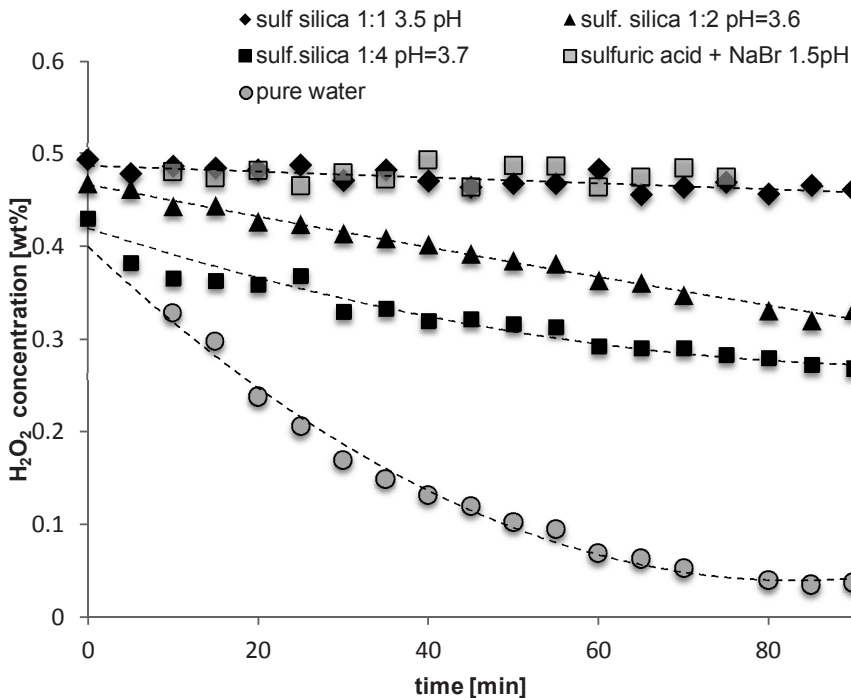


Figure 7.1. Hydrogen peroxide decomposition over time in pure water, aqueous phase with additives and in aqueous phase after addition of various sulfonated silicas ($T=30^{\circ}\text{C}$).

7.2.1. Application of solid acid as a catalyst support

Some of applications of hydrogen peroxide require ultra-pure peroxide grades. Typically, the direct synthesis process involves acidification of the liquid phase to prevent peroxide disproportionation to water. Acid is also added in the conventional process in the extraction phase in order to prevent peroxide decomposition during downstream processing and

storage. Ultra-pure grades of hydrogen peroxide are obtained after an additional purification step involving ion-exchange columns.

In case of the on-site application of hydrogen peroxide, the addition of mineral acids can be overcome by the application of a solid acid as a catalyst support. Following this approach, in our group the attempt has been made to sulfonate the conventionally used silica support. The effect of sulfonated silicas obtained by varying the silica to MPTS ratios (affecting the pH of solution) on peroxide decomposition is given below (Fig. 7.1):

From those results obtained in batch testing we can conclude that the application of solid acids is rather effective in preventing peroxide decomposition inside the reactor.

The next step would involve the sulfonation of the silica-washcoated layer inside the microchannel and testing its ability to inhibit the decomposition in the direct synthesis of hydrogen peroxide. In this case, all downstream parts of the set-up would need to be passivated to avoid peroxide decomposition catalysed by equipment fabrication material.

7.2.2. Polyelectrolyte multilayers (PEM) AuPd catalyst as an upgrade in the catalyst preparation procedure

The method used throughout this thesis for the preparation of an AuPd catalyst in microchannels was a two-phase synthesis. Although significantly faster and effective than conventional impregnation due to the higher vapour pressure of dichloromethane in comparison to water, preparation of catalytic layers via this method is still time consuming considering that solvent removal needs to be done at relatively mild conditions to ensure a uniform catalyst distribution along the channel. Recently, we identified the method known as polyelectrolyte multilayer (PEM) deposition for preparation of AuPd catalytic layers. This method involves cyclic deposition of a polyanionic (polyacrylic acid) layer and a polycationic layer (polyethylene imine) followed by ion exchange with AuCl_4 and PdCl_4 ions from solution and NaBH_4 reduction. Results from microchannel testing are given in Fig. 7.2. One of the main advantages of this method is that the catalyst loading can be tuned by choosing the number of layers deposited (Fig. 7.2a). Besides shortening in the preparation procedure (one week to one day), this method resulted in a highly active catalyst. It is interesting to notice that when comparing the performance of the AuPd PEMs (1 and 3 layers) catalyst with the AuPd colloidal nanoparticles in terms of the conversion-selectivity-peroxide concentration relationship (Fig. 7.3), both type of catalysts behave rather similar.

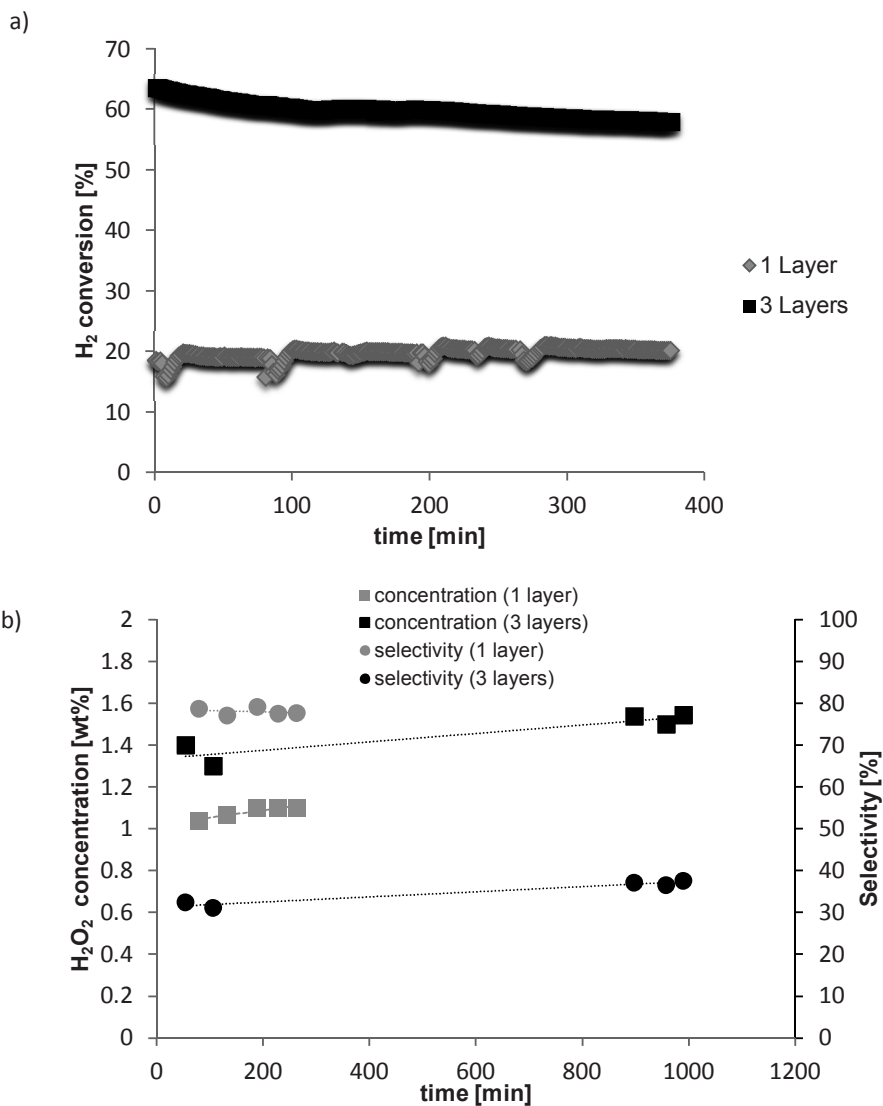


Figure 7.2. Performance of AuPd PEM's in a wall-coated microchannel (a) H_2 conversion as a function of number of AuPd PEM layers and (b) Peroxide concentration and selectivity as a function of number of PEM layers (Total gas flow rate 5 mL/min, $H_2/O_2 = 1$, liquid phase 0.05M $H_2SO_4 + 10$ ppm NaBr, liquid flow rate 0.05 mL/min, $p = 20$ bar).

Future work on the direct synthesis of hydrogen peroxide in a microchannel with respect to the catalysis aspect should incorporate a detailed study on the long-term stability of PEMs

and the effectiveness of sulfonated silica inside the microchannel as solid acid able to suppress peroxide decomposition. Application of PEMs would significantly simplify catalyst preparation procedure, while application of solid acids instead of mineral acids would enable production of ultra-pure peroxide grades inside the microchannels. Eventually, the techno-economical evaluation is needed to assess advantages and disadvantages of microreactor application for the direct synthesis of hydrogen peroxide and economic competitiveness of the direct synthesis process in microreactor with the conventional process.

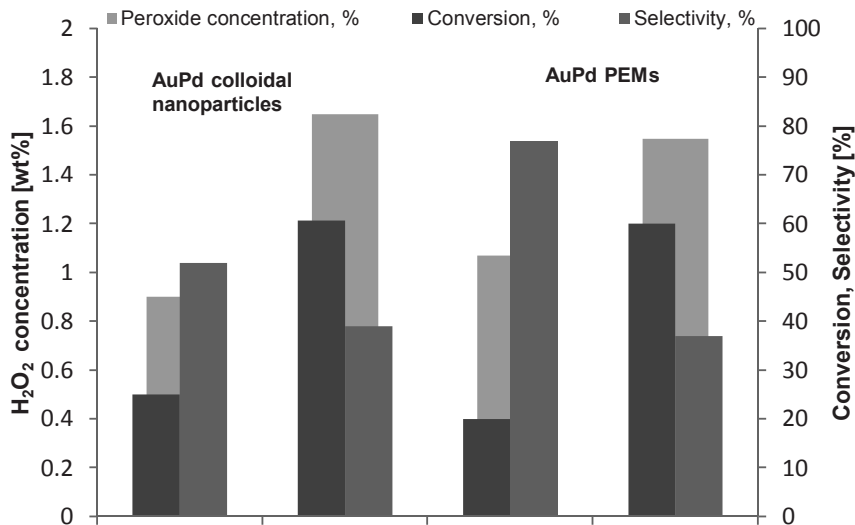


Figure 7.3. Comparison of microchannel performance of AuPd colloidal nanoparticles and PEMs.

References:

- [1] J. García-Serna, T. Moreno, P. Biasi, M. J. Cocero, J.-P. Mikkola, T. O. Salmi, *Green Chem.* **2014**, *16*, 2320–2343.
- [2] M. Al-Rawashdeh, Barrier-Based Micro/Milli Channels Reactor, PhD Thesis, Eindhoven University of Technology, **2013**.
- [3] T. R. Dietrich, *Microchemical Engineering in Practice*, John Wiley & Sons, Inc., New Jersey, **2009**.

List of publications

Journal Articles

Paunovic, V., Ordonsky, V., Neira d'Angelo, M.F., Schouten, J.C. & Nijhuis, T.A. (2014). Direct synthesis of hydrogen peroxide over Au-Pd catalyst in a wall-coated microchannel. *Journal of Catalysis*, 309, 325-332.

Paunovic, V., Schouten, J.C. & Nijhuis, T.A. (2014). Direct synthesis of hydrogen peroxide in a wall-coated microchanne over Au-Pd catalyst- A microchannel performance study. *Catalysis Today*, 248, 160-168.

Neira d'Angelo, M.F., Ordonsky, V., **Paunovic, V.**, Schaaf, J. van der, Schouten, J.C. & Nijhuis, T.A. (2013). Hydrogen production through aqueous-phase reforming of ethylene glycol in a washcoated microchannel. *ChemSusChem*, 6(9), 1708-1716.

Paunovic, V., V.Ordonsky, V. Suschievisch, J.C.Schouten, T.A. Nijhuis (2015), Direct synthesis of hydrogen peroxide over Au-Pd catalyst -Effect of co-solvent addition. *ChemCatChem*, 7 (7), 1161-1176.

Paunovic, V., Ordonsky, V., Neira d'Angelo, M.F., Schouten, J.C. & Nijhuis, T.A. (2015). Coating catalyst on prefabricated capillary microchannels for the direct synthesis of hydrogen peroxide. *Industrial and Engineering Chemistry Research*, 54(11), 2919-2929..

Paunovic, V., Schouten, J.C. & Nijhuis, T.A. (2015).Direct synthesis of hydrogen peroxide over Au-Pd catalyst in a wall-coated microchannel- Kinetic study. *Applied Catalysis A: General*. accepted.

Conference Proceedings

Paunovic, V., Ordonskiy, V., Nijhuis, T.A. & Schouten, J.C. (2013). Direct synthesis of hydrogen peroxide in a wall coated microreactor. Proceedings of the 9th World Congress of Chemical Engineering (WCCE9), August 18-23, 2013, Seoul, Korea.

Neira d'Angelo, M.F., Ordonskiy, V., **Paunovic, V.,** Schouten, J.C., Schaaf, J. van der & Nijhuis, T.A. (2013). Hydrogen production by aqueous phase reforming of renewable carbohydrates in a washcoated microchannel. Proceedings of the 14th Netherlands Catalysis and Chemistry Conference (NCCC-XIV), 11-13 March 2013, Noordwijkerhout, The Netherlands.

Paunovic, V., Ordonskiy, V., Nijhuis, T.A. & Schouten, J.C. (2013). Direct synthesis of hydrogen peroxide in a wall coated microreactor using Au-Pd catalyst. Proceedings of the 9th European Conference of Chemical Engineering (ECCE9), 21-25 April 2013, The Hague, The Netherlands.

Paunovic, V., Ordonskiy, V., Nijhuis, T.A. & Schouten, J.C. (2013). Direct synthesis of hydrogen peroxide in a wall coated reactor using Au-Pd. Proceedings of the 23rd North American Catalysis Meeting (NAM23), June 2-7 2013, Louisville, Kentucky.

Paunovic, V., Ordonskiy, V., Nijhuis, T.A. & Schouten, J.C. (2013). Direct synthesis of hydrogen peroxide in a wall coated microreactor. Proceedings of the 15th Netherlands Catalysis and Chemistry Conference, March 11-13, 2013, Noordwijkerhout, The Netherlands.

Paunovic, V., Ordonskiy, V., Nijhuis, T.A. & Schouten, J.C. (2013). Direct synthesis of hydrogen peroxide in a wall coated microreactor using Au-Pd catalyst. Proceedings of the 3rd North American Symposium on Chemical Reaction Engineering (NASCRE-3), March 17-20, 2013, Houston, Texas.

Paunovic, V., Neira d'Angelo, M.F., Ordonskiy, V., Nijhuis, T.A. & Schouten, J.C. (2012). Development of uniform silica-based catalytic coatings for catalytic microreactors. Proceedings of the 22nd International Symposium on Chemical Reaction and Engineering (ISCRE 2012), 2-5 September 2012, Maastricht, The Netherlands., submitted / in press.

Paunovic, V., Neira d'Angelo, M.F., Ordonskiy, V., Nijhuis, T.A. & Schouten, J.C. (2012). Development of uniform silica-based coatings for catalytic reactors. Proceedings of the 13th Netherlands Catalysis and Chemistry Congress (NCCC XIII), 5-7 March 2012, Noordwijkerhout, The Netherlands., submitted / in press.

Neira d'Angelo, M.F., Ordonskiy, V., **Paunovic, V.**, Schouten, J.C., Schaaf, J. van der & Nijhuis, T.A. (2012). Catalytic coatings on microchannels for aqueous phase reforming of biofeedstocks. *Proceedings of the 13th Netherlands Catalysis and Chemistry Congress (NCCC XIII), 5-7 March 2012, Noordwijkerhout, The Netherlands.*, submitted / in press.

Neira d'Angelo, M.F., Ordonskiy, V., **Paunovic, V.**, Schouten, J.C., Schaaf, J. van der & Nijhuis, T.A. (2012). Catalytic coatings on microchannels for aqueous phase reforming of biofeedstocks. *Proceedings of the 15th International Congress on Catalysis (ICC 2012), 1-6 July 2012, Munich, Germany*, submitted / in press.

Paunovic, V., Nijhuis, T.A. & Schouten, J.C. (2011). Direct hydrogen peroxide synthesis in a capillary micro reactor. *Proceedings of the Netherlands Process Technology Meeting (NPS-11), 24-26 October 2011, Arnhem, The Netherlands.* (pp. 207-207).

Acknowledgments

As the curtain comes down on my academic pursuit, I would like to acknowledge many people who contributed to the realization and quality of this PhD thesis and to those who stood next to me during this journey.

First of all, I would like to express my sincere gratitude to prof. Jaap Schouten. Dear Jaap, thank you for opening the door of the scientific world to me and giving me the privilege to work in the SCR group. You created a proficient and agreeable working environment in which every one of us could develop professionally bringing out the very best of ourselves. Looking back, there was nothing I thought of that could not have been technically realized. I enjoyed learning from you and I sincerely appreciate your guidance and support during the past four years.

Many thanks to my daily supervisor, dr. Xander Nijhuis. Dear Xander, thank you for recognizing my strengths and weaknesses, for challenging me to think further and making me a better and independent researcher. Thank you for teaching me that sometimes you simply have to take the risk when making a decision. Otherwise, as Einstein said, "If we knew what it was we were doing, it would not be called research, would it?"

A very special gratitude goes to dr. Vitaly Ordonsky, my non-official supervisor during the past three years. Vitaly, you are one of the most passionate and imaginative researchers I know. Thank you for a number of brilliant ideas and thank you for encouraging me to work and to think beyond my comfort zone. Your enthusiasm is sometimes viral. Besides being a great colleague and coach, thank you for being a great friend outside the Helix building together with Liza.

In addition, I would like to thank dr. Mart de Croon for our pragmatic discussions on kinetics, members of the committee, prof. dr. Y. Cheng, prof. dr. F. Kapteijn and prof.dr.ir. E.J.M. Hensen, for taking their time to read this thesis and their encouraging comments. Special thanks to prof. Kapteijn for sharing his expertise and putting final touches to this manuscript. To prof. Cheng I would like to thank you for a few wonderful months in Beijing. It was a pleasure to be a guest researcher in your group at the Tsinghua University.

This research would not have been possible without funding provided by NRSC-Catalysis, the Dutch Institute for Catalysis Research. I gratefully acknowledge their financial support.

Finally, I would like to thank all those people whose names are not visible between the covers of this book, but without whom my experimental work would not have been possible

- Carlo, Marlies, Peter, Erik, Theo, Dolf, Madan, Joris and Joost. Carlo, I hope I did not bother you too much with SEM, TEM, my set-ups and particularly with safety. I believe that by now you know everything about hydrogen and oxygen mixtures and ways how to and how not to explode them ☹. Peter, thank you for learning the ICP analysis technique, to be able to help us. I have to say that I also enjoyed sharing an office with you (until Vitaly stole that position☺). Marlies, I always found it impressive how patient you can be with us and our GCs. Besides, it was often so nice sitting in the lab or in the coffee room next to you and talk about ordinary life, escaping the scientific bubble that we are all surrounded with more or less. Erik, thank you for creating miracles fast. So often, I was impressed with your technical creativity and so often I was relying on you to find a solution.

Denise, I am grateful beyond words for all your help with this thesis and moreover with all the administration I had to do in the past few years. Thank you for being so dedicated to the work you do, so organized. Whenever I had a question or a doubt about something, you always knew what to do. Luckily, you are still not on holidays while I am finalizing those lines. Your sharp eye will locate all the remaining typos I might have made☺.

My dear laddies... Lara, Emila, Dulce, Fer, Paola, Shohreh... Thanks to you, TU/e became my second home. I can say that your company I will miss the most. This little hood, a mix of different cultures, languages, accents, characters... is so unique. Lara... thank you for sharing with me the office, several labs, hydrogen in STW 1.09 the past few years ☺☺☺ and air in Beijing... Without your company and encouragement, I would ask for the return ticket soon after I arrived! Thank you for telling me “focus!” the last few months of my PhD when I started panicking about many many things... You were often actually the rational big sister! Emi... your colourful clothes and shoes so well reflects your personality... It's always joyful to be in your company! I cannot thank you enough for accompanying me to Soleil... I will never forget the two of us pulling that funny large grey box with ‘suspicious’ content through Gare du Nord, surrounded by armed soldiers checking suspicious passengers ☺☺☺... Dulceeeeeee, our PO/gold/TS-1 expert... you are one of the most emphatic and friendly people I met... Fer, it would be much more difficult to coat those capillaries without your help ☺... Thank you for teaching me to trade perfectionism for pragmatism ☺! I am looking forward to see you in your new roles - a mother and a professor. Pao and Shohreh, it would not be nice if I would split the male part of the fantastic four, Michiel and Slavisa... thank you for always organizing some nice activities and trying to persuade me to join... Nopi, I am so glad that you are back in the Netherlands and in Eindhoven...

Dear Faysal, without you it would be much more difficult to rebuild my life in the Netherlands ... thank you for being a great colleague, friend, real estate agent when needed☺, for helping me with moving, fixing electricity in my apartment, cooking dinners

... Ma'moun, I was always admiring that natural tranquillity you possess ... it's a true gift. Carlos, I will always remember that poster with Gisele Bundchen advertising biomass as a new carbon feedstock on the door of our office (it could be it's still there and no one knows why) ... you are a true marketing genius 😊 among scientists. I also need to thank Jovan and Ivana for giving me first instructions how to survive as a Serbian in the Netherlands 😊 ...

I must thank all other people that I shared many nice moments with in SCR and SFP groups: my office mates Michiel, Ana and Shamayita, Qi, Ivana, Minjing, Bruno, Jun, Lana, Anto, Frans, Jiaqi, Christine, Stefan, Elnaz, Bhaskar, Carlos, Lida, Marco, Tom, Serdar, Narendra, Jack, Halabi, Wim, Joost, Miguel, Aleksandra...and some others I might have forgotten to mention here. Tom thank you for trying to teach me Dutch and for organizing the SCR outing together with me ...

Almost five years ago, I replanted myself on the Dutch soil ... In the meantime, I feel here like at home thanks to my Dutch-Serbian family, Dada and Martijn, Aleksandar and Natasa, and mostly of all thanks to Tobias, who kept loving me despite all my curves and edges and supporting me throughout. Now I know that it would be worth the journey to here just to meet you 😊. Finally, I want to thank my parents for giving me always a lot of love and freedom and for never disputing my choices. To my brother, for always being my accomplice, even in chemical and most recently in catalysis engineering 😊. Hvala Vace! Hvala mama I tata sto ste nas uvek podrzavali u svemu, bez obzira na velicinu snova. I sto ste nas naucili da za velike cipele moramo da porastemo.

Curriculum Vitae

Violeta Paunović was born on April 29th 1985 in Prijepolje, Serbia. She studied at the Faculty of Technology and Metallurgy of the University of Belgrade (Belgrade, Serbia). In 2009 she graduated with the diploma work at the Department of Pharmaceutical Engineering on a topic of Diffusion of drugs from hydrogels and gels with encapsulated microparticles under the supervision of Prof.Dr. Nevenka Bosković-Vragolović and Prof.Dr. Branko Bugarski. During the graduate studies, she was awarded 'Student of the Year' for outstanding academic performance.

In 2010 she joined the Chemical Reactor Engineering group at the Eindhoven University of Technology (Eindhoven, The Netherlands) as a PhD student supervised by dr.ir. Xander Nijhuis and prof.dr.ir. Jaap Schouten. The results of her PhD research project dealing with direct synthesis of hydrogen peroxide in a wall-coated microchannel are presented in this dissertation. Since April 2015 she is employed at DSM (Geleen, NL) as a process development engineer.